MODELLING STORMWATER POLLUTANTS IN HAMILTON, CANADA

By

SHIVALINGAIAH BOREGOWDA, M. E.

A thesis

Submitted to the School of Graduate Studies in

Partial Fulfilment of the Requirements

for the Degree

Doctor of Philosophy

McMaster University

MODELLING STORMWATER POLLUTANTS IN HAMILTON, CANADA

DOCTOR OF PHILOSOPHY (1984)
(Civil Engineering)

McMASTER UNIVERSITY
Hamilton, Ontario

TITLE: Modelling stormwater pollutants in Hamilton, Canada.

AUTHOR: Shivalingaiah Boregowda,

B.E. (Mysore University, India)

M.E. (Bangalore University, India)

SUPERVISOR: Dr.W. James

NUMBER OF PAGES: XV, 252

DEDICATED

TO

MY PARENTS

ABSTRACT

The fact that considerable quantities of solids, toxic metals and hazardous contaminants are washed off urban surfaces has been well documented in recent literature.

It is generally recognised that urban runoff models predict runoff quantity quite well. However, due to lack of understanding of the various processes involved in pollutant buildup, washoff and routing and insufficient, and faulty data collection, urban runoff models depict runoff quality poorly. This research therefore attempts to introduce new concepts and algorithms, based on the physical processes involved, to improve runoff quality prediction. The problem has been segmented into three broad areas: a) pollutant buildup, b) pollutant washoff and, c) routing and fate of pollutants.

The interaction of addition and removal processes in pollutant buildup has been further disaggregated. Estimates are made of the daily mass balance of pollutants over a dry period, considering meteorological and geographical effects. Additions from atmospheric dustfall, vehicles, population and special activities; removal due to biological decay, vehicle and wind created eddies and intentional removals (street sweeping) are formulated individually. Scavenging of aerosols and gases and washoff from canopies during

precipitation are also modelled and added to conventional washoff. Expressions for the impact of raindrops, shear due to overland flow, and vehicle-induced eddies are used to develop a new washoff equation which is compared to conventional washoff equations. An established pollutant routing algorithm is modified to minimise summation error. All these pollutant concentration prediction algorithms are interfaced with one of the most comprehensive models, the Storm Water Management Model Version 3 (SWMM3), preserving the runoff quantity prediction algorithms. Provision has been made for variable time steps for both runoff quantity and quality. The modified SWMM3 is called CHGQUAL in the present work. CHGQUAL was applied to the Chedoke Creek Catchment in Hamilton, Canada, for verification, calibration and validation. The pollutional parameters used in the study are suspended solids(SS), biochemical oxygen demand (BOD), total nitrogen (TKN) and total phosphorous (TP). The CHGQUAL computed pollutant concentration results were statistically compared to both SWMM3 results and observed data.

The new runoff water quality algorithms showed improved predictability for the test catchment. The CHGQUAL model can readily be applied to other catchments.

ACKNOWLEDGMENTS

I wish to express my sincere gratitude to my advisor Dr. William James for his constant encouragement and valuable guidance throughout my research work. I am thankful to my supervisory committee members, Mr. J. Marsalek, Dr. C. R. Murthy, and Dr. J. Kramer, for their continuing guidance, understanding and suggestions.

I appreciate the assistance of Mark Stirrup, Dale Henry, Peter Nimmrichter, Ron Scheckenberger, Alaa El Zawahary, Kathryn Bradshaw, and Mr. Mark Robinson who have helped me collectively and individualy in completing this study.

I am grateful to the Civil Engineering Department and McMaster University for providing support and a generally creative environment to enrich my knowledge and also to Water Resources Research Support Programme, Environment Canada, for funding through a 3-year research grant to Dr. James.

I am also thankful to P.E.S. College of Engineering, Mandya, India, for having provided study leave.

Finally, I must thank my wife Meera and family for their patience and support during my study.

TABLE OF CONTENTS

LIST OF TABLES

LIST OF FIGURES

CHAPTER I

INTRODUCTION

Urban runoff contributes a considerable mass of pollutants to receiving water bodies (Novotny and Goodrich-Mahoney, 1978). A growing population, increasing motorization and industrial production all augment pollutant loadings in an urban environment (Shaheen, 1975). Storm water serves as a vector for all these pollutants. Despite laws governing the safe disposal of point source pollutants, the deterioration of surface water quality continues to be an important problem. Since the early seventies this has inspired much research into non-point pollutant sources (urban runoff is an example of a non-point source). Many researchers have attempted to model the mechanisms of pollutant buildup and washoff due to rainfall.

Various human activities initiate pollutant accumulation on the ground surface and in the atmosphere. Atmospheric pollutants ultimately reach the ground with or without chemical interaction, either by gravitational settling or by precipitation scavenging. The contribution of atmospheric pollutants to runoff water quality was assumed to be negligible, but recent studies have revealed that considerable quantities of solids and nutrients are contributed from this source. Most runoff water quality

models use dust and dirt buildup equations, without distinguishing between pollutant sources such as street pavements, vehicles, atmospheric fallout, scavenging, vegetation, land surface, litter, spills, anti-skid compounds, chemicals, construction and drainage networks. Existing urban runoff quantity and quality prediction models usually lump all these sources together in estimating the buildup rates during dry days for different conventional land uses. Overland flow ultimately washes pollutants from pavements and transports them through sewer networks to the receiving water.

1.1 Scope of the study:

The concensus amongst storm water quantity and quality model users is that runoff quantity simulations are usually good, whereas runoff water quality simulations are fair to poor. The present study has therefore attempted to analyze the problem more thoroughly and to develop better algorithms for urban runoff quality prediction based on the physical processes. The study has been divided into four major parts: (1) Sources and buildup of pollutants, (2) Washoff, (3) Routing and fate of pollutants, and (4) Model application. Runoff water quality processes described herein may also be classified as major and minor processes. Major process include (a) dust and dirt (DD) buildup on both pervious and impervious surfaces during inter storm periods, (b) DD

washoff from impervious surface, and (c) routing of pollutants during storm events. The minor processes are (a) pollutant scavenging from the atmosphere, (b) pollutant washoff from pervious areas including canopy washoff, and (c) the effect of baseflow and weir on runoff water quality including variable timestep simulation. The source of pollutants in runoff water is mainly from the surface (pervious and impervious), the atmosphere during dry days, and scavenging at the time of precipitation. The algorithms for these processes have been developed and tested individually and collectively against the available data. Pollutants from pervious areas due to the vegetation canopy and soil erosion from unprotected surfaces have also been added to total pollutant concentrations. All these algorithms are discussed in detail in the subsequent chapters. The complete model is calibrated and validated using Chedoke Creek catchment data of Hamilton. The schematic of existing stormwater quality models and the present study is given in Figure 1.1.

1.2 Geographical and meteorological features of Hamilton:

Hamilton is located on the south western shore of Lake Ontario. It is one of Canada's major industrial cities. The iron and steel industry is the major activity in this city of 306 640 (1980), occupies most of the southern shore of Hamilton Harbour, with the downtown area to the southwest. The Niagara Escarpment almost surrounds Hamilton and the

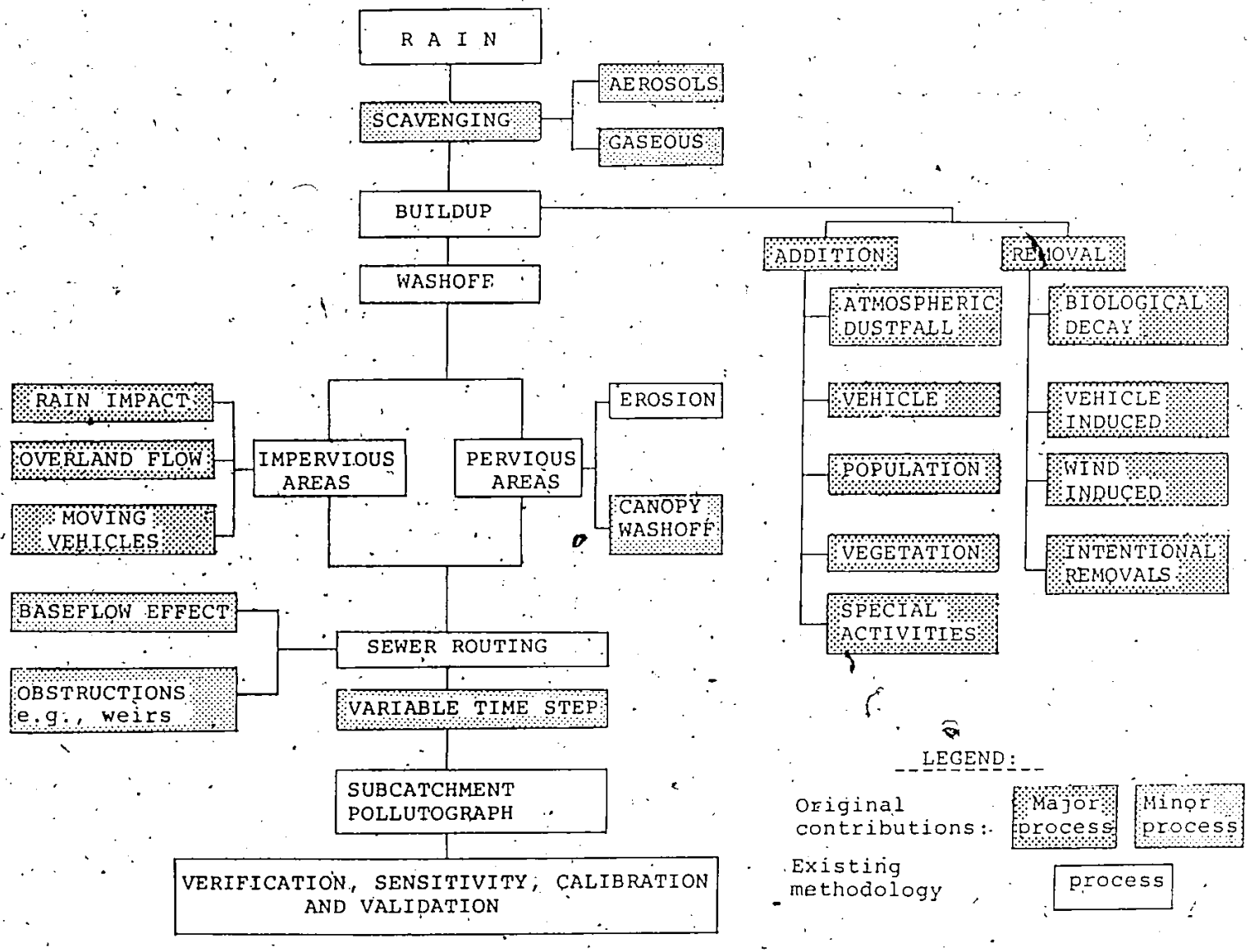

Figure 1.1 Schematic of existing stormwater quality models and present work.

southern arm divides the city into upper and lower sectors having an average height difference of 108 m (see Figure 1.2). The terrain of both the upper and lower city sectors is essentially flat. The escarpment is cut by a number of deep valleys of which the most important is the southwest-northeast aligned Dundas Valley. The main morphological features of the city with respect to pollution are the heavy industrial sector concentrated along the southern side of Burlington Bay and the central business district. The major steel plants are located in the former together with associated industries including machinery, electrical and chemical manufacturing. The business district comprises a core of multistorey commercial buildings of limited areal extent surrounded by a lower level of mixed commercial and residential properties.

The prevailing wind is dominantly west and southwest which helps advect the air borne pollutants away from Hamilton towards Lake Ontario. Northeast and easterly winds play an important role in distributing pollutants over the city. The meteorological data from the hydrometeorological station at the Royal Botanical Gardens show an increase in the frequency of northeast and easterly wind from March to September (Shivalingaiah and James, 1982). This was found to be higher during the day compared to night in the lower part of the city (Farhang, 1982). This effect may be due to the

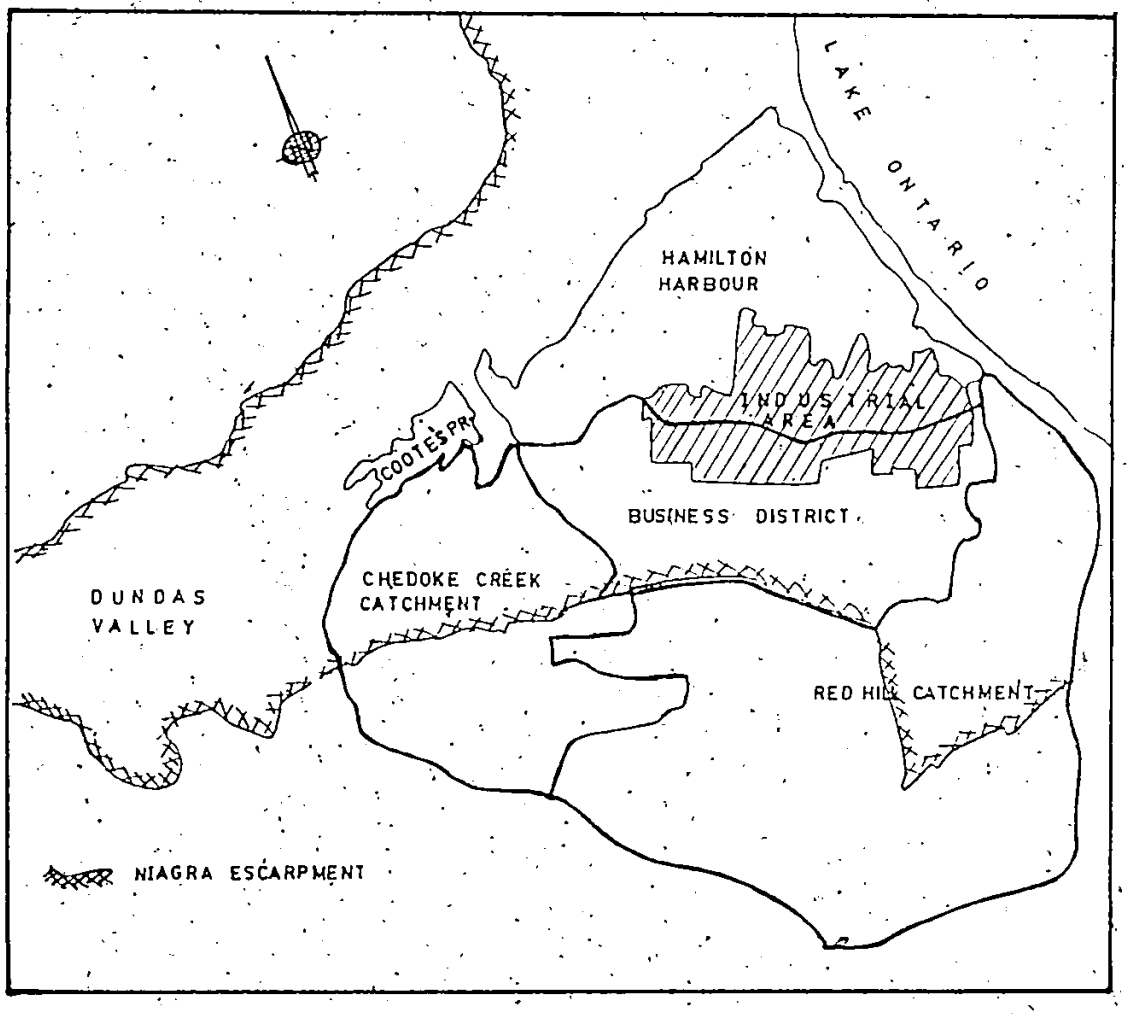

Figure 1.2 Geographical map of Hamilton.

influence of lake breezes. A clockwise shift in the northeast and easterly wind was observed because of the Niagara Escarpment and Dundas Valley (Rouse et al., 1972, Farhang, 1982). Hamilton is highly susceptible to atmospheric inversions because of differential heating between the lake and the land surface. A persistant sharp elevated inversion anywhere between 1070 and 1080 m in height over the heavy industrial zone has been observed (Rouse et al., 1972). The height of the inversion depends upon the season, but it is strongly developed in the morning, diminished in magnitude towards solar noon and strengthened again towards sunset.

The city is divided into three major catchments as shown in Figure 1.3 for storm runoff water quantity and quality modelling based on elevation contours and storm sewer net work. The catchments are the central business district, Chedoke Creek and Redhill Creek. These catchments are further discretized into a number of subcatchments considering the utility of the area for detailed analyses as shown in Figure 1.4. The location of the industrial area with respect to catchments is also shown in Figure 1.3.

The central business district catchment consists of multistorey buildings with the highest degree of imperviousness. It is also encompassed by a lower level of mixed, commercial and residential areas. This catchment is in very close proximity to the industrial area.

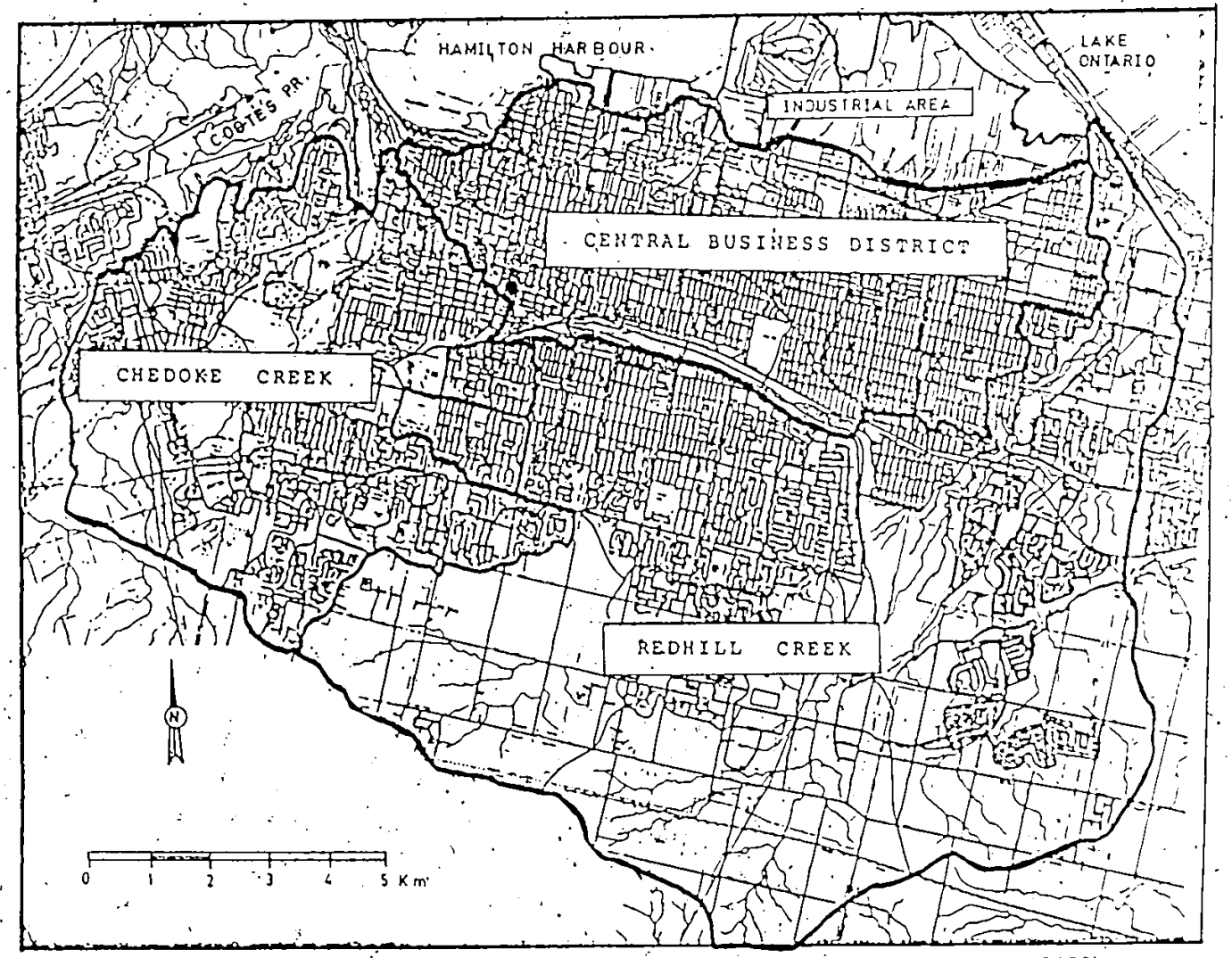

Figure 1.3 The three major catchments of Hamilton(source: James and Henry, 1982).

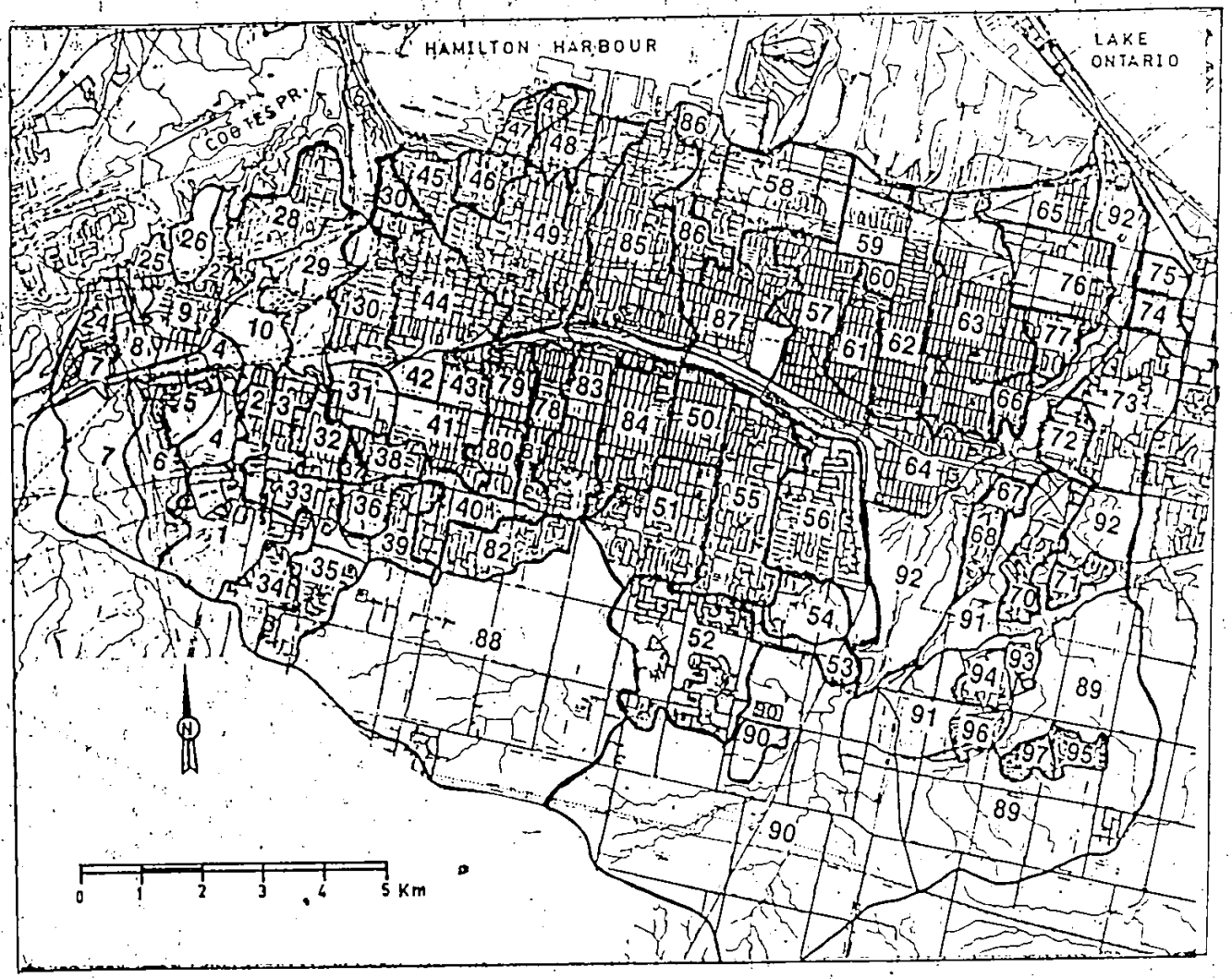

Figure 1.4 Discretized map of Hamilton catchments(source: James and Henry, 1982).

The Chedoke Creek Catchment consists of mainly single and multistorey residential areas, schools, parks, and forested areas. The Chedoke Creek runs almost through the middle of the catchment. This catchment has been further discretized for extensive study.

The Redhill Creek Catchment is the largest of the three. Only about 25% of the area is used for residential purposes, the remainder being undeveloped farm land.

PART 1

POLLUTANT BUILDUP

CHAPTER II

SOURCE AND BUILDUP OF POLLUTANTS.

2.1 Sources of pollutants:

In the early 1960's, it was found that in a few isolated cities urban runoff quality could be as "degraded" as domestic sewage. Since then, the problem has received more attention and the quality of the runoff has grown even more ominously degraded as new substances were found in it. New concerns about trace chemicals have surfaced.

There are many and diverse sources of pollutants, man-made and natural. In urban situations, industries, automobiles, house heating, combined sewer overflows, nutrients, insecticides, and pesticides contribute significant quantities of pollutants to surface waters and the atmosphere. Generally, pollutants derived from natural sources can be related to swampgas, salt sprays from the sea, dust picked up by winds, smoke from naturally lit fires, terpenes, resins and pollens from forests, fog, photochemical ozone, nitrogen oxide and other oxidants, gases, vapours, and particulates derived from volcanoes, geysers and fissures and climatic factors. Most of the natural pollutants depend on the geographical location of the city under consideration. Table 2.1 summarizes pollutants in urban runoff and their commonly attributed

Table 2.1 Major pollutants and sources

Pollutant	Sources
Inorganic suspended solids (sand, silt, and clay)	Soil erosion, farming, vehicle movements.
Inorganic dissolved solids (NH_3-N, NO_2-N, NO_3-N, PO_4-P)	Decomposition of organic solids in farms, lawns, street litters (leaves, branches and seeds).
Organic suspended and dissolved (decomposable substances) solids.	Various human activities (farming, wastefood products, vegetables etc.)
Heavy metals (lead, zinc, copper, iron, nickel, chromium, manganese).	Burning petrol, vehicles and industrial activities.
Toxic chemicals (insecticides, pesticides, herbicides etc.)	Farming etc.
Chemicals (hexachlorobenzene, hexachlorocyclohexane isomers, polychlorobiphenyles, DDT, dieldrin, chlordane, phalate-ester plasticizers)	Chemical industries.
Organisms (Fecal coliforms)	Live stock.

sources. Rain falling on an urban area gains pollutants from the air, dusty roofs, littered and dirty streets, sidewalks, traffic byproducts (gasoline and oil drippings, tire residuals, brake wear, vehicular exhaust), metallic corrosion, hazardous material spills and chemicals applied for fertilization, control of ice, rodents, insects and weeds.

2.2. Pollutant buildup on impervious areas:

Various human activities in urbanised areas increase the pollutant load accumulating on the surface and in the atmosphere. This accumulation occurs between storms and is known as "pollutant buildup". Various pollutant generating activities are more intense on impervious areas than on pervious areas. Impervious areas contribute higher BOD, COD, toxic metals, nutrients, oil and grease etc. However, solids eroded from unprotected and bare lands, and nutrients from pervious farm lands cannot be neglected. Pollutant contribution from pervious areas is discussed separately in section 6.2.

Most of the pollutant quantities correlate reasonably well with the mass of dust and dirt (DD) accumulated over dry periods. Therefore DD may be taken as a reference for estimating concentrations of various pollutants. A detailed analysis of the accumulation of DD on impervious areas is considered in this chapter.

Due to the inadequacy of the generally available urban stormwater quality data base, the deposition and removal processes are not completely or even adequately understood. Some urban non-point source pollution prediction models assume linear accumulation rates, but there is general consensus that the DD accumulation rate should be a decreasing function of time. A wide variety of accumulation relationships have appeared in the storm water literature as shown in Table 2.2 (Ammon, 1979). The accumulated DD loading rate has been related to the elapsed time since street sweeping, or time since one half inch rainfall, whichever comes last (Sartor and Boyd, 1972). The equations developed for different land uses with their correlation coefficients were summarized by Sartor and Boyd in Table 2.3; the observed data and fitted curves are shown in Figure 2.1. The poor correlations show that land use classifications and antecedent time period may not adequately depict the accumulation process. Geomorphologic and climatic variables may also be important independent variables.

McQuen and Sutherland (1975) used a pattern search technique to fit equations to Sartor and Boyd's approximate curves and their best fit equations are given in Table 2.4.

The San Jose study (Pitt, 1978) showed that, immediately after street cleaning, the street DD loading increases rapidly but levels off after several days.

TABLE 2.2 DUST AND DIRT ACCUMULATION RELATIONSHIPS (SOURCE: AMMON, 1979)

Relationship	Definition of L	Definition of t	General Category	Reference	Comment
$L=(1-\frac{at+1}{bt+ct+1})L_m$	BOD_5 or SS (kg/ha)	Number of 5min. antecedent dry intervals	Asymptotic	Geiger and Dorsch(1979)	
$L=L_m(1-\exp(-Kt))$	Dust and Dirt near curb(g/curb mi)	Accumulation period(d)	Asymptotic	Novotny and Goodrich-Mahoney(1978)	Milwaukee, Wisc. data
$L=830.7+32.9t$	BOD_5(lb/acre)	Antecedent dry period(d)	Linear	Nunno(1978)	Greenfield, Mass. data
$L=2.79t/(t+7.88)$	BOD_5(lb/acre)	Antecedent dry period(d)	Asymptotic	Nunno(1978)	Greenfield, Mass. data
$L=1849(1-\exp(-0.123t))$	BOD_5(lb/acre)	Antecedent dry Period(d)	Asymptotic	Nunno(1978)	Greenfield, Mass. data
$L=426\exp(0.0565t)$	Total solids (lb/curb mi)	Time since rainfall or street sweeping(d)	Increasing rate	Sartor and Boyd(1972)	Residential land use
$L=t/(0.00187+0.000601\ t)$	Total solids (lb/curb mi)	Time since rainfall or street sweeping(d)	Asymptotic	Sartor and Boyd(1972)	Industrial land use

TABLE 2.2 continued

Relationship	Definition of L	Definition of t	General Category	Reference	Comment
$L=694-519/t$	Total solids (lb/curb mi)	Time since rainfall or street sweeping (d)	Asymptotic	Sartor and Boyd (1972)	Commercial land use
$L=294t^{0.511}$	Total solids (lb/curb mi)	Time since rainfall or street sweeping (d)	Declining rate	Sartor and Boyd (1972)	All land use combined
$L=L_m(1-\exp(-Kt))$	Dust and dirt dry weight (lb/curb mi)	Accumulation period (d) or traffic count (axles)	Asymptotic	Shaheen (1975)	
$L=1388(1-\exp(-0.19t))$	Total solids (lb/curb mi)	Time since rainfall or street sweeping (d)	Asymptotic	Sutherland McCuen (1976)	Industrial land use
$L=500(1-\exp(-0.335t))$	Total solids (lb/curb mi)	Time since rainfall or street sweeping (d)	Asymptotic	Sutherland McCuen (1976)	Commercial land use
$L=1089/(1.0+1.3t)$	Total solids (lb/curb mi)	Time since rainfall or street sweeping	Asymptotic	Sutherland McCuen (1976)	Residential land use

t = time elapsed since rainfall or street sweeping, days

L_m = maximum accumulation DD, kg/ha.

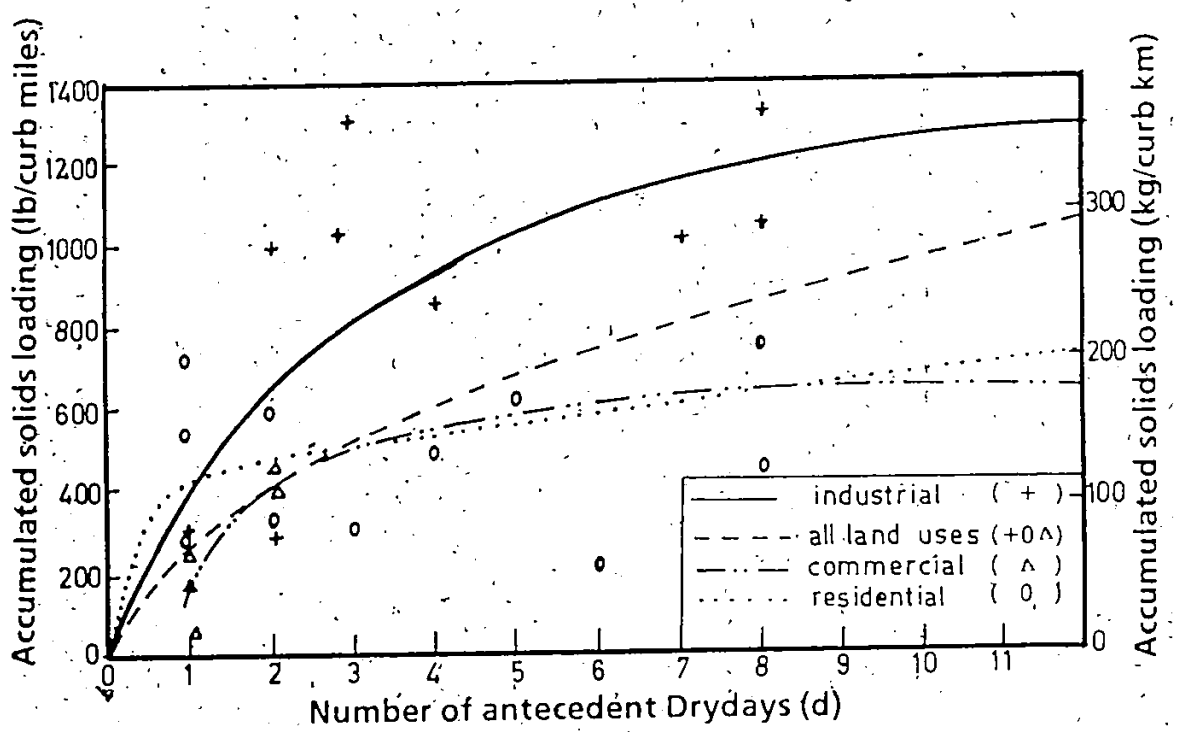

Figure 2.1 Observed and fitted curve for DD accumulation (source: Sartor and Boyd, 1972).

TABLE 2.3 ACCUMULATION RELATIONSHIPS FROM MULTI-CITY DATA (SOURCE: SARTOR AND BOYD, 1972)

Land use category	Equation[1]	Correlation coefficient	Number of observations
Residential	$L=426(e^{0.0565t})$	0.17	12
Industrial	$L=t/(0.00187 + 0.000601t)$	0.32	10
Commercial	$L=694-519/t$	0.88	5
All combined	$L=294(t^{0.511})$	0.31	27

[1]Extreme ten percent values disregarded
t = time elapsed since rainfall or street sweeping(d)
L = solids loading on streets(lb/curb mi)

TABLE 2.4 POLLUTANT BUILDUP EQUATIONS (McCuen and Sutherland, 1975)

Land use	R^2	Standard error (lbs/curb mile)	Equation
Industrial	0.83	194	$P_I = 1388(1-e^{-0.19t})$
Commercial	0.50	165	$P_C = 500(1-e^{-0.335t})$
Residential	0.24	268	$P_R = 1089t/(1+1.3t)$

Nunno (1978) found that the non-linear buildup of a pollutant (BOD) between storms has a limit, regardless of the length of the dry period. The best fits between the initial pollutant loads and the antecedent dry days were fitted to the exponential and Michaelis-Menton relationships. The relationships formulated are listed in Table 2.5, and the observed data and fitted curves are shown in Figure 2.2.

Shaheen (1975) examined samples collected from roadways over various deposition periods. These data revealed that the deposition rate of non-traffic related pollutants is linear with time while the accumulation levels off substantially on the pavements after several days due to the displacement of the material onto areas adjacent to the road ways. For traffic related loadings the net accumulation rate is given by:

$$\frac{dL}{dT} = K_d - K_1 L \qquad [2.1]$$

where: L = the pollutant loading, kg/km.

T = total traffic, axles

K_d = deposition rate per axle, kg/axle-km.

K_1 = loss rate per axle,

On integration, the equation [2.1] leads to

$$L = L_m(1 - e^{-K_1 T}) \qquad [2.2]$$

TABLE 2.5 SUMMARY STATISTICS FOR BOD_5 ACCUMULATION FUNCTION CURVE FITTING RESULTS, GREENFIELD, MASSACHUSETTS (NUNNO 1978)

Model	Fitted equation	Maximum pollutant accumulation P_o (lb BOD_5)	No. of days required for 90 percent of maximum pollutant buildup	Coefficient of determination (R^2) for Linearized form[1]	Standard error of estimate (SEE)
Linear	$P_0=32.9t+830.7$	infinite	-	0.422	406
Hyperbolic	$P_0=\frac{2179t}{t+7.88}$	2179	71	0.960	294
Exponential	$P_0=1849(1-e^{-0.123t})$	1849	19	0.867	293

[1]Non-linear equations were linearized to obtain constants by method of least squares fit.

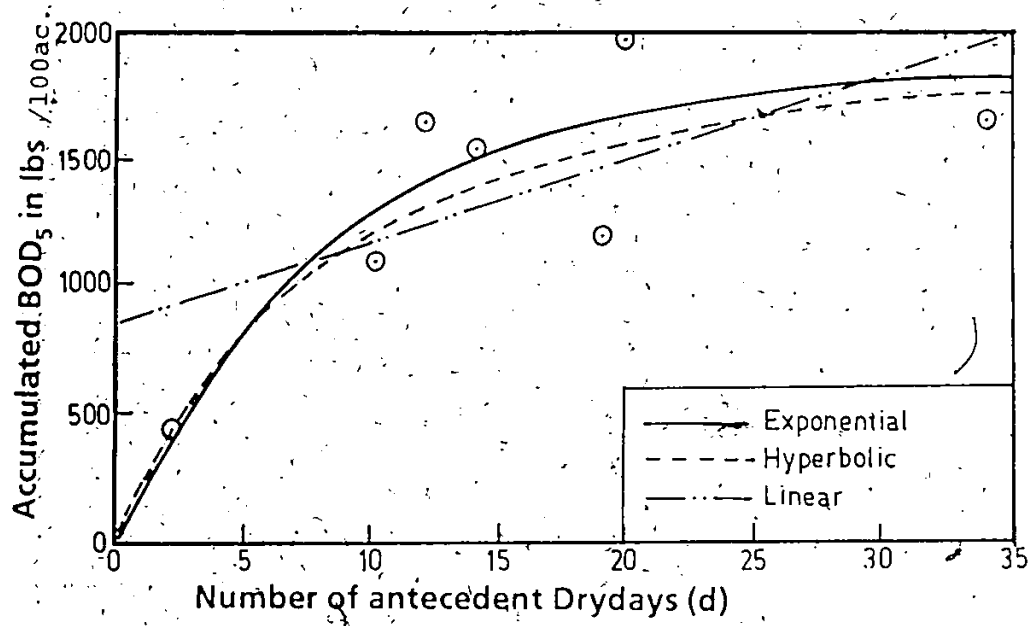

Figure 2.2 Observed and fitted curves for BOD_5 accumulation (Nunno, 1978)

where: $L_m = K_d / K_1$ = maximum pollutant loading, kg/km.

This equation can be transformed into an accumulation equation by assuming $t = T/N$, where, t is accumulation period in days and N is average daily traffic in axles/day. In this case:

$$L = L_m(1 - e^{-Kt}) \qquad [2.3]$$

where: $K = K_1 N$

For the high and slow-speed lanes of North Capitol Street, Washington, D.C., Shaheen estimates:

K_d = 0.00288 lb/axle-mile (0.0008kg/axle-km),

K_1 = 0.00001 to 0.00003 per axle and

N = 40,000 axle/d

this leads to $96 \leq L_m \leq 288$ lb/mile ($28 \leq L_m \leq 82$ kg/km)

$0.4 \leq K \leq 1.2\ d^{-1}$

Terstriep et al. (1978) sampled total solids accumulated on the streets of Urbana-Champaign, Illinois, sequentially during a 10 day period following a runoff event. The total solids increased during the dry period for all three sites as shown in Figure 2.3. The accumulation rate was quite high in commercial streets compared to the other two residential streets.

In a 57.6 acre residential catchment study in Burlington, Ontario, Canada, Marsalek (1976) found the

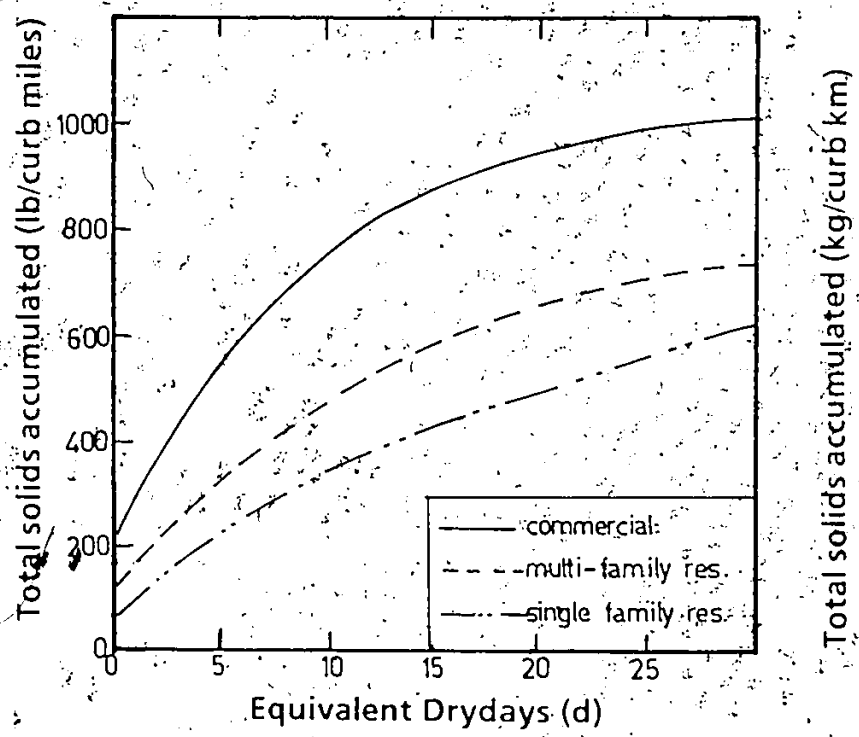

Figure 2.3 Dust and dirt accumulation for three different land uses (source: Terstriep et al. 1978).

antecedent dry period to be the most imporant variable in a linear regression model for suspended solids concentration.

Mance and Harman (1978) found that for most pollutants studied, between 60 and 90 percent of the variance in the data could be explained with total volume discharged by multiple regression analysis using antecedent dry period, and magnitude of the previous runoff as independent variables. However, the latter two variables only accounted for a maximum of six percent of the variance. In other words the characteristics of the latest event were primarily responsible for determining the mass of pollutants discharged. This would seem to indicate an ample DD supply; one that is not time constrained. Waller (1972) also observed at Halifax that the antecedent dry period had little statistical effect on the quality of runoff.

In an extensive statistical data analysis of a 47 acre residential catchment and a 39 acre transportation catchment in Broward county, Florida, Miller et al. (1978) found the antecedent dry period to be a significant independent variable. Peak discharge was the most important variable in the regression analysis.

Novotny and Goodrich-Mahoney (1978) derived an equation for DD accumulation near the curb:

$$D = \frac{A}{B}(1 - e^{-Bt}) \qquad [2.4]$$

where: $A = A_f \frac{W}{2} - 5.02 R_d - 6.29 P_a + 1.15 T_d$

$B = 0.0166 (e^{-0.0884H})(T_s + W_s)$

D = dust and dirt (suspended solids) accumulated near the curb (g/m).

W = street width (m).

A_f = atmospheric fallout (g/m^2-d).

R_d = residential density (dwellings/ha).

P_a = percent open area near the site,

t_d = time, d

T_d = traffic density (1000 axles/d).

H = curb height (cm).

T_s = traffic speed (km/h) and

W_s = wind speed (km/h).

Ammon C. D. (1979) reported the relationship developed by Meta System after reanalyzing the data from APWA (1969), Sartor and Boyd (1972) and Pitt (1978):

$$L = \frac{-a}{1 + bt} + \frac{ac}{b^2} \ln(1 + bt)e^{-ct} + c(1 + bt)e^{-ct} + c^2(1 + bt)^2 e^{-ct} + \frac{a}{b} + c + \frac{c^2}{4} \qquad [2.5]$$

where: L = accumulated loading, mg

t = accumulation period, d

and a, b, c = constants (typical values are not given).

It was found that climate and average daily traffic

have a larger effect on loadings than land use. Loadings were low, both at very high and very low traffic counts, and higher at intermediate levels. This suggests that both deposition from traffic-related activities and scour are important factors.

A simplified equation for calculating the buildup rate on street pavements was developed by Gupta (1978):

$$T_s = 0.002N^{0.89} \qquad [2.6]$$

where: T_s = total solids(kg/km-d)

N = average daily traffic (vehicles/d).

After reviewing the existing theories on DD buildup, it is evident that the buildup process is usually described by an empirical relationship. Except for the work of Novotony and Goodrich (1978), all other equations do not consider meteorological parameters. But DD accumulation is the constant interaction of addition and removal processes due to vacious activities in the catchment along with the influence of meteorological parameters. The daily mass balance of pollutant buildup on impervious areas over a dry day period represents the buildup process better than empirical relationships. Hence, a new approach has been adopted in this study for obtaining DD accumulation: discretizing and modelling all the accumulation and washoff processes and integrating them with the meteorological parameters of the catchment.

Pollutant concentration in storm water is governed by three types of process: buildup, washoff and transport. Pollutants scavenged during rainfall, and materials previously deposited in storm sewers and catchbasins, also add to the instantaneous concentration. The mass balance for pollutants in urban storm runoff for a single storm event and for a single catchment is:

$$P_r = P_i + P_s + P_p + P_d \qquad [2.7]$$

where: P_r = total mass flux of pollutants in the subcatchment pollutograph mg/s

P_i = total mass flux of accumulated pollutants washed off impervious areas, mg/s.

P_s = total mass flux of pollutants scavenged by rain during its motion through the atmosphere, mg/s.

P_p = total mass flux of pollutants washed off pervious areas, mg/s.

P_d = total mass flux of previously deposited pollutants scoured from storm sewers and catch basins, mg/s.

The accumulation process on impervious surfaces areas can be expressed as:

$$P_a = (\text{Atmospheric dustfall} + \text{Surface input}) - \text{Removals} \qquad [2.8]$$

or:

$$P_a = L_a + L_v + L_s + L_p + L_e - R_v - R_b - R_i - R_w \qquad [2.9]$$

where: P_a = daily mass flux of pollutant accumulated mg/d

L_a = daily mass flux of atmospheric dustfall, mg/d

L_v = daily mass flux of pollutants from vehicles, mg/d

L_s = daily mass flux of pollutants from special activities such as construction, demolition of structures, mg/d

L_p = daily mass flux of pollutants from population related activities such as lawn cutting, insecticides and pesticides, spray and fertilizer on lawns, mg/d

L_e = daily mass flux of pollutants from vegetation mg/d

R_v = daily mass flux of pollutants removed by vehicle generated eddies, mg/d

R_b = daily mass flux of pollutants removed by biological decomposition, mg/d

R_i = daily intentional removal of pollutants, e.g. street cleaning, mg/d

R_w = daily removal of pollutants by natural wind, mg/d

Each of the above processes is now discussed in detail.

2.3. ATMOSPHERIC INPUT TO POLLUTANT BUILDUP

2.3.1. Introduction:

Particulates from man-made sources are formed in the combustion processes, and by catalytic and photochemical reactions involving oxides of sulphur, unburned or partially burned hydrocarbons and nitrogen oxides. The proportion of water insoluble matter in dust deposits generally grows with increase of industrial activity. During each season of the year, the total deposition varies

in both quantity and composition. One of the peak deposition rates occurs in spring when the wind raises loose dust prior to the sprouting of vegetation. In summer, the amount of various natural particulates, such as pollen grains and seeds, is at a maximum. In autumn, when vegetation withers, storms raise mineral dust and organic material into the atmosphere. In winter, snow prevents recirculation of the particulates deposited on the ground, but the emission of particulates from heating, energy production and other activities are at a maximum.

The mass of volatiles deposited is approximately equal to the amount of organic matter in the deposited dust. A portion of volatile deposition originates from natural sources, such as soil, vegetation and animal. In summer this fraction contains pollen grains, seeds and other particulates originating from plants. In winter the volatile deposition consists mainly of soot, tar compounds and other anthropogenic compounds originating from heating and traffic.

The amount of organic carbon in dust fallout reflects the quantity of organic matter. The ratio of total organic matter to carbon is highest in complex compounds (e.g. proteins and fats), as they contain a large quantity of oxygen, nitrogen and other ingredients and smallest in pure hydrocarbons. Pollen grains and seeds contain a large portion of proteins and fats.

Phosphorus is emitted into the atmosphere from mineral dust, as phosphates. Organogenic substances also contribute phosphorus into air as organically fixed calcium phosphate. In summer, organic particulates orginating from vegetation increases the amount of phosphorus compounds in the air, far more than do the anthropogenic sources such as industrial processes and the spreading of fertilizers.

The important nitrogen compounds in the atmosphere are: nitrogen oxides, nitrates and ammonium salts, nitric acid and ammonia. Of all the oxides of nitrogen, nitric oxide (NO) and nitrogen-dioxide (NO_2) are air pollutants. The principal man-made source of nitric oxide is the burning of fuels at high temperatures (heat and power stations, refuse incineration plants, motor vehicles and some chemical plants). On a global scale, roughly 50% of the anthropogenic nitrogen oxides come from coal combustion and 40% from petroleum processing and combustion (Seinfeld 1975).

Very little ammonia occurs in the atmosphere as it is oxidised to nitrate. Ammonia is produced by biological decay on the earth's surface and chemical industry emissions. Nitrates and ammonium salts are mainly formed from the conversion of nitric oxide, nitrogen-dioxide and ammonia. Ultimately most of these oxides are converted into nitrate particulates, which in turn are removed from the

atmosphere by rainout, washout and dry deposition. Most of the ammonia is converted to ammonium compounds and roughly one fourth is oxidized to nitrates.

During the last decade a number of studies were carried out on the quantity and quality of precipitation and runoff. The major pollutants investigated were suspended solids, BOD, COD, TOC, nitrate and phosphate. The average concentrations of COD and TOC in rain water were found to be 20.7-322.0 mg/l and 2.8-18.0 mg/l respectively (Randall et al., 1978; Malmquist, 1978). Nitrates and phosphates in rain water exceeded the concentration recommended for controlling eutrophication (Novotny 1981, Randall et al. 1978, Rutherford 1967, Frizzola and Joseph 1975, Goettle 1978, Jeffries 1975, Chan and Kuntz 1981). The concentration of pollutants in the atmosphere and rain water is site specific in a highly industrialized city. Similar to the runoff first flush effect, high pollutant concentrations were observed during the early stages of rain (Randall et al. 1978).

2.3.2. Removal of pollutants from the atmosphere

Pollutants in the atmosphere are removed by natural processes which are referred to as either precipitation scavenging (wet process) or dry deposition (dry process). Washout is the removal of pollutants from the atmosphere by precipitation. Dry deposition is the removal of pollutants by gravitational settling, Brownian and eddy diffusion in

the absence of precipitation. A distinction is also made between below cloud scavenging (washout) and in-cloud scavenging (rainout) depending on the elevation of the pollutant with respect to the cloud base. Consider the efficiency with which pollutants are removed from an air stream by obstacles such as rain, snow, grass, leaves and water surfaces. The flux of free stream pollutant is given by the product of concentration X_a and velocity v_a. For a particle of projected area A_c heading towards a collision with an obstacle of projected area A_x, then, collision efficiency E, and collection efficiency F are calculated as:

$$E = A_c / A_x \qquad [2.10]$$

$$F = RE \qquad [2.11]$$

where: E = collision efficiency

F = collection efficiency

A_c = area leading to collision, cm^2

A_x = projected area of obstacle, cm^2

R = retention efficiency (approximately equal to unity)

After the collection efficiency has been determined, it is summed over all collecting elements to obtain an overall removal rate.

a) Dry deposition:

The removal of particulates or gases at the air solid surface interface is described in meteorological

transport models by the term "dry deposition" or "dry deposition velocity". The dry deposition flux to the combined vegetative canopy and ground surface is the product of dry deposition velocity and airborne concentration above the vegetative canopy, say typically one meter above the ground surface. For monodispersed aerosol, the deposition velocity is:

$$V_d = -F/X = K_{1m} \qquad [2.12]$$

where: V_d = deposition velocity, m/s.

F = flux of pollutant per unit area, mg/s-m^2

X = air-borne concentration, mg/m^3

The deposition velocity is a function of particle diameter. The subscript 1m indicates a pollutant concentration at a height of one meter. The relationship between V_d and K_{1m} for a poly-dispersed aerosol of particle size 'i' is:

$$V_d = \frac{\Sigma(K_{1m})_i X_i}{\Sigma X_i} \qquad [2.13]$$

The value of V_d is highly dependent on the characteristic size distribution.

The gravitational settling velocity and the Brownian diffusion are two principal parameters used for predicting the dry deposition velocity. The Brownian diffusion coefficient increases as the particle diameter decreases

(<0.1 μm) and approaches that of a gas coefficient. When the particle is larger than 1 μm diameter (1 μm = 10^{-6} m) eddy diffusivity becomes important because of gravitational settling and particle inertia. Within one millimeter of the deposition surface Brownian diffusion is more important than particle inertia, eddy diffusion, and gravitational settling.

Because of the approximate nature of the theory, analysis difficulties, and the existence of atmospheric layers where different transfer processes dominate, it has become common to construct layer or resistance models of dry deposition. These layers might include: the loft layer A, above the atmospheric boundary layer ($Z \geq 1$ km); the boundary layer B (1 km$\geq Z \geq$100 m); the constant flux layer C (100 m$>Z>\delta$); and the deposition or viscous sublayer D ($Z<\delta$), where δ is the thickness of the deposition layer. The constant flux layer and viscous sublayer are shown in Figure 2.4. A general equation for the magnitude of the vertical component of the average dry flux considering all the layers is:

Total dry flux	=	Brownian diffusion flux	+	particle settling velocity flux	+	slip velocity flux	-	air and slip velocity fluctuation flux

$$\overline{L} = \overline{V_d \chi} = D \frac{\partial \overline{\chi}}{\partial z} + V_g \overline{\chi} - \overline{W_s} \overline{\chi} - \overline{W_a \chi} - \overline{W_s \chi} \qquad [2.14]$$

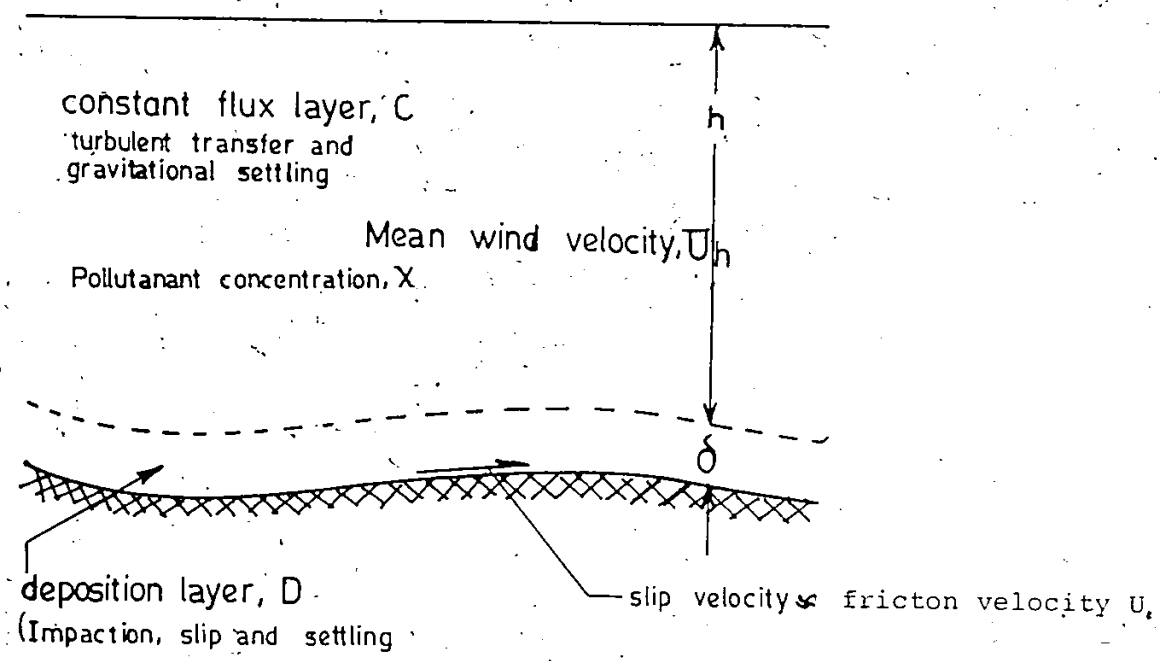

Figure 2.4 Schematic of constant and deposition layers.
(source: Eisenreich J, 1981)

where: $\overline{L}$ = average vertical component of dry flux, mg/m^2-s

$\overline{V_d}$ = the time average, deposition velocity, m/s

V_g = gravitational settling speed m/s

W_a, W_s = the vertical components (positive, up) of the air and slip velocities, m/s

W_a', W_s' = the fluctuation in air and slip velocities, m/s

D = Brownian or molecular diffusivity, cm^2/s

$\overline{X}$ = pollutant concentration in air, mg/m^3

X' = pollutant concentration fluctuations in air, mg/m^3

z = vertical height, m

Note: Time averages are denoted by bar (e. g., $\overline{X}$) and fluctuations about the averages by primes (e. g., X').

The turbulent flux terms in equation [2.14] can be approximated in terms of mean concentration gradient by the introduction of the eddy diffusivity:

$$-\overline{W_a'X'} = K_z \frac{\partial \overline{X}}{\partial z} \qquad [2.15]$$

$$-\overline{W_s'X'} = \epsilon_p \frac{\partial \overline{X}}{\partial z} \qquad [2.16]$$

where K_z = the Z component of turbulent diffusivity, m^2/s

ϵ_p = particle eddy diffusivity, m^2/s

Far from the air/ground surface interface, turbulence usually dominates in the vertical transfer of air pollutants; i.e. the other terms in equation [2.14] are

usually negligible compared to $\overline{W_a' X'}$. A first estimate for $\overline{W_a' X'}$ is $U_* \bar{X}$; consequently, $\bar{V}_d \approx U_*$, where U_* is the friction velocity, defined by $\sqrt{\frac{\tau}{\rho_a}}$. Where ρ_a is the air density and τ is the viscous stress. A better estimate for the contribution to $\overline{V_d}$ from turbulence far from the interface may be obtained from an analogy with the deposition velocity for momentum transfer

$$\overline{V_{dm}(z)} = \frac{\tau}{\rho_a \overline{U(z)}} = \frac{\rho_a U_*^2}{\rho_a \overline{U}} = \frac{U_*^2}{\overline{U}^2}\overline{U} = C_D \overline{U(z)} \qquad [2.17]$$

where $C_D = \frac{U_*^2}{\overline{U}^2}$ is the drag coefficient and $\overline{U}$ = mean value of the horizontal wind velocity (m/s). For solid surfaces, the deposition velocity for a pollutant (with $V_g \leq 0.01 m\ s^{-1}$) is less than $\overline{V_{dm}}$ because of the no-velocity-slip condition at solid surfaces and momentum transfer by pressure forces (from drag).

Conditions near an interface are complicated. For a solid interface, it is clear that turbulent transfer must vanish at the surface. The vertical turbulent flux of momentum $\rho_a \overline{U_a W_a}$, at a solid surface is zero because both the horizontal component of the air's velocity, U_a, and the vertical component W_a, and their fluctuations U_a' and W_a' in horizontal and vertical direction must vanish. Since the vertical turbulent transfer of pollutants is given by $\overline{W_a X'}$, we must focus on W_a' at an interface, not U_a'. At a solid

interface $W_a' = 0$, therefore the second last term in equation [2.14] $(\overline{W_a' \chi'})$ is zero at a solid interface. Because W_a' vanishes at the interface, and therefore transfer of momentum by turbulence is suppressed at the interface, there must be a region near the interface where viscosity dominates momentum transfer, even though the no-slip condition is violated (i.e. $U_a' \neq 0$). The thickness δ of this viscous sublayer may be less than for a solid surface (with $U_a = 0$ at the interface) but a first estimate for δ can be obtained in the usual manner:

$$\rho_a \nu \frac{U_*}{\delta} \approx \mu \frac{\partial U}{\partial z} = \tau = \rho_a U_*^2 \qquad [2.18]$$

where $\nu = \frac{\mu}{\rho_a} \approx 0.15 cm^2 s^{-1}$ at STP is the kinematic viscosity of air. Thus from equation [2.18]

$$\delta \approx \frac{\nu}{U_*} \qquad [2.19]$$

For $Z \leq \delta$, it is assumed herein that turbulent transfer of pollution is negligible. Then equation [2.14] becomes

$$\overline{L} = \overline{V}_d \overline{\chi} = D \frac{\partial \overline{\chi}}{\partial z} + (\overline{V}_g - \overline{W}_s)\overline{\chi} - \overline{W_s \chi'} \qquad [2.20]$$

Even for the simple case when only Brownian diffusion is important and equation [2.20] reduces to $\overline{L} = D \frac{\partial \overline{\chi}}{\partial Z}$, there are some uncertainties, whether V_d varies with the diffusivity as D^1, $D^{2/3}$, $D^{0.6}$ or $D^{1/2}$ (Eisenreich, 1981). The

term $w_s X$ causes additional difficulties in estimating slip velocity turbulent flux . An estimate of the contribution to V_d from particle inertia was calculated by Slinn (1976) assuming particles are convected to the surface at the leading edge of Joukowski's caterpillar-tread model of turbulent eddies. If sufficiently massive, the particles are impacted on the surface from the viscous jet at the leading edge of the tread. The result suggested that for V_d based on a 1 cm reference height:

$$\overline{V}_d = V_g - \alpha m' + \frac{U_*^2}{kU}\left[S_c^{-0.6} + 10^{-3/S_t} \right] \qquad [2.21]$$

where: $\alpha m'$ = a mean slip velocity caused by diffusiophoresis in which $\alpha = (10^3 \text{ cm s}^{-1})/(1 \text{ g cm}^{-2} \text{ s}^{-1})$ and m' is the rate of water evaporation from the surface.

k = 0.4 = Von Karman's constant

$S_c = \frac{\nu}{D}$ = the Schmidt number

$S_t = \frac{\tau U_*}{\delta_1} = \frac{\tau U_*^2}{\nu}$ the Stokes or impaction parameter based on the height of the viscous sublayer, δ_1, and on the particle relaxation time $\tau = V_g/g$, in which g is the acceleration of gravity.

Particle deposition in a canopy is different from smooth solid surfaces. Assuming pollutant particle fluxes as shown in Figure 2.5, a general continuity equation for a steady state condition could be written as (Slinn 1977):

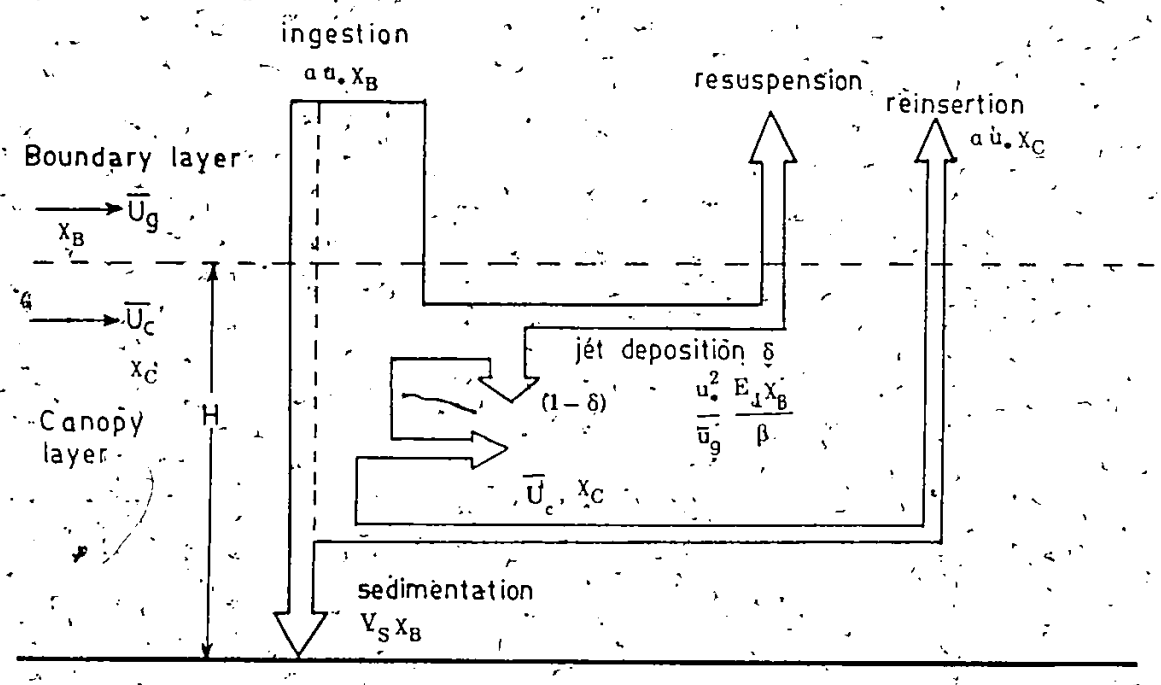

Figure 2.5 Pollutant flux in a canopy (source: Slinn, 1977).

$$\frac{\partial \chi_c}{\partial x} + \left[\frac{aU_* + CH}{\overline{U}_c H}\right]\chi_c = \left[aU_* - \frac{U_*^2 E_j}{\overline{U}_g \beta}\right]\chi_B \qquad [2.22]$$

where C, is the fraction of the a-particles filtered out per second by the canopy. If χ_B is a constant then equation [2.22] predicts an x-independent solution in a distance which is typically about 10 canopy heights. Then for x-independent conditions, equation [2.22] can easily be solved to give χ_C in terms of χ_B. From this result the deposition velocity, the net flux to the canopy divided by χ_B, becomes:

$$V_d = V_s - \frac{\delta U_*^2 E_j}{U_g \beta} + \frac{aU_*}{aU_* + CH}\left[CH + \frac{U_*^2 E_j}{\overline{U}_g \beta}\right] \qquad [2.23]$$

where: V_d = particle deposition velocity, m/s.

V_s = particle settling velocity, m/s.

δ = fraction of particles resuspended from the canopy.

U_* = friction velocity, m/s.

E_j = jet collection efficiency.

$\overline{U}_g$ = mean wind above canopy, m/s.

a, β = empirical constants.

C = canopy removal rate (fraction of a-particles filtered out per second), s^{-1}.

$$C = \frac{\overline{U}_c B}{\lambda \rho} \exists (a, \lambda) \qquad [2.24]$$

$\overline{U}_c$ = mean wind speed in canopy, m/s.

B = biomass per unit volume, mass/m^3

λ = typical length scale of individual fibres, m.

$\bar{\rho}$ = average mass density of the foliage, mass/m^3

β = particle/canopy collection efficiency.

H = canopy depth, m

χ_C = pollutant concentration in the canopy layer per m^3

χ_B = pollutant concentration in the boundary layer per m^3

The theory developed by Slinn (1977) is consistent with the experimental results of Hill and Chamberlain (1975) Sehmel (1975) ; Heinemann et al. (1975); and Chamberlain (1967), but sufficient data are not yet available to test equation [2.22] and to evaluate the parameters α, β, γ, and δ.

Deposition velocities for various particulates and gases on different surfaces have been well documented in the literature (Sehmel, 1980). Though deposition velocities could be used along with the observed pollutant concentration to obtain dry deposition flux on the ground surface, the complexity and uncertainity involved in the theory, geography of the place and composition of dry deposit make it impossible. In view of this problem and also considering the main objective of the research, a statistical approach was adopted to compute atmospheric dustfall over Hamilton catchment. The statistical method used in the present work is discussed in section 2.3.4.

2.3.3. Review of air pollution and rainwater quality studies in Hamilton:

As a result of public concern, a municipal survey was begun in the early 1950's, to study the effects of air pollution on metropolitan Hamilton and surrounding communities. The first report was published in 1956 by the Department of Chemistry, Ontario Research Foundation. The study focused on dust, aerosols and sulphur dioxide (SO_2). Transport and dispersion of pollutants depend on prevailing meteorological conditions in the city. Stewart and Matheson (1967) analysed data from all the meteorological stations in Hamilton and found that data from the Royal Botanical Gardens (RBG) station was representative of conditions in Hamilton.

A number of studies on pollutant quantity were conducted in relation to wind direction with diurnal, weekly, seasonal and annual changes (Weisman et al. 1969). Rouse and McCutcheon (1970) showed that Hamilton is among the most polluted cities in Canada in terms of suspended particulate matter. Rouse identified pollution islands in the city and also significant shifts with various wind directions, during the study period. Pollutional levels observed under east winds with accompanying atmospheric stability were twice as great as in all other directions. The composite wind picture before the maximum API in Hamilton showed a preference for moderately consistent east and northeast winds at speeds

less than 6 miles/hour (Heidorn, 1978).

An effective control of air pollutants at the point sources in Hamilton minimized pollutant quantities except dust (Ministry of Environment Report, 1977). Dust concentration was found to be almost constant from 1970. Fugitive dust sources such as uncontrolled stock piles, excavation and construction and recycling of road dust were shown to be important in explaining the persistent levels of dust concentration (Barton, et al. 1981). About 15 square kilometers were encompassed by the 9.0 grams of dust/m^2 -30 days isopleth (yearly average) which was twice the MOE yearly objective. Another 57 square kilometers (46% of the city area) is covered by the 4.5 grams dust/m^2 -30 days isopleth. The remaining area receives less than 4.5 gram/m^2 -30 days. An yearly average of 77 $\mu g/m^3$ of suspended particulates was observed in the city (MOE report 1980). An average concentration of 3.5 $\mu g/m^3$ of nitrate and 3 - 24.0 $\mu g/m^3$ of organic carbon (4 - 14% of TSP) was observed in the suspended particulates (Barton, et al. 1981).

Gross Ontario rain and snow chemistry was determined by collecting samples from a precipitation sampling network established in Hamilton and Northern Ontario. Relative to surface waters, precipitation normally has a low conductivity (mean value = 34 μmho/cm), low pH (4.3) with elevated heavy metal (10 - 100 $\mu g/l$) and nutrient concentrations (50 - 100 $\mu g/l$ of phosphate; 400 - 2000 $\mu g/l$

of nitrate, (Jefferies, D. 1975, Kramer J. 1982)).

A study on atmospheric deposition on Lake Ontario (1969 - 1978 data) showed that yearly average concentrations of phosphorous, nitrite and nitrate were higher at the Burlington station (near the Canada Centre for Inland Waters) than the Ancaster station (Chan and Kuntz, 1981). A prevailing westerly wind might have favoured advection of nutrients from Hamilton towards the Burlington station. The close proximity of the highway also might have influenced the Burlington station. A study of atmospheric loadings of the lower Great Lakes and the Great Lakes drainage basin (1973 - 1976) showed an average value of 10 ng/cm^2-d of total phosphorus and 0.4 $\mu g/cm^2-d$ of total nitrogen (Acres report, 1977). The increase in total particulates for the year 2000 was estimated to be 0.8 $\mu g/cm^2-d$ in that report.

2.3.4. Prediction of dust fall on Hamilton subcatchments:

In an industrial city, the contribution of solids and nutrients to surface loadings from atmospheric dustfall is quite significant. Deterministic estimation of dustfall rates due to various human activities and processes is difficult or impossible in an urban situation. Therefore a statistical approach is used in this study to quantify atmospheric input. Correlations to achieve the required accuracy in predicting atmospheric dustfall on individual subcatchments were carried out. These results are used as

input in estimating total dust and dirt available on the surface before the commencement of storm events and thus to predict the quality of urban stormwater runoff.

(a) Availability of data:

Data have been collected over the past decade by the Ontario Ministry of the Environment (MOE) from an atmospheric monitoring network in Hamilton. About eighteen dustfall collection stations were used as shown in Figure 2.6. The MOE also collects data on suspended solids (high volume air sampling) and gases (sulphur dioxide, carbon monoxide, nitrogen dioxide, nitric oxide, nitrogen oxides, reactive hydrocarbons, ozone and fluoridation rates) only at a few selected stations.

Dustfall data are being collected for integration periods of one month in plastic open jars placed 1 to 2 m above the ground surface. Dustfall collection stations were selected by careful analysis of the nearby surroundings to avoid any local influences on the data. Since the collection jar is open for a period of one month, the data were measured in g/m^2-30 d. This includes both dry and wet deposition. Atmospheric pollutants are scavenged by both snow and rain and accumulate in the dust collection jar. During the interstorm period, dry deposition also accumulates in the same jar. Thus the data obtained from the collection jar reflect bulk deposition. Accidental

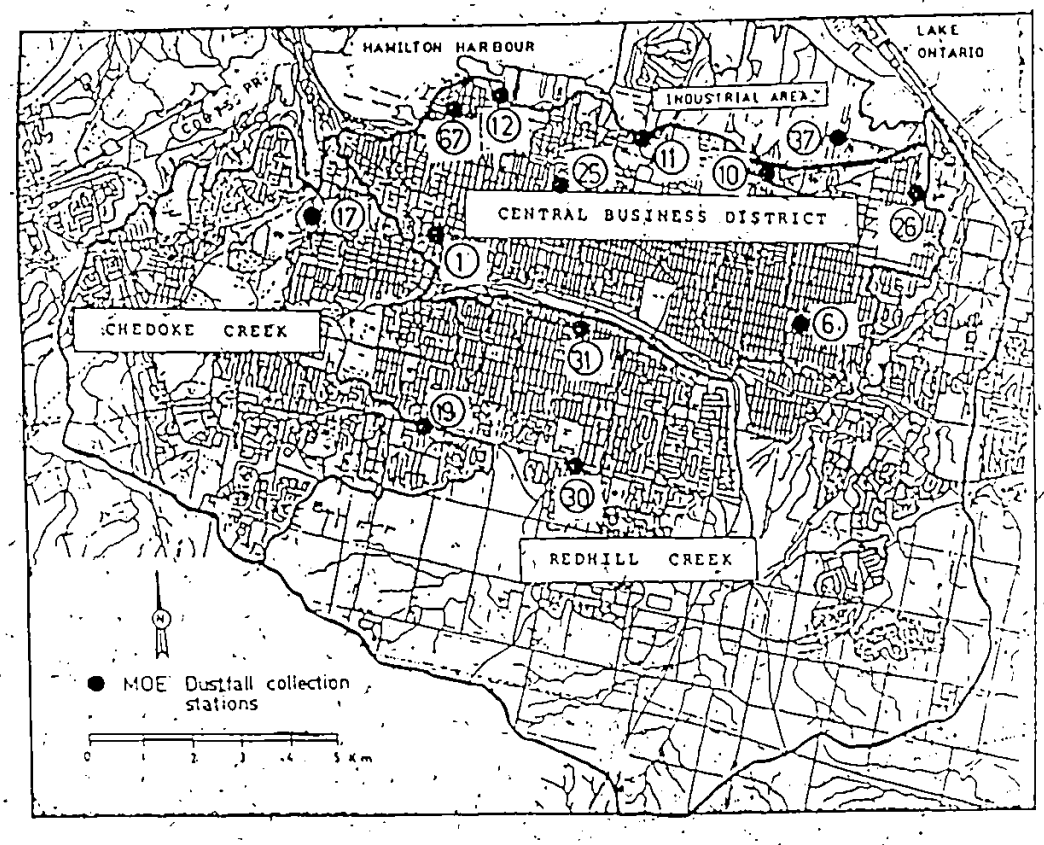

Figure 2.6 Location of dustfall collection stations in Hamilton.

contamination (leaves, bird droppings, etc) is removed before calculating the total dust deposition. The accumulated dust was analysed for characteristics such as grain size distribution. Since dustfall data at ground level are not available and the dust collection height is within the constant flux layer, it was decided to assume that the available dust collection jar data are representative of dustfall on the ground surface.

After analysing the meteorological data from the Atmospheric Environment Service (AES) stations near Hamilton, Stewart (1968) found that the data from Royal Botanical Gardens (RBG) station were representative of conditions in Hamilton. Hence the RBG meteorological data were used in this work. Wind velocity and frequency, and total precipitation were used to develop the model, Monthly average wind velocities and frequencies were abstracted for all the eight primary directions of the compass along with dustfall data. The velocity and frequency of wind and total precipitation were measured in km/h, fraction of time and mm water equivalent (snow + rain) respectively. Even though snow scavenges more pollutants than rain, all precipitation was assumed to be rain because the present work is limited to urban storm runoff water quality modelling between the months of April and October.

(b) Model development:

The available dustfall record was divided into

two, the first part used for model derivation and the second part to validate the model. The complete record covers 1970 - 1981; 1978 - 1980 data were used for model derivation and 1981 for validation. Data form 1970-1977 were not used because of the decreasing DD sources in this period.

i) Model 1: (Average Model)

In model 1 we postulate that the mean for each month will repeat every year:

$$Y_{im} = \frac{\Sigma y_{im}}{n} \qquad [2.25]$$

where: Y_{im} = predicted average dustfall for month m and station i, g/m^2 -30 d

y_{im} = observed dustfall for month m and station i, g/m^2 - 30 d

n = number of records for the month m and station i

Model 1 is not sensitive to any of the physical or meteorological processes and produces estimates that differ widely from observed values. The average dustfall values of Model 1 and observed dustfall data of 1981 are tabulated in columns 3 and 8 of Table 2.6.

ii) Model 2: (Linear Regression Model)

Here it is assumed that accurate estimates of the dispersion of dust and pollutants in the atmosphere require a knowledge of the frequency distribution of wind direction and wind speed. This type of information varies

Table 2.6 Summary of the results obtained by all the models.

Stan.	Month	Predicted results in grams/sq.m/30days					Observed results
		MODEL1	MODEL2		MODEL3		
			all dire.	NE	all dire.	NE	
29001	Jan	5.40	3.34	3.34	6.30	6.60	3.60
	Feb	6.03	2.29	2.29	8.40	6.80	6.80
	Mar	10.40	2.28	2.28	7.80	7.00	7.10
	Apr	10.13	5.56	5.56	9.20	7.30	6.90
	May	9.70	9.04	9.04	7.70	6.90	8.40
	Jul	5.43	5.07	5.07	5.60	7.40	5.60
	Aug	5.67	2.22	2.22	6.30	7.40	9.20
	Sep	5.93	2.55	2.55	7.80	7.40	6.90
Stand.deviation			3.77	3.77	1.78	1.50	
29006	Jan	5.60	3.39	3.39	6.10	6.60	4.50
	Feb	5.86	2.31	2.31	7.10	6.50	8.40
	Mar	10.16	2.31	2.31	7.20	7.40	8.10
	Apr	12.13	5.65	5.65	7.30	7.60	5.60
	May	7.73	9.16	9.16	7.30	6.80	5.70
	Jul	6.17	5.15	5.15	6.10	7.50	13.00
	Aug	5.06	2.25	2.25	7.10	6.80	6.30
	Sep	5.93	2.59	2.59	6.40	7.30	6.50
Stand.deviation			4.71	4.71	2.73	2.38	
29008	Jan	19.70	16.30	7.19	17.20	12.40	20.70
	Feb	13.63	25.24	4.91	15.40	12.40	20.60
	Mar	13.50	15.07	4.91	12.20	14.00	17.20
	Apr	9.90	22.20	12.02	11.80	14.40	10.50
	May	9.93	3.34	19.46	16.20	12.90	13.50
	Jul	11.87	0.19	10.95	16.90	14.30	11.30
	Aug	10.45	0.33	4.79	16.40	13.40	8.30
	Sep	11.97	0.46	5.51	16.70	14.10	9.80
Stand.deviaton			8.37	9.00	5.20	5.21	
29009	Jan	5.36	7.95	2.81	5.30	5.60	3.90
	Feb	5.86	12.30	1.92	5.80	5.30	5.80
	Mar	7.70	7.35	1.92	5.80	6.30	7.00
	Apr	7.90	10.81	4.69	5.90	6.30	5.30
	May	8.00	1.63	7.60	5.90	5.60	7.00
	Jul	4.23	0.99	4.27	5.40	6.10	5.80
	Aug	5.16	0.16	1.87	5.90	5.30	6.90
	Sep	5.90	0.23	2.15	5.60	5.90	8.80
Stand. deviation			5.80	3.79	1.44	1.48	
29011	Jan	11.20	7.38	7.38	14.10	14.70	7.20
	Feb	15.70	5.04	5.04	18.30	14.70	13.70
	Mar	22.06	5.02	5.02	17.20	16.00	16.30
	Apr	23.20	12.29	12.29	19.80	16.30	14.60
	May	20.10	19.95	19.95	16.80	15.10	23.60
	Jul	10.47	11.20	11.20	12.50	16.20	16.40
	Aug	12.70	4.91	4.91	13.80	15.50	12.10
	Sep	15.43	5.64	5.64	16.80	16.10	11.20
Stand. deviation			6.43	6.43	4.90	4.59	

Table 2.6 continuation

1	2	3	4	5	6	7	8
29012	Jan	8.87	4.60	4.60	6.50	6.70	5.20
	Feb	7.86	3.14	3.14	9.80	9.50	8.60
	Mar	13.65	3.14	3.14	7.50	7.60	9.30
	Apr	12.16	7.68	7.68	10.10	10.20	9.40
	May	11.90	12.44	12.44	9.10	8.80	11.00
	Jul	7.20	7.00	7.00	10.80	11.40	11.10
	Aug	6.97	3.06	3.06	15.20	14.90	8.50
	Sep	13.57	3.52	3.52	12.70	13.00	8.70
Stand. deviation			4.28	4.28	2.98	2.98	
29017	Jan	9.00	13.39	5.40	10.10	10.10	4.50
	Feb	6.96	20.67	3.70	11.40	11.40	11.30
	Mar	14.50	12.37	3.65	8.80	8.80	21.10
	Apr	10.66	18.14	8.91	9.40	9.40	10.00
	May	11.43	2.75	14.56	10.50	10.50	10.50
	Jul	8.57	0.16	8.12	10.10	10.10	15.00
	Aug	8.57	0.28	3.58	12.60	12.60	35.10
	Sep	8.87	0.38	4.10	11.00	11.00	6.10
Stand. deviation			15.15	13.35	9.60	9.60	
29019	Jan	2.40	5.56	2.04	3.60	3.60	2.70
	Feb	2.40	8.56	1.40	4.80	4.80	3.50
	Mar	6.13	5.13	1.38	2.80	2.80	3.60
	Apr	4.37	7.50	3.36	3.60	3.60	4.20
	May	4.60	1.14	5.51	4.10	4.10	4.30
	Jul	4.40	0.72	3.07	4.20	4.20	3.60
	Aug	3.03	0.12	1.35	6.40	6.40	6.60
	Sep	5.53	0.16	1.55	5.00	5.00	5.00
Stand. deviation			4.11	2.54	0.69	0.69	
29025	Jan	7.00	4.60	4.60	7.90	8.50	4.40
	Feb	7.10	3.14	3.14	9.60	10.10	10.10
	Mar	14.10	3.12	3.12	9.00	8.40	6.60
	Apr	12.90	7.63	7.63	8.70	9.70	8.50
	May	14.13	12.42	12.42	8.60	9.50	13.30
	Jul	6.80	6.95	6.95	10.40	10.40	8.30
	Aug	8.45	3.05	3.05	12.70	12.70	14.00
	Sep	10.47	3.50	3.50	10.80	11.40	8.80
Stand. deviation			5.15	5.15	2.52	2.47	
29026	Jan	5.00	5.53	2.74	5.40	5.60	4.20
	Feb	5.06	3.70	1.87	6.30	5.50	5.00
	Mar	6.56	14.17	1.86	6.40	5.50	7.00
	Apr	6.43	11.81	4.54	6.80	5.40	6.40
	May	7.00	7.82	7.40	6.00	5.50	5.80
	Jul	4.50	3.60	4.14	4.30	5.40	9.90
	Aug	4.20	3.55	1.82	4.10	5.20	4.10
	Sep	4.80	4.76	2.09	5.40	5.30	11.00
Stand. deviation			4.57	4.50	2.88	2.74	
29030	Jan	3.70	[illegible]	2.85	4.80	5.80	2.90
	Feb	4.00	[illegible]	1.95	5.30	6.40	7.90
	Mar	7.20	[illegible]	1.92	5.90	5.00	6.30
	Apr	5.77	[illegible]	4.68	6.10	5.10	6.20

Table 2.6 continuation

1	2	3	4	5	6	7	8
	May	8.00	1.58	7.67	5.10	5.90	5.00
	Jul	6.53	0.99	4.27	5.00	5.40	7.90
	Aug	6.20	0.16	1.89	5.30	6.70	7.60
	Sep	5.53	0.22	2.15	5.20	5.80	8.00
Stand.	deviation		5.53	4.24	2.00	1.82	
29031	Jan	6.66	10.23	3.59	6.30	6.60	4.60
	Feb	7.90	15.84	2.45	7.50	6.80	7.60
	Mar	10.83	9.46	2.46	7.10	7.70	8.70
	Apr	9.97	13.93	6.01	7.70	8.20	6.00
	May	8.70	2.10	9.72	7.50	7.10	8.70
	Jul	4.60	0.12	5.48	7.10	8.20	8.40
	Aug	5.87	0.21	2.39	8.60	7.90	7.60
	Sep	7.74	0.29	2.76	7.70	8.20	8.10
Stand.	deviation		6.99	4.06	1.25	1.28	
29036	Jan	6.93	16.08	6.68	9.60	10.40	6.60
	Feb	8.60	24.89	4.57	15.90	13.20	10.70
	Mar	14.40	14.87	4.54	13.70	9.70	9.30
	Apr	14.27	21.88	11.10	17.80	11.80	8.60
	May	13.53	3.29	18.05	13.70	12.00	13.70
	Jul	10.23	0.19	10.12	9.30	13.10	11.70
	Aug	8.47	0.32	4.44	12.40	17.50	11.70
	Sep	9.43	0.46	5.10	15.30	14.90	11.00
Stand.	deviation		11.07	4.68	4.52	3.25	
29037	Jan	17.73	26.16	9.75	15.20	17.40	11.90
	Feb	12.36	40.39	6.67	19.10	22.04	19.90
	Mar	26.83	24.17	6.60	18.80	14.90	14.90
	Apr	25.23	35.44	16.12	15.70	18.10	22.30
	May	18.93	5.37	26.32	16.00	19.80	25.50
	Jul	17.86	0.31	14.70	21.00	20.50	13.80
	Aug	22.67	0.54	6.47	26.50	29.00	18.90
	Sept	14.75	0.75	7.41	21.00	23.70	23.40
Stand.	deviation		17.02	9.34	5.89	5.40	
29044	Jan	13.40	14.44	5.56	9.90	10.30	7.70
	Feb	10.50	22.33	3.80	11.10	10.30	10.20
	Mar	14.43	13.35	3.79	10.80	11.40	7.60
	Apr	11.00	19.62	9.28	11.30	11.80	9.00
	May	11.23	2.96	15.03	11.20	10.70	8.00
	Jul	10.50	0.17	8.45	10.50	11.70	9.60
	Aug	9.43	0.29	3.70	12.00	11.20	8.90
	Sep	9.73	0.41	4.26	11.10	11.70	9.20
Stand.	deviation		8.69	4.51	2.38	2.57	
29046	Jan	3.33	6.70	2.55	5.20	5.60	2.90
	Feb	2.70	10.29	1.75	4.10	5.80	3.80
	Mar	3.90	6.18	1.71	5.10	4.40	3.50
	Apr	4.10	8.99	4.16	3.20	4.10	3.40
	May	9.60	1.38	6.85	5.70	5.30	1.10
	Jul	10.23	0.88	3.80	7.90	4.30	5.70
	Aug	3.63	0.15	1.68	8.00	5.20	3.30
	Sept	4.70	0.20	1.92	7.20	4.50	3.20

Table 2.6continuation

1	2	3	4	5	6	7	8
Stand. deviation			4.27	2.48	3.00	2.18	
29067	Jan	4.90	8.28	2.82	5.20	5.40	5.30
	Feb	5.30	12.79	1.93	7.20	5.80	6.10
	Mar	9.26	7.65	1.92	6.50	5.80	4.30
	Apr	7.63	11.23	4.70	7.80	6.20	6.30
	May	8.16	1.70	7.63	6.50	5.80	9.70
	Jul	4.67	0.10	4.28	4.90	6.30	4.50
	Aug	4.53	0.17	1.88	5.70	6.70	11.20
	Sep	6.17	0.24	2.16	6.80	6.50	4.50
Stand. deviation			6.25	4.01	2.60	2.38	

significantly from city to city, and varies considerably for a given city from month to month. The characteristic patterns of local air movement may be represented in either tabular or graphical form. In the graphical representation, the frequencies of various observed wind directions are plotted proportional to the total length of radiating lines, called a windrose. The distribution of wind speeds within each direction is indicated by the width of the individual sections of a given line. The wind rose gives directly the joint frequency distribution of wind speed and direction. The wind direction indicated in the wind rose is the direction from which the wind is blowing. For predicting dust and pollutant dispersion in the local atmosphere, a complete set of wind roses for the year should be available, because of seasonal variations in wind speed and direction. The monthly averaged (1977-1980) wind rose for the RBG is plotted in Figure 2.7. The corresponding monthly averaged dustfall calculated from all the dust collection stations in Hamilton is plotted as dustfall concentration contour lines (isopleths) in Figure 2.8. Figure 2.7 and Figures 2.8 a-f reveal that an increase in NE wind velocity and frequency spreads the isopleths away from the industrial sources. The reverse is observed in Figure 2.8d. A linear regression with wind velocity as an independent parameter and dustfall as a dependent parameter was performed using 1977-80 data:

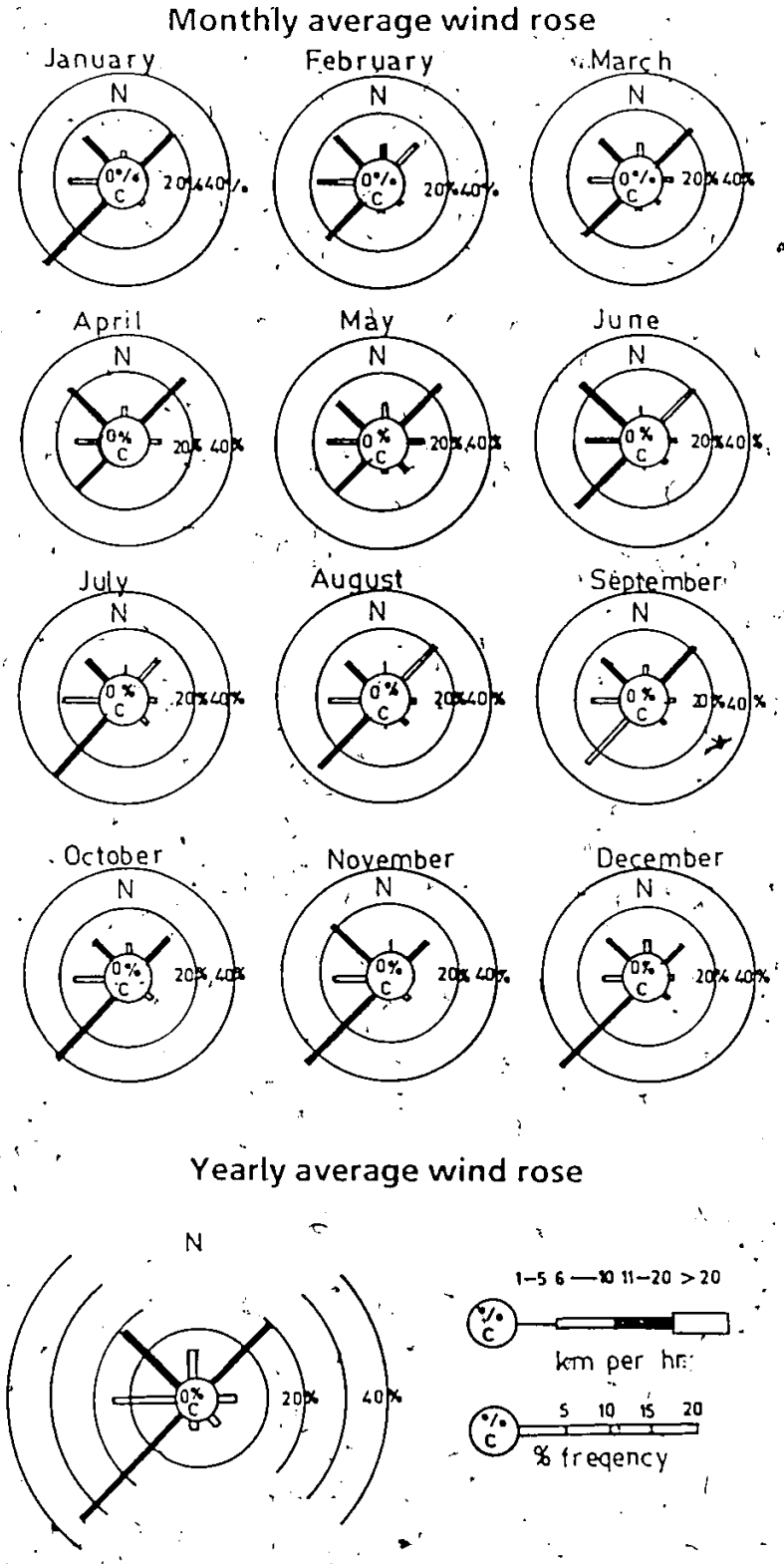

Figure 2.7 Monthly and yearly average wind rose of Hamilton. (RBG data, 1977-80)

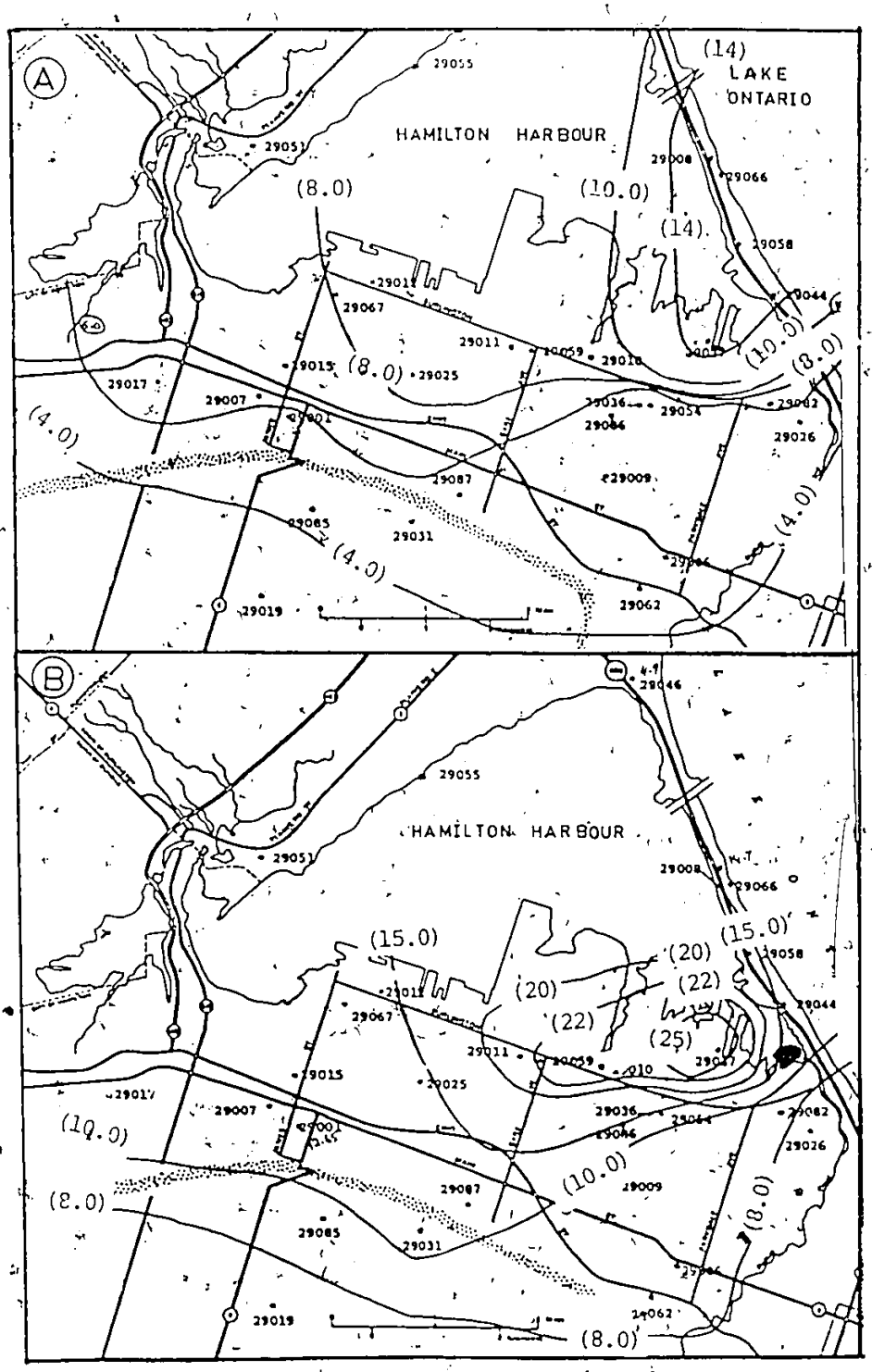

Figure 2.8 Monthly average dustfall isopleths over Hamilton.

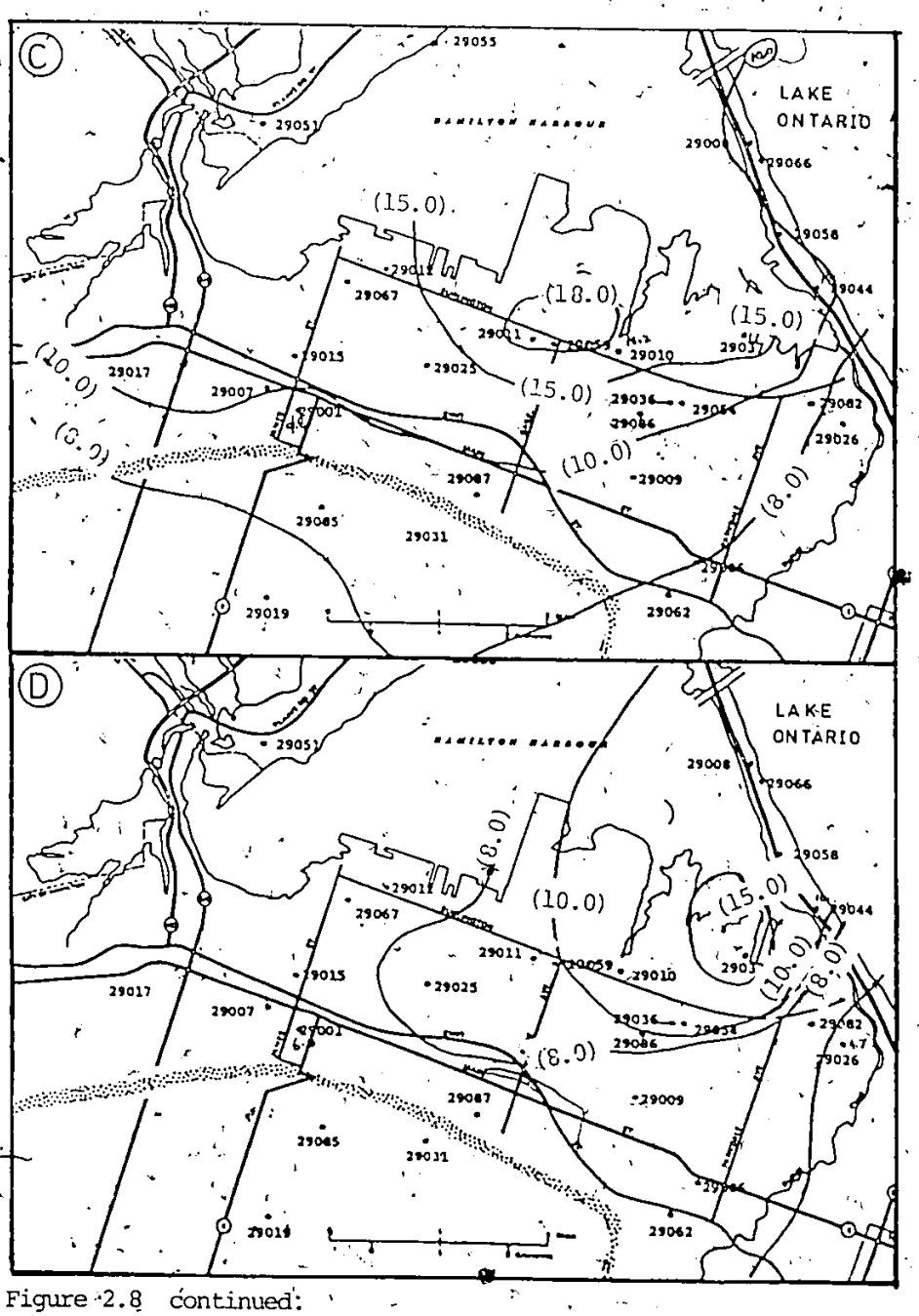

Figure 2.8 continued:

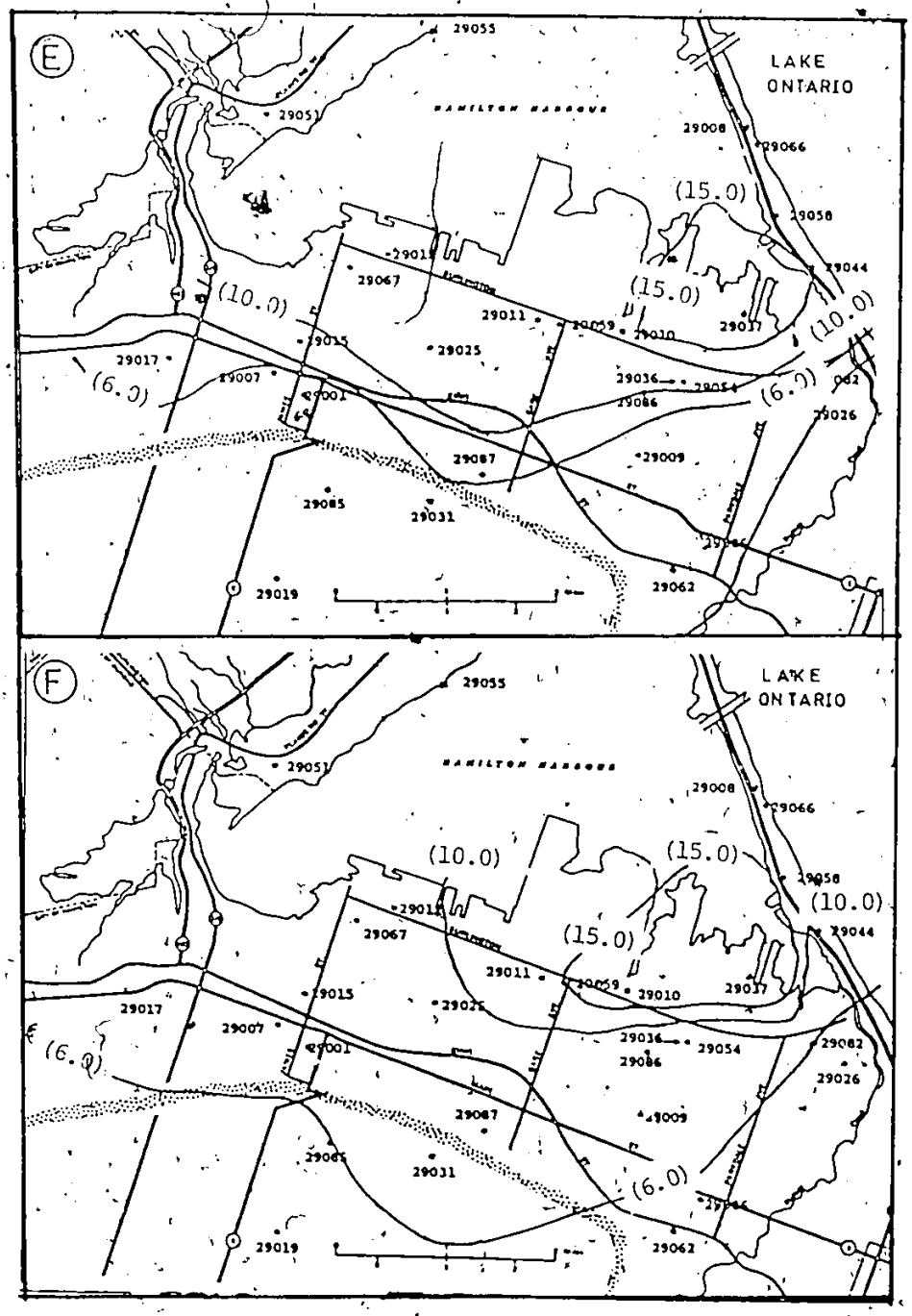

Figure 2.8 continued.

$$Y_{im} = a_i + b_i V_{md} \qquad [2.26]$$

where: V_{md} = average wind velocity for the month m and direction d, (km/h)

a_i, b_i = regression constants for dustfall station i.

The regression constants for all the dustfall collection stations were calculated using NE direction information at first and all eight directions later. The direction for each individual dust collection station that produced the minimum standard deviation between observed and predicted data was calculated and the corresponding wind velocity and frequency were used to calculate regression constants.

Model 2 was then tested against 1981 data, and the standard deviation between observed and predicted data for both NE and optimised direction were calculated. These results are tabulated in column 4 and 5 of Table 2.6.

iii) Model 3: (Multiple linear regression model)

Since dustfall data has both wet and dry deposition components, total precipitation was included as one more independent parameter in the linear regression equation:

$$Y_{im} = a_i + b_i \Sigma V_{md} + c_i \Sigma P_m \qquad [2.27]$$

where a_i, b_i and c_i = multiregression constants

P_m = total water precipitation during month, mm (water equivalent).

The subscripts i, m and d correspond to dust collection station, month and direction. Multi-regression constants were calculated for the conditions similar to the conditions discussed in Model 2.

Inclusion of the precipitation parameter improved the predicted results and reduced the standard deviation between observed and predicted values. The results are tabulated in column 6 and 7 of Table 2.5. Multiple linear regression constants corresponding to NE meteorological information are tabulated in Table 2.7.

The model is sensitive to seasonal variations because of the sensitivity of the independent variables to seasonal variations. The results showed, that the NE direction wind data correlates better with dust collection, having lower standard deviations for most collection stations.

Dustfall predicted by the three models were compared statistically to determine the best model, using i) regression analysis (regression coefficients a, b and correlation coefficient r), ii) relative error, iii) root mean square error (RMSE) and iv) standard deviation and coefficient variation (Thomann, 1982). The FORTRAN code for these statistical analyses are included in the program

Table 2.7 Multiregression coefficients

Stat.	Dire.	Const-a	Const-b	Const-c
9001	NE	5584.695	3.092	4.088
9006	NE	4677.929	6.449	-0.750
9008	NE	8058.933	14.286	-0.020
9009	NE	4004.965	5.310	-2.712
9011	NE	11997.335	8.688	3.490
9012	NE	5265.253	2.398	49.905
9017	NE	13110.332	-10.602	17.028
9019	NE	3553.187	-7.462	19.451
9025	NE	8929.253	-2.649	26.513
9026	NE	5831.605	-0.599	-2.191
9030	NE	7962.386	-7.282	6.993
9031	NE	4319.199	7.230	5.948
9036	NE	12053.507	-7.755	44.986
9037	NE	24161.562	-25.879	77.735
9044	NE	7249.218	9.962	1.332
9046	NE	3432.210	-9.443	0.214
9067	NE	4689.531	2.138	7.063

Verification of Water Quality Models (VWQM). Observed data were regressed against predicted results to find the best fit line as shown in Figure 2.9a. If the predicted results are the same as the observed data, the points fall on 45 degree ideal line. The statistics between best fit line and ideal line are used for comparison. Median relative error versus percent samples were also plotted in Figure 2.9b. The statistical results calculated for all the models are tabulated in Table 2.8. These results show that Model 3b i.e. multiregression model with NE direction meteorological input, has better predictability compared to other models and is also sensitive to meteorological data. The results from Model 3b were used to plot dustfall isopleths along with observed dustfall isopleth for the final comparison shown in Figure 2.10. The accuracy of the results obtained by the model 3b is satisfactory for the present work.

2.3.5. Interpolation of predicted dustfall over subcatchments:

Finally, it is necessary to predict the spatially averaged dustfall rate for each subcatchment. In doing so, the wet deposition component was deducted from the predicted total dustfall (bulk data) and converted from units of g/m^2-30 d to g/m^2-effective hour. An "effective hour" is the product of wind frequency of a given direction and total number of hours under consideration. Effective

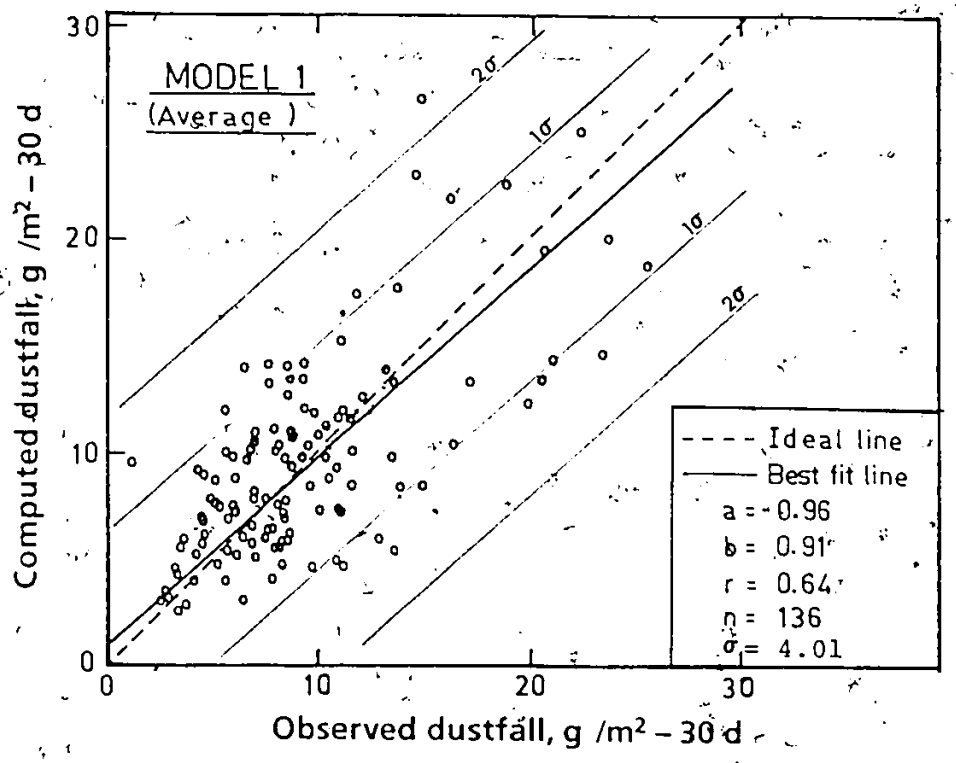

Figure 2.9 Statistical comparison between observed and computed dustfall.

Figure 2.9 continued.

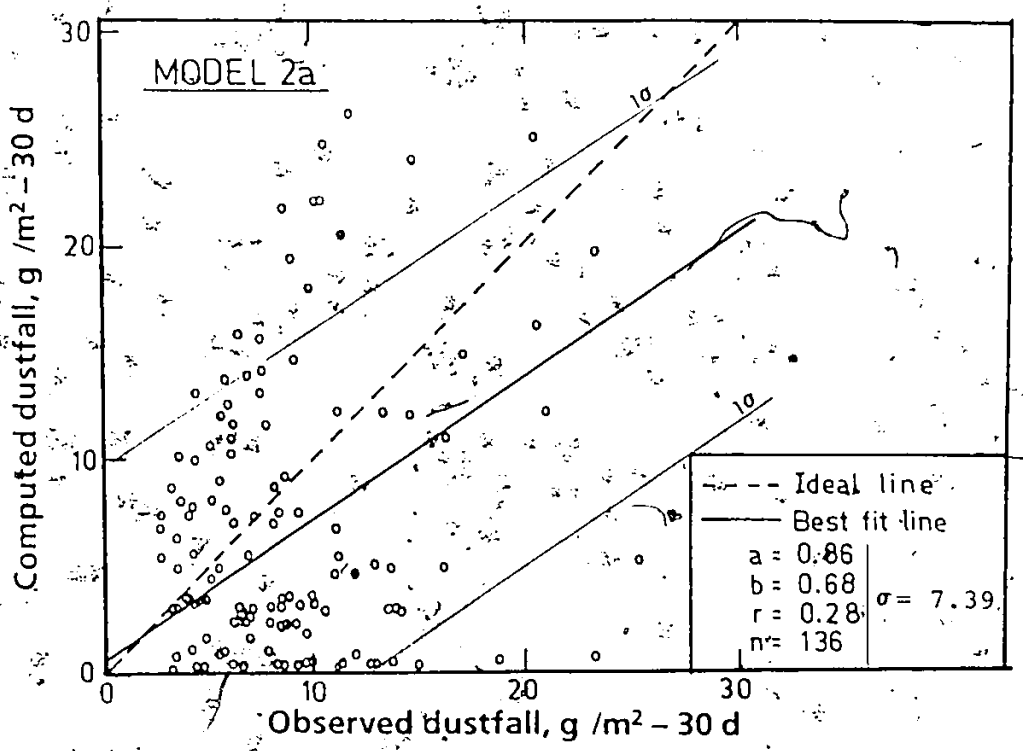

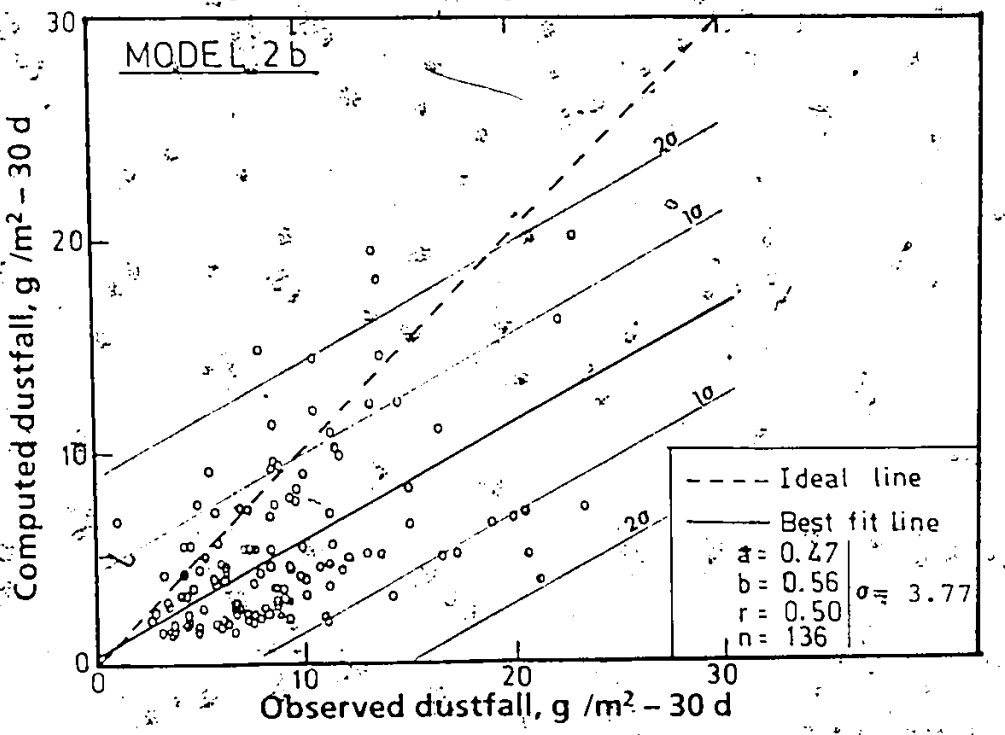

Figure 2.9 continued.

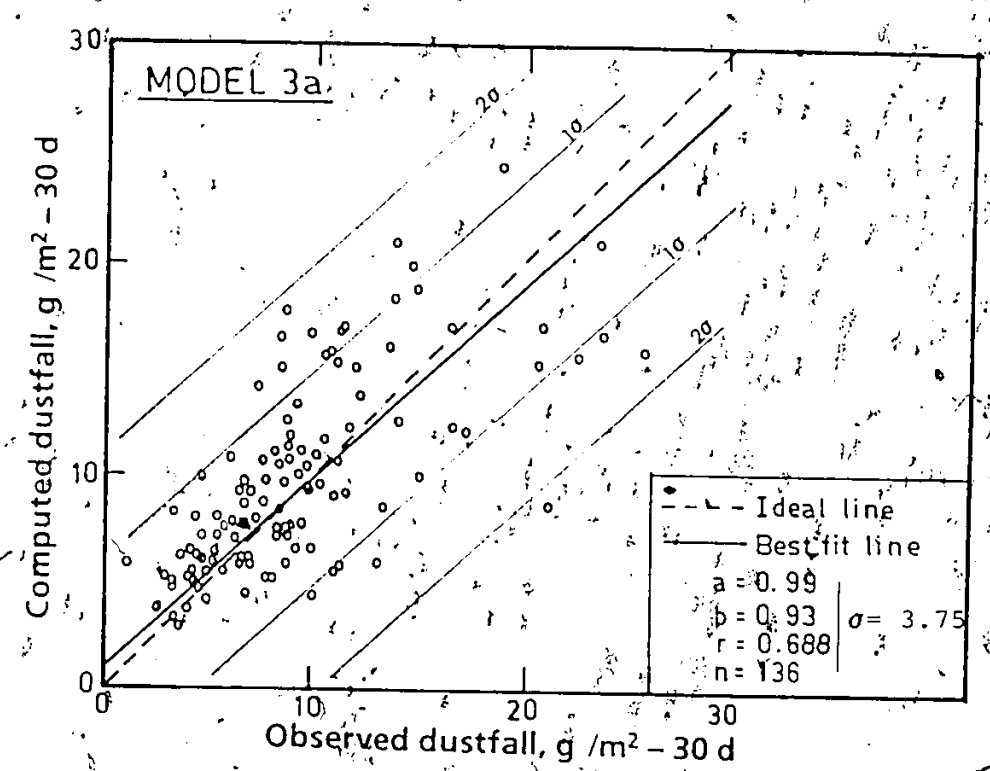

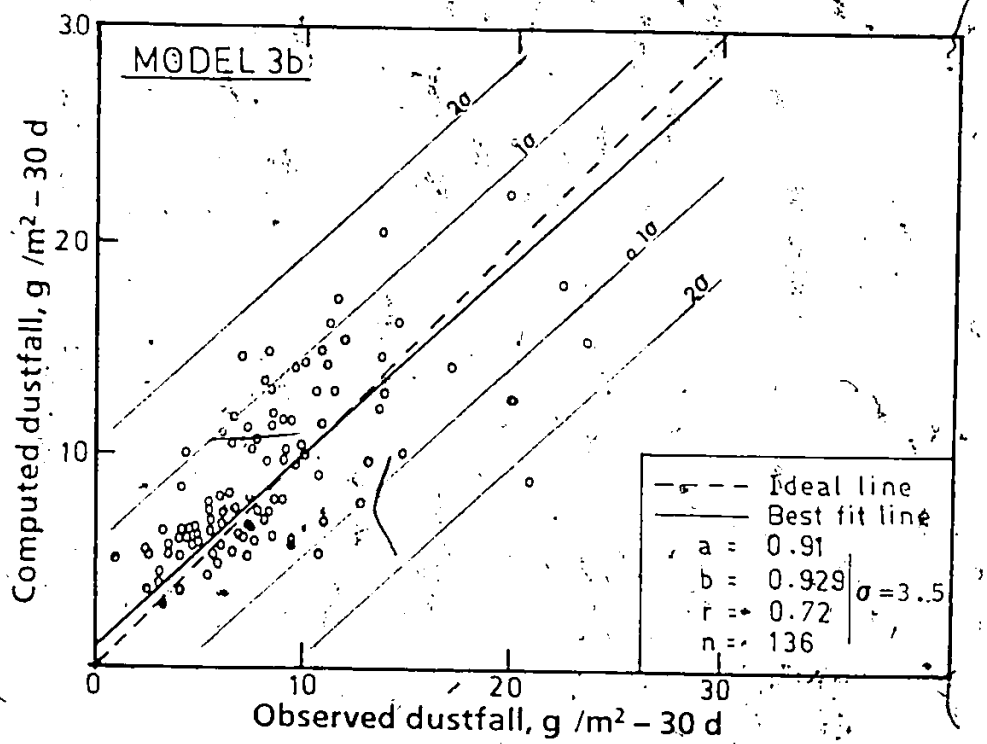

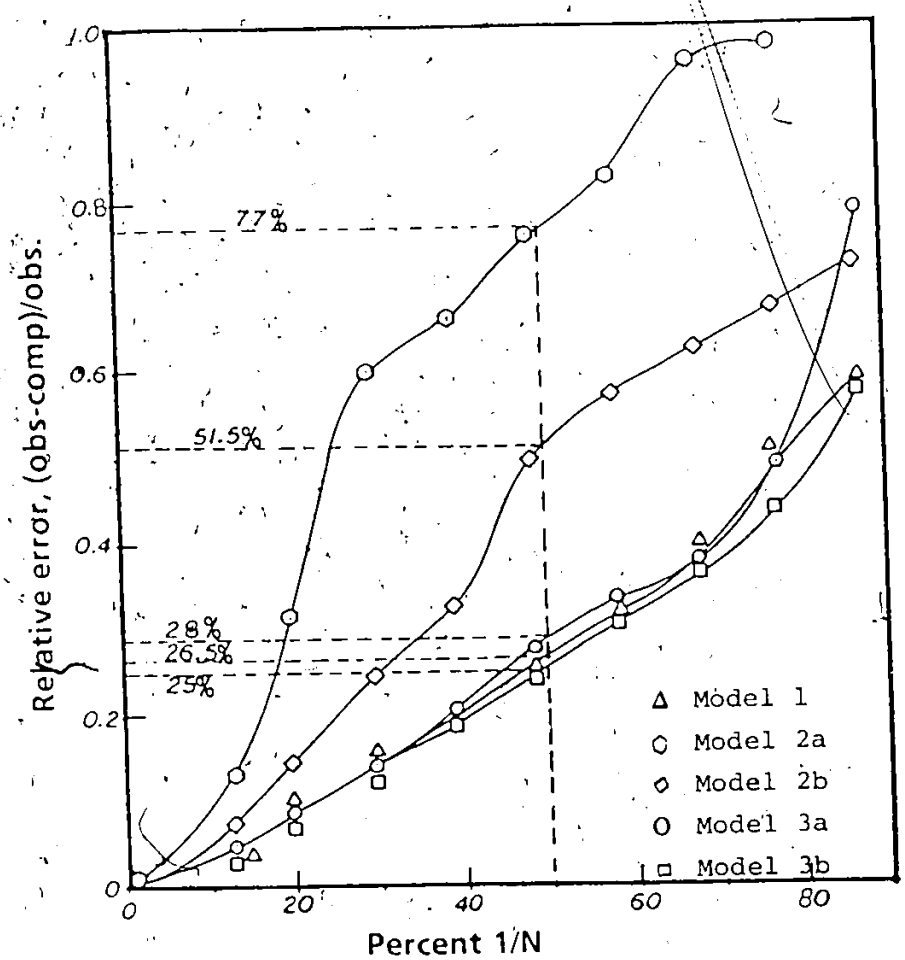

Figure 2.9b continued.

TABLE 2.8 STATISTICAL COMPARISON OF DUSTFALL PREDICTION MODELS

Parameter	Model				
	1	2a	2b	3a	3b
a	0.9617	0.8636	0.4671	0.9991	0.9197
b	0.1908	0.6844	0.5555	0.9312	0.9290
r	0.6493	0.2779	0.4966	0.6882	0.7202
Stdev.	4.0154	7.3947	3.7730	3.7570	3.5468
Coe.Var.	43.6252	104.775	68.6745	39.8554	38.0285
Med.Rel.Er	76.5000	77.000	51.5000	29.0000	25.0000
RMSE	3.9858	7.3401	3.7451	3.7292	3.5207
Tot.Samp.	136.0000	136.0000	136.0000	136.0000	136.0000

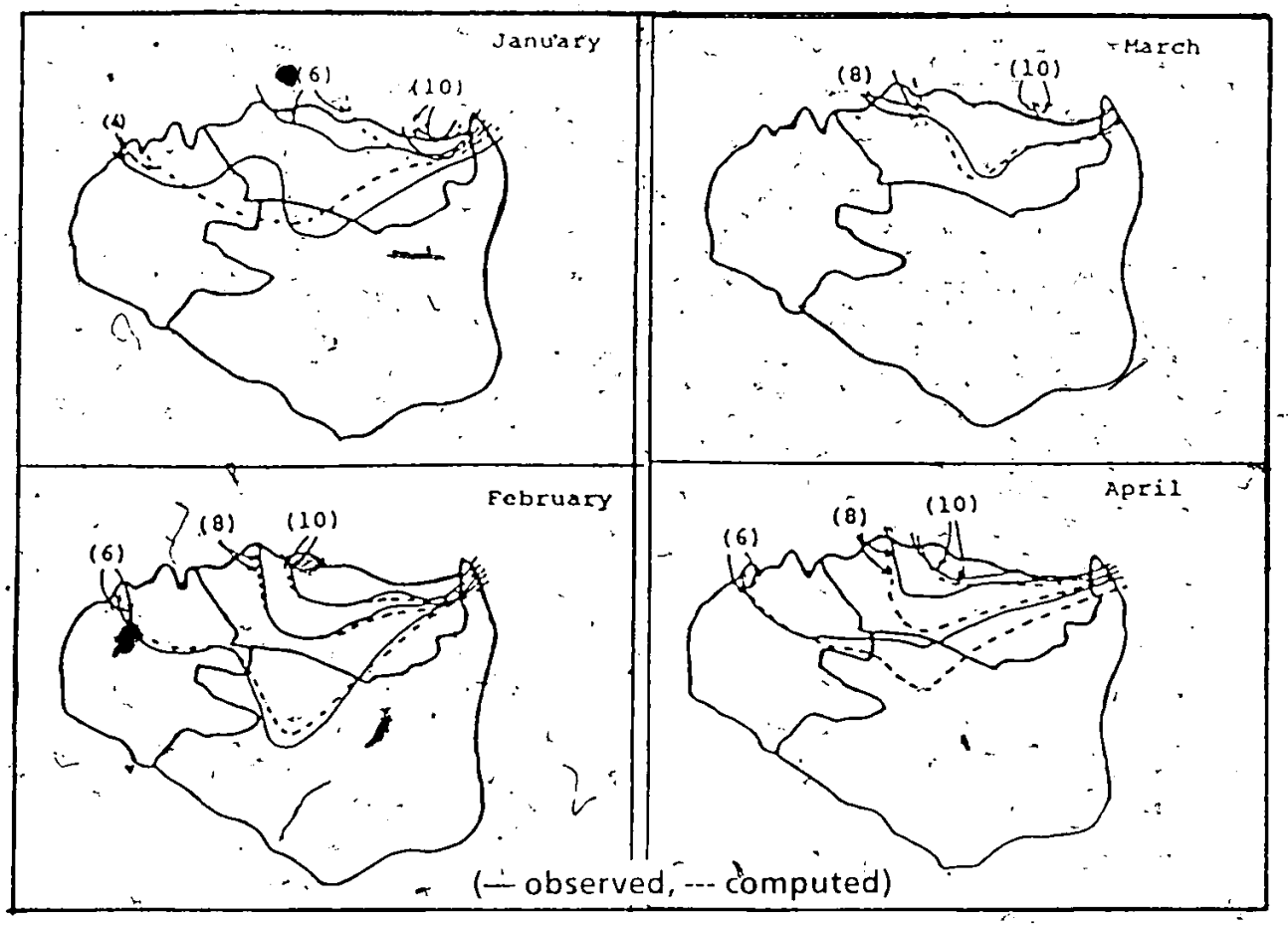

Figure 2.10 Observed and computed dustfall isopleths over Hamilton.

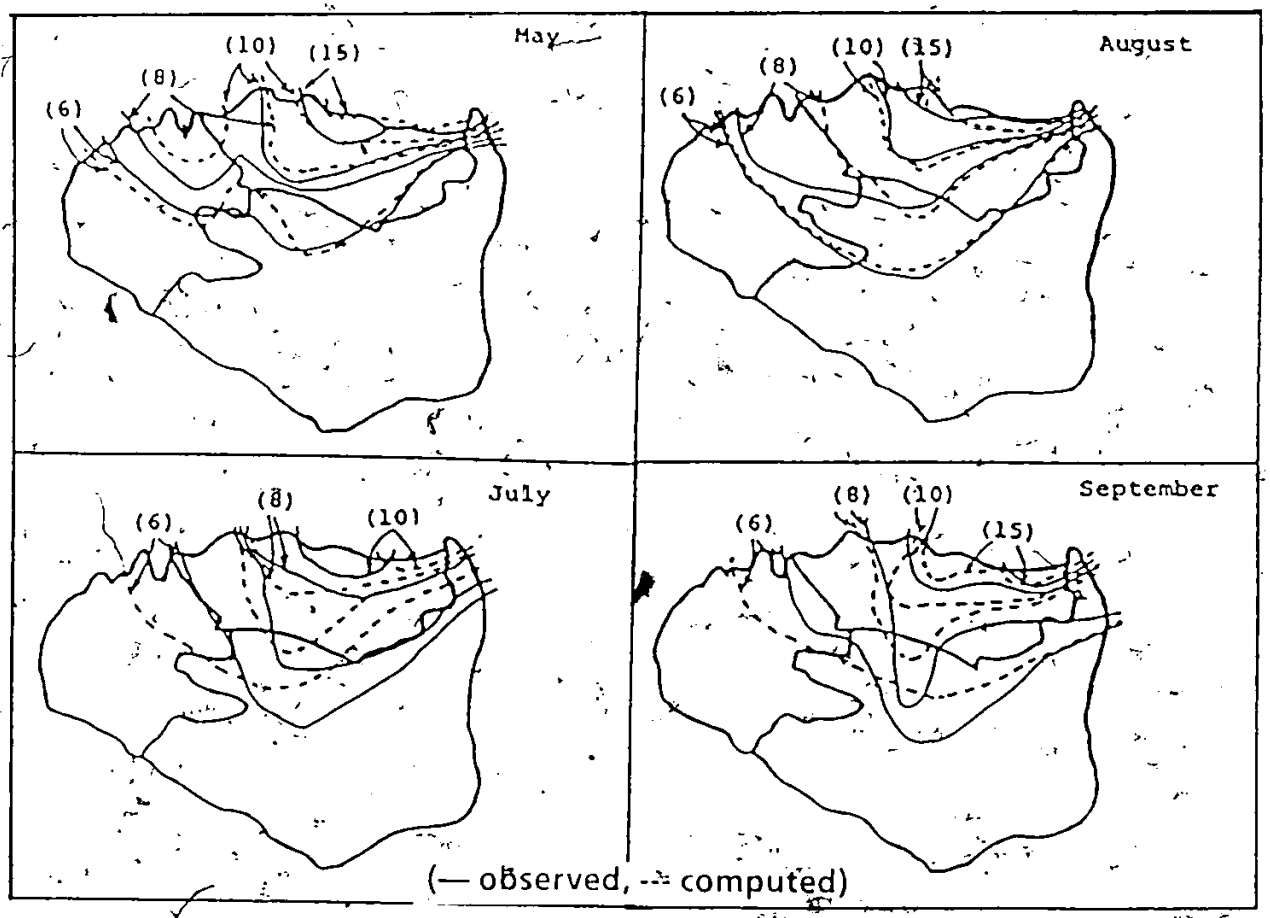

Figure 2.10 continued.

hours are calculated by assuming that the wind velocity and the direction used to produce the minimum standard deviation between observed and predicted dustfall distributes dust over the catchment only during that proportion of the time. In addition to the assumption that dust falls on the subcatchments only during the effective hours, it is also assumed that there is a linear distribution of dust concentration from 2 m to ground level. These two assumptions allow use of the observed dust data for calculating mass dust flux on a given subcatchment.

On a map of the area, all dust sampling stations were connected by straight lines as shown in Figure 2.11. Dust fall rate was interpolated between two collection stations assuming a linear distribution. Since all dust collection stations are located within the catchments, the results were extrapolated to the outmost catchment boundary. A provision is also made in the model to interpolate the data, assuming an imaginary station at the catchment boundary and equating these to expected background concentrations. The computed results for different subcatchments are tabulated in Table 2.9. These results are added to the remaining component contributed by various surface activities to obtain total dust accumulation rate on the surface considering physical, chemical and biological processes. The algorithms for predicting atmospheric dustfall at dustfall collection stations and on individual subcatchments for any given

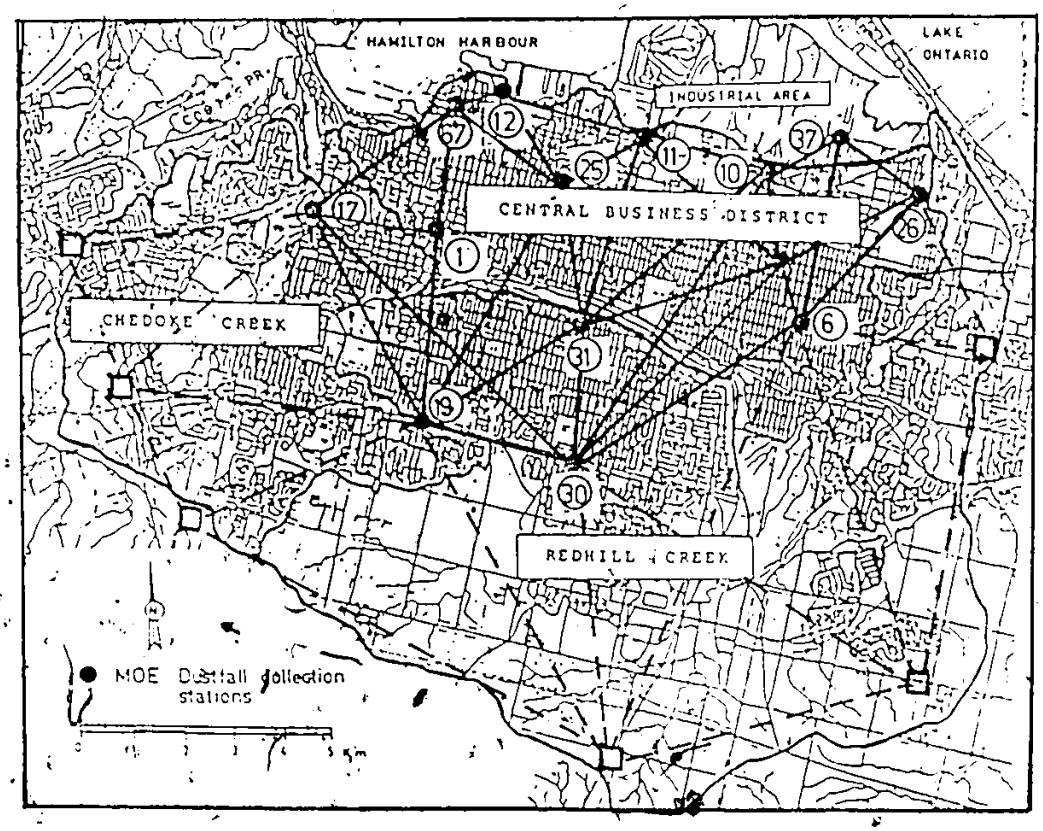

Figure 2.11 Dustfall collection station network.

Table 2.9 Predicted dustfall on subcatchments, mg/m^2 -eff.h

Subcat. #	Jan.	Feb.	Mar.	Apr.	May	July	Aug.	Sept.
1	15.27	22.32	24.06	10.62	6.33	11.24	23.49	21.93
2	37.73	54.96	63.49	27.32	14.97	28.96	59.62	57.06
3	44.02	64.71	72.49	30.93	17.23	32.83	69.27	65.54
4	33.32	43.72	55.19	23.77	13.23	25.20	52.40	49.81
5	40.05	57.96	68.79	29.66	15.96	31.41	63.63	61.48
6	5.19	7.50	7.00	3.44	2.51	3.62	7.43	6.65
7	1.00	1.00	1.00	1.00	1.00	1.00	1.00	1.00
8	9.38	14.00	12.99	5.83	4.01	6.23	13.86	12.31
10	66.05	95.93	113.99	48.76	25.94	51.68	105.38	101.81
24	9.38	4.00	12.99	5.83	4.01	6.23	13.86	12.31
25	27.03	38.97	46.19	20.10	10.97	21.27	42.75	41.32
26	53.06	76.94	91.39	39.21	20.95	41.55	84.50	81.65
27	53.06	76.94	91.39	39.21	20.95	41.55	84.50	81.65
28	105.12	152.89	181.78	77.42	40.90	82.09	168.01	162.29
29	98.62	143.39	170.45	72.64	38.40	77.02	157.57	152.21
30	107.54	153.63	196.73	84.08	42.19	89.01	174.65	173.13
31	56.60	84.21	90.48	38.30	21.75	40.72	88.57	82.51
32	21.96	33.49	30.99	13.20	8.53	14.08	33.16	29.27
33	21.96	33.49	30.99	13.20	8.53	14.08	33.16	29.27
34	9.38	14.00	12.99	5.88	4.01	6.23	13.86	12.31
35	13.58	20.50	18.99	8.32	5.52	8.85	20.30	17.96
36	26.15	39.99	36.93	15.64	10.03	16.69	39.59	34.93
37	26.15	39.99	36.93	15.64	10.03	16.69	39.59	34.93
38	26.15	39.99	36.93	15.64	10.03	16.69	39.59	34.93
39	26.15	39.99	36.93	15.64	10.03	16.69	39.59	34.93
40	32.44	49.74	45.98	19.30	12.29	20.81	49.24	43.41
42	87.04	128.42	143.97	60.96	33.46	64.76	137.54	130.05
43	109.12	159.19	187.33	79.60	42.26	84.45	174.14	167.58
44	106.65	153.19	192.13	82.00	41.71	86.85	172.45	169.74
79	84.59	121.97	150.63	64.22	33.00	68.05	136.34	133.47
82	32.44	49.74	45.98	19.30	12.29	20.61	49.24	43.41
45	107.54	153.65	196.73	84.03	42.19	89.01	174.65	173.13
46	95.73	135.10	181.61	77.86	37.85	82.32	157.09	158.38
47	83.93	116.51	166.49	71.64	33.51	75.64	139.54	143.64
48	40.22	54.95	81.92	35.62	16.48	37.55	67.20	70.21
49	41.35	55.89	36.79	37.80	17.06	39.82	69.77	73.89
57	85.73	113.97	139.11	82.02	35.09	86.36	147.29	159.26
58	163.92	221.38	343.53	150.77	66.50	158.89	278.37	295.93
59	117.03	164.83	223.25	95.75	46.33	101.23	192.35	194.44
60	88.55	117.61	195.98	85.02	36.28	39.21	152.34	164.94
61	81.71	108.80	179.60	77.88	33.41	82.01	140.23	151.38
62	87.40	117.61	187.45	81.14	35.53	85.49	148.83	158.85

Table 2.9 continuation:

Subcat. #	Jan.	Feb.	Mar.	Apr.	May	July	Aug.	Sept.
63	76.57	107.82	145.28	82.48	30.49	66.05	125.51	126.67
65	110.65	158.46	201.20	85.94	43.36	91.00	179.40	177.33
76	80.17	109.61	165.39	71.53	32.30	75.29	134.88	141.40
85	75.96	105.59	150.43	64.84	30.45	65.46	126.14	129.83
86	142.05	193.31	296.48	128.07	57.38	135.05	239.84	252.79
87	105.02	144.22	214.25	92.39	42.20	97.48	176.08	183.64
41	78.22	115.93	127.37	53.85	29.98	57.24	123.10	115.52
50	83.82	114.72	172.50	74.41	33.75	78.52	140.92	147.56
51	1.00	1.00	1.00	1.00	1.00	1.00	1.00	1.00
52	46.04	67.48	77.12	32.94	18.00	34.94	72.83	69.42
53	38.54	56.35	64.43	27.61	15.17	29.29	60.86	58.02
54	46.04	67.42	77.12	32.94	18.00	34.94	72.83	69.42
55	78.98	111.03	151.23	64.89	31.29	68.59	129.95	131.59
56	83.18	115.48	164.97	70.98	33.21	74.95	138.28	148.34
64	72.43	95.61	161.85	70.33	29.86	74.07	124.88	135.91
66	63.50	83.75	141.74	61.71	26.26	64.93	109.39	119.05
67	54.57	71.96	121.64	53.04	22.65	55.80	93.91	102.15
68	54.57	71.96	121.64	53.04	22.65	55.80	93.91	102.15
70	36.71	48.30	51.43	35.69	15.43	37.53	62.94	68.46
73	18.86	24.65	41.21	18.35	8.22	19.27	31.97	34.73
74	38.42	53.24	75.34	32.69	15.62	34.49	63.45	65.15
75	45.90	63.69	90.21	39.03	18.55	41.19	75.94	77.98
77	83.06	112.37	175.87	76.05	33.66	80.16	140.87	149.47
78	76.91	108.89	144.56	61.83	30.35	65.50	125.87	126.36
80	54.24	79.32	82.41	39.24	20.97	41.64	86.39	52.83
81	52.14	76.14	89.23	37.91	20.13	40.22	83.14	79.89
83	80.53	115.06	147.43	63.01	31.60	66.70	130.81	129.72
84	79.20	109.40	159.17	68.56	31.71	72.37	132.19	136.91
88	21.96	33.49	30.99	13.20	8.59	14.08	33.16	29.27
89	1.00	1.00	1.00	1.00	1.00	1.00	1.00	1.00
90	23.52	34.21	39.06	16.97	9.50	17.97	36.92	35.21
91	31.03	45.25	31.75	22.29	12.33	23.63	48.89	46.61
92	43.84	60.52	37.14	37.18	17.81	39.86	72.74	75.12
93	18.86	24.65	41.21	18.35	8.22	19.27	31.97	34.73
95	1.00	1.00	1.00	1.00	1.00	1.00	1.00	1.00
96	16.01	23.14	26.37	11.65	6.67	12.31	24.94	23.81
97	16.01	23.14	26.37	11.65	6.67	12.31	24.94	23.81

months and meteorological information are collected under a common model named ATMDST. This model is written as a separate block of the "Storm Water Management Model (SWMM3, Huber 1981). SWMM3 is a widely used package in the field of urban hydrology and has been enhanced by the computational Hydraulics group (the enhanced program is called FASTSWMM3). The model structure of FASTSWMM3 and ATMDST are shown in Figures 2.12 and 2.13 respectively.

2.4. SURFACE INPUT FOR DUST AND DIRT BUILDUP:

Apart from dustfall, other surface activities also play an important role in DD buildup on impervious areas. The net buildup depends on the addition and removal processes on the surface. The effects of major surface activities on DD buildup are discussed here.

2.4.1. Vehicle input:

Highway runoff pollutants important to water quality are vehicle dependent. Metals (lead, zinc, copper, chromium, and iron), nutrients (nitrogen and phosphorous) and hydrocarbons are largely contributed by motor vehicle traffic. The specific source and type of these solids depends on where the vehicle has travelled and where the pollutants were picked up. Probable common sources of these solids include parking lots, urban and industrial areas, construction sites, unpaved roads and farming areas. Traffic byproducts, gasoline and oil drippings, tire residuals,

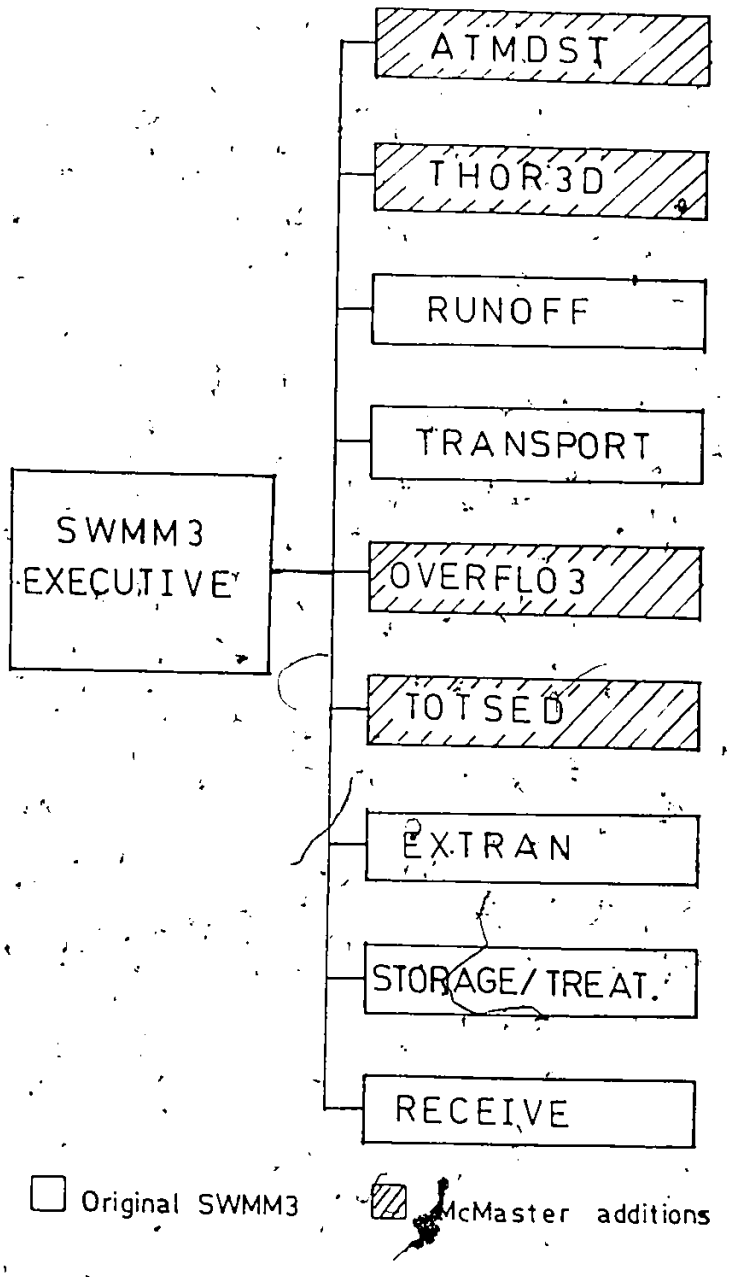

Figure 2.12 SWMM3 model structure schematic diagram.

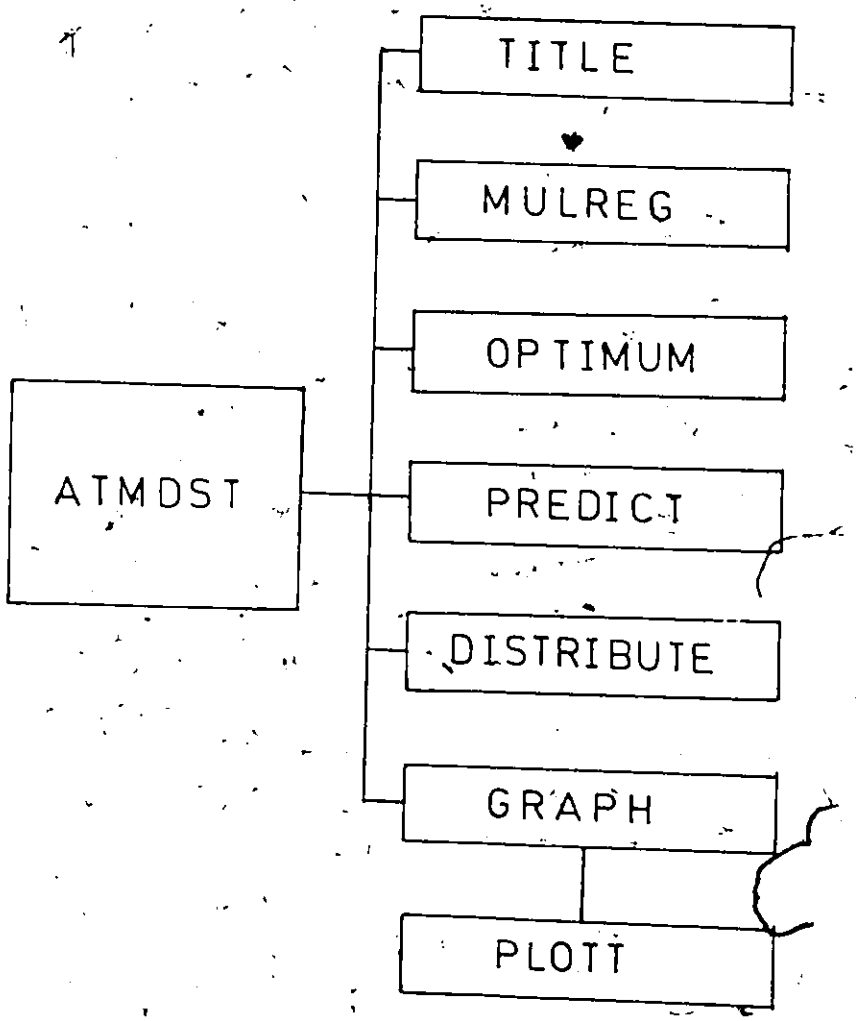

Figure 2.13 ATMDST model structure diagram.

brakewear, vehicle exhaust and metallic corrosion are also major contributors to pollutant accumulation. Many studies have focussed on vehicle input and developed algorithms for the prediction of runoff quality (Shaheen, 1975). These daily quantities produced per subcatchment could be quantified:

$$L_v = NLM \qquad [2.28]$$

where: L_v = mass of DD produced by vehicles mg/d.

N = number of vehicle axles active each day in a subcatchment, assuming two axles per vehicle (product of total population and P)

P = population to vehicle ratio = 0.4 to 0.5

L = mass of DD produced per vehicle per km travelled (800mg/axle-km in Hamilton)

M = total length of road in subcatchment, km.

2.4.2. Population input.

Litter deposits in urban areas include solid wastes deposited on surfaces, private and municipal waste collection operations, animal and bird fecal droppings, and other cultural deposits. The DD component of litter (materials less than 3.5 mm size) is regarded as having the greatest pollution potential of street surface refuse materials.

Although most of the litter is originally greater in size than that of DD, it is possible that a significant

portion of the street DD originates from the mechanical fracture of litter. An American Public Works Association study (1969) reported that street DD in residential areas increased as population density increases, because of additional pedestrian and roadway traffic.

Therefore, population input is formulated as:

$$L_p = P\ L \qquad [2.29]$$

where: L_p = total mass of DD due to population, mg/d.

P = total population in a subcatchment

L = per capita mass of pollutants/day, (200mg/cap-d in Hamilton)

2.4.3. Vegetation input:

Fallen dead leaves and grass clippings in urban areas also contribute significant quantities of DD on both pervious and impervious areas. The rate of vegetation input increases substantially during the fall and depends on the density of vegetation. In addition to DD load nutrients and other chemicals are leached to runoff water, depending upon the contact period with water (Prasad et al. 1980; Chen et al. 1983). The study conducted by Prasad in the Borough of Etobicoke in the Municipality of Metropolitan Toronto on autumn leaves showed that potentially large organic loads originate from leaves in an urban area. The amount of leaf fallout per tree per year is about 14.5 to 26 kg/yr (Heaney and Huber 1973). The tree density could vary from 10 - 500 trees/ha depending upon the utility of land. Since most of

the leaves are removed by regular street cleaning or arrested in the vegetation, only a fraction joins the runoff. Therefore an averge rate of 0.3 to 6.0 kg/ha-d (assuming leaves fall over a period of 90 days and a tree density of 10 - 400 trees/ha) is assumed in modelling vegetation input. The vegetation input is given by:

$$L_o = V\ A \qquad [2.30]$$

where: L_o = Vegetation input DD, mg/d.

V = Vegetation load rate to DD which varies with the landuse, and density of trees, mg/ha-d.

A = area, ha

2.4.4. Special activities:

This component is added to the DD accumulation only in the case of construction, demolition of structures or any other pollutant producing activities in the subcatchment. This is very site-specific and could be treated as a separate subcatchment with an additional pollutant load. DD produced by special activities is estimated by:

$$L_s = S_L\ A \qquad [2.31]$$

where: L_s = total mass of DD produced by special activities in mg/d.

S_L = DD loading, mg/ha-d

A = special activity area, ha.

2.5. Removals:

The DD accumulated on pavements is subjected to physical, chemical and biological processes which ultimately reduces the accumulation rate almost to zero over an extended period of dry days. This may be due to biological decomposition of organic material, wind and vehicle induced eddies and regular street cleaning practices.

2.5.1. Biological removal:

Organic pollutants decompose into simple substances in the presence of organisms, with or without oxygen. This reduces the total quantity of pollutants available at the time of washoff. Nitrate and phosphate are exceptions to the above process as they are normally increased by the addition of decomposed end products. This removal of solids by biological decomposition is calculated as:

$$R_b = P\,F(1 - e^{-Kt}) \qquad [2.32]$$

where: R_b = total mass of DD removed by biological decomposition, mg/d.

P = average mass of DD available on the surface, mg/d.

F = fraction of decomposable DD

K = decay coefficient, 1/d.

t = number of days.

2.5.2. Vehicle removal.

Vehicle generated eddies transport pollutants from the streets to ineffective impervious and pervious

areas from which they may not be washed off during storm events (Sehmel, 1973). The physical transfer of solids from effective to ineffective surfaces results in a loss in the net DD. This could be calculated as:

$$R_v = N\ F\ P \qquad [2.33]$$

where: R_v = mass of DD removed due to vehicle generated eddies, mg/d.

N = number of vehicles in a subcatchment

P = DD available for eddy transport, mg/d.

$$F = \theta_1(1 - e^{-\theta_2 S}) \qquad [2.34]$$

θ_1 = maximum fraction of DD that could be removed

θ_2 = decay coefficient, h/km.

S = vehicle speed, km/h.

2.5.3. Wind removal:

The transport of accumulated DD due to natural wind also reduces the available quantity for washoff. Dust removal is a function of wind speed, curb height, and presence or absence of an adjacent pervious area which acts as a pollutant sink. The general pattern of airflow on street pavements dictates the loss rate. Natural wind induced losses may be expressed (Novotny and Goodrich Mahoney 1978) as:

$$R_w = 0.0116(e^{-0.088\ H})W \qquad [2.35]$$

where: R_w = fraction of DD lost due to wind

H = curb height, cm

W = wind speed, km/h.

2.5.4. Intentional removal:

Regular street cleaning enhances aesthetics and minimises pollutant loadings to the receiving water. The frequency and efficiency of cleaning depends on traffic density and cleaning equipment respectively. Solids remaining on the pavement after street cleaning finally are washed off by rain. DD remaining on the catchment after street cleaning is given by (Huber et al. 1981):

$$R_i = \frac{L_a - R_{ma}}{L_a}$$

or

$$R_{ma} = L_a(1 - R_i) \qquad [2.36]$$

where: R_{ma} = DD remaining on subcatchment surface, mg

L_a = DD present before sweeping, mg

R_i = DD removed by sweeping = $A_v \; R_f$

A_v = availability factor = $0.6(2.5 \; P_d)^{0.2}$ [2.37]

P_d = population density, persons/ha.

R_f = removal efficiency.

The net DD accumlation on an impervious area is then calculated on a daily basis considering both addition and removal quantities. Subroutine NEWBLD was developed

using the algorithms discussed above (equations 2.27-2.37) for the prediction of DD accumulation over a dry day period on individual subcatchments. A provision to input the sweeping dates as timeseries for all the subcatchments is also included in the subroutine. The fraction of DD arrested in vegetation and buildings due to the canopy effect is also added to the accumulation. NEWBLD has been inserted in our version of the RUNOFF block of SWMM3 and is called CHGQUAL herein.

CHAPTER III

MODEL DEVELOPMENT - POLLUTANT BUILDUP

3.1. EXISTING DD BUILDUP ALGORITHMS:

Many urban runoff quantity and quality models have been developed during the last two decades some of them are listed in Table 3.1. In SWMM3 options for both linear and nonlinear (exponential and Michaelis-Menton) pollutant accumulation over a dry day period are given:

$$C_f = D_f D_m \qquad [3.1]$$

$$U_L = D_d D_m \qquad [3.2]$$

$$E_L = C_f t^P \qquad \text{(power linear)} \qquad [3.3]$$

$$E_L = U_L(1 - e^{-Pt}) \qquad \text{(exponential)} \qquad [3.4]$$

$$E_L = \frac{U_L t}{(C_f + t)} \qquad \text{(Michaelis Menton)} \qquad [3.5]$$

where: E_L = pollutant buildup, (mg or MPN)

C_f = coefficient, kg/d.

t = time in days

P = exponent, constant

U_L = upper limit for load, kg.

D_f = DD buildup rate, kg/100 m, curb-d. or kg/ha-d.

D_m = gutter length, 100m or subcatchment area, ha.

Table 3.1 Major runoff quantity and quality models developed during last two decades(Wanielista, 1979).

Corps of Engineers Storm.

Environmental Protection Agency SWMM.

Illinois Urban Drainage Area Simulator Illudas.

British Road Research Laboratory Model.

Hydrocomp Simulation Program.

Battelle Urban Waste Water Mangement Model.

University of Cincinnati Urban Runoff Model.

Massachusetts Institute of Technology Urban Watershed Model.

Metropolitian Sanitary District of Greater Chicago Flow simulation Program.

Water Resources Engineers Storm Water Mangement Model.

Environmental Protection Agency(EPA) Pesticide Transport Runoff(PTR) Model.

Simplified Storm Water Mangement Model for Planning.

Agricultural Chemical Transport Model.

Florida Technological University(FTU) Nonpoint Model.

FTU Best Mangement Practices Model (BMP).

Texas Water Board Water Yield Model.

D_d = limiting buildup quantity, kg/100m or kg/ha.

In STORM (HEC, 1976) pollutant accumulation for each one hour time step when runoff is less than 0.0005 inch/h (0.0122 mm/h) is given by:

$$L_t = D_d Q G t + L_{t-1} \qquad [3.6]$$

where: L_t = pollutant loading on subcatchment at time 't'(mg).

D_d = dust and dirt loading rate (g/d-100 m)

Q = fraction of dust and dirt consisting of pollutant, in mg/g

G = total gutter or curb length in subcatchment, 100 m

t = time step, d.

L_{t-1} = pollutant loading on subcatchment at t-1,(mg)

The pollutant accumulation in the Hydrologic Simulation Program (HSP), Agricultural Runoff Mangement Model (ARM), and the Nonpoint Source Pollutant loading model (NPS) is formulated as:

$$L_t = L_{t-1}(1 - R_g) + D \qquad [3.7]$$

where: L_t = pollutant accumulation at time t, (t/ha).

L_{t-1} = pollutant accumulation at time(t-1), (t/ha)

R_g = general removal fraction

D = pollutant deposition during time interval, (t/ha)

The general removal fraction is as follows in HSP and ARM:

$$R_g = F \frac{E}{f} R_W K_b \qquad [3.8]$$

where: F = fraction of impervious area.

E = efficiency of street cleaning on the impervious area.

f = frequency of street cleaning.

R_W = fraction of pollutant removal by wind

K_b = fraction of pollutant decay by biochemical processes.

The general removal rate in the NPS Model is an input parameter and there is one value for each month.

The Quantity Quality Simulation (QQS) program (Geiger and Dørsch,1979) has an asymptotic accumulation relationship formulated as:

$$L = (1-\{(az+1)/(bz+cz+1)\})\ L_m \qquad [3.9]$$

where: L = pollutant accumulation during dry period, kg/ha

z = dry period (number of 5 minute intervals).

a, b and c = empirical coefficients.

L_m = maximum pollutant loading (kg/ha).

The magnitude of the coefficients a,b and c is in the range 0.0001 to 0.0000001 and depends on the pollutant being accumulated.

3.2. Modified accumulation algorithm:

A wide variety of pollutant accumulation relationships have been proposed by many investigators,

depending upon their field data. A relationship suitable for all catchments is yet to be derived. In view of this problem, subroutine NEWBLD was developed as a substitute to the BUILD routine of SWMM3 RUNOFF based on individual buildup processes. The equations discussed in section 2.3.6 to 2.5.4 are used in the NEWBLD subroutines. The flow diagram of the NEWBLD subroutines and the block diagram for SWMM3 RUNOFF are given in Figure 3.1 and 3.2 respectively. NEWBLD accounts for daily addition and removal processes depending on the prevailing meteorological and geological conditions of an individual subcatchment. The ATMDST routine predicts atmospheric dustfall which is then transferred to NEWBLD. The new buildup algorithm does not follow any conventional accumulation rate curve even though it is non-linear in nature. The FORTRAN code is given in the CHGQUAL User's Manual (Shivalingaiah and James, 1984).

3.3. Sensitivity test on DD buildup:

DD buildup rate decreases over a period of dry days and becomes almost zero, attaining steady state. Both addition and removal processes are governed by wind velocity and source concentration. Even if the pollutant input from all the sources is constant, the dispersion and advection processes, mainly controlled by meteorological factors, distribute pollutants on to the subcatchments. Therefore a sensitivity test on the buildup algorithm was performed for

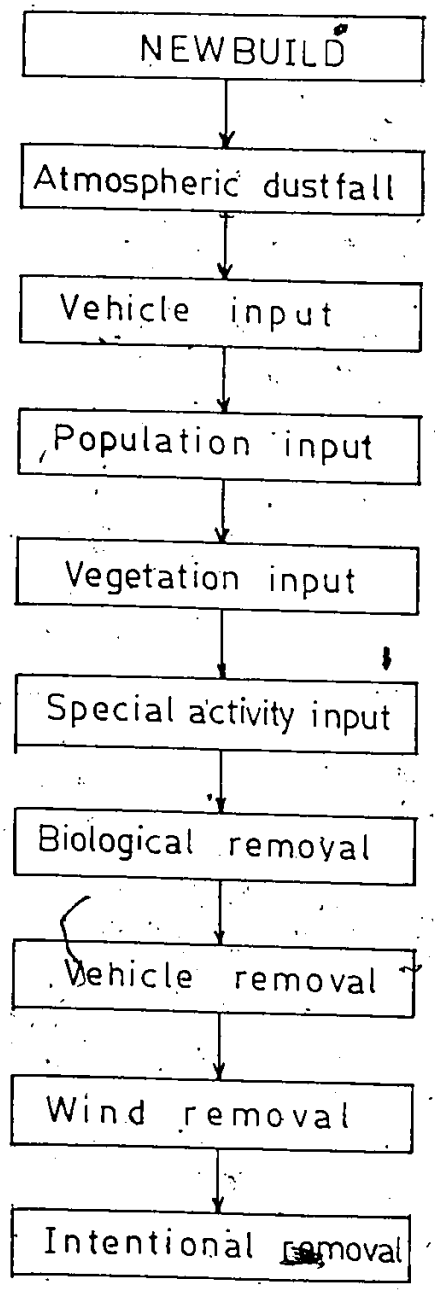

Figure 3.1 Flow chart for NEWBLD subroutine.

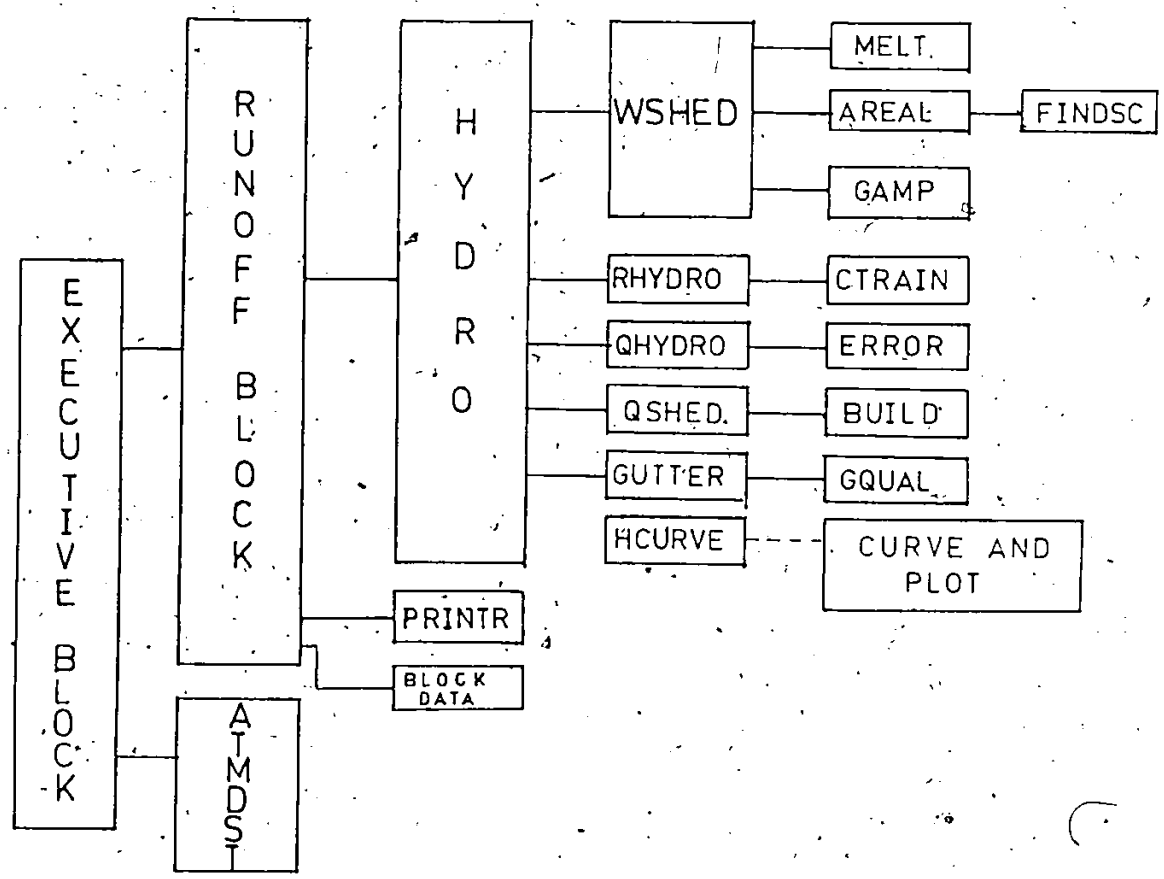

Figure 3.2 SWMM3 Runoff Block Subroutines.

three different land uses using an actual data set for the Chedoke creek catchment in Hamilton. The parameters used in the sensitivity analysis are given in Tables 3.2, 3.3, and 3.4. The results obtained for highly impervious area are plotted in Figure 3.3. The analysis showed that buildup is very sensitive to wind velocity and vehicle speed. Constant values were used in the analysis for complete dry day period. But it is not true in nature. Meteorological parameter fluctuates widely. Therefore random values of wind velocity and frequency and average values of remaining parameters were used to generate Figure 3.4. This plot appears to be very similar to the DD buildup data observed by various researchers. The effect of street cleaning frequency on DD buildup was also studied and the results are presented in Figure 3.5.

Table 3.2 Sensitivity analysis on buildup algorithm. (highly impervious area, subcatchment # 40, pollutant DD).

Days	average values	wind vel. km/h (8.3)[1]		wind freq. (0.44)[1]		vehicle speed km/h. (30.0)[1]		PVR[2] (0.5)[1]	
		3	90	0.05	0.60	15	90	0.1	0.9
1	7.66	7.79	5.67	6.57	8.11	14.20	3.27	2.56	12.61
2	14.93	15.31	9.65	12.80	15.81	27.80	6.28	5.02	24.48
3	21.85	22.58	12.46	18.70	23.13	40.84	9.05	7.40	35.49
4	28.42	29.61	14.44	24.37	30.08	53.34	11.60	9.69	45.87
5	34.68	36.41	15.83	29.73	36.71	65.34	13.94	11.90	55.61
6	40.63	42.99	16.82	34.84	43.01	76.86	16.11	14.04	64.75
7	46.31	49.37	17.52	39.70	49.02	87.94	18.11	16.10	73.35
8	51.72	55.55	18.02	44.34	54.75	98.59	19.95	18.09	81.43
9	56.89	61.55	18.37	48.77	60.21	108.84	21.66	20.02	89.03
10	61.81	67.37	18.63	53.00	65.43	118.70	23.23	21.88	96.19
11	66.52	73.02	18.81	57.03	70.41	128.20	24.69	23.69	102.93
12	71.02	78.51	18.95	60.89	75.17	137.35	26.04	25.44	109.28
13	75.32	83.83	19.05	64.57	79.72	146.17	27.29	27.13	115.27
14	79.43	89.01	19.12	68.10	84.07	154.68	28.45	28.78	120.92
15	83.36	94.05	19.18	71.47	88.23	162.88	29.52	30.37	126.25
16	87.12	98.95	19.22	74.69	92.22	170.79	30.52	31.91	131.28
17	90.72	103.71	19.25	77.78	96.03	178.43	31.44	33.41	136.04
18	94.17	108.34	19.28	80.73	99.68	185.80	32.30	34.86	140.53
19	97.47	112.85	19.30	83.56	103.17	192.92	33.10	36.27	144.77
20	100.60	117.24	19.32	86.28	106.52	199.79	33.84	37.64	148.78
21	103.66	121.51	19.34	88.87	109.72	206.43	34.53	38.97	152.57

Note: 1 - average values.
2 - population to vehicle ratio.

Table 3.3 Sensitivity analysis on buildup algorithm. (medium impervious area, subcatchment # 7, pollutant DD).

Days	average values	wind vel. km/h. (8.3)[1]		wind freq. (0.44)[1]		vehicle speed km/h. (30.0)[1]		PVR[2] (0.5)[1]	
		3	90	0.05	0.60	15	90	0.1	0.9
1	0.13	0.13	0.09	0.12	0.12	0.25	0.04	0.03	0.22
2	0.25	0.25	0.16	0.24	0.25	0.49	0.08	0.058	0.44
3	0.36	0.38	0.21	0.36	0.37	0.72	0.13	0.086	0.64
4	0.48	0.50	0.24	0.47	0.48	0.95	0.17	0.11	0.85
5	0.59	0.62	0.26	0.58	0.60	1.17	0.21	0.13	1.04
6	0.70	0.74	0.28	0.68	0.70	1.38	0.24	0.16	1.22
7	0.80	0.85	0.29	0.78	0.81	1.58	0.28	0.18	1.40
8	0.90	0.97	0.30	0.88	0.91	1.78	0.31	0.21	1.58
9	1.00	1.08	0.31	0.97	1.01	1.97	0.35	0.23	1.74
10	1.09	1.19	0.32	1.06	1.10	2.16	0.38	0.25	1.90
11	1.18	1.30	0.30	1.15	1.19	2.34	0.41	0.27	2.06
12	1.27	1.41	0.33	1.32	1.37	2.68	0.47	0.32	2.36
13	1.35	1.51	0.33	1.32	1.37	2.68	0.47	0.32	2.36
14	1.44	1.62	0.33	1.40	1.45	2.85	0.50	0.34	2.50
15	1.52	1.72	0.33	1.48	1.53	3.01	0.52	0.35	2.64
16	1.59	1.82	0.33	1.55	1.61	3.16	0.55	0.37	2.77
17	1.67	1.92	0.33	1.63	1.69	3.31	0.57	0.39	2.90
18	1.74	2.02	0.33	1.70	1.76	3.46	0.60	0.41	3.02
19	1.81	2.12	0.33	1.77	1.83	3.60	0.62	0.43	3.14
20	1.88	2.21	0.33	1.84	1.90	3.74	0.64	0.44	3.26
21	1.95	2.31	0.33	1.90	1.97	3.88	0.66	0.46	3.37

Note: 1 - average value.
2 - population to vehicle ratio.

Table 3.4 Sensitivity analysis on buildup algorithm. (pervious area, subcatchment # 5, pollutant DD).

Days	average values	wind vel. km/h (8.3)[1]		wind freq. (0.44)[1]		vehicle speed km/h. (30.0)[1]		PVR[2] (0.5)[1]	
		3	90	0.05	0.60	15	90	0.1	0.9
1	1.34	1.36	0.99	1.11	1.44	2.43	0.64	0.48	2.19
2	2.63	2.71	1.70	2.17	2.82	4.77	1.21	0.95	4.29
3	3.88	4.01	2.20	3.20	4.15	7.03	1.76	1.40	6.30
4	5.07	5.29	2.56	4.19	5.43	9.20	2.29	1.84	8.22
5	6.22	6.53	2.82	5.13	6.66	11.30	2.80	2.26	10.05
6	7.32	7.75	3.00	6.05	7.84	13.30	3.28	2.67	11.81
7	8.39	8.95	3.14	6.93	8.98	15.29	3.73	3.07	13.50
8	9.41	10.12	3.23	7.77	10.08	17.19	4.17	3.45	15.11
9	10.40	11.27	3.29	8.59	11.14	19.02	4.58	3.82	16.66
10	11.36	12.40	3.34	9.38	12.17	20.80	4.98	4.18	18.15
11	12.28	13.50	3.38	10.14	13.15	22.51	5.35	4.53	19.58
12	13.17	14.59	3.41	10.88	14.11	24.18	5.71	4.87	20.95
13	14.03	15.65	3.43	11.59	15.03	25.79	6.06	5.20	22.27
14	14.86	16.70	3.44	12.27	15.92	27.35	6.38	5.52	23.54
15	15.66	17.73	3.45	12.93	16.78	28.87	6.70	5.83	24.76
16	16.44	18.74	3.46	13.58	17.61	30.34	7.00	6.13	25.93
17	17.19	19.73	3.47	14.20	18.41	31.77	7.28	6.43	27.06
18	17.91	20.71	3.47	14.80	19.19	33.15	7.56	6.71	28.15
19	18.62	21.67	3.48	15.38	19.94	34.49	7.82	6.99	29.20
20	19.30	22.61	3.48	15.94	20.67	35.80	8.07	7.26	30.21
21	19.75	23.54	3.48	16.48	21.38	37.06	8.31	7.52	31.11

Note: 1 - averge values.
2 - population to vehicle ratio.

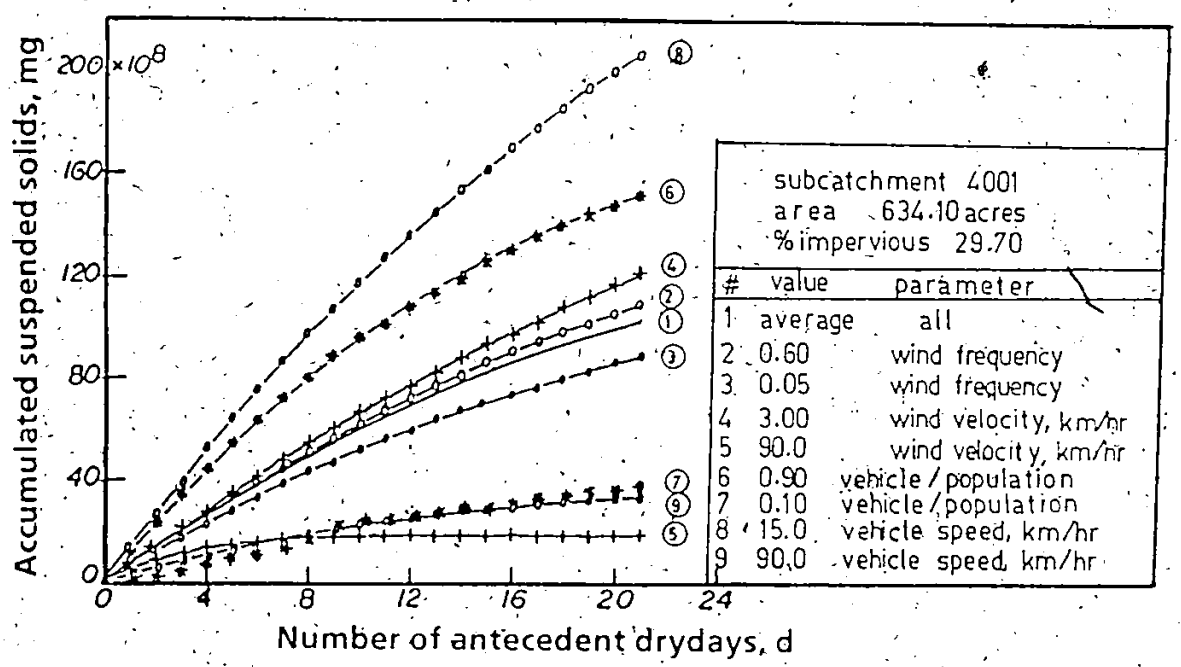

Figure 3.3 Sensitivity analysis on new buildup algorithms.

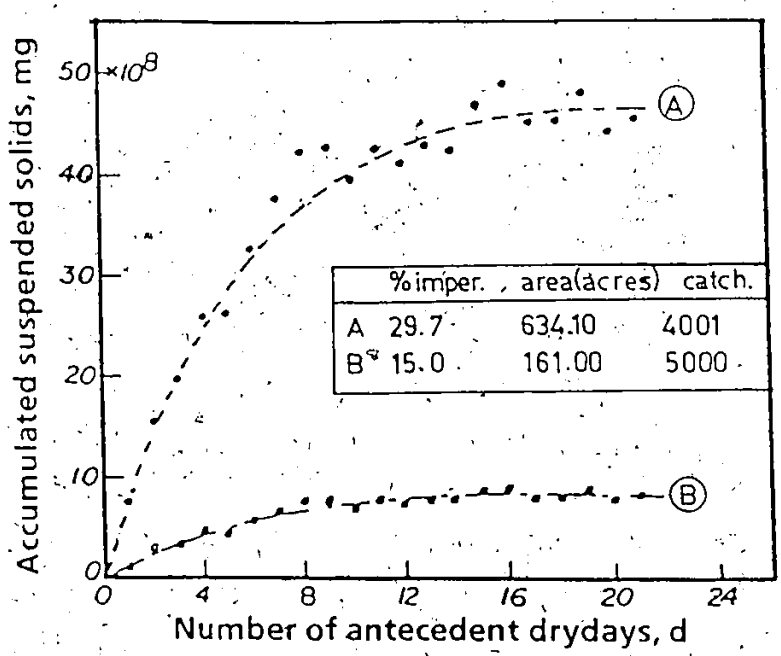

Figure 3.4 Dust and dirt buildup under random wind velocity and frequency.

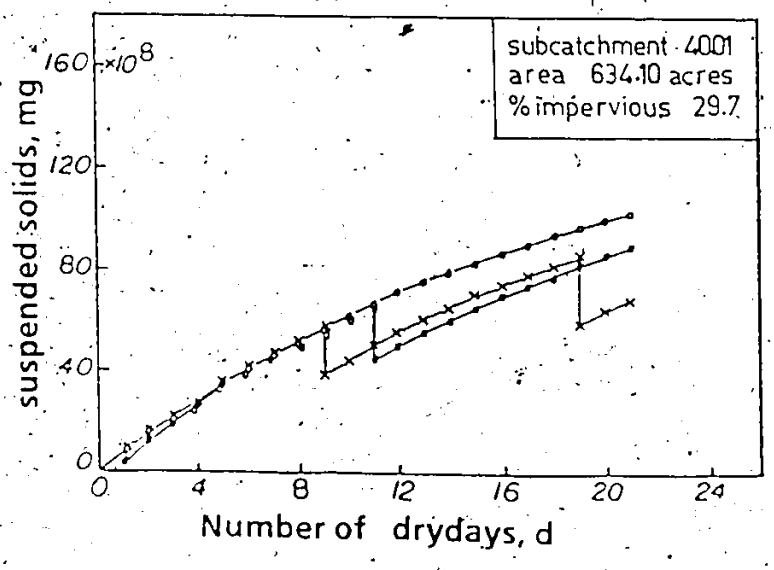

Figure 3.5 Effect of street cleaning frequency on DD accumulation.

PART 2

POLLUTANT WASHOFF

CHAPTER IV

POLLUTANT WASHOFF FROM IMPERVIOUS AREAS

4.1. Introduction:

Pollutants which accumulate on effectively impervious areas after the complex processes of addition and removal described in Part 1 are further removed during wet and dry periods respectively by overland flow and intentional removals such as regular street cleaning operations. The purpose of street cleaning operations is to control the quantity of pollutants entering a water body. Since the potential for pollution depends on the smaller size particles present, the type of cleaning equipment and cleaning method are important. Street cleaning removes 20 to 60% of the solids. The remaining solids continue to buildup, until the next cleaning operation or storm occurrence.

4.2. Literature review:

Washoff is the process of removing DD from the accumulated effective impervious areas by storm runoff. Washoff depends mainly on hydrodynamic forces acting on a grain or an aggregate of particles of a cohesive or noncohesive DD. Amount of material available to washoff and transport capacity of the runoff dictates the total quantity

to be washed off. In urban areas, material available on the impervious area to washoff is equal to material accumulated over a dry day period. Hence, washoff rate is mostly limited by the accumulated quantity rather than transport capacity of runoff water. The washoff experiments conducted by Sartor and Boyd (1972) were perhaps the first step in defining the washoff equation as an exponential (detail analysis is given in section 4.2.2). Since then, exponential washoff of DD has become more common in urban runoff quality modelling.

The exponential washoff equation (Sartor and Boyd, 1972) is empirical. The only driving force in the equation is runoff rate. But washoff of DD in an urban area is dominated by the rain impact, overland flow rate and number of moving vehicles during the storm. It would be more realistic to include terms for the shear stresses caused by these processes, making it semi-empirical in nature rather than empirical.

4.2.1. Rain impact: Rain drops, varying in size, fall on the surface and cause a splatter of dust and dirt particles in the solid aggregates which are then carried away by surface runoff. Measurments made by Hudson (1964) and Blanchard (1950) showed that the biggest raindrops are approximately 5 mm. in diameter. Raindrops greater than this will split into smaller drops. Regional low intensity

precipitation usually comprises small drops, whereas high intensity rainfall events are usually characterised by drops of much larger diameter. Figure 4.1 presents the relation between raindrop size and rainfall intensity (Hudson 1964).

Raindrop velocity is affected by gravity, and by the resistance of the air. A raindrop falls freely under the force of gravity and is accelerated until the frictional resistance of the air is equal to the gravitational force at a constant velocity. This terminal velocity depends upon the size and shape of the raindrop. Figure 4.2 presents the relationship between terminal velocity and drop diameter (Laws, 1941).

The kinetic energy of raindrops is of fundamental importance to the washoff process. Raindrops impinging on the soil surface break down the soil aggregates and detach the soil particles splashing them short distances and increasing the turbulence of overland flow. The relation between kinetic energy and intensity of rainfall is shown in Figure 4.3.

To determine the energy flux, detailed information on the distribution of raindrops is required. Since data on raindrop size distributions are not typically available on an event basis, it would be desirable to be able to estimate rainfall energy from commonly measured variables such as rainfall intensity and total precipitation. This may be

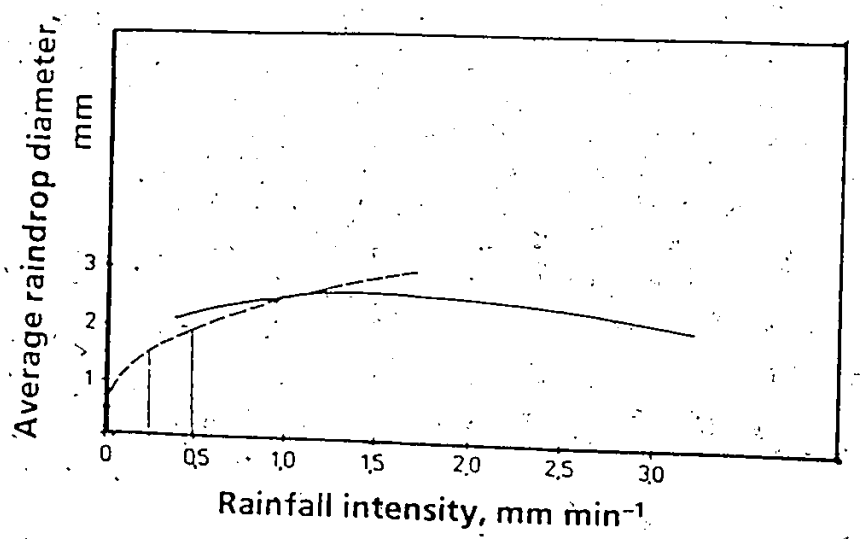

Figure 4.1 Relation between the average diameter of raindrops and rainfall intensity.

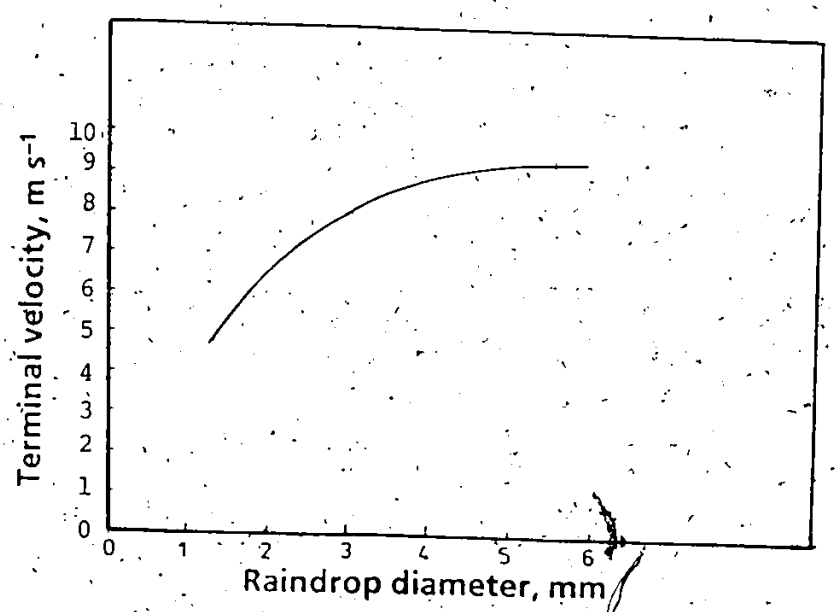

Figure 4.2 Relation between raindrop velocity and raindrop diameter.

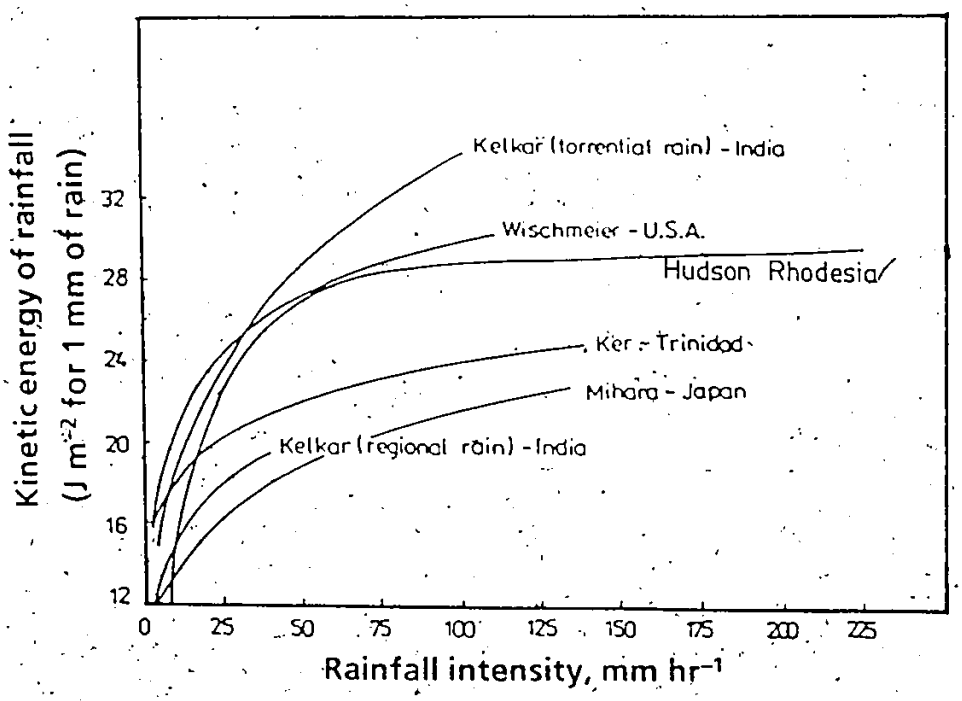

Figure 4.3 Relation between rainfall kinetic energy and rainfall intensity.

obtained by calculating the energy content of storms from available drop size data and parameterizing the resulting relation. Wischmeier and Smith(1965), and Quimpo and Brohi (1983) developed equations [4.1] and [4.2] respectively for drop kinetic energy per unit area per unit depth of rainfall

$$E = 12.1 + 8.9 \ln(I) \qquad [4.1]$$

where: E = energy per unit area per unit depth, t-m/ha-mm,

I = intensity of rainfall, mm/h.

$$\ln(Es) = 2.32 + 1.2 \ln(I) \qquad [4.2]$$

where: Es = energy per unit area per unit depth, ergs/cm^2-mm.

4.2.2. Overland flow impact: Overland flow transports the particles already detached by raindrops. The tangential stress of overland flow detaches further particles and chemical substances for transportation. Sartor and Boyd (1972) were perhaps the first to use a rain simulator for investigating washoff of pollutants from streets. A portable simulator with small jets, 0.018 inch in diameter, was used to spray water 4 to 8 feet high to simulate moderate to heavy rainfall. Samples were collected at every 15 minutes for a total period of 2.25 hours for generated intensities of 0.2 and 0.8 inch/h from three typical surfaces: new asphalt, old asphalt and concrete. The results are shown for total solids in Figure 4.4. The study concluded that the rate of washoff depends on storm

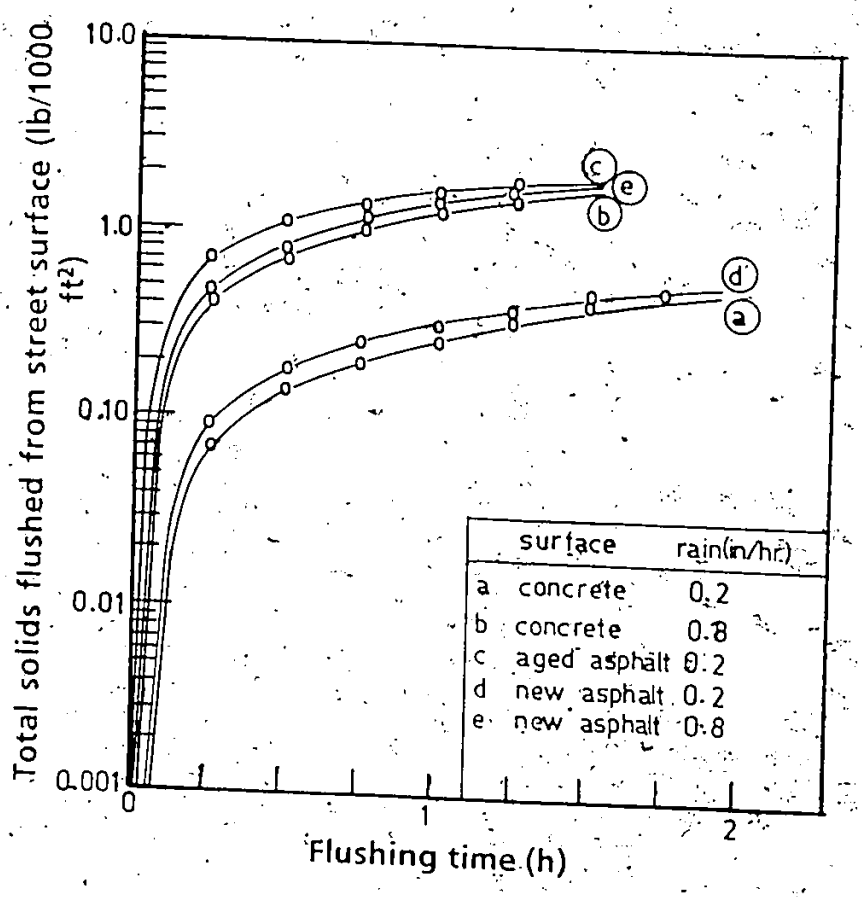

Figure 4.4 Particle transport across street surfaces by particle size, street character and rainfall intensity (Sartor and Boyd, 1972).

intensity, street surface characteristics and particle size. A simple exponentiaal decay equation for washoff was formulated as (Sartor and Boyd, 1972):

$$L = L_0(1 - e^{-kt}) \qquad [4.3]$$

where: L = cumulative weight of material of a given particle washed off, kg/1000 m^2

L_0 = initial load of material of a given particle kg/1000 m^2

k = bR = proportionality constant, 1/h.

b = washoff coefficient, 1/mm.

R = runoff rate, mm/h.

t = time since beginning of runoff, h.

Generally, the value of the decay coefficient (washoff coefficient) b is held constant at 0.18 1/mm. This assumes that a uniform runoff of 0.5 inch per hour (12.7 mm/h) would washoff 90% of a constituent from effective impervious surfaces, regardless of duration and the uniformity of the runoff.

Several studies have reported that washoff coefficient b varies for different constituents and for different watersheds (Barkdoll 1975; Smith and Jennings 1979; Ellis and Sutherland 1979). Alley(1981) described an optimization technique for determining the best fit value of the decay coefficient for a storm or set of storms. The relationship of the optimal value of "b" to average runoff rate and total

runoff volume was investigated. No significant relationship between the optimized 'b' values and these storm variables was evident.

Donigian and Crawford (1976) developed an equation for washoff of sediment from an impervious area similar to that for a pervious area:

$$T = KQ_t^j \quad \text{for } T < L_t \qquad [4.4]$$

$$T = L_t \quad \text{for } T > L_t \qquad [4.5]$$

$$E = TF_o \qquad [4.6]$$

where: T = sediment transport for time interval t, t/ha.

Q_t = impervious area overland flow occuring in time interval t, mm.

K = impervious area coefficient of transport.

j = impervious area exponent of transport.

L_t = amount of material on the impervious surface, t/ha.

F_o = fraction of impervious overland flow reaching the stream in time t.

E = sediment loss to stream from impervious areas in time t, t/ha.

All other pollutants are specified as fractions of the sediment loss.

4.2.3. Vehicle induced washoff:

Solids removal from highways during wet periods is due to scrubbing of the pavement by mechanical energy from vehicles during the storm. In addition to this, washing of

the tires and chassis of vehicles also contributes pollutants. The energy transferred to the highway by 1300 vehicles per hour per lane is equal to the amount of energy imparted during a 0.5 in/h rainstorm (Asplund, et al. 1982). On high traffic volume sections of highways, this is probably the primary removal mechanism during low intensity rainfall periods. Studies conducted at ten sites by Asplund et al. (1982) in Washington State showed that a linear relationship exists between cumulative total suspended solids and cumulative vehicles during storms.

CHAPTER V

MODEL DEVELOPMENT - POLLUTANT WASHOFF

5.1. Existing washoff algorithm:

Most urban runoff models use an exponential decay relationship for describing pollutant washoff. The SWMM was one of the first to use this form of relationship (Metcalf and Eddy et al. 1971). The washoff algorithm used in SWMM2 (1971-77) and STORM (1974) is as follows:

$$P_{nj} = A_j L_{nj(t-1)} (1 - e^{-bR\Delta t}) \qquad [5.1]$$

$$L_{njt} = L_{nj(t-1)} - P_{nj} \qquad [5.2]$$

where: P_{nj} = quantity of pollutant 'j' washed off subcatchment 'n', mg.

$L_{nj(t-1)}$ = quantity of pollutant 'j' on subcatchment 'n', at timestep (t-1), mg.

L_{njt} = quantity of pollutant 'j' on subcatchment 'n' at timestep t, mg.

b = washoff coefficient, 1/mm.

Δt = timestep, h

A_j = availability factor, dimensionless.

R = runoff rate, mm/h

The availability factor for settleable solids is given by:

$$A_1 = 0.028 + \left(\frac{R}{25.4}\right)^{1.8} \qquad [5.3]$$

and for suspended solids:

$$A_2 = 0.057 + 1.4\left(\frac{R}{25.4}\right)^{1.1} \qquad [5.4]$$

where: R = runoff rate mm/h.

The maximum value for the availability factor is 1.0 for all pollutants. The concept of an availability factor was introduced into SWMM when modelling water quality for Laguna Street, San Francisco. Though it was originally site specific, the availability factor was still used in SWMM.

The SWMM3 washoff algorithm for computing pollutant concentration is an improvement over SWMM2 (Huber et al. 1981). In SWMM2 concentration always decreased with time since the runoff rate R is cancelled out in the equation and the quantity remaining Pn,j continues to decrease:

$$C = \frac{1}{Q}\frac{d}{dt}(P_{nj}) \qquad [5.5]$$

or

$$C = \frac{const}{AR} bRP_{nj} \qquad [5.6]$$

where: C = concentration of pollutants

Q = flow rate = AR, m^3 /h

A = subcatchment area in ha.

R = runoff rate, mm/h.

$P_{n,j}$ = quantity of pollutant j available for washoff from catchment n, mg.

b = washoff coefficient, 1/mm.

In SWMM3 (1981) this problem was rectified by setting washoff rate at each time step proportional to the runoff

rate raised to the power W as follows:

$$\frac{d}{dt}(P_{nj}) = -C_f R^W P_{nj} \qquad [5.7]$$

where: P_{nj} = constituent available for washoff at time t, mg

C_f = washoff coefficient, $(mm/h)^{-W} s^{-1}$.

W = exponent.

R = runoff rate, mm/h.

The concentration of any constituent is proportional to R^{W-1}. Hence, an increase in runoff rate results in an increase in the constituent concentration.

The Quantity Quality Simulation model (QQS) uses washoff algorithms which are based on the unit hydrograph method (Geiger and Dorsch, 1979):

$$P_t = R_n D_i U_{n-1} I \Delta t \qquad [5.8]$$

where: P_t = pollutant washed off at time t, kg/ha.

t = time since start of effective precipitation, min.

n = t/5

R_n = rainfall duration factor, dimensionless. (1.0 at the beginning and decreases to 0.2 within one hour)

D_i = diurnal variation factor at time of the day d, dimensionless, varies from 0.7 to 1.0

U_{n-1} = transformation function, kg/ha-mm

I = effective precipitationn, mm/5 min

Δt = time step.

HSP-F treats washoff from impervious areas similar to pervious areas as follows:

$$T_s = K_o O_V^J \qquad \text{for } T_s < L_t \qquad [5.9]$$

$$T_s = L_t \qquad \text{for } T_s > L_t \qquad [5.10]$$

$$E_i = T_s F_0 \qquad [5.11]$$

where: T_s = sediment transport for time interval t, t/ha.

O_V = impervious area overland flow occuring in time interval t, min.

K_o = impervious area coefficient at transport.

L_t = amount of material on the impervious surface, t/ha.

F_0 = fraction of impervious overland flow reaching the stream.

E_i = sediment loss to stream from impervious area, t/ha.

The remaining pollutants are taken to be a fraction of the sediment lost.

5.2. Modified washoff equation:

The review of existing formulations for DD washoff from impervious areas indicated that washoff equations are more empirical rather than process oriented. The writer has now attempted to develop process oriented semi-empirical algorithms to permit modelling of managment strategies for runoff water quality.

Washoff of DD is affected by the following factors: raindrop sizes; drop splash and bounce; surface tension; depth of overland flow; raindrop momentum; shearstress at the water surface due to wind and raindrops; shearstress at the bottom surface of water due to overland flow; and shear stress induced by the moving vehicles during storm. The kinetic energy of a raindrop is one of the important factors in washoff. As disscussed in section 4.2.1, raindrop size increases with the intensity of rain and the velocity of the drop increases with the mass. The kinetic energy is proportional to the intensity of rainfall, and drop size. Since, information on kinetic energy of drop mass and drop size distribution is not easily available washoff may be directly related to rainfall intensity. The breakdown of DD aggregates and transport by splashing is reduced with increased overland flow depth. Under these conditions, drop kinetic energy helps keep the solids in suspension, and splashing and splitting of raindrops helps advect the solids from one place to another.

Increased overland flow due to the increased rainfall intensity increases overland flow momentum and bed shear stress which in turn ultimately accelerates the erosion process. This process dominates over rainfall impact after sufficient depth of overland flow is attained. The momentum balance should include terms for external forces (wind, raindrop and bed friction) as well as internal

hydrostatic forces (ground surface and water surface slopes). The overall schematic is shown in Figure 5.1 and a general equation may be formulated as follows:

Let V_{dx} be the resultant drop velocity with a intensity of rainfall i, hitting the surface at an angle θ. The horizontal component of raindrop velocity is:

$$v_{dx} = v_{dr} \cos\theta \qquad [5.12]$$

Force = (mass) (change in velocity)

Force due to rain drop/unit mass $= i A \rho v_{dx}/y A \rho = i(v_{dx} - v_w)/y$ [5.13]

where:

i = excess rainfall, cm/s.

y = depth of water, cm

v_{dx} = drop velocity component in x direction, cm/s.

ρ = mass density of water, g/cm^3

A = area, cm^2

Force induced due to rain drop shear stress/unit mass $= \frac{\tau_i A}{\rho y A} = \frac{\tau_i}{\rho y}$ [5.14]

Force induced due to wind shear stress at the top of the flow/unit mass $= \frac{\tau_w A}{\rho A y} = \frac{\tau_w}{\rho y}$ [5.15]

Force due to bed shear/unit mass $= \frac{-\tau_b A}{\rho A y} = \frac{-\tau_b}{\rho y}$ [5.16]

Using the continuity principle

$$i = \frac{\partial y}{\partial t} + \frac{\partial}{\partial x}(v_w y) \qquad [5.17]$$

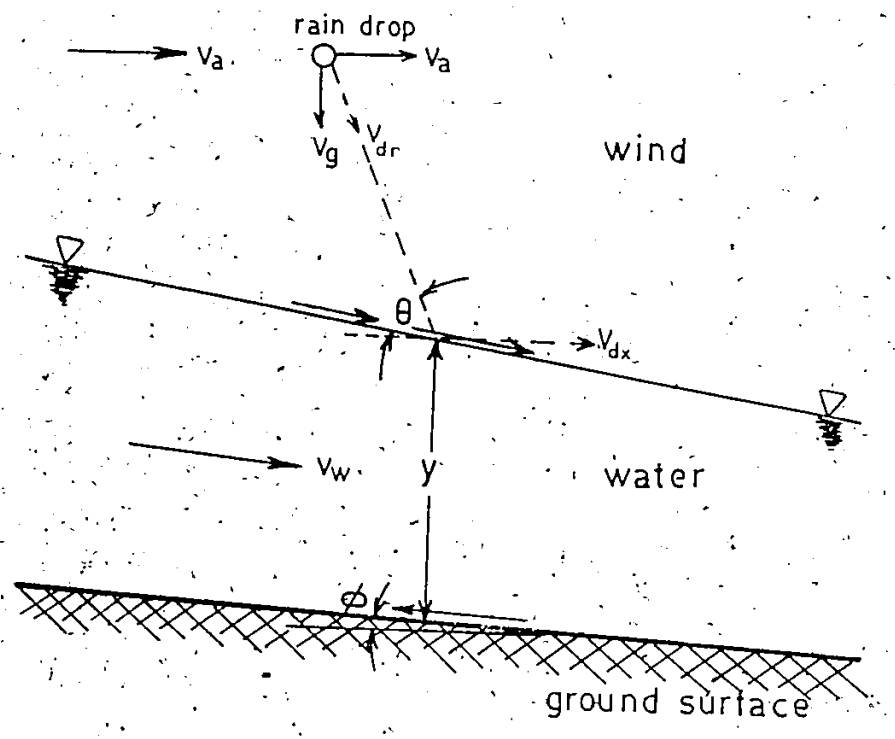

Figure 5.1 Schematic diagram for pollutant washoff.

$$i = \frac{\partial y}{\partial t} + v_w \frac{\partial}{\partial x}(y) + y \frac{\partial}{\partial x}(v_w) \qquad [5.18]$$

or $i = \frac{\partial y}{\partial t} + \frac{\partial q}{\partial x}$, where $q = v_w y$, and

i = effective or "excess" rainfall.

Considering force per unit mass of overland flow, the total summation of all the forces must be equal to zero. A general equation for the forces could be written as:

local force/unit mass due to acceleration of overland flow + force/unit mass due to convective flow + change of momentum due to rain + force/unit mass due to change in water level

+ force/unit mass due to wind shear in direction of flow + force/unit mass due to rain drop momentum in direction of flow + force/unit mass due to surface friction due to rain drops

= force/unit mass due to shear at the bottom of the flow + force/unit mass due to surface slope at gravitational forces.

The usual term is $\frac{\partial v_w}{\partial t} + v_w \frac{\partial v_w}{\partial x} + i \frac{v_w}{y} + g \frac{\partial y}{\partial t} = - \frac{\tau_b}{\rho y} + g \phi$

thus

$$\frac{\partial}{\partial t}(v_w) + v_w \frac{\partial}{\partial x}(v_w) + i \frac{v_w}{y} + g \frac{\partial(y)}{\partial x} - \frac{\tau_w}{\rho y} - \frac{i}{y}(v_{dx} - v_w) + \frac{\tau_i}{\rho y} = - \frac{\tau_b}{\rho y} + g \phi \qquad [5.19]$$

where: v_w = mean horizontal velocity of the overland flow cm/s

t = time in s.

x = horizontal distance in the x-direction, cm

i = excess intensity of rainfall, cm/h

$$i = \frac{\partial y}{\partial t} + v_w \frac{\partial}{\partial x}(y) + y \frac{\partial}{\partial x}(v_w) \qquad [5.18]$$

or $$i = \frac{\partial y}{\partial t} + \frac{\partial q}{\partial x}$$, where $q = v_w y$, and

i = effective or "excess" rainfall.

Considering force per unit mass of overland flow, the total summation of all the forces must be equal to zero. A general equation for the forces could be written as:

local force/unit mass due to acceleration of overland flow + force/unit mass due to convective flow + change of momentum due to rain + force/unit mass due to change in water level

+ force/unit mass due to wind shear in direction of flow + force/unit mass due to rain drop momentum in direction of flow + force/unit mass due to surface friction due to rain drops

= force/unit mass due to shear at the bottom of the flow + force/unit mass due to surface slope at gravitational forces.

The usual term is $\frac{\partial v_w}{\partial t} + v_w \frac{\partial v_w}{\partial x} + i \frac{v_w}{y} + g \frac{\partial y}{\partial t} = -\frac{\tau_b}{\rho y} + g\phi$

thus

$$\frac{\partial}{\partial t}(v_w) + v_w \frac{\partial}{\partial x}(v_w) + i \frac{v_w}{y} + g \frac{\partial(y)}{\partial x} - \frac{\tau_w}{\rho y} - \frac{i}{y}(v_w - v_w) + \frac{\tau_b}{\rho y} = -\frac{\tau_b}{\rho y} + g\phi \qquad [5.19]$$

where: v_w = mean horizontal velocity of the overland flow - cm/s

t = time in s.

x = horizontal distance in the x-direction, cm

i = excess intensity of rainfall, cm/h

y = depth of overland flow, cm

τ_w = wind shear stress on the water air, g/cm^2

ρ = density of water, g/cm^3

τ_i = shear stress due to rain drop, g/cm^2

τ_b = bed shear stress, g/cm^2

g = acceleration due to gravity, cm/s^2

ϕ = surface slope.

Vehicles moving over the road during the storm also induce momentum changes in the overland flow. This should be added to the total momentum budget. Equation [5.19] is not considered in any of the urban runoff models known to the writer to obtain a general equation for pollutant washoff from impervious areas. An order of magnitude analysis is required to find the effect of individual terms in equation [5.19]. It is expected that the effect of wind and rain in the total momentum budget is considerable. In view of the nonavailability of individual process data and complexity of the problem in the real washoff situation, semi-empirical equations were developed for raindrop, overland flow and moving vehicles by the present writer. The formulation of this washoff algorithm is now discussed in detail.

The rainfall impact on accumulated DD over an impervious area increases with increasing storm intensity and decreases exponentially with increased depth of runoff.

Overland flow absorbs a certain amount of drop energy. This process may be formulated as:

$$r_i = K_1\left(\frac{I}{25.4}\right)^{K_2} e^{-\left(\frac{R}{25.4}\right)W_1} \qquad [5.20]$$

where: r_i = rain impact component, 1/h.

K_1 = constant, in empirical units, usually = 1.0

K_2 = rain impact exponent = 2.0

I = rain intensity, mm/h.

W_1 = drop energy damping exponent, h/mm.

R = runoff rate, mm/h.

Particles dislodged by the rainfall impact are then transported further by the overland flow. The tangential stress of overland flow also detaches particles from the surface. Rainfall impact on overland flow helps the solids to stay in suspension. This process could be formulated similar to SWMM3 as:

$$O_i = C_f\left(\frac{R}{25.4}\right)^{W_2} \qquad [5.21]$$

where: O_i = overland flow washoff component, 1/h

C_f = washoff coefficient in empirical units

W_2 = washoff exponent.

R = runoff rate, mm/h.

Suspension of solids in runoff depends mainly on the turbulence created by the rain impact and on the number of vehicles moving on the street during the storm period. In

addition to creating turbulence, vehicles scrub the pavement. The total solids removal by vehicles is linearly related to the total number of vehicles during the storm (VDS) on the street. This relationship can be written as:

$$V_i = W_3 N \frac{R}{25.4} \qquad [5.22]$$

where: V_i = vehicle induced washoff component, 1/h.

W_3 = vehicle washoff constant, 1/in per 1000 veh.

N = number of vehicles in thousands,

R = runoff rate, mm/h.

The above three individual processes are aggregated to derive the total washoff coefficient:

$$P_W = (r_i + O_i + V_i)t \qquad [5.23]$$

$$P_L = P_0 \left[\frac{1}{1 + P_W^n} \right] \qquad [5.24]$$

where: P_L = solids remaining after washoff at time t, mg.

P_W = total washoff coefficient, 1/h.

P_0 = solids accumulated on the impervious area, mg.

t = time, h.

n = washoff exponent = 0.8

r_i = rain impact component, 1/h

O_i = overland flow washoff component, 1/h

V_i = vehicle induced washoff component

Finally, washoff of pp during the time interval 't' is given by:

$$P_t = P_0 - P_L \qquad [5.25]$$

The constants W_1, W_2, and W_3 were obtained by calibrating the modified washoff equation against Sartor and Boyd's experimental data. The calibrated and experimental curves are shown in Figure 5.2. The discrepancy in the results may be due to the nonavailability of information on vehicle numbers during the experimental period. For the purpose of calibration it was assumed that 1500 vehicles pass during the storm period. The calibrated values derived for W_1, W_2 and W_3 were 1.1, 4.5 and 2.5 respectively. Equation [5.20] to [5.24] were coded by the writer and the new algorithms is called CHGWASH herein.

5.3. Sensitivity test on the CHGWASH:

The calibrated CHGWASH algorithm was further subjected to sensitivity analysis. The sensitivity of the overall washoff of pollutant to W_1, W_2, W_3 was investigated using a small test catchment (10 acres in area and 100 percent imperviousness) and a constant rainfall intensity of 1.5 inch/h. The results are given in Table 5.1, and also plotted in Figures 5.3, 5.4 and 5.5. The sensitivity analysis indicated that the total washoff is more sensitive to constant W_2 than W_1 and W_3.

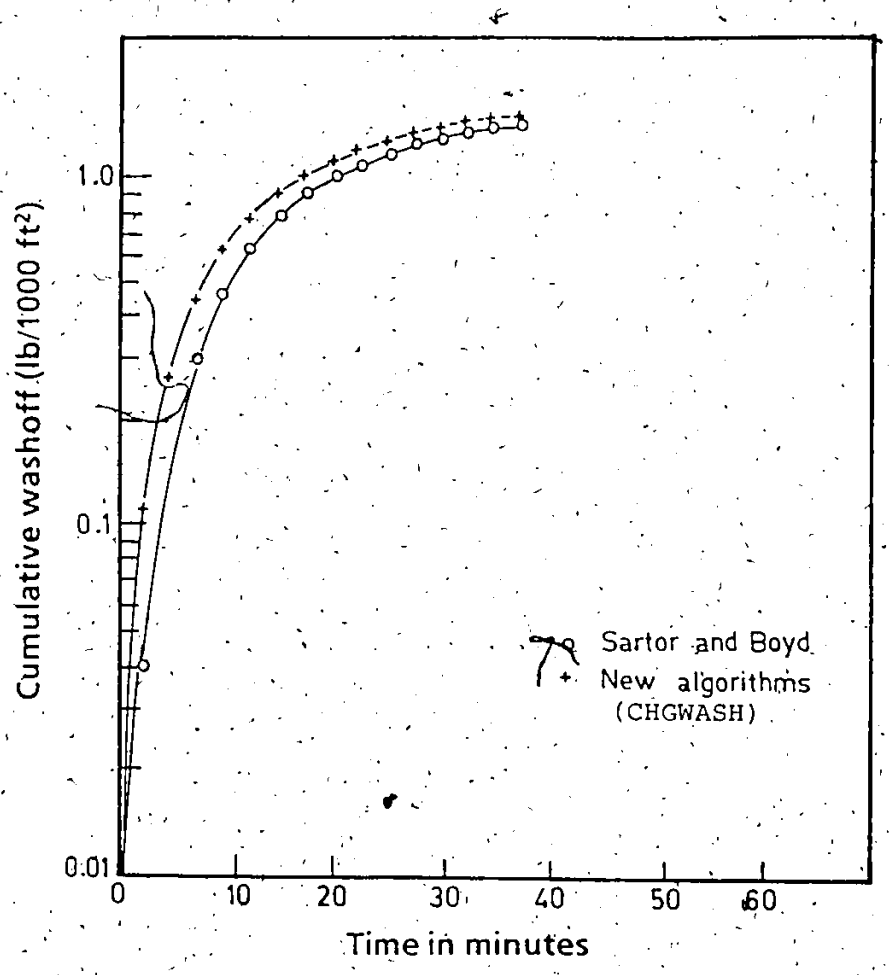

Figure 5.2 Comparison of cumulative washoff of pollutants between calibrated and Sartor and Boyd data.

Table 5.1 Sensitivity to washoff constants W_1, W_2, W_3 (constant rainfall intensity of 1.5 inch/h for 25 minutes).

W_1	W_2	W_3	Total % of BOD washed off	Remarks
1.1	4.5	2.5	96.5	calibrated values
0.5	4.5	2.5	97.0	
2.5	4.5	2.5	96.0	
5.0	4.5	2.5	95.0	
10.0	4.5	2.5	94.0	
1.1	0.1	2.5	80.0	
1.1	1.0	2.5	86.3	
1.1	2.0	2.5	90.0	
1.1	9.0	2.5	99.5	
1.1	4.5	0.05	92.0	
1.1	4.5	0.5	93.0	
1.1	4.5	1.5	95.0	
1.1	4.5	5.0	98.6	

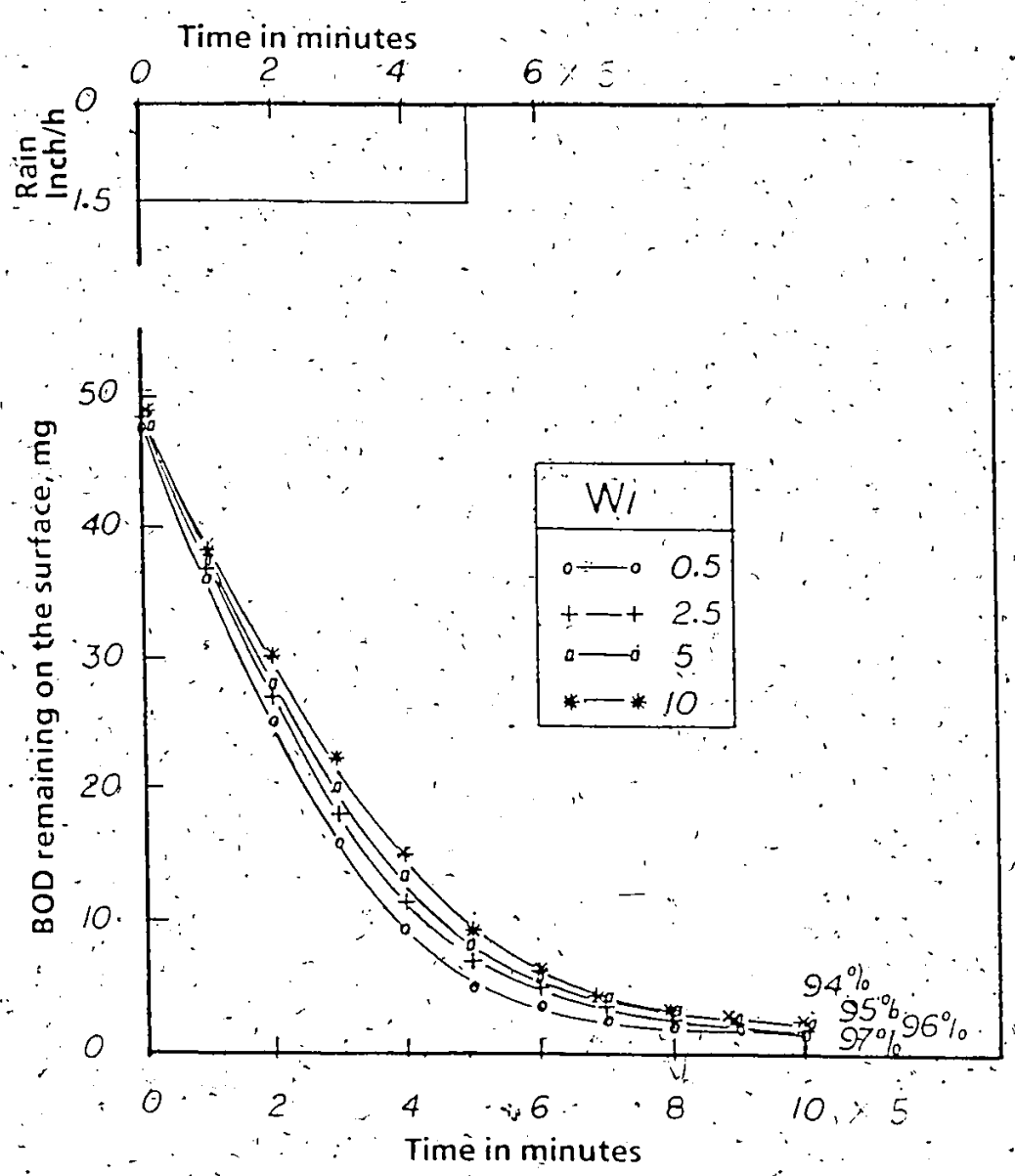

Figure 5.3 Sensitivity analysis for washoff constant W_1.

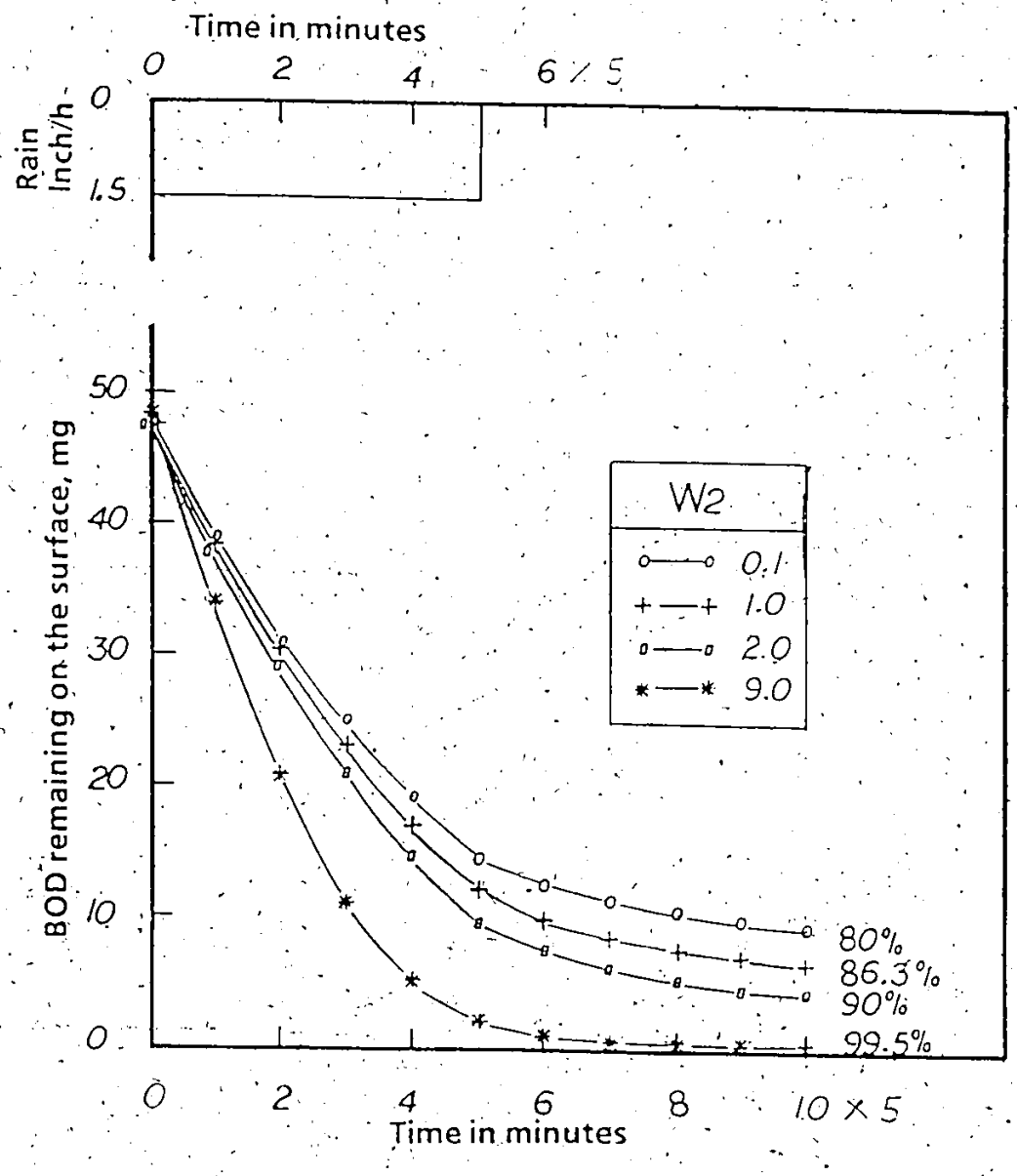

Figure 5.4 Sensitivity analysis on washoff constant W_2.

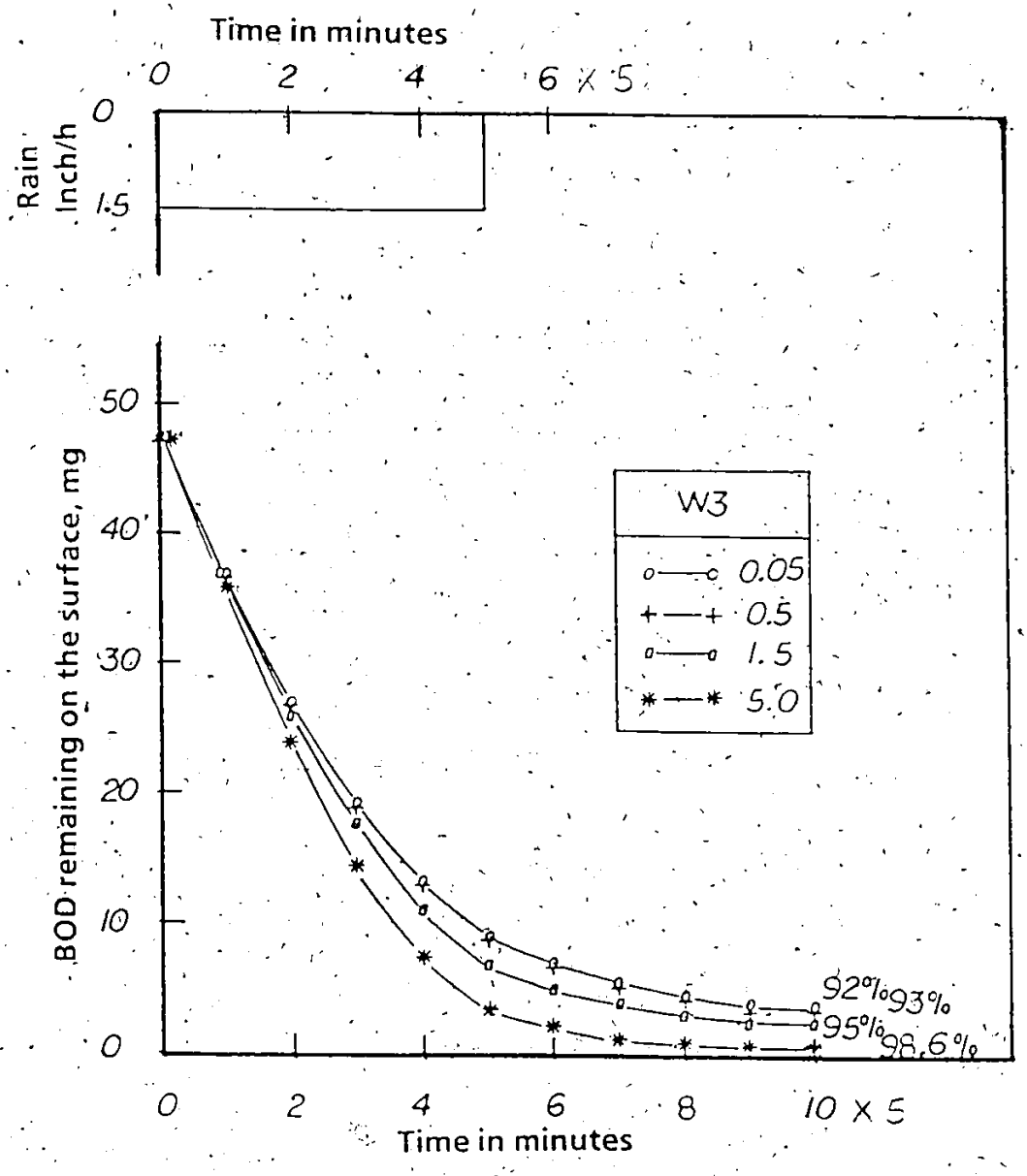

Figure 5.5 Sensitivity analysis on washoff constant W_3.

CHAPTER VI

ALGORITHMS FOR MINOR PROCESSES.

6.1. Pollutant scavenging

The removal of aerosols and gaseous pollutants present in the atmosphere by scavenging is dependent upon the rate of pollutant attachment to the falling raindrop and the pollutant flux at the ground. The basic mathematical concepts of precipitation scavenging are presented in the next two sections.

6.1.1. Scavenging of Aerosol Particles by Precipitation:

The general formulation for scavenging of aerosol particles considers the amount of contaminant per unit volume 'χ', associated with particulates of radii 'a' to 'a + da' (Slinn 1977):

$$\frac{D\chi}{Dt} = K \cdot \nabla^2\chi - \psi\chi + G\chi - L(\chi) \qquad [6.1]$$

where: $\frac{D}{Dt} = \frac{\partial}{\partial t} + V \cdot \nabla$ is the total time derivative

V = wind speed, m/s.

K = turbulent diffusivity, m^2/s

Ψ = precipitation scavenging rate coefficient, 1/s.

G, L = gain and loss of contaminant associated with particles because of condensation, evaporation, coagulation etc.) 1/s

χ = amount of contaminant per unit volume, mg/m^3

t = time in s.

By averaging over all particle sizes, equation [6.1] becomes:

$$\frac{D\chi_t}{Dt} = K \cdot \nabla^2 \chi_t - \overline{\Psi}(z,t)\chi_t \qquad [6.2]$$

where: $\chi_t = \int_0^\infty \chi(z,t;a)\,da$ the total contaminant density.

The particle average removal rate:

$$\overline{\Psi}(z,t) = \int_0^\infty \frac{\chi\Psi(z,t;a)}{\chi_t}\,da \qquad [6.3]$$

The subscripts z, a and t are elevation, particle radius and time respectively.

In developing equation [6.2] from [6.1] particles are assumed to be subjected to homogenous turbulence and use has been made of the observation that in all processes contributing to gain (G) and loss (L) the contaminant is not lost from the space volume. If equation [6.2] is integrated over a large enough volume of space, so that no contaminant is convected from the volume by the wind, then use of the divergence theorem ($\nabla \cdot V = 0$) and ignoring dry deposition leads to:

$$\frac{\partial Q_t}{\partial t} = -\langle \overline{\Psi}(t) \rangle Q_t \qquad [6.4]$$

where the total amount of contaminant present per unit area is:

$$Q_t = \int \chi_t(z,t)\,dz \qquad [6.5]$$

and the space and particle average removal rate is:

$$<\overline{\Psi}(t)> = \int \frac{\overline{\Psi}(z,t)\chi_t(z,t)}{Q_t} dz \qquad [6.6]$$

for the case that $<\overline{\Psi}>$ is time independent. Then the total contaminant present per unit area in the atmosphere at time t is:

$$Q_t = Q_{to}\, e^{-<\overline{\Psi}>t} \qquad [6.7]$$

This is the equation used in many precipitation scavenging studies. The total contaminant removed from the atmosphere at time t is given by:

$$Q_t = Q_{to}(1 - e^{-<\overline{\Psi}>t}) \qquad [6.8]$$

where the rain scavenging rate Ψ is approximated (Slinn, 1974) by:

$$\Psi(a) \approx \frac{P(z,t)}{2R_m} E(a, R_m) \qquad [6.9]$$

where: E = collection efficiency, (collision efficiency multiplied by retention efficiency which is taken to be unity)

$P_{(z,t)}$ = precipitation rate at elevation 'z' and time 't' mm/s.

A suggested semi-empirical expression for the collection efficiency, which accounts for particle diffusion, interception and internal impaction (Slinn,1974), is

E = diffusion + interception + impaction.

$$E = \frac{4}{P_e}\left(1 + 0.4\, R_e^{1/2} S_c^{1/3}\right) + \frac{4a}{R}\left(\frac{a}{R} + \frac{1 + 2V\frac{a}{R}}{1 + V R_e^{-1/2}}\right) + \left(\frac{S - S_o}{S + C}\right)^{3/2} \qquad [6.10]$$

where: R_m = volume mean drop radius, m

P_e = Peclet number $= \frac{R_e V_t}{D}$

V_t = terminal drop velocity, m/s.

D = molecular diffusion coefficient, m^2/s.

R_e = Reynold's number $= \frac{R V_t}{\nu}$

R = rain drop radius, m.

ν = kinematic viscosity of air, m^2/s.

S_c = Schmidt number $= \frac{\nu}{D}$

V = ratio of dynamic viscosities, water to air $= \mu_w/\mu_a$

a = aerosol particle radius, m

S = Stoke's number $= \frac{tV_t}{R}$

S* = critical Stoke's number

$$\approx \frac{1.2 + \frac{1}{12}\ln(1+Re)}{1+\ln(1+Re)}$$

c = (2/3) - S*

The average flux of pollutant due to scavenging of aerosols over any interval of time t is given by :

$$Q = (Q_t - Q_{t-1})/t \qquad [6.11]$$

where: Q = average pollutant flux, mg/m^2-s.

Q_t and Q_{t-1} = pollutants concentration at time, t and t-1, mg

t = time, s.

6.1.2. Scavenging of Gases by precipitation:

The scavenging of gases by rain could be developed in a similar way to equation [6.1]: total removal rate

calculated by considering gases diffusing to each drop size and then integrating the expression over all drop sizes to obtain a total removal rate (Slinn 1976). Molecular diffusion to the drop or droplets will occur in accordance with the vapour pressure and solubilities of the free and collected gases (Junge 1963, Chamberlain and Chadwick 1966). Gas captured by a drop is quickly well-mixed with the fluid in the drop either because of internal circulation with a large ($\geq$ 1 mm) drop, or because of the relatively small volume to surface ratio of a small drop. Consider the initial concentration of the pollutant gas in the drop, say C (mg/litre). If irreversible chemical reactions during the short raindrop flight time are ignored, then the gas concentration changes according to:

$$V_t \frac{d}{dz}\left(\frac{4}{3}\pi R^3 C\right) = \frac{D}{R}\left[1 + 0.4\, R_e^{1/2} S_c^{1/3}\right] 4\pi R^2 (C_e - C) \qquad [6.12]$$

where C_e is the equilibrium concentration of the gas in the drop for the existing air concentration X , and C is the gas concentration in precipitation. For some gases, $C_e = HX$, where H is the solubility coefficient or Henry's law constant. The driving force is the difference between C_e and the actual concentration C. For $C > C_e$, the gas can be desorbed from the drop. The concentration of gas in the drop attains its equilibrium concentration, C_e, relatively rapidly, in less than 10 seconds (Postma,

1970; Hales, 1972). Consequently, it is reasonable to assume $C = C_e$ for a well mixed gas layer depth between 100 to 1000 m in height above the ground. Then the pollutant flux due to gas scavenging is given by:

$$D_g = I\,C_e \qquad [6.13]$$

where: D_g = surface deposition, mg/m^2-s.

I = the precipitation rate, m/s.

C_e = equilibrium concentration of gaseous pollutant in the drop = X_g/H

H = Henry's law constant.

X_g = pollutant concentration in the gas, mg/m^3

6.1.3. Scavenging algorithms:

The quantity of pollutant scavenged during a storm depends on the quantity available, intensity of rainfall, collection efficiency and the areal coverage of the storm. The scavenging rate of pollutant is exponential in nature (Randall et al. 1978, Slinn, 1977). The process may be simplified for modelling purposes, for interfacing with CHGQUAL. The algorithm for aerosol scavenging was formulated as:

$$S_c = S_o\,e^{-R_a t} \qquad [6.14]$$

where: S_c = quantity of aerosol remaining in the atmosphere at time t, mg

S_0 = quantity of aerosol present before the scavenging, mg.

R_a = rain scavenging rate constant, 1/s.

t = time, s

The quantity of aerosol present before the scavenging is calculated assuming a triangular distribution of pollutant concentration within the atmospheric mixing zone. The total mass is given by:

$$S_o = AHCF \qquad [6.15]$$

where: A = area of subcatchment, m^2

H = atmospheric mixing height, m

C = mean atmosphric aerosol concentration, mg/m^3

F = pollutant fraction in aerosol, mg/mg

Rain scavenging rate, as calculated by Slinn (1975) is:

$$R_a = \frac{1}{0.0045}\left(\frac{I}{25.4}\right)^{3/4} C_f \qquad [6.16]$$

where: I = intensity of rainfall, mm/h

C_f = collection efficiency, (10^{-2} to 10^{-1} for particle size 1-5 μm and drop radius 0.1 - 1.00mm; Slinn, 1977)

The rate of pollutant scavenging is obtained by differentiating equation [6.14]:

$$\frac{dS_c}{dt} = S_0 (-R_a) \cdot e^{-R_a t}$$

or:

$$P_s = -S_c \cdot R_a \qquad [6.17]$$

where: P_s = aerosol pollutant scavenging rate, mg/s

S_c = aerosol pollutant quantity remaining in the atmosphere, mg

R_a = rain scavenging rate, 1/s

The amount of gaseous pollutant absorbed into rain droplets depends on the pollutant concentration potential between the drop and the gas. The equilibrium concentration in the droplet is attained in a short period of travel and is assumed not to be rate limited. Therefore pollutant concentration is constant throughout the storm. The total pollutant quantity depends on the quantity of runoff and pollutant equilibrium concentration. Hence, gas scavenging is written as:

$$P_g = 1000\,Q\,C_q \qquad [6.18]$$

where: P_g = rate of gaseous pollutant added to the runoff water, mg/s

Q = runoff rate, m^3/s

C = equilibrium concentration, mg/l

1000 = conversion factor, m^3 to litre

6.2. POLLUTANTS WASHOFF FROM PERVIOUS AREAS:

Pollutants will buildup on both pervious and impervious areas during the interstorm periods. Atmospheric dustfall is distributed more or less equally on both types of surface, but other surface activities cause more pollutants buildup on impervious areas than to pervious areas. Impervious area buildup was discussed in detail in Chapter 2. In this section only pervious area contributions are discussed. Pervious areas may be bareland (unprotected) or vegetation (protected). Vegetated land collects more

atmospheric dust due to the canopy effect, where pollutants accumulate on leaves over the interstorm period, and are washed off during storms. In addition to this, direct leaching of dead and growing leaves also adds pollutants. Unprotected land contributes suspended solids and nutrients due to overland flow erosion, depending on the type of soil and intensity and duration of the storm.

6.2.1. Canopy washoff algorithms:

The leaf canopy provides an additional lodging area for atmospheric dust. The quantity of dust arrested in the canopy depends mainly on wind velocity and frequency, area density of leaves and atmospheric dust concentration. A detailed mathematical representation of canopy removal is given in section 2.3.2. A simplified formulation is developed in this section, suitable for adaptation to stormwater management modelling. Pollutant buildup in the canopy may be modelled by assuming a linear buildup over an interevent period using dustfall rates predicted by ATMDST for individual subcatchments. The canopy pollutants similarly may be washed off using an exponential relation between pollutant flux and storm intensity and duration. Of course, not all pollutants washed off the canopy will reach the overland flow because of soil infiltration and also because of filtration due to motion through vegetation. For these reasons it is often assumed that pollutants from

canopy washoff are not significant. Algorithms for simulating the canopy contribution may easily be developed as follows:

$$P_c = D t A E_f F \qquad [6.19]$$

where: P_c = total pollutant quantity on the canopy before the rain, mg

D = atmospheric dust, mg/eff.h-m^2

t = drydays, d

A = total canopy area, m^2

F = fraction of pollutants in atm. dust, mg/mg

E_f = number of effective hours, h (24 X wind frequency)

The quantity of pollutant remaining after wash off in the canopy is given by:

$$P_w = P_c \, e^{-C_1 I t/3600} \qquad [6.20]$$

where: P_w = quantity of pollutant remaining in the canopy after wash off at time t, mg

P_c = quantity of pollutant available initially on the canopy, mg

C_1 = canopy washoff constant (0.4), 1/mm

I = rain intensity, mm/h

t = time, s

Washoff rate in mg/s could be calculated by differentiating equation [6.20]:

$$P_r = \frac{-P_w}{3600} \cdot I \cdot C_I \qquad [6.21]$$

The concentration of pollutant in mg/l within the canopy is written as:

$$C_c = \frac{Pr}{IA} 3600 \qquad [6.22]$$

and pollutant flux to runoff water is given by:

$$F_c = C_c q \qquad [6.23]$$

where: F_c = pollutant flux in canopy, mg/s

C_c = pollutant concentration in canopy, mg/l

q = quantity of flow joining to runoff water, l/s

A = area of canopy, m^2

P_r = $d(P_w)/dt$, mg/s

6.2.2. Algorithms for erosion:

Erosion is caused by rainfall impact and the shear stress exerted on dislodged soil particulates by overland flow. Unprotected surfaces are subject to more erosion. A widely used empirical approach, the Universal Soil Loss Equation (USLE), has been adopted for use in SWMM and CHGQUAL. The USLE was developed by Wischmeier and Smith (1958) to estimate the average annual soil erosion from rainstorms for a given upland area. The average annual soil loss per unit area (tons per acre per year) is:

$$L = R_f K L_s C P \qquad [6.24]$$

where: R_f = the rainfall factor,

K = the soil erodibility factor,

L_s = the slope length gradient ratio,

$$L_s = L_m^{1/2} - 0.0076 + 0.53\,S + 7.6\,S^2$$

L_m = the length in feet from the point of origin of overland flow to the point where the slope decreases to the extent that deposition begins or to the point at which runoff enters a defined channel eg., gutter/pipe or inlet,

S = the average slope over the given runoff length, ft/ft

C = the cropping mangement factor or cover index factor, and

P = the erosion control practice factor.

The rainfall factor R in equation [6.24] is the product of the maximum thirty minute intensity and the sum of the rainfall energy for the time of simulation, i.e.

$$R_f = E_n R_t \qquad [6.25]$$

where:

R_t = maximum average 30 minute rainfall intensity for the storm (single event) or the period of simulation (continuous), inch/h

Rainfall energy may be written:

$$E_n = (9.16 + 3.31\,\ell n(I))\,I\,t \qquad [6.26]$$

where: E_n = total rainfall energy, 100 ft-t/ac,

I = rainfall intensity at the time interval, in/h

t = time interval, such that the product I and

t equals rainfall depth during the time interval.

6.3. Variable time step for single event simulation:

In Storm Water Management Models, constant timesteps are used, even for single event simulation. As is the case for all modelling, the longer the time step, the greater the deviation from reality but the smaller the computational cost. In CHGQUAL an attempt was made to reduce the computational cost without sacrificing accuracy by modifying the algorithms to accept variable timesteps. SWMM3 RUNOFF uses constant timesteps down to one minute for single event simulation. For small rainfall intensities, the timestep may not influence the runoff quality results but for intense rains, the computed pollutographs are sensitive to time step. A sensitivity analysis showed that computed concentrations are particularly sensitive to timestep during the initial period of washoff, so provision was made for smaller initial timesteps, e. g. one minute timesteps during the initial stage of a washoff event, and subsequently at user discretion, this may be changed to 5 minutes or to a larger integration period. Tests showed this improves accuracy without greatly increasing computation time. The detailed changes to the FORTRAN code are documented in the CHGQUAL User's Manual (Shivalingaiah and James, 1984).

PART 3

ROUTING AND FATE OF POLLUTANTS

CHAPTER VII

ROUTING AND FATE OF POLLUTANTS

7.1. POLLUTANT ROUTING IN SEWER NETWORK

7.1.1. Literature review:-

Pollutants washed off from impervious areas during a storm enter the waterbody through natural drainage or man-made sewer networks. Hydrographs and pollutographs undergo attenuation while flowing through conduits. The induced lag time and reduced peak in quantity and pollutant concentration between the inlet and outlet of a sewer is known as routing.

Muskingum or reservoir routing techniques are widely used in flow routing. In the case of pollutant routing one of two methods are used: completely mixed flow or plug flow. In completely mixed flow, particles entering the tank are mixed immediately throughout the tank. Particles that leave the tank are in proportion to their statistical population. In plug flow, fluid particles pass through the tank and are discharged in the same sequence in which they enter. The particles retain their identity and remain in the tank for a time equal to the theoretical detention time.

Routing of pollutographs through a sewer system is complex due to turbulent processes of dispersion, mixing and advection during transient flow and concentrations. The

changes in flow cause wave formation which moves with a celerity higher than the fluid parcel which contains the pollutant plug. Therefore the changed flow propagates much faster to the outlet of the sewer than does the actual parcel of fluid with its advected pollutant load. This is similar to an unsteady plug flow reactor.

If a continuous flow of conservative (non reactive) tracer is injected into the inlet at concentration C_o, the appearance of the tracer at the outlet of a completely mixed tank would occur as shown in Figure 7.1. The effluent concentration as a function of time can be determined from a materials mass balance for tracer around the reactor as follows (Metcalf and Eddy, Inc., 1972):

Rate of change in amount of tracer in reactor	=	Rate of tracer inflow to reactor	+	Rate of tracer outflow from reactor

$$V\frac{d}{dt}(C) = QC_o - QC \qquad [7.1]$$

where: C = effluent concentration at any time t, mg/l

V = volume of reactor, l

Q = flow rate, l/s

C_0 = influent concentration of tracer, mg/l

Simplifying and integrating:

$$C_t = C_o\left(1 - e^{-\frac{tQ}{V}}\right) \qquad [7.2]$$

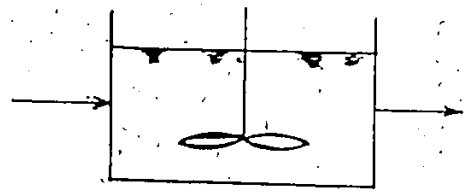

Complete mix

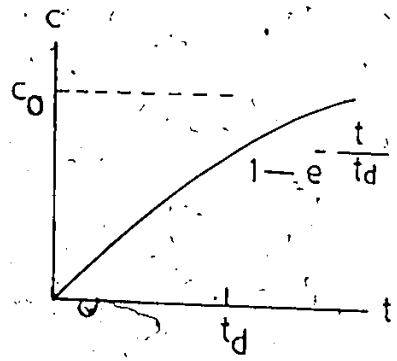

Figure 7.1 Continuous tracer input

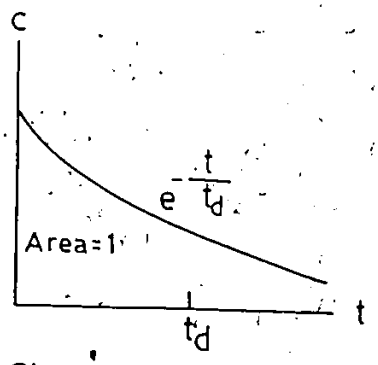

Figure 7.2 Slug tracer input

$$C_t = C_o\left(1 - e^{-\frac{t}{t_d}}\right) \qquad [7.3]$$

where: t_d = detention time = V/Q

C_t = outlet concentration at time t, mg/l

Medina (1976), developed an equation for predicting effluent concentration of a nonconservative pollutant from a completely mixed tank. The mass balance equation for a well mixed, variable volume reservoir is:

$$\frac{d}{dt}(VC) = I_t C_{it} - O_t C_t - K C_t V_t \qquad [7.4]$$

where: V = reservoir volume, l

C_{it} = influent pollutant concentration, mg/l

C_t = effluent and reservoir pollutant concentration, mg/l

I_t = inflow rate, l/s

O_t = outflow rate, l/s

t = time, s

K = decay coefficient, 1/s

Equation [7.4] is further rewritten over an interval Δt as:

Change in mass in basin during Δt = Mass entering during Δt − Mass leaving during Δt − Decay during Δt

$$C_2 V_2 - C_1 V_1 = \frac{C_1^I I_1 + C_2^I I_2}{2}\Delta t - \frac{C_1 O_1 + C_2 O_2}{2}\Delta t - K\left(\frac{C_1 V_1 + C_2 V_2}{2}\right)\Delta t \qquad [7.5]$$

where: subscripts 1 and 2 refer to the begining and end of the time step, respectively.

The tracer from a purged source (a continuous source which is suddenly stopped) in a completely mixed tank appears in the effluent as shown in Figure 7.2. The mass balance of the tracer could be written:

$$V \frac{dC}{dt} = - QC \qquad [7.6]$$

By rearranging:

$$\frac{dC}{C} = - \frac{Q}{V} dt \qquad [7.7]$$

On integration:

$$\ell n C = - \frac{Q}{V} dt = - t/t_d \qquad [7.8]$$

$$C_t = C_o e^{-t/t_d} \qquad [7.9]$$

where: C_t = effluent concentration, mg/l

C_0 = influent concentration, mg/l

t = time, s

t_d = detention period, s ($t_d = V/Q$)

V = volume of the tank, l

Q = flow, l/s.

A purged source condition exists in a completely mixed conduit only when t_d increases due to the reduction in incoming fluid quantity and is large compared to the simulation timestep. Otherwise the previous timestep concentration leaves the pipe without joining the coming concentration as a purged source.

A general equation for the prediction of

concentration in the sewer using advection and diffusion terms could be formulated:

$$\frac{\partial C}{\partial t} = -V\frac{\partial C}{\partial x} + D_x\frac{\partial^2 C}{\partial x^2} + D_y\frac{\partial^2 C}{\partial y^2} + \frac{1}{A(x)}\frac{\partial Q}{\partial x}(C_D - C) - KC \qquad [7.10]$$

The terms on the right side represent advection, diffusion in x and y direction, dilution and decay or sedimentation of pollutants in the sewer. Assuming that hydrographs and pollutographs from other sewers are added only at the node points (at the begining or end of the sewer), the dilution term can be deleted from the general equation. In pipe flow, the diameter is very small compared to the length and in most cases the concentration across the section becomes constant within small distances of the entry. Hence diffusion in the y direction is neglected. The diffusion term, being the second derivative of the concentration, is small compared to the first derivative advection term. Therefore the diffusion term is also neglected. Thus equation [7.10] becomes:

$$\frac{\partial C}{\partial t} = -V\frac{\partial C}{\partial x} - KC \qquad [7.11]$$

The actual hydrographs and pollutographs are unsteady, but a simplifying assumption of constant flow and concentration over a time interval reduces the complete process to a quasi-transient condition. The final steady state equation over a single time step is written:

$$V \frac{\partial C}{\partial x} = - KC \qquad [7.12]$$

By rearranging:

$$\frac{\partial C}{C} = - \frac{K}{V} \partial x \qquad [7.13]$$

integration leads to:

$$C_o = C_i \, e^{-\frac{Kx}{V}} \qquad [7.14]$$

where: C_0 = concentration of pollutant at the outflow, mg/l

C_i = concentration of pollutant at the inflow, mg/l

x = longitudinal distance, m

V = horizontal velocity, m/s

K = decay coefficient (decomposition) or solid removal rate, w/d (sedimentation), 1/s

w = solids settling velocity, m/s

d = depth of flow, m.

Equation [7.14] is the plug flow reactor equation from which the change in concentration over a distance travelled during the timestep can be calculated. The change of pollutant concentration over a complete simulation period is obtained by routing the pollutant concentration over a complete distance. Let the first and second parcel of fluid of concentration C_1 and C_2 move with velocity V_1 and V_2. The corresponding depths are d_1, and d_2. By application of the continuity and momentum equations to the volume shown in

broken lines in Figure 7.3, the average velocity is:

$$V_a = V_1 - 2\sqrt{g}\left(\sqrt{d_2} - \sqrt{d}\right) \qquad [7.15]$$

where: V_a = average fluid velocity with which pollutant concentration is moving, m/s

g = acceleration due to gravity, m/s^2

d_1 = depth of incoming fluid parcel, m

d_2 = average depth between first and the second fluid parcel, m

V_1 = velocity of oncoming fluid, m/s

But the wave celerity V_c is greater than the average velocity V_a of the parcel of water. The wave celerity V_c is given by:

$$V_c = V_a + 2\sqrt{gd} \qquad [7.16]$$

where: V_c = celerity, m/s

V_a = average fluid velocity, m/s

g = acceleration due to gravity, m/s^2

d = average depth of fluid, m

Time taken by the fluid parcel to carry the pollutant to the end of the sewer after the wave arrives is known as the lag time. The interaction of wave propagation and the fluid parcel transport determines the pollutant concentration at the end of pipe at every time step. If the pollutograph and hydrograph coincide at this point, the resultant concentration is:

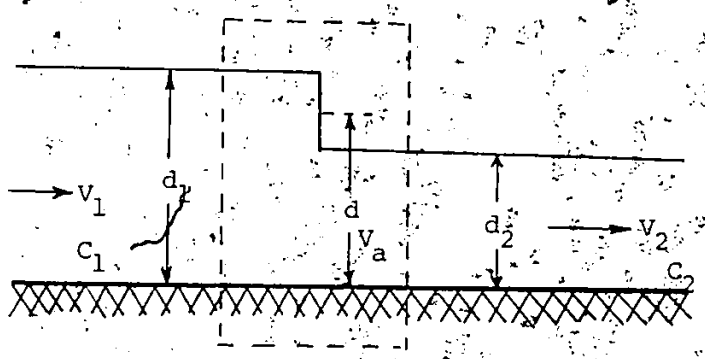

Figure 7.3. Schematic diagram of unsteady flow.

$$C_a = \frac{C_1 Q_1 + C_2 Q_2}{Q_1 + Q_2} \qquad [7.17]$$

where: C_a = average pollutant concentration, mg/l.

C_1, C_2 = pollutant concentration from pipe 1 and 2, mg/l.

Q_1, Q_2 = flow from pipe 1 and 2, l/s

The procedures discussed above could be used for pollutant routing in a sewer network. However, keeping track of all changes in velocities and celerities and their interactions is very complex, and the completely mixed reactor approach has been preferred in most urban runoff quality modelling.

The algorithm used for pollutant routing in SWMM is based on the assumptions that the pollutant in the gutter is completely mixed and that both the effect of continuous source and purged source of present and previous time steps may be added together to calculate the outflow pollutant concentration:

Outlet concentration = continuous input + purged input

$$C_j = \frac{F_a}{Q_a}\left(1 - e^{-R_c}\right) + C_c e^{-R_c} \qquad [7.18]$$

where: C_j = outlet pollutant concentration for gutter number j, mg/l

F_a = average pollutant flux over the timestep, mg/s

Q_a = average flow rate over the timestep, l/s

$R_c = \frac{\Delta t Q_a}{V}$ = constant

Δt = timestep, s

V = average volume of water in the gutter over the timestep, l

C_c = pollutant concentration at the previous timestep, mg/l

Equation [7.18] is used in SWMM3 until R_c is greater than 16.0. Beyond this range the outlet concentration is equal to the inlet concentration since e^{-R_c} tends to zero.

7.1.2. Modified routing equation:

The equation used by the present writer for routing pollutants is similar to the equations used in SWMM3, but the applicability differs as discussed below.

When $\Delta t < td$, the detention period in the sewer is longer than timestep. Since the concentration is required at the end of the pipe, and the flow has not left the pipe, the previous timestep pollutant flux gets mixed with incoming pollutant. The outlet concentration for the present timestep is then given by:

$$C = C_o\left(1 - e^{-R_c}\right) + C_c e^{-R_c} \qquad [7.19]$$

where:

C = gutter outlet concentration at time t, mg/l

C_0 = gutter continuous source influent concentration, mg/l

C_c = gutter purged source concentration (previous time step concentration), mg/l

R_c = constant = $\Delta t/td$

Δt = timestep, s

t_d = detention period, s

At the end of the first timestep, the pollutant concentration inside the gutter and at outlet is C_c and this acts as a purged source to the incoming continuous pollutant. Different values of R_c are used for different pollutants to minimise the total summation error, R_c ranges between 0.5 and 1.5.

When $\Delta t > t_d$ or $\Delta t/t_d > R_c$, the detention period is less than the timestep; therefore, inflow leaves the sewer during the timestep. During the timestep complete mixing involves only the incoming flow, there is no effect of previous timestep concentration on the following timestep:

$$C = C_o\left(1 - e^{-\Delta t/t_d}\right) \qquad [7.20]$$

7.2. Algorithms for deposition and scour at weirs:

Weirs are generally used to measure stormwater discharge. Installation of a weir increases the depth of flow upstream and hence reduces the horizontal velocity and increases sedimentation. Horizontal velocity changes considerably during the passage of a floodwave. Deposition of solids decreases as horizontal velocity increases, and at a critical condition, there will be no deposition or removal. Beyond the critical condition, flowing water starts to scour the previously deposited solids.

In urban drainage, storm runoff carries large quantities of silt, sand, debris, etc., which settle out at low horizontal velocities. Most stormwater management models do not consider the effect of obstructions such as weirs used for flow measurement or other purposes. In this case, computed pollutant prediction will be high at the onset of the flow event because of low flow. As flow increases the deposited solids are then resuspended and carried over the weir. This is especially true if sampling is carried out at the weir overflow. These concepts have been modelled by the writer using a simple formulation for deposition and scour of solids at weirs using a detention period approach:

detention period = t_d = volume / flow

t_d is inversly proportional to horizontal velocity. Critical detention period t_c occurs at the critical velocity when there is no solids deposition or removal.

If t_d is greater than t_c, the deposition of solids is given by:

$$S_d = C\left(1 - e^{-W_r(t_d - t_c)}\right) \qquad [7.21]$$

where: S_d = concentration of removed solids, mg/l

C = weir influent solids concentration, mg/l

W_r = deposition rate exponent, 1/s

t_d, t_c = detention and critical detention periods, s

The total quantity of solids removed during the time step is given by:

$$T_R = S_d Q \Delta t \qquad [7.22]$$

where: T_R = quantity of solids removed during time step mg.

Q = flow rate, l/s

Δt = time step, s

When t_d is less than t_c, the increased horizontal velocity scours the previously deposited solids:

$$T_C = S_a\left(1 - e^{-\frac{W_s}{t_d}}\right)/\Delta t \qquad [7.23]$$

where: T_c = average flux of solids scoured during the time step, mg/s

S_a = total quantity of deposited solids at the weir, mg

W_s = scour exponent, s

t_d = detention period, s

The additional pollutant concentration due to scour (added to incoming concentration) is given by:

$$C_a = T_c/Q \qquad [7.24]$$

$$C_T = C_a + C_i \qquad [7.25]$$

where: C_a = additional concentration due to scouring in mg/l

T_c = scoured pollutant flux, mg/s

C_i = incoming concentration in mg/l

C_T = total concentration in mg/l

Q = runoff flow rate, l/s

The values for t_c, W_r and W_s are user input variables and depend principally on the type and size of solids associated with the flow to be modelled. Usually, the value for t_c lies between 10 and 60 seconds. These deposition and scour algorithms were coded into CHGQUAL. The computed pollutographs display an improved shape of rising limb, when compared to observed pollutographs.

7.3. EFFECT OF BASEFLOW:

Computed pollutant washoff from impervious areas has an exceptionally high initial concentration due to low runoff rates and the larger mass of pollutant buildup. This is unlikely in the real situation because of dilution with baseflow having low concentrations. Present stormwater management models do not model this effect, which is important in the rising limb. Moreover computed washoff, based on accumulated DD, tends to zero after DD is computed to be completely washed off. However observed pollutant loads tend to background constant concentration towards the end of a pollutograph. Prevailing background or base flow concentrations have been identified, by carefull analysis of Chedoke Creek catchment data bank as follows: 8 mg/l, 3 mg/l, 0.8 mg/l, for BOD, TKN and total phosphorous respectively. These average baseflow pollutant

baseflow pollutant concentrations were used to find the resultant concentrations by dilution. As a result of this, high dilution in the beginning of storm and constant concentration towards the end of the storm was obtained. CHGQUAL was modified accordingly and the output produced better fits to the rising and recession limbs of observed pollutographs. The FORTRAN code is given in subroutine GQUAL in the CHGQUAL user's manual (Shivalingaiah and James, 1984).

7.4. Fate of pollutants at the outfall zone:

Pollutants washed off the catchment eventually reach the receiving water and undergo changes in concentration due to advection, diffusion, sedimentation or decay. These processes are controlled by the particle size, type of pollutants and hydrodynamics of the receiving water. Runoff from the Chedoke Creek catchment in Hamilton, drains to Coote's Paradise. Coote's Paradise, Hamilton Harbour and Lake Ontario are inter-connected as shown in Figure 7.4.

Chedoke Creek ends in an artificial concrete channel 6.4m (20 ft) wide followed by a natural channel of 1000m (3120 ft) long (Chedoke Creek outfall channel, CCOC). CCOC has an irregular natural cross section with a minimum width of 9.6m (30 ft) at the upstream end and a maximum width of 32m (100 ft) at the downstream end. The depth of water varies between 0.6 and 1.3m (2 and 4 ft). The CCOC

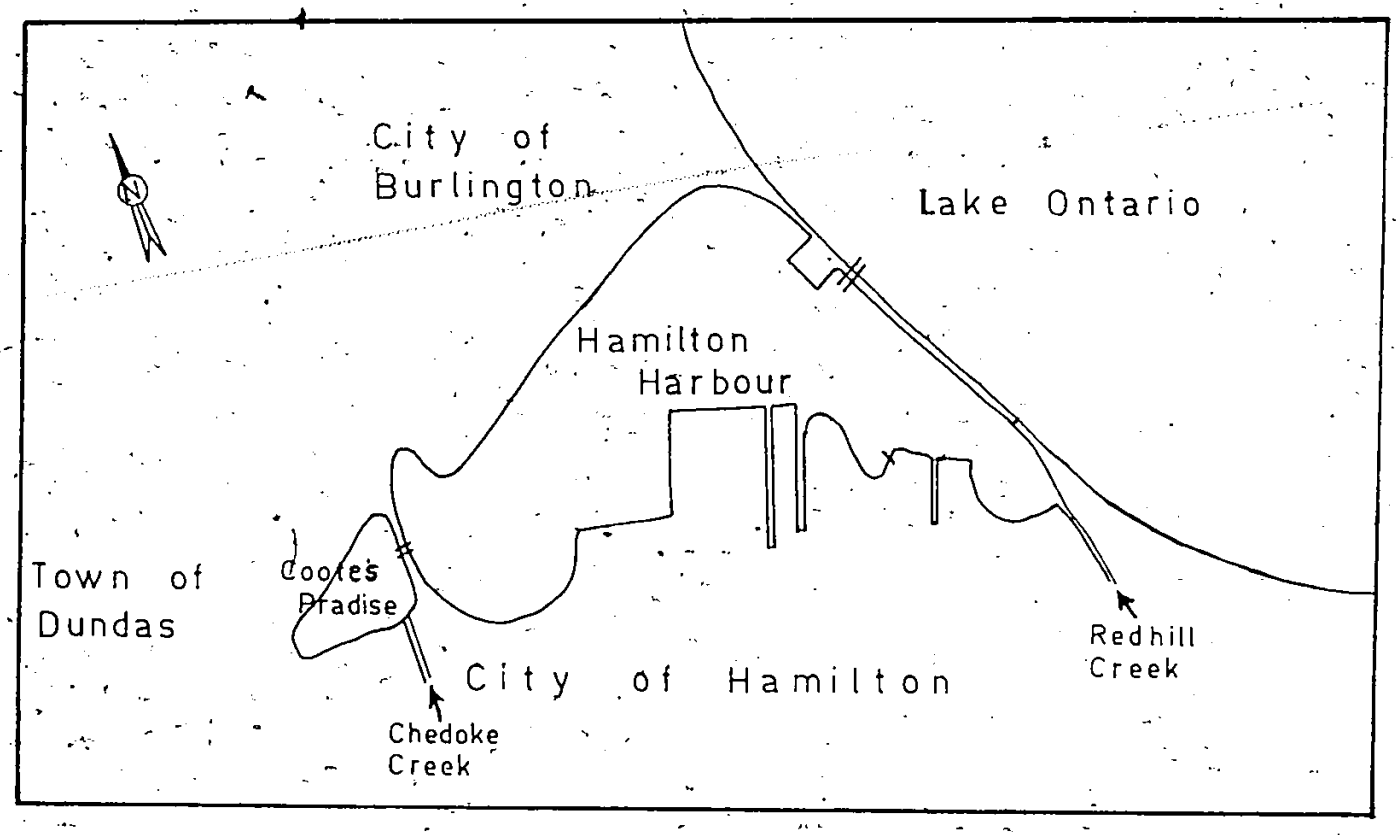

Figure 7.4 The three water bodies and their tributories.

downstream depth has been found to be constant at 1.3m (4 ft). Depending upon the horizontal velocity which decreases due to increased cross sectional area towards the stagnant receiving water, the unsteady flow condition in the channel might favour the sedimentation or scouring of solids. A detailed model(TOTSHED) was developed by Alaa El Zawahary (1981) for computation of suspended solids concentration along COCC for any given inflow hydrograph and suspended solids pollutograph. The study concluded that 80 to 90% of suspended solids were trapped in the COCC. Since the COCC has not been dredged for the past 2 to 3 decades either the trap efficiency may be wrong or low frequency floods must scour the accumulated sediments. The remaining fraction of pollutants reaches Coote's Paradise.

Coote's Paradise is a Crown game preserve comprising approximately 430 ha (1200 acres) of forest, marsh and open water located at the extreme western end of Hamilton Harbour. The mean depth of 160 ha (400 acres) of open water is about 45cm (1.5ft), but seasonal variations in water level due to fluctuations in the level of Lake Ontario can be extreme enough to expose large areas of mud flats. Numerous streams as well as the discharge from the sewage treatment plant in Dundas provide a constant through flow of water into Hamilton Harbour. The various streams entering Coote's Paradise are: Hickory Brook, Long valley Brook, Vine Brook, Hopkins Creek, Spencer Creek, Westdale Brook and

Chedoke Creek. The relative input of pollutants in kilograms per day from Chedoke Creek was estimated to be less than other major sources, but the observed mean concentrations were higher (Semkin et al. 1977). The observed data also revealed that Chedoke Creek was enriched in phosphorous and nitrogen, had higher levels of BOD, COD, suspended solids and heavy metals and considerably higher bacteria counts. Based on historical flows and seasonal variations, the residence time for Coote's Paradise varies between 0.014 - 0.054 years (5 - 20 days). Most suspended solids should settle in this time, but for agitation of bottom sediment by the wind induced waves. This was confirmed by turbidity data. Unstable organic substances (external to Coote's Paradise) decomposed into simple end products within the residence time and are exchanged with Hamilton harbour. Since the average inflow is the same as the average outflow and the residence time much smaller than the Harbour residence time, the input from Coote's Paradise to Hamilton Harbour is considered to be direct, neglecting the effect of the residence time in Coote's Paradise.

The amount of surface runoff to the harbour has been influenced by changes due to urbanization and by a small expansion of the drainage area through the transfer of approximately 10 km from the Lake Ontario watershed to the Hamilton Harbour watershed. A more significant impact has

been the substantial increase in municipal consumption of water, since water taken from Lake Ontario is contaminated and discharged to the two receiving waters. In addition to this, new industries and the expansion of existing industries have also affected Harbour water quality. The major contributors to Hamilton Harbour are Coote's Paradise, Grindstone Creek and Red hill Creek. Stormwater overflows drain the combined stormwater-sanitary sewer network into both receiving waters. The area of the Harbour is about 21.25 km and the depth varies between 1.8 and 18 m. The calculated average detention periods for the harbour including lake-harbour exchange are 0.92 and 1.23 years for average land runoff and average total inflow respectively for the period 1975 - 1977. The total percentage contributions from major sources were calculated using the pollutant mass balances for 1977 by Snodgrass, (1981). All the major sources were grouped into two sources, point sources (industries and municipal) and nonpoint sources (all streams and CSO from the central business district). The percentage contributions of total phosphorous, total nitrogen, BOD and suspended solids from nonpoint sources to Hamilton Harbour were 54, 10, 32 and 71 respectively. Continuous simulation using SWMM2 on the three major catchments from 1971 to 1980 (Robinson and James, 1981) showed increases in total load of TP, TN, BOD and SS of 1.3, 1.0, 1.1 and 2.1 compared to the loads calculated by

Snodgrass. This discrepancy indicates the lack of input data to estimate total pollutant quantity reaching Hamilton Harbour.

The exchange of flow and pollutants between Hamilton harbour and Lake Ontario is important in estimating pollutant concentration in the harbour. The 107m by 9.5 m Burlington canal is the main path for flow and pollutant exchange between the Harbour and the Lake. The exchange is of two types: (a) Unidirectional flow or so-called Helmholtz mode, which changes direction depending upon the relative difference in lake and harbour water levels and persists throughout the year. (b) Densimetric flow during thermal stratification in which warm harbour water flows out to the lake in the top layer and colder lake water moves into the harbour in the bottom layer (Eid, 1981) Though stratified two layer flow has been observed in the canal, densimetric flow is small compared to flow due to change in water elevation (Dick and Marsalek, 1973). The exchange coefficient was calculated to be (Snodgrass, 1981):

$$a = (C_i - C_h)/(C_l - C_h) \qquad [7.26]$$

where: a = exchange coefficient

C_i = average input concentration to Harbour, mg/l

C_h = average concentration in the Harbour, mg/l

C_l = average Lake concentration, mg/l

then $E = aQ$ [7.27]

where: E = average annual Lake exchange rate, m^3/s

Q = average annual inflow rate to Harbour, m^3/s

Kohli (1977) estimated the exchange flows from lake to harbour and harbour to lake to be 8 m^3/s and 25 m^3/s respectively using continuous current data in the ship canal for the period September 1 - 13, 1975. This lowers the harbour depth by 0.5 m but the observed data showed no decrease in the depth. Again in 1979, Kohli made a similar calculation of average exchange for the months of June, July, August, October and November, 1976. The calculated average net outflow and inflow to harbour were 25.4 and 5.8 m^3/s indicating a net lowering of 11 meters in depth over those of 5 months or, more likely, a fundamental error in basic data. The exact magnitude of exchange awaits proper mass budgets calculated over a peroid of a few years.

Stormwater runoff contributes significant quantities of TN, TP, BOD and SS to Coote's Paradise and Hamilton Harbour, compared to municipal and industrial point sources. Since the exchange of pollutant and flow between Coote's Paradise, Hamilton Harbour and Lake Ontario is still uncertain, an estimate of total pollutant budget for Hamilton Harbour is premature.

PART 4

MODEL APPLICATION

CHAPTER VIII

CHGQUAL VALIDATION

8.1. Introduction:

A mathematical model is simply a quantitative expression of a process or phenomenon one is observing, analyzing, or predicting. Since no process can be completely observed, any mathematical expression of a process will involve some element of uncertainity. Hence, any mathematical model formulated to represent a process or phenomenon will be conceptual to some extent and the reliability of the model will be based upon the extent to which it can be or has been verified. Model verification is a function of the data available to test the model scientifically and the resources available to perform the scientific tests. A reliable data acquisition system simplifies the problem of model building and testing. After ensuring the availability of good data, a series of verification, sensitivity tests, calibration, and validation can be designed to produce sufficient information to answer a wide range of questions about the model's performance (James and Robinson, 1981).

8.2. DATA ACQUISITION:

Hamilton's urban drainage system comprises an area of approximately 120 km^2 which drains through 20 major

combined sewer outfalls to Hamilton Harbour and Coote's Paradise. Among the three major drainage areas of Hamilton, the Chedoke Creek Catchment was chosen for examination in this study (see Figure 8.1).

The Chedoke Creek drainage system is 26.8 sq.km. in area, and about 46% of the area is served by separate sewers. The predominant land use is low to medium density single family residential. The Chedoke Creek outfall channel receives runoff from 93% of the area and ultimately drains to Coote's Paradise (James and Henry, 1982).

At the turn of the century Hamilton was prospering, due to its rapidly expanding steel industry. The population increased by 40% in less than a decade. This in turn over-taxed the sewer network causing flooding and pollution problems during storm events. Remotely operated diversion structures were built into the existing sewers system in the late 1960's and early 1970's. These diversion structures enabled diversion of combined waste water to the receiving waters during storm events which increased the pollutional load to the receiving waters. Subsequent to deterioration of receiving water quality, in the late 1970's and in early 1980's, a study was initiated to investigate the pollutional potential due to runoff. The Computational Hydraulics Group (CHG) McMaster University, set up a hydrometerological data acquisition network heavily in the test catchment. Figure

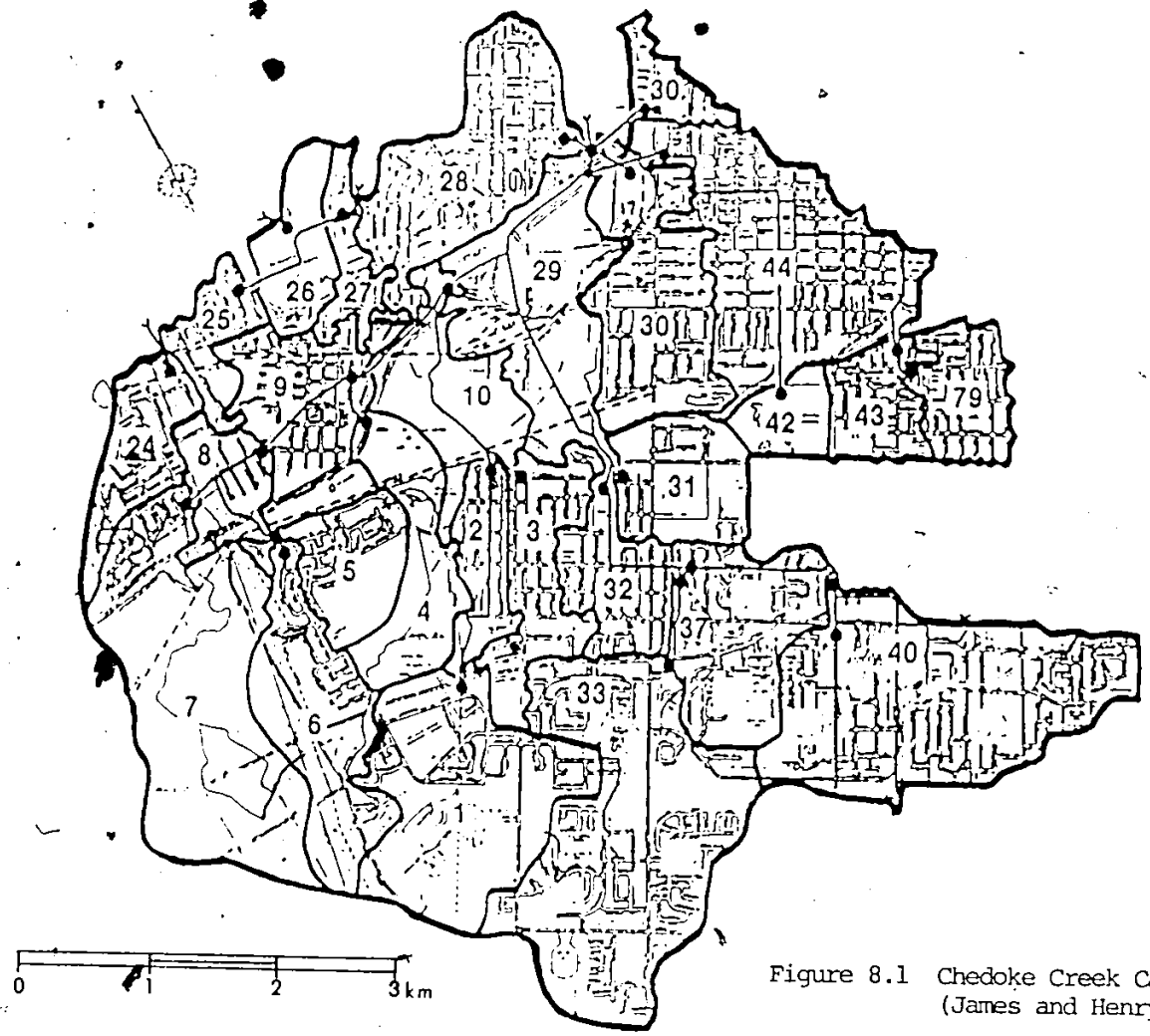

Figure 8.1 Chedoke Creek Catchment.
(James and Henry, 1982)

8.2 presents an overview of the CHG data acqusition network; and Tables 8.1 and 8.2 indicate the type of instruments and their locations for stream flow and rain recorders respectively (James and Henry, 1982). Simultaneously, a side weir overflow model (James and Mitri, 1982), and continuous and interactive storm water models (James and Robinson, 1982), were developed and tested for Hamilton.

Since the storm cells are dynamic, stationary rain data are too unrealistic to use in urban runoff studies (Shtifter,1980; Schekenberger, 1983). A higher density of rain recording stations was necessary to track the storm direction and intensity. An inexpensive, higher precision and resolution, reliable and automatic system for rainfall data was developed (James et al. 1982; Haro et al. 1983). The rain recorder consists basically of three components: a) The rain sensor collects precipitation and converts it into water drops of almost constant size, b) The data logger senses the drops and counts them for a programmable time interval. The logger processes the time series and stores it on standard audio cassette magnetic tape. The cassettes are removed, transported to the CHG laboratory, and read and interpreted by a decoder. (c) The decoder communicates with a PDP 11/23 computer for further analysis of the data.

Runoff samples were collected at three points (HYDRO, HOTPOINT and MAIN STREET) in the Chedoke Creek Catchment at

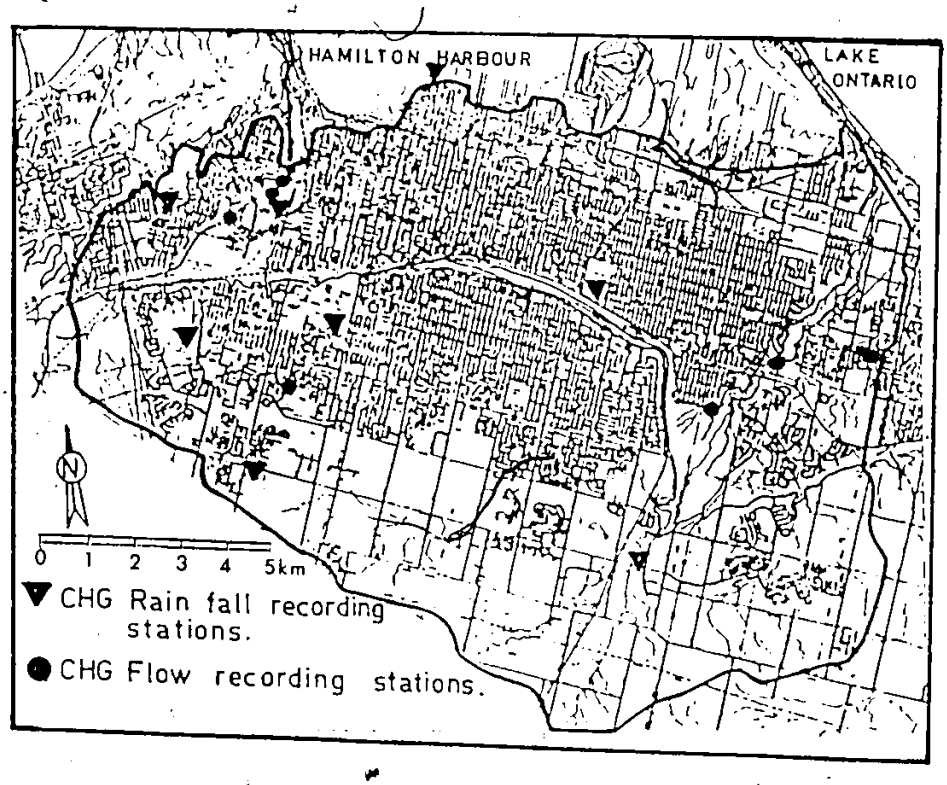

Figure 8.2 CHG data acquisition network(James and Henry, 1982).

Table 8.1 Rain recording instrument(James and Henry, 1982).

Basin	Location	rain gauges
Chedoke Creek	McMaster University	Weathertronics Tipping Bucket(Imperial) Honeywell Electronic 194 recorder.
	Chedoke Hospital	AES (Metric) Tipping Bucket 30 day step chart recorder.
	Hotpoint warehouse	AES (Imperial) Tipping Bucket 30 day step chart recorder.
Redhill Creek	Garth street	Belfort Tipping Bucket (Imperial) Rustrak recorder.
	Mohawk college	AES (metric) Tipping Bucket Rustrak Recorder.
Central Business district	Gauge park	AES (metric) Tipping Bucket 30 day step chart recorder.
	Circle Racquetball	AES (metric) Tipping Bucket 30 day step chart recorder.
	Hamilton Harbour Commission	AES (metric) Tipping Bucket Rustrak recorder.

Note: Imperial raingauges are calibrated to 0.01 in/tip (0.254mm/tip).

Metric raingauges are calibrated to 0.00787 in/tip (0.2mm/tip).

Table 8.2 Streamflow recording instruments(James and Henry, 1982).

Basin	Location	Instruments
Chedoke Creek	Main street crossing	Steven's float recorder
	Hydro substation	Pneumatic level sensor
	Hotpoint warehouse	Steven's float recorder
Redhill Creek	Greenhill CSO	Pneumatic level sensor
	Queenston road	Steven's float recorder
Central business district	Ferguson and Ferrie	new sampler proposed

approximately 5 minute intervals during storm events. The sample collection team synchronized their watches with a quartz chronometer kept at the CHG laboratory which was set to National Research Council time in Ottawa before sample collection. The collected runoff water samples were labeled and transported to the Ministry of Environment (MOE) laboratary for analyses. The runoff water samples were analysed for BOD, suspended solids, total nitrogen, total phosphorous and total coliform organisms.

Information pertaining to street cleaning, population and vehicle density, was obtained from the Hamilton City Hall. The CHG archive provided all the geographical maps of the catchment needed for model development.

8.3. MODEL VERIFICATION

8.3.1. Introduction:

Verification tests use some specific conditions for which the model response can be exactly predicted to check if indeed the model is structured and coded as intended. Verification tests are not conducted by comparision of model responses with those of the actual system to be modelled; rather comparisions between model responses and theoretically anticipated results are made in as many cases as possible. The input data need not be physically reasonable (James and Robinson, 1981)

8.3.2. Verification tests on CHGQUAL:

Before the new buildup, washoff and routing algorithms were interfaced with the SWMM3 RUNOFF Block, CHGQUAL was extensively subjected to verification tests. The verification showed that the runoff quantity prediction was quite satisfactory. But the runoff quality prediction was not satisfactory because of code errors in unit conversions and because the total percentage of DD washoff decreased with increased rain intensity.

The quantity of DD washed off is calculated in subroutine QSHED and is then transferred to subroutine HYDRO where the total quantity of DD remaining on the land surface is calculated and subsequently passed to subroutine PRINTER where final results are printed. The units of variables PSHED(J,1) and PBASN(J,1) were not converted to pounds from kilograms in subroutine HYDRO. Changes were made in HYDRO as follows:

PSHED(J,1) = SUMSRF * 2.2 [8.1]

PBASN(J,1) = SUMCAT * 2.2 [8.2]

Similarly, the precipitation load PP calculated in subroutine QSHED was also not converted into mg/s. The following correction was made in subroutine QSHED:

PP = WFLOW (N) * CONCRN (K) * 28.3 [8.3]

Decrease of total pollutant washoff with increased rainfall intensity was mainly due to linear integration of washoff rate over a timestep using Simpson's 1/3 rule (see Figure 8.3). The quantity of DD washed off in the first timestep is large compared to subsequent timesteps when the washoff rate may not be linear. Due to the assumption of linearity the total quantity of pollutant washed off is under estimated. This error grows with increased rain intensity and timestep interval. The error can be corrected by reducing the timestep interval so that the linear washoff rate assumption holds good or summing the individual quantity washed off in each timestep rather than integrating washoff rate.

$$P = \Sigma\left(P_{(t-1)} - P_{(t)}\right) \qquad [8.4]$$

where: P = total quantity of pollutants washed off, mg.

P_t = quantity of pollutants present on the surface at time 't', mg.

P_{t-1} = quantity of pollutants present on the surface at time t-1, mg.

The verification results produced by both CHGQUAL and SWMM3 algorithms are shown in Figure 8.4.

After the above correction was coded, in addition to pollutant buildup, washoff, routing and other processes the CHGQUAL was then subjected to sensitivity analyses, calibration and validation.

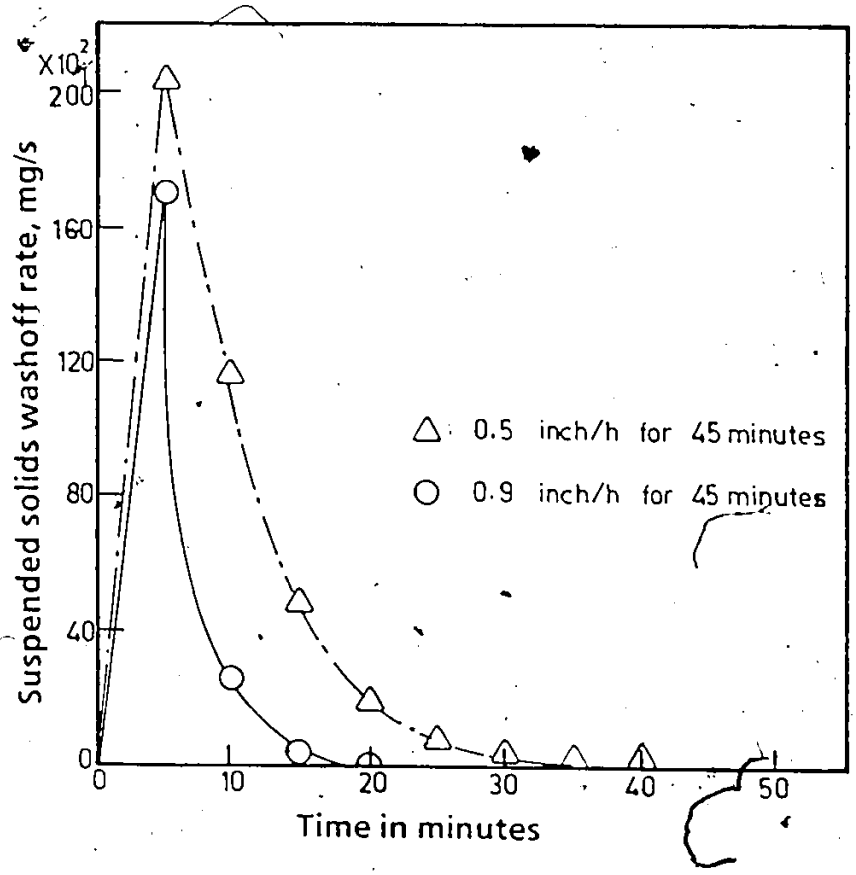

Figure 8.3 Washoff rate of suspended solids during a simulation period(SWMM3 algorithms).

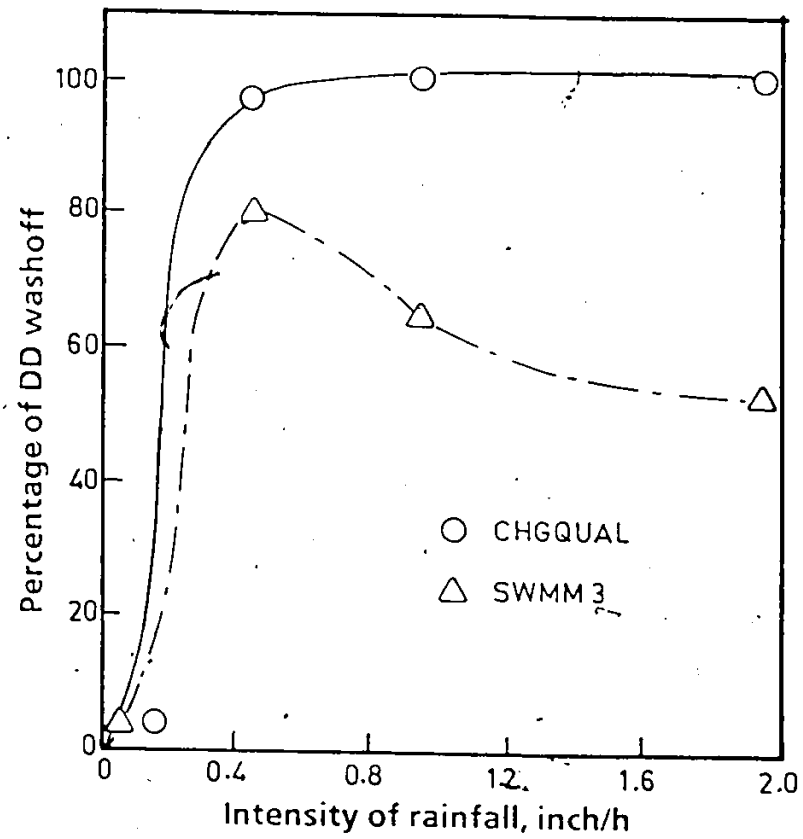

Figure 8.4. Comparison of total DD washoff between SWMM3 and CHGQUAL.

8.4. SENSITIVITY ANALYSIS

8.4.1. Introduction:

Sensitivity analysis proceeds by holding all parameters but one constant at their expected values, and perturbing that parameter within reasonable expected limits such that the variations of the objective function can be examined. If apparently small perturbations of the parameter produce large changes in the objective function, the system is said to be sensitive to that parameter (James and Robinson, 1981). This gives a measure of how accurate that parameter must be examined if the model is to be used in prediction. If the objective function is not sensitive to the perturbed parameter, then the parameter need not be accurately estimated. If the system is extremely insensitive to the perturbed parameter, the parameter and its associated system component may be redundant and could be deleted from the model. The tests are done using the full design problem input data set. It must be stressed that the actual values of the constant parameters may affect the sensitivity analysis, and so their values should be typical of the conditions being modeled.

8.4.2. Sensitivity analysis on CHGQUAL:

Sensitivity analysis on the CHGQUAL was carried out using the Chedoke Creek catchment geographic data file,

Parameters used in the analysis are listed in Table 8.3. The sensitivity of individual parameters was studied keeping all other parameters at their expected values. The perturbed parameter's effect on suspended solids peak concentration and total load is shown in Figure 8.5. The results revealed that vehicle speed, pollutant load rate of vehicle and vegetation, simulation timestep and aerosol concentration are highly sensitive; wind velocity and frequency, cleaning interval, number of vehicles during storm, curb height, atmospheric mixing height, dustfall, dry days, rainfall washoff coefficient and weir removal coefficient are moderately sensitive; and population load, vehicle washoff coefficient, rainfall energy exponent and overland washoff coefficient are less sensitive parameters in computing urban runoff water quality. This information is used in calibrating CHGQUAL to the observed data set. Simulation timestep is effective, because of increased summation error due to increase in timestep interval.

8.5. CALIBRATION

8.5.1. Introduction:

Calibration is the comparision of model simulation results to field measurements, or to another model known to be accurate, or to some other adequate criteria to ensure that the model of the system is producing accurate data. If these comparisions indicate that the model results are not

Table 8.3 Parameters used in the CHGQUAL sensitivity analysis.

parameter	unit	values		
		minimum	maximum	average
wind velocity	km/h	1.00	50.00	8.30
wind frequency	-	0.05	0.60	0.44
vehicle speed	km/h	10.00	100.00	30.00
vehicle/population	ratio	0.10	1.00	0.50
vehicle load rate	mg/vehicle	500.00	25000.00	15000.00
population load rate	mg/p-d	50.00	1000.00	200.00
curb height	cm	2.00	25.00	15.00
atm. mixing height	m	100.00	900.00	500.00
aerosol con.	ug/m	5.00	150.00	35.00
dustfall	%	-50.00	+100.00	1.00
dry days	d	5.00	21.00	15.00
cleaning interval	d	2.00	30.00	15.00
veg. load rate	mg/ha-d	1.00	50.00	5.50
W1		0.10	5.00	1.10
W2		1.00	10.00	5.50
W3		0.50	5.00	3.50
time step	min	1.00	5.00	1&5

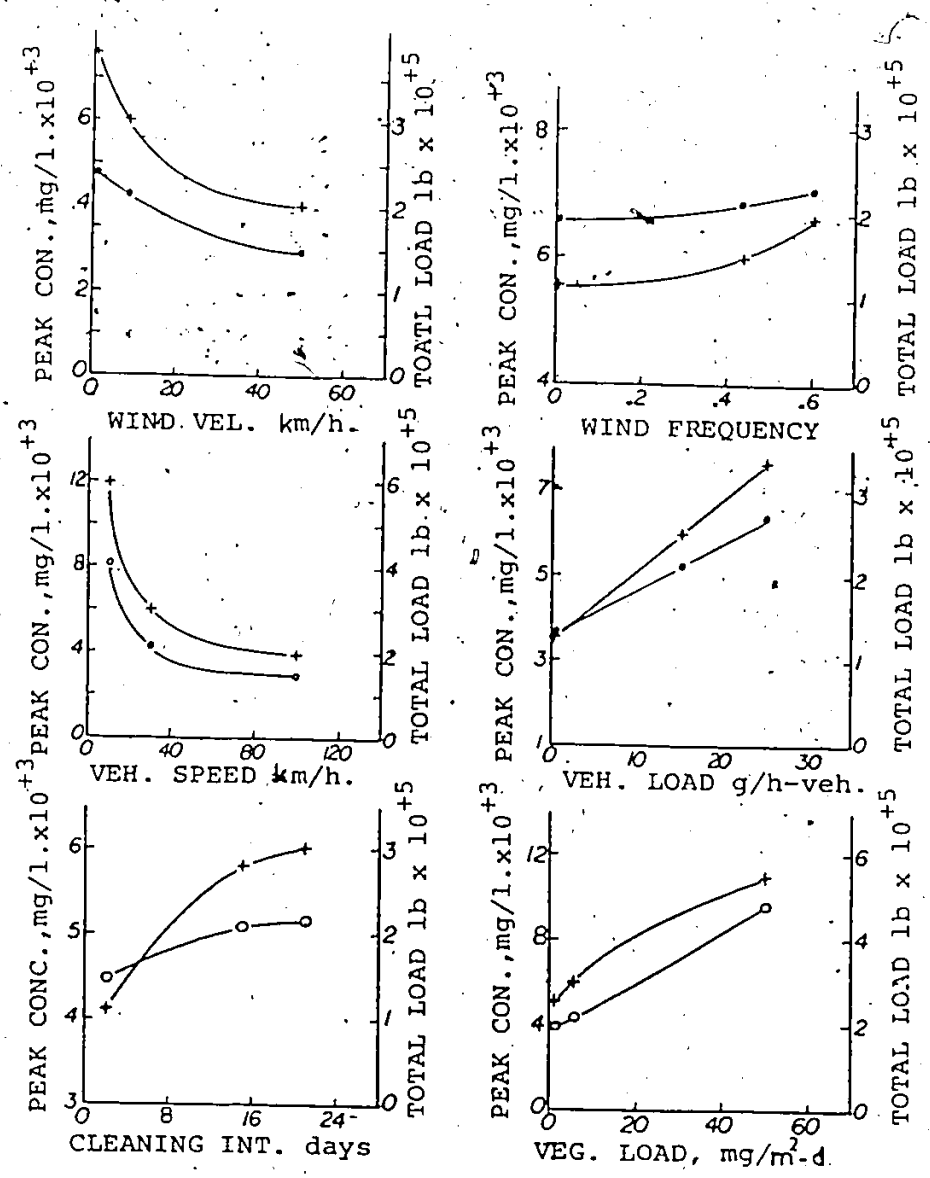

Figure 8.5 Sensitivity analysis on peak concentration and the total load of suspended solids. (0 total load, + peak concentration)

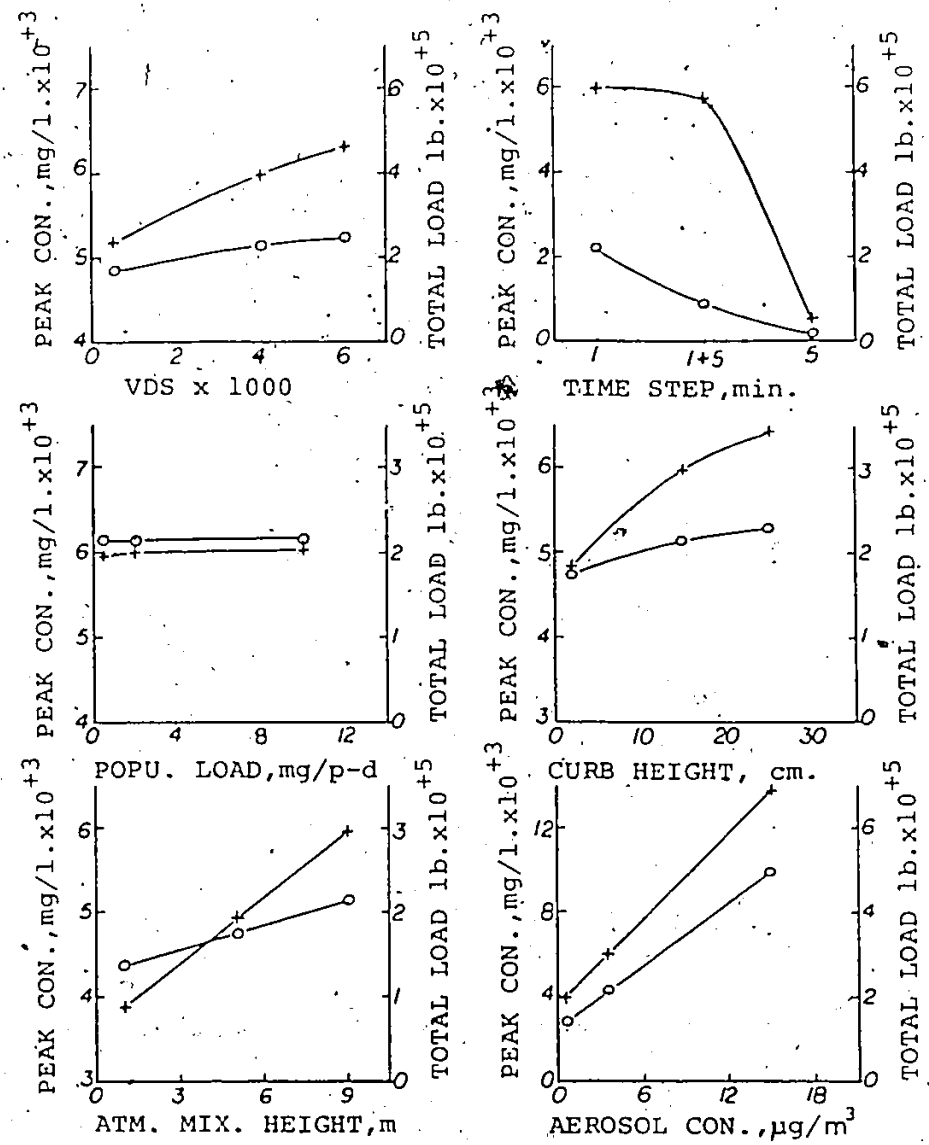

Figure 8.5 continued. (o total load, + peak concentration)

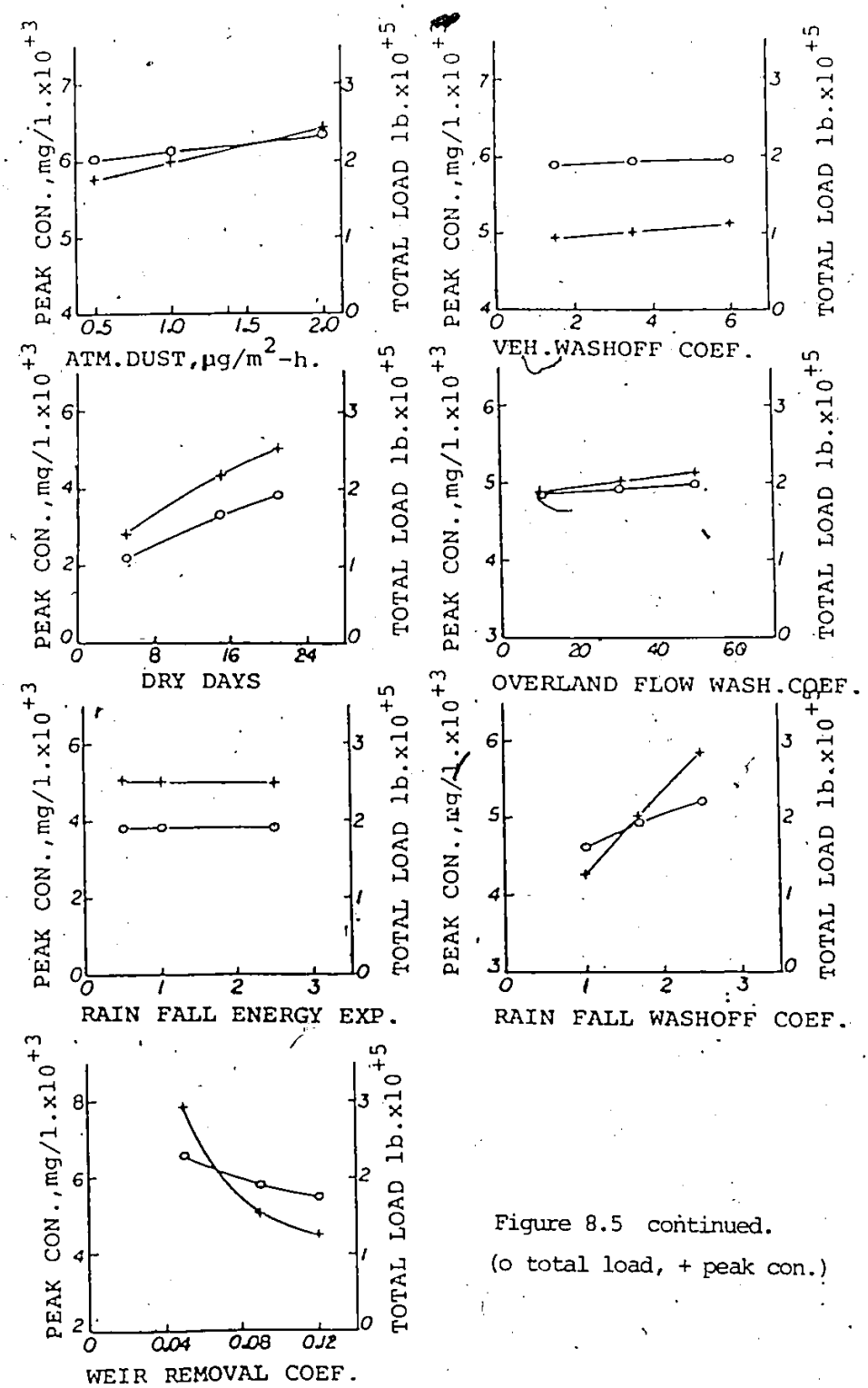

Figure 8.5 continued.

(o total load, + peak con.)

sufficiently accurate, then the model of the system is altered, usually by adjusting one or more program parameters, and the procedure is repeated. This process generally involves several iterations before a satisfactory confidence level is achieved. Techniques used in calibration include: (a) comparison of results against field observations, (b) cross-correlation of continuous model results with those of another proved, usually discrete event, or process model equivalently initialized, and (c) some combination of field observations and modelling (James and Robinson, 1981).

8.5.2. CHGQUAL model calibration:

The CHGQUAL was applied to Chedoke Creek catchment, Hamilton for calibration. Data collected on storm 8-13 during summer 1980 on flow, BOD, SS, total Kel. nitro. and total phosporous at Hotpoint and Hydro were used for calibration. The catchment details along with storm sewer network details are given in Tables 8.4 and 8.5 respectively. The hyetographs used in the calibration correspond to McMaster University, Mohawk and Hamilton Airport rain recorders (James and Henry, 1982). Since storms are dynamic, the hyetograph for an individual subcatchment is not the same as the observed hyetographs at the rain recording stations. Identifying the individual hyetographs for all the subcatchments was done by careful study of the three observed hyetographs and fixing the direction and

Table 8.4 Chedoke Creek Catchment details.

* * * * * S U B C A T C H M E N T D A T A * * * * *

SUBCATCH-MENT NO.	GUTTER OR INLET	WIDTH (FT)	AREA (AC)	PERCENT IMPERV.	SLOPE (FT/FT)	RESISTANCE FACTOR IMPERV.	RESISTANCE FACTOR PERV.	DEPRES. STORAGE(IN) IMPERV.	DEPRES. STORAGE(IN) PERV.	INFILTRATION RATE(IN/HR) MAXIMUM	INFILTRATION RATE(IN/HR) MINIMUM	DECAY RATE (1/SEC)
1 1000	6011	4440.33	427.00	11.30	.0230	.017	.025	.050	.100	2.00	.50	.00150
2 2000	3011	730.03	107.00	18.00	.0100	.017	.025	.050	.100	2.00	.50	.00115
3 3000	1015	1510.30	163.00	23.00	.0070	.017	.025	.050	.100	2.00	.50	.00115
4 4000	4011	1320.30	190.00	11.00	.0520	.017	.025	.050	.200	1.30	.18	.00150
5 5000	1612	3810.00	151.00	15.00	.0250	.017	.025	.050	.100	2.00	.50	.00115
6 6000	2412	4495.33	256.00	9.00	.0340	.017	.025	.050	.100	2.30	.50	.00115
7 7000	2915	1390.30	515.00	2.00	.0740	.017	.025	.050	.100	2.30	.50	.00115
8 8000	3112	1895.33	92.00	12.00	.0250	.017	.025	.050	.100	2.00	.50	.00115
9 9000	3612	4365.30	239.00	21.00	.0170	.017	.025	.050	.100	2.00	.50	.00115
10 10000	4311	1400.33	214.00	4.00	.0630	.017	.025	.050	.100	2.00	.50	.00115
11 2901	291	7130.33	113.90	27.70	.0300	.017	.025	.050	.100	2.00	.50	.00115
12 3100	2921	5210.00	166.50	21.00	.0078	.017	.025	.050	.100	2.00	.50	.00115
13 3200	2921	4460.30	195.70	27.90	.0173	.017	.025	.050	.100	1.00	.18	.00115
14 3300	3310	9526.30	611.70	22.80	.0071	.017	.025	.050	.100	1.30	.18	.00150
15 3700	3710	5110.30	272.30	26.00	.0143	.017	.025	.050	.100	1.00	.18	.00115
16 4001	4060	9999.33	634.10	29.70	.0063	.017	.025	.050	.100	1.00	.18	.00115
17 2900	299	2890.33	205.00	14.10	.0458	.017	.025	.050	.100	1.00	.18	.00115

TOTAL NUMBER OF SUBCATCHMENTS.. 17

TOTAL TRIBUTARY AREA (ACRES).... 4518.20

IMPERVIOUS AREA (ACRES)..... 789.00

PERVIOUS AREA (ACRES)..... 3729.20

TOTAL WIDTH (FEET)..... 70400.00

PERCENT IMPERVIOUSNESS..... 17.46

Table 8.5 Chedoke Creek Catchment sewer network details.

* * * * * GUTTER AND PIPE DATA * * * * *

GUTTER NUMBER	GUTTER CONNECTION	WIDTH (FT)	LENGTH (FT)	SLOPE (FT/FT)	SIDE SLOPES L	SIDE SLOPES R	MANNING N	MAX DEPTH (FT)
1 4060	3840	7.50	3250.0	.0031	0.00	0.00	.013	9.50
2 3840	3710	7.50	300.0	.0058	0.00	0.00	.013	13.00
3 3330	3712	6.00	1320.0	.0110	0.00	0.00	.013	6.50
4 3712	3840	7.75	550.0	.0044	0.00	0.00	.013	8.50
5 3710	2921	7.25	2950.0	.0063	0.00	0.00	.013	13.00
6 2921	2922	10.00	1350.0	.1100	0.00	0.00	.050	6.00
7 2922	2941	7.00	3250.0	.0058	0.00	0.00	.013	9.00
8 2941	293	12.00	950.0	.0045	0.00	0.00	.013	10.00
9 $ 293	294	0.00	0.0	0.0000	0.00	0.00	0.000	0.00
10 *6011	7011	6.00	350.0	.0095	0.00	0.00	.015	0.00
11 7011	7012	5.00	1000.0	.0140	1.67	1.67	.022	3.00
12 *7012	7013	6.00	500.0	.0075	0.00	0.00	.015	0.00
13 7013	8011	6.50	3200.0	.0077	0.00	0.00	.015	6.00
14 8011	4411	7.50	110.0	.0193	0.00	0.00	.015	7.00
15 *1015	4411	5.00	300.0	.0046	0.00	0.00	.015	0.00
16 2915	3112	6.50	600.0	.0090	0.00	0.00	.015	5.50
17 2412	3111	5.00	120.0	.3820	0.00	0.00	.015	5.00
18 3111	3112	4.00	1150.0	.0175	2.60	2.00	.030	3.50
19 3112	3211	7.00	1300.0	.0090	0.00	0.00	.015	7.00
20 3211	3311	9.50	1300.0	.0025	0.00	0.00	.015	7.75
21 3311	3612	9.50	800.0	.0060	0.00	0.00	.015	7.75
22 3612	4012	9.50	400.0	.0030	0.00	0.00	.015	7.75
23 *1612	3711	4.00	435.0	.0370	0.00	0.00	.015	0.00
24 3711	4311	5.00	620.0	.0060	3.00	3.00	.020	5.00
25 4011	4012	7.00	740.0	.0060	3.00	3.00	.020	5.00
26 4012	4013	9.50	200.0	.0030	0.00	0.00	.015	7.75
27 4013	4211	8.00	500.0	.0035	2.00	2.00	.020	6.50
28 4211	4212	12.00	300.0	.0036	0.00	0.00	.015	8.00
29 4212	4311	6.00	1100.0	.0026	1.10	1.10	.015	8.00
30 4411	4413	5.00	1447.0	.0770	0.00	0.00	.035	6.00
31 4413	4414	11.00	167.0	.0420	.58	.58	.040	6.00
32 4414	4415	33.00	143.0	.0090	0.00	0.00	.035	3.00
33 4415	4416	12.00	983.0	.0330	0.00	0.00	.035	3.00
34 4416	4417	8.00	420.0	.0071	0.00	0.00	.015	4.70
35 4417	4418	6.00	850.0	.0500	1.00	1.00	.040	5.00
36 4418	4311	12.00	325.0	.0090	0.00	0.00	.015	5.00
37 4311	430	8.00	750.0	.0026	1.10	1.10	.015	9.00
38 430	2992	8.00	150.0	.0026	1.36	1.36	.015	9.00
39 2992	2942	10.00	600.0	.0026	0.00	0.00	.015	9.00
40 2942	292	8.00	260.0	.0026	1.36	1.36	.015	9.00
41 $ 292	294	0.00	0.0	0.0000	0.00	0.00	0.000	0.00
42 294	299	8.00	2400.0	.0026	1.36	1.36	.015	9.00
43 299	2990	24.00	910.0	.0026	0.00	0.00	.015	11.00

TOTAL NUMBER OF GUTTERS/PIPES, 43

ASTERISK (*) DENOTES CIRCULAR PIPE, DIAMETER=WIDTH.
DOLLAR SIGN ($) DENOTES DUMMY GUTTER, USED TO OBTAIN PRINT OUTS ONLY.

Table 8.6 Fraction of pollutants for different DD sources (mg of pollutant/mg of DD).

Source	BOD	Suspended solids	Total solids	Total nitrogen (TKN)	Total phosphorus
Traffic related	0.0023	0.80	1.00	0.0016	0.00060
Dustfall	0.1000	0.80	1.00	0.0050	0.00075
Vegetation	0.2500	0.80	1.00	0.0010	0.00080
Population	0.0030	0.80	1.00	0.001	0.00040
Aerosols	0.0200	0.80	1.00	0.0100	0.00500
Canopy	0.1000	0.80	1.00	0.0050	0.00075

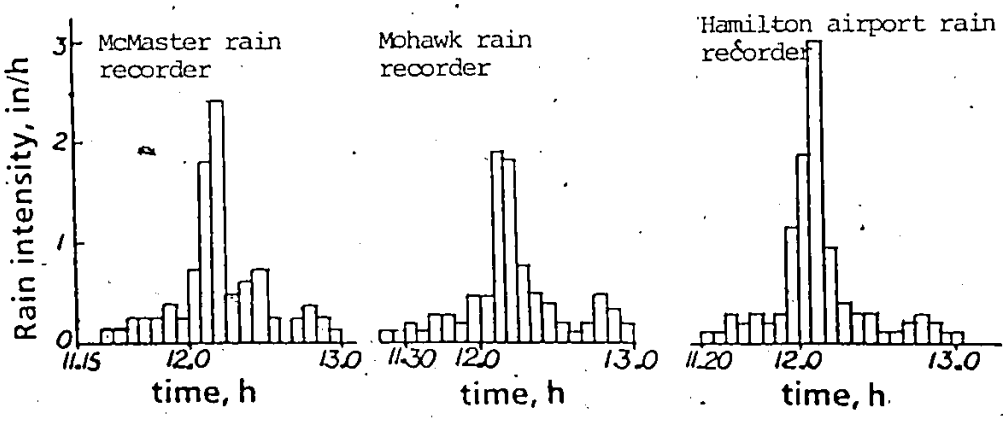

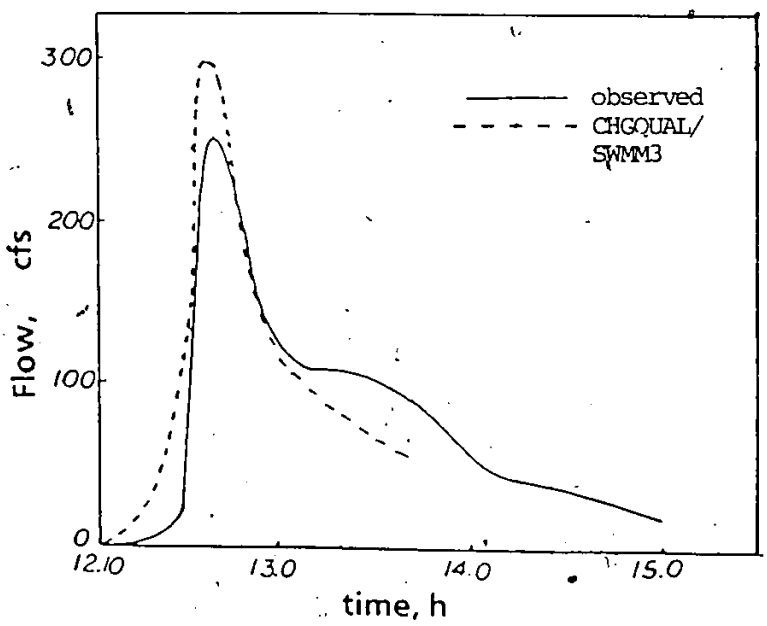

Figure 8.6 CHGQUAL and SWMM3 calibrated and observed hydrograph and pollutograph(storm#8, June 28,1980, Hydro station).

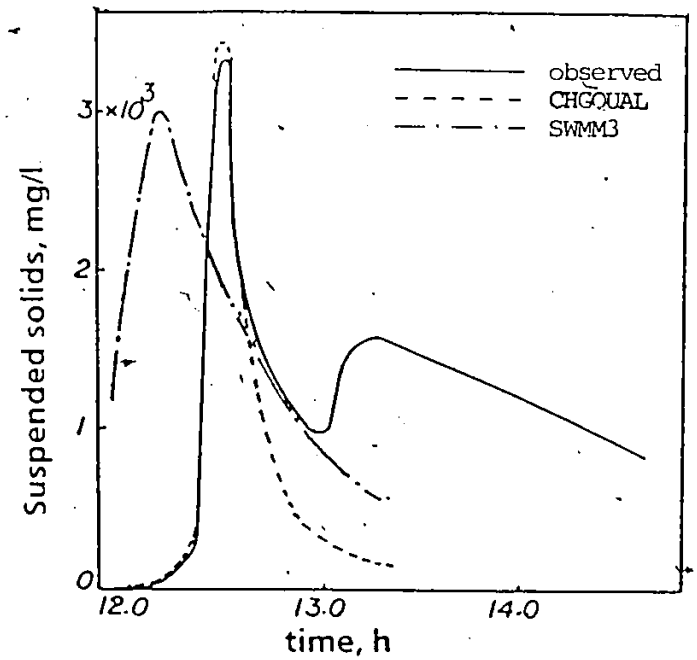

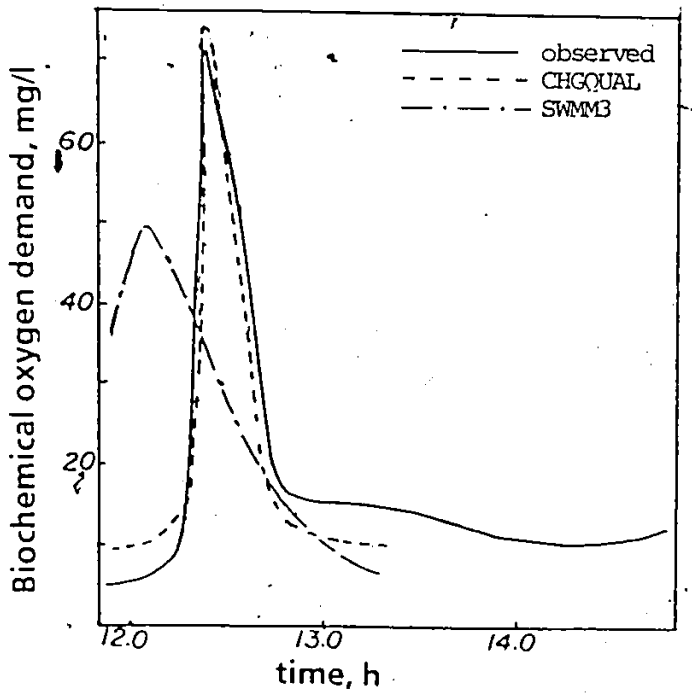

Figure 8.6 continued.
(storm#8, June 28, 1980, Hydro station)

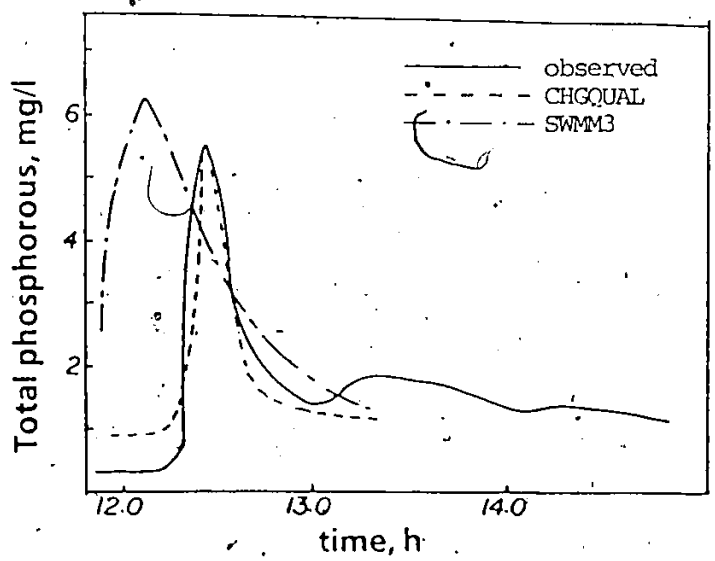

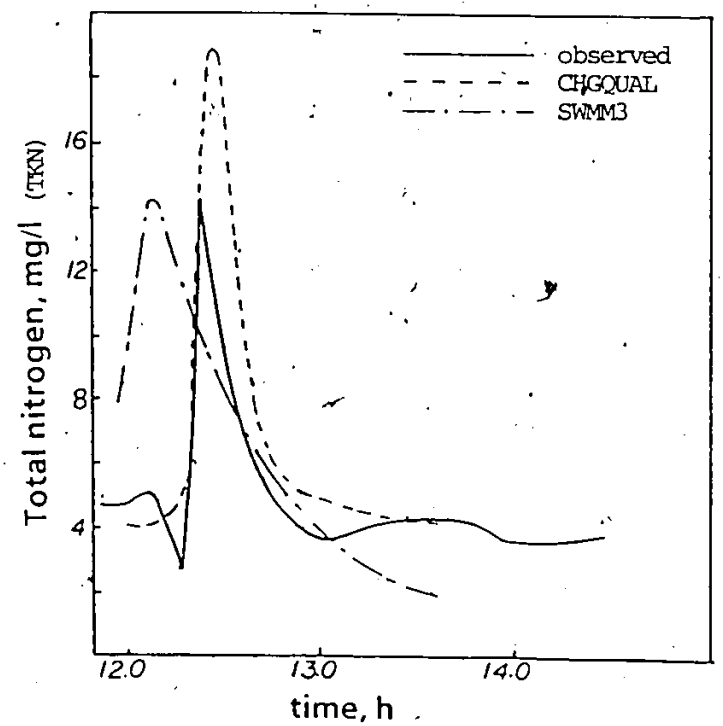

Figure 8.6 continued.
(storm#8, June 28, 1980, Hydro station)

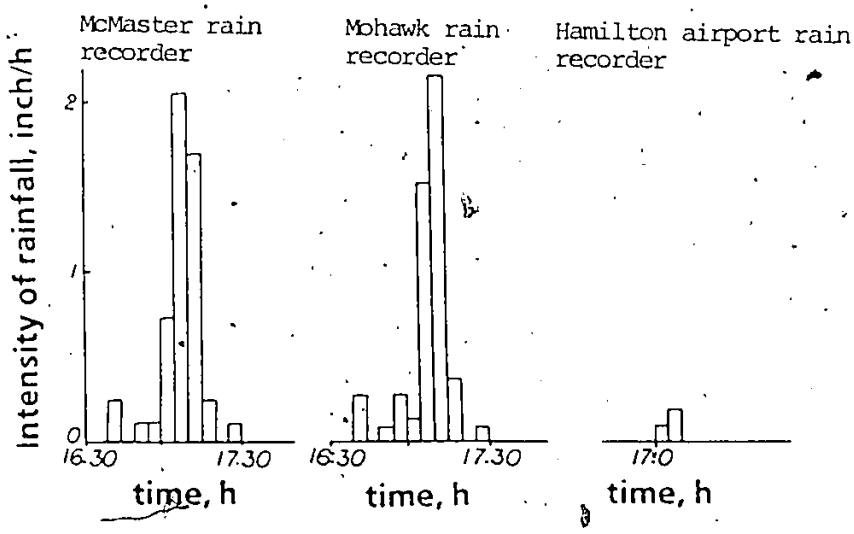

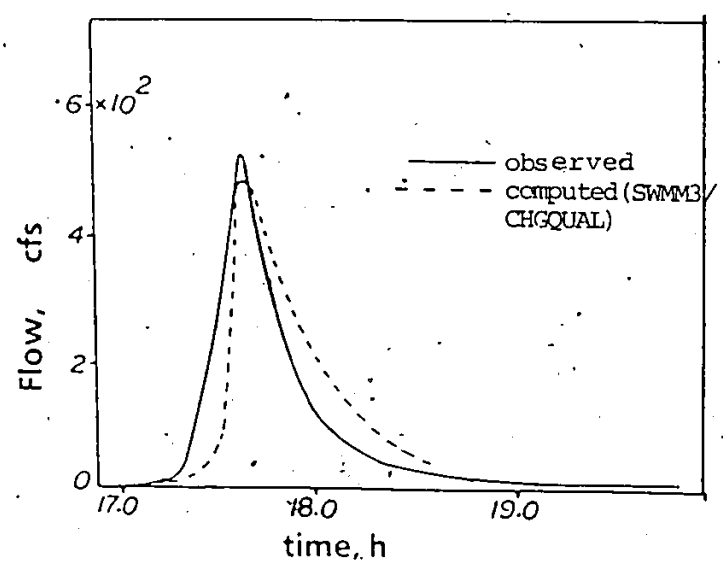

Figure 8.7 CHGQUAL and SWMM3 calibrated and observed hydrograph and pollutographs(storm#9, July 19,1980, Hotpoint station).

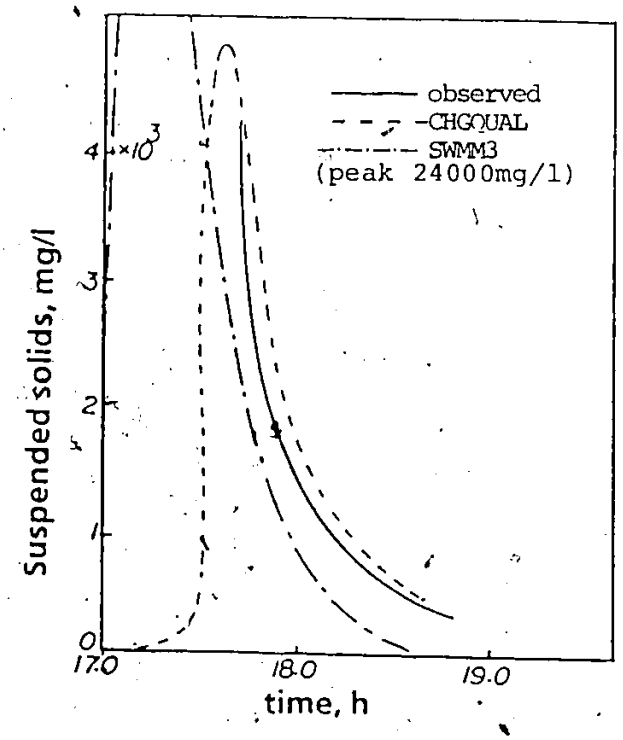

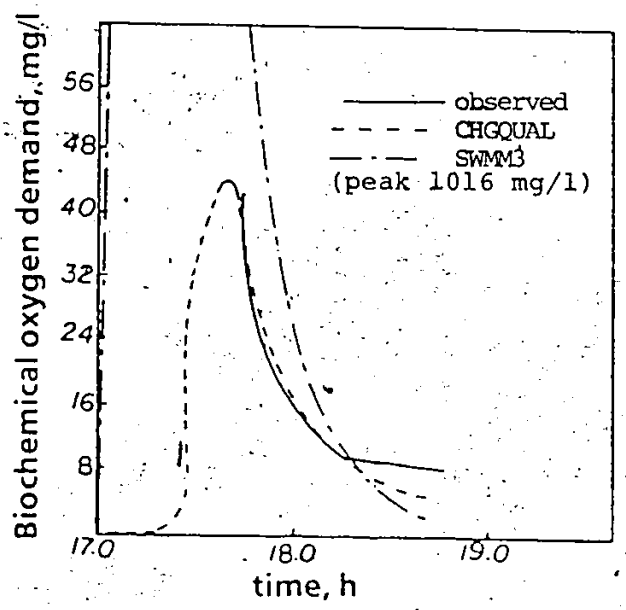

Figure 8.7 continued.(storm#9, July 19,1980, Hotpoint station)

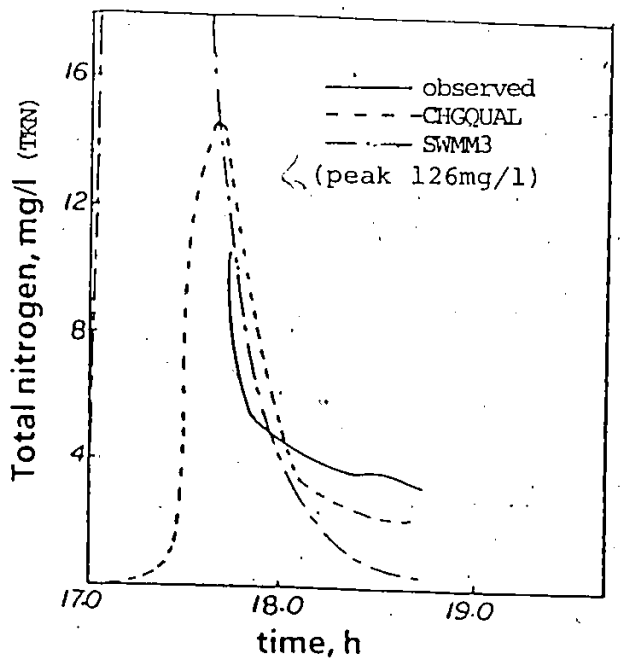

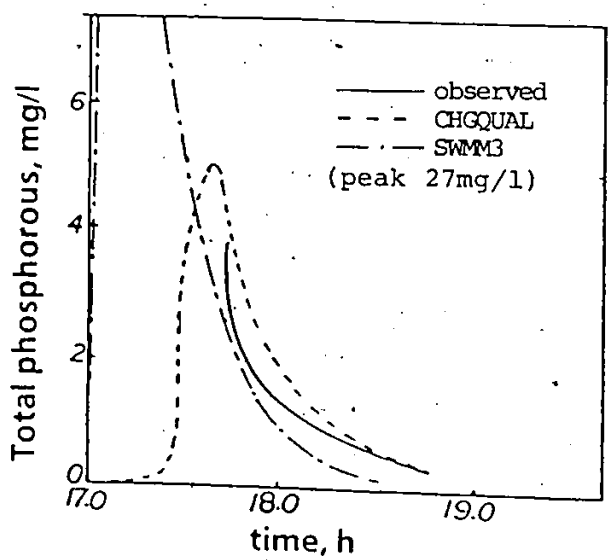

Figure 8.7 continued. (storm#9, July 19, 1980, Hotpoint station)

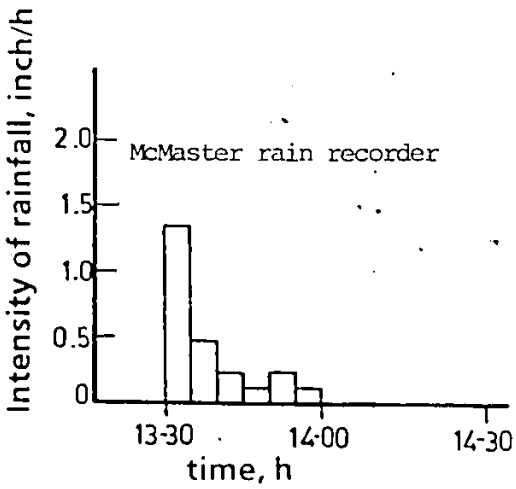

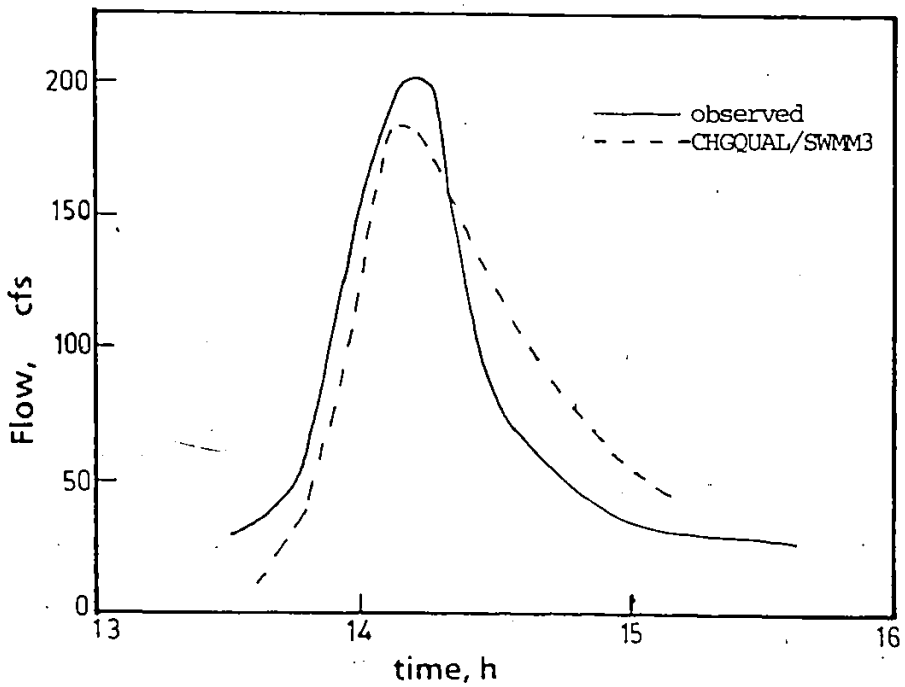

Figure 8.8 CHGQUAL and SWMM3 calibrated and observed hydrograph and pollutographs(storm #10, July 22, 1980, Hotpoint station).

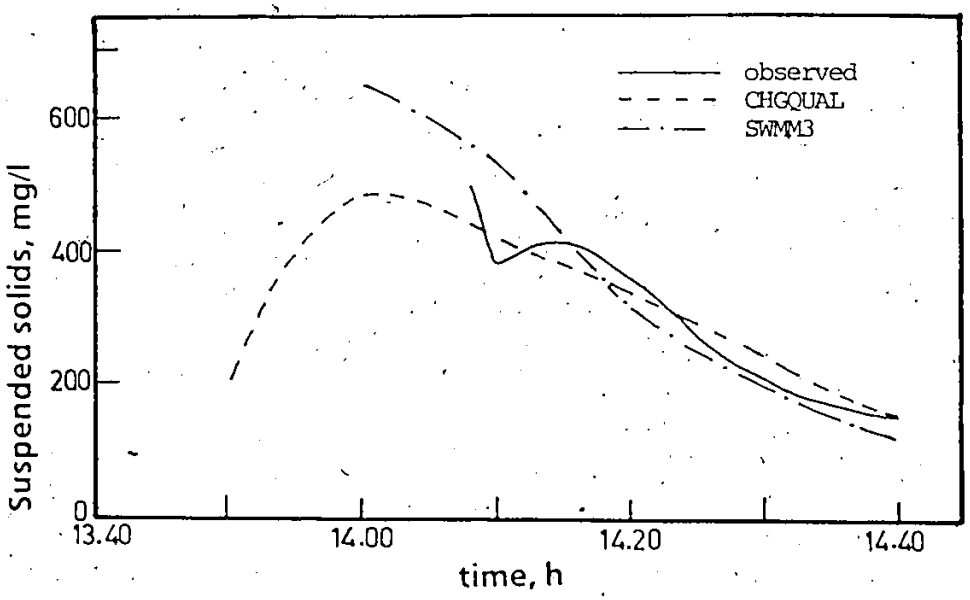

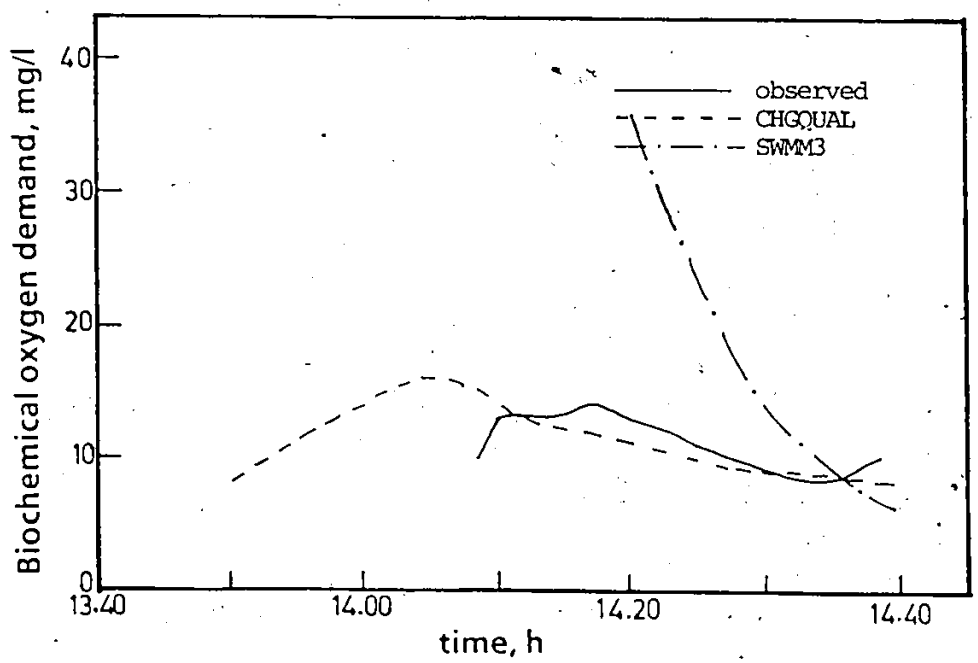

Figure 8.8 continued. (storm #10, July 22, 1980, Hotpoint station)

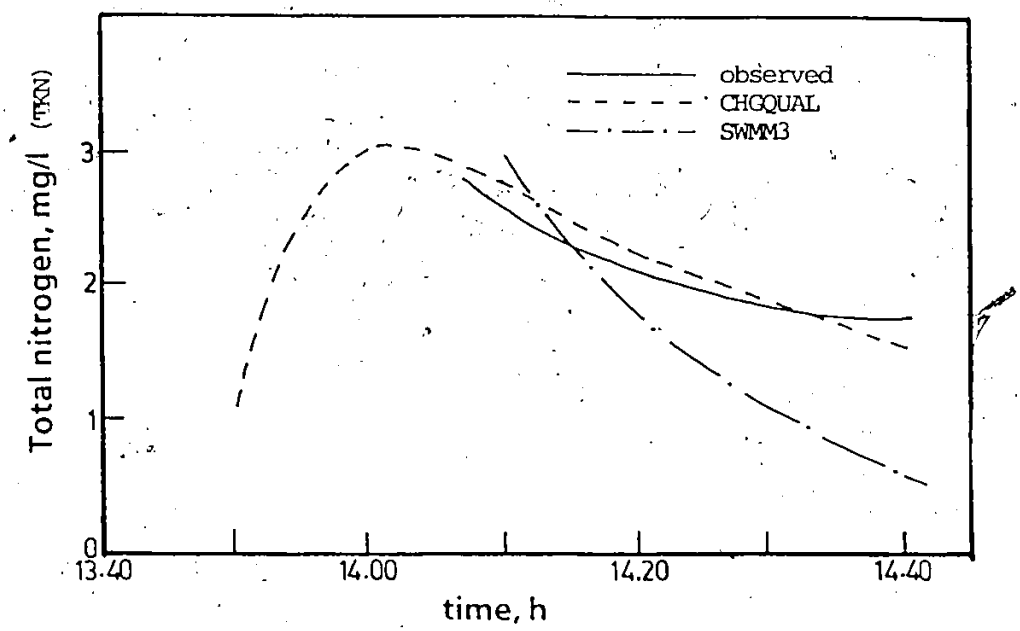

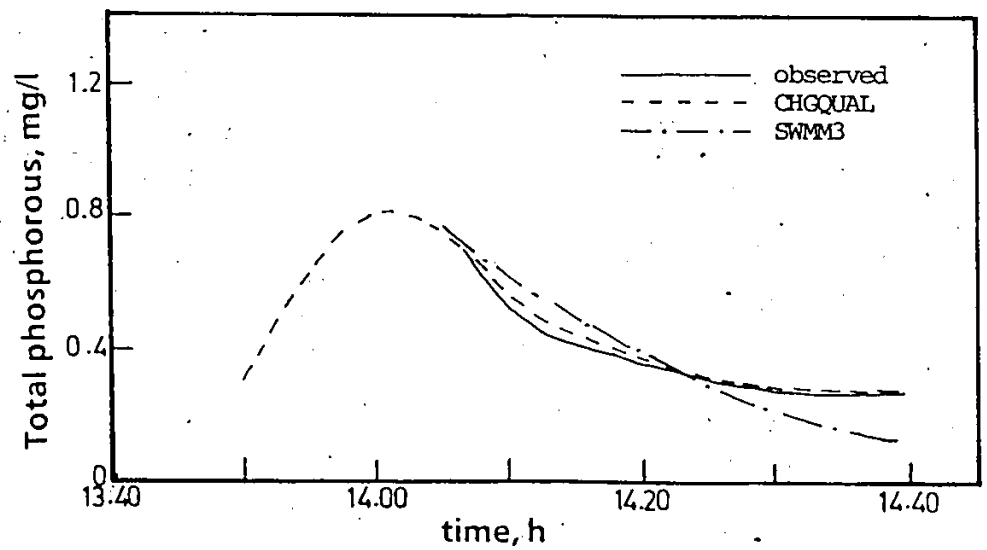

Figure 8.8 continued. (storm#10, July 22, 1980, Hotpoint station)

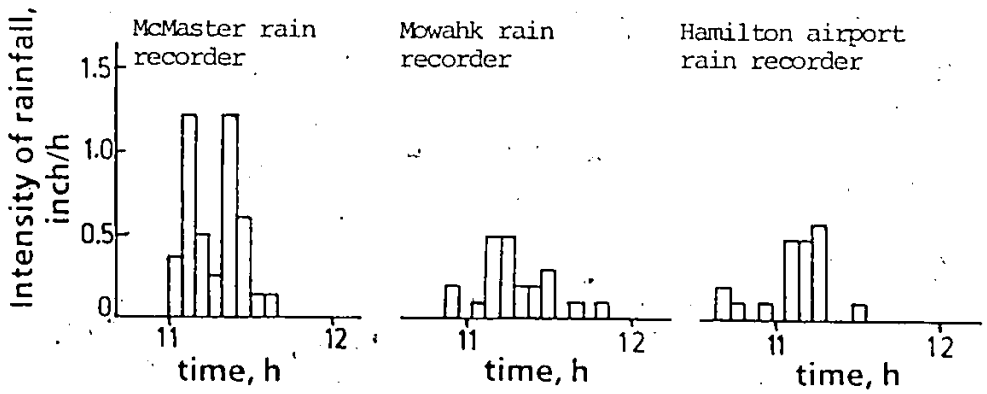

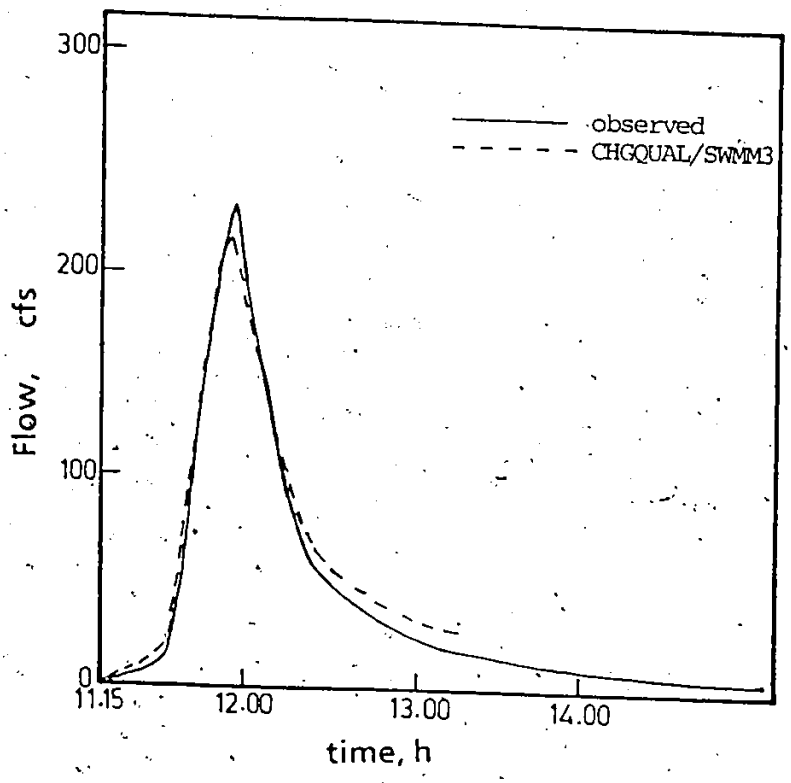

Figure 8.9 CHGQUAL and SWMM3 calibrated and observed hydrograph and pollutographs(storm#12, August 14, 1980, Hotpoint station).

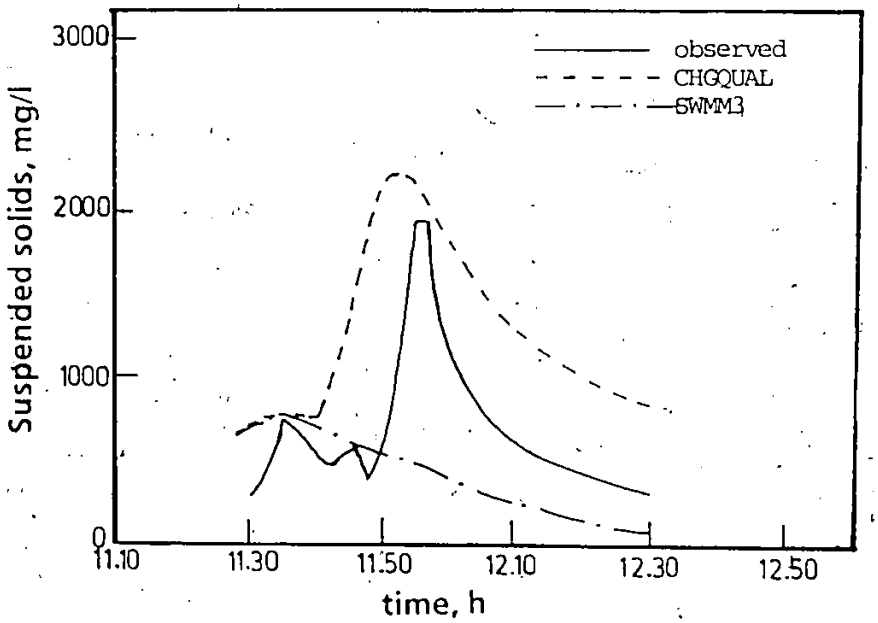

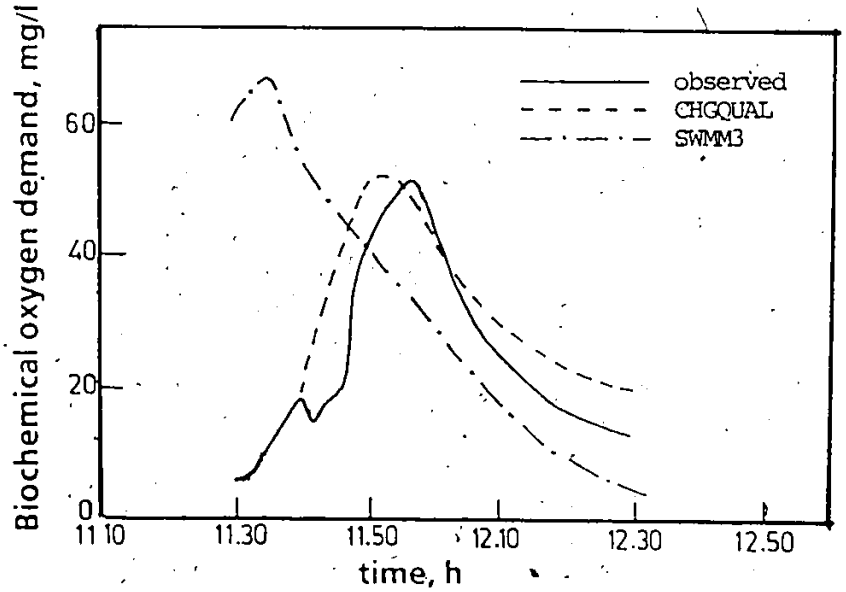

Figure 8.9 continued. (storm#12, August 14, 1980, Hotpoint station)

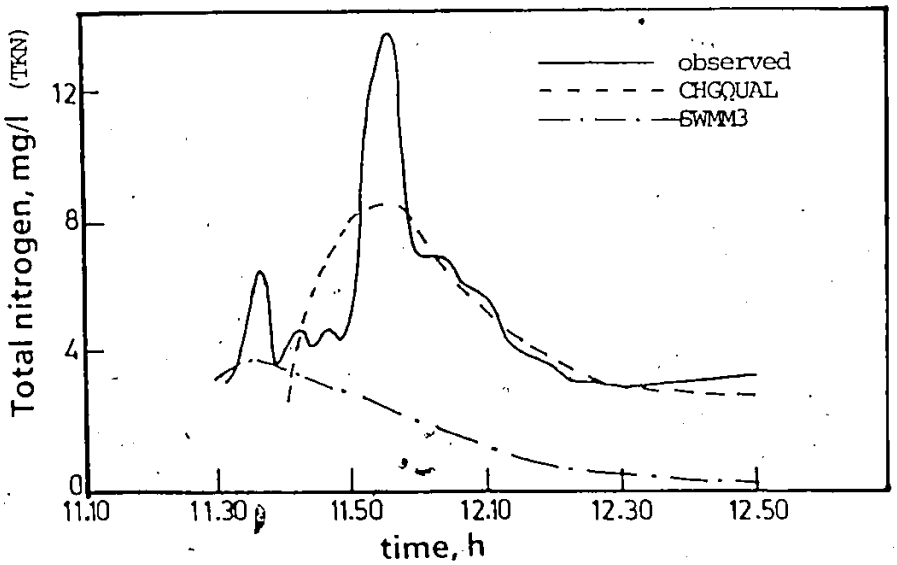

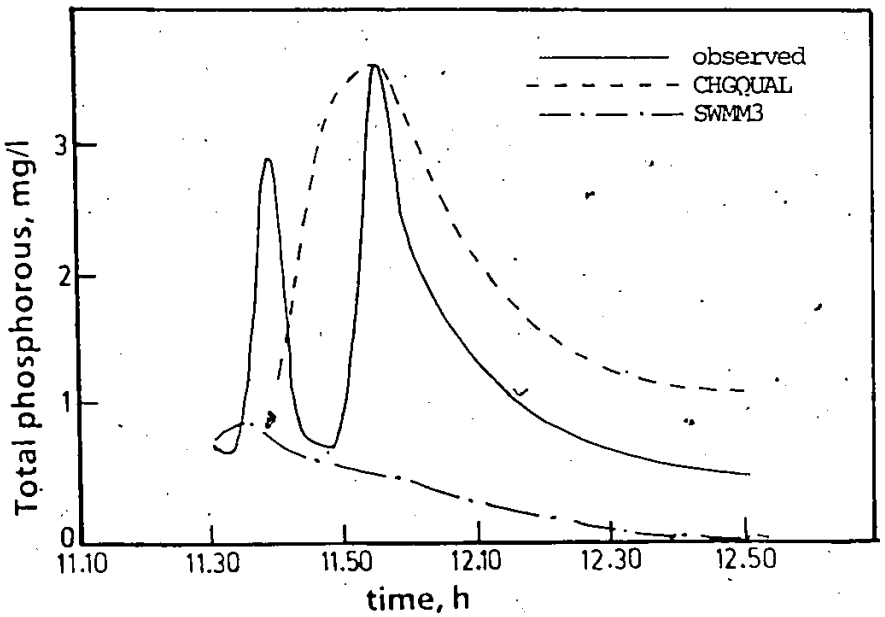

Figure 8.9 continued.(storm#12, August 14, 1980, Hotpoint station).

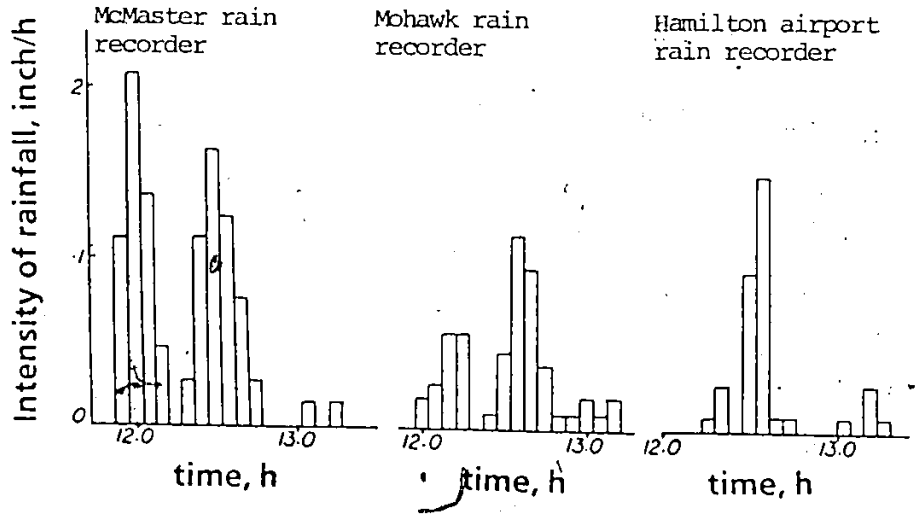

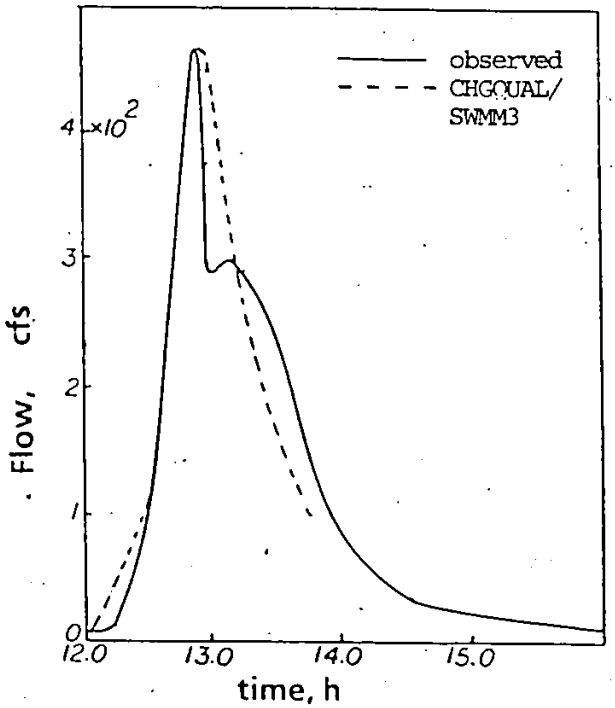

Figure 8.10 CHGQUAL and SWMM3 calibrated and observed hydrograph and pollutographs(storm#13, August 22, 1980, Hotpoint station)

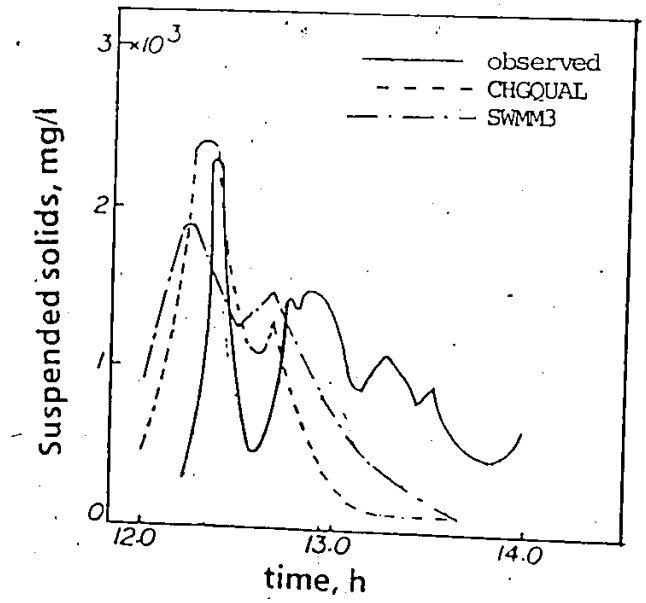

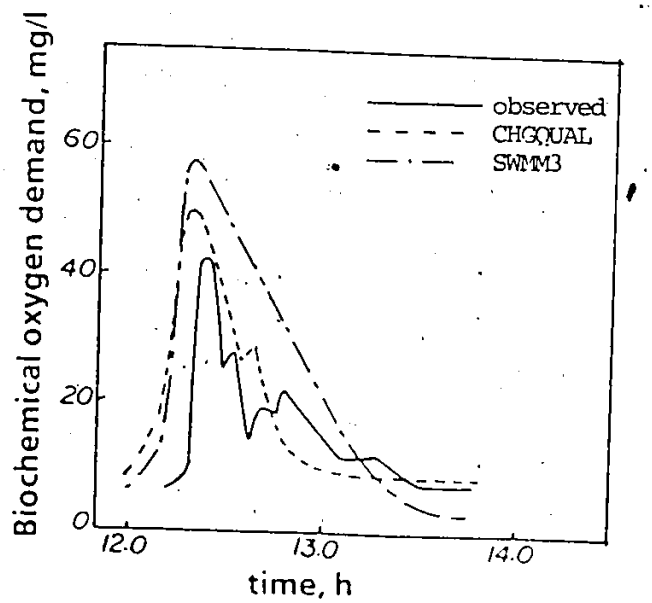

Figure 8.10 continued. (storm#13, August 22, 1980, Hotpoint station)

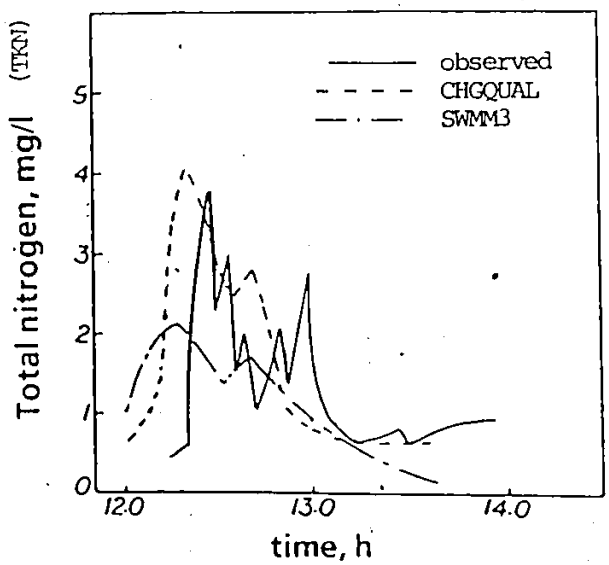

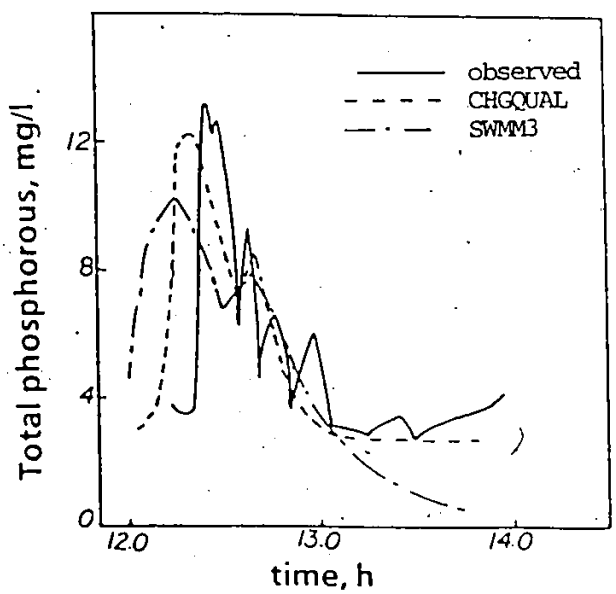

Figure 8.10 continued. (storm#13, August 22, 1980, Hotpoint station)

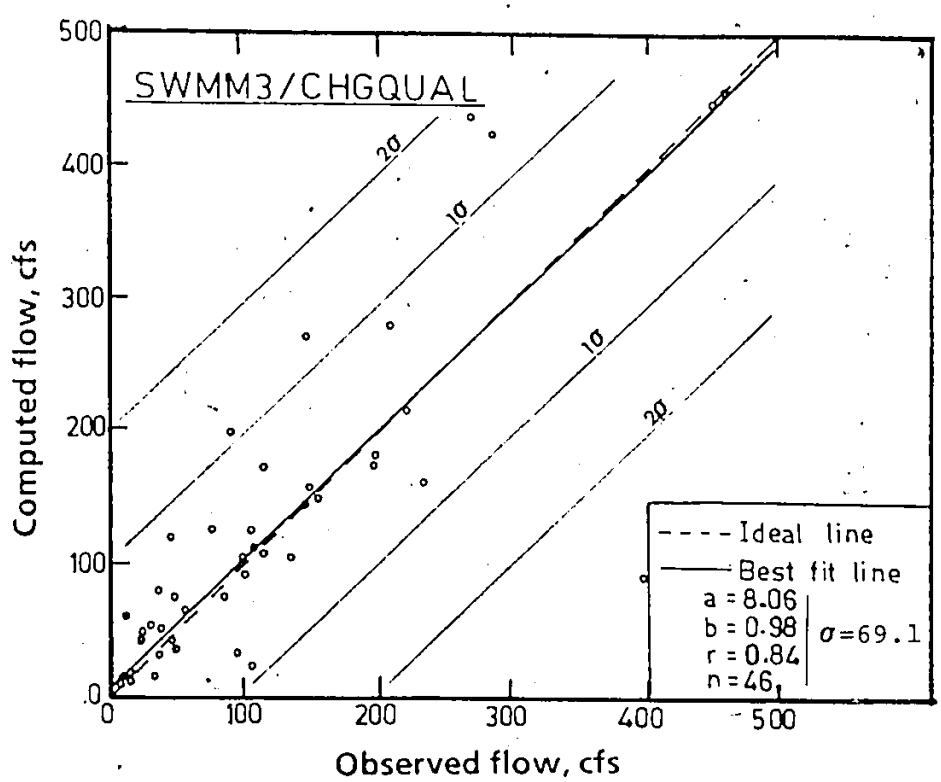

Figure 8.11 Statistical comparison between observed and calibrated hydrograph and pollutographs.

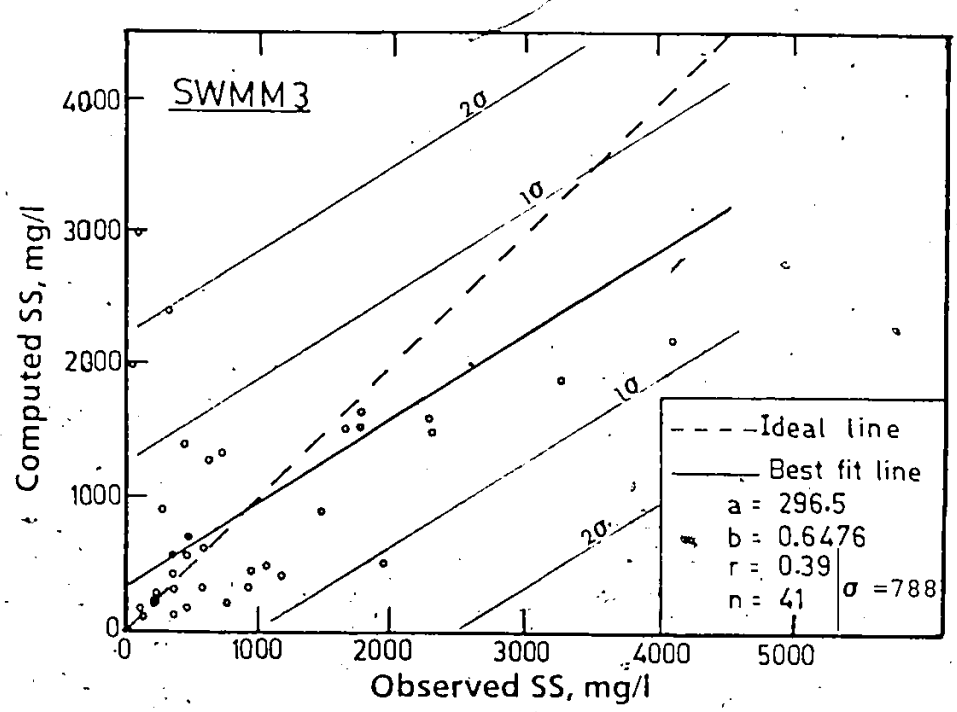

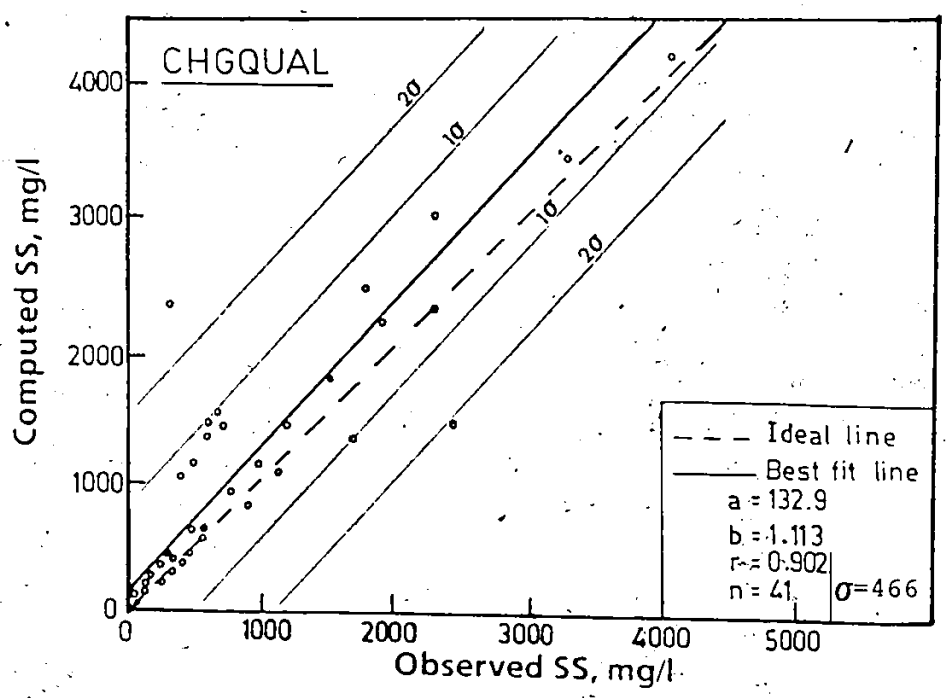

Figure 8.11 continued.

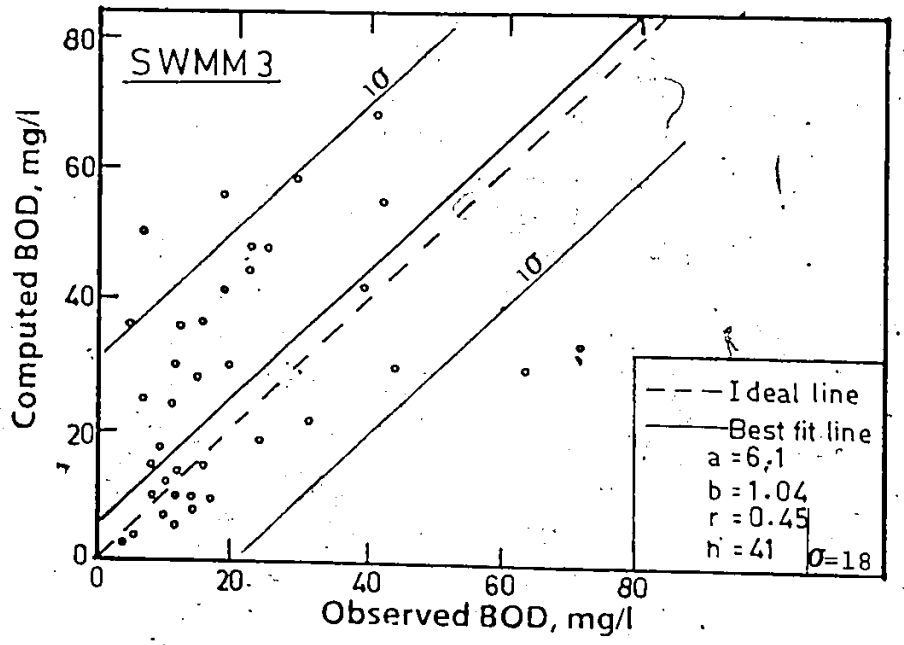

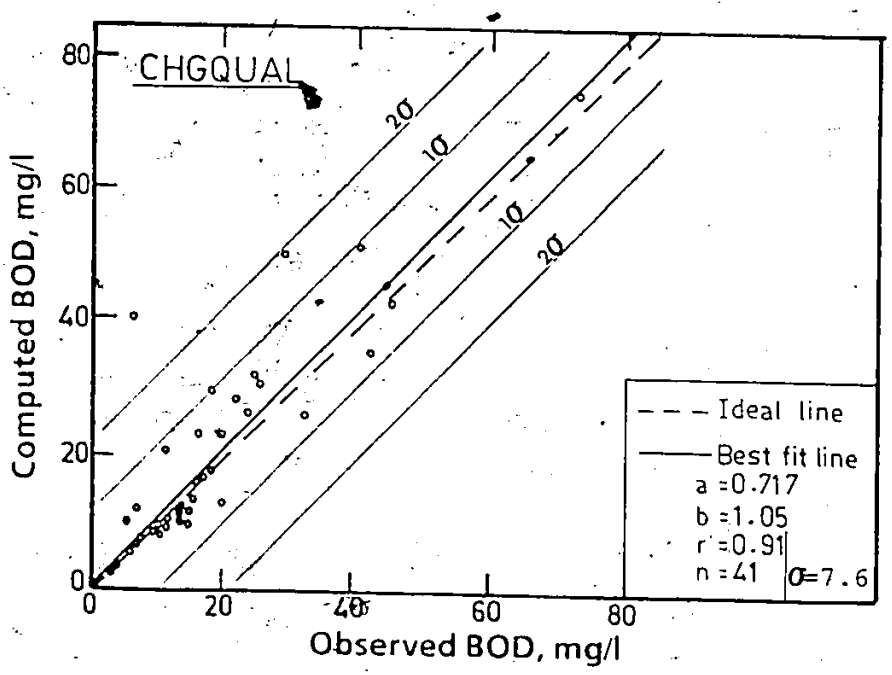

Figure 8.11 continued.

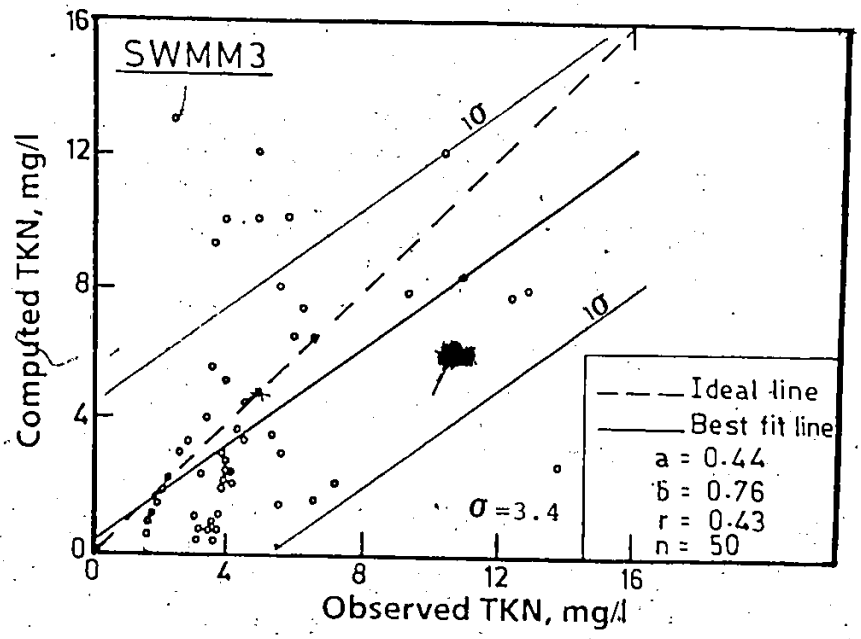

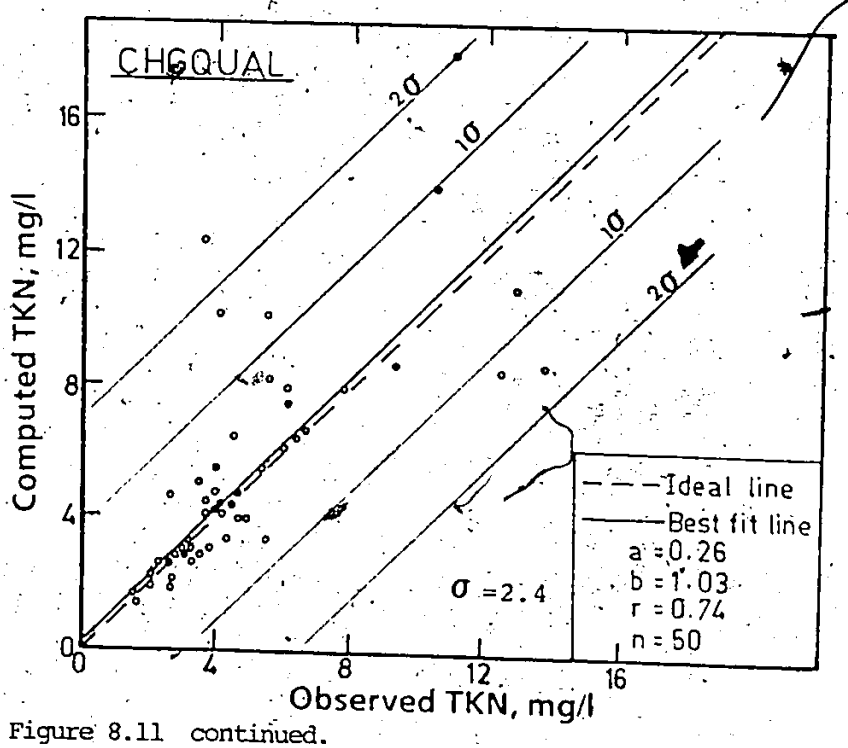

Figure 8.11 continued.

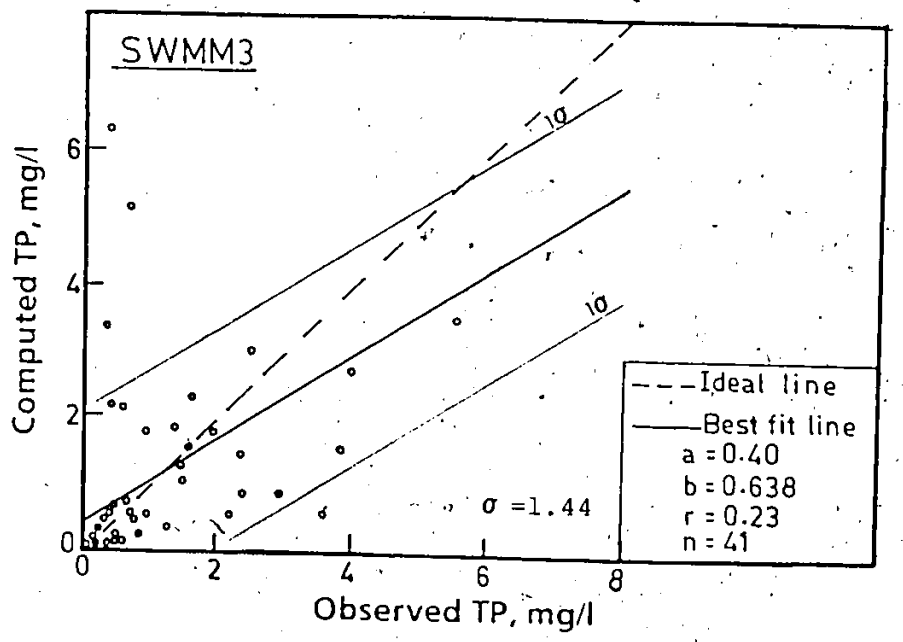

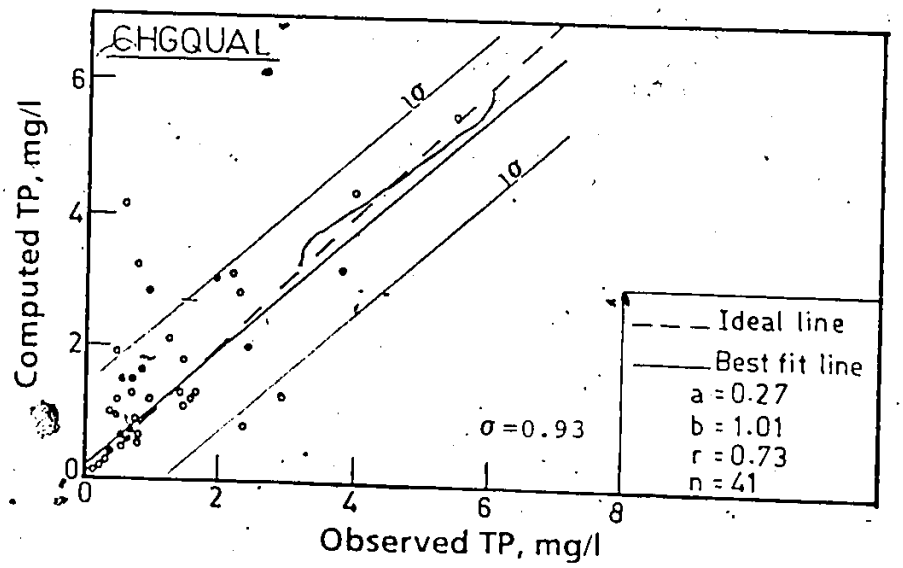

Figure 8.11 continued.

Table 8.7 Statistical comparison between CHGQUAL and SWMM3 (calibrated results)

Statistical parameter	values for best fit lines								
	flow	SS		BOD		TKN		TP	
	CHGQUAL/SWMM3	CHGQUAL	SWMM3	CHGQUAL	SWMM3	CHGQUAL	SWMM3	CHGQUAL	SWMM3
a	8.06	132.99	296.46	0.72	6.10	0.26	0.44	0.27	0.40
b	0.98	1.11	0.65	1.05	1.04	1.04	0.76	1.01	0.64
standard deviation	69.10	466.20	788.16	7.56	17.74	2.39	3.38	0.93	1.44
covariance	50.61	37.82	84.22	34.28	65.48	44.38	80.16	57.07	115.15
correlation coefficient	0.84	0.90	0.39	0.90	0.46	0.74	0.40	0.73	0.23
RMSE	67.58	452.00	764.62	7.36	17.27	2.35	3.32	0.91	1.41
relative error	0.22	0.13	0.45	0.15	0.50	0.12	0.44	0.20	0.50

approximate speed of the storm. The observed peak flow and time to peak were also used as guidelines to fit the hyetograph to each individual subcatchment. The minor adjustment for the flow and pollutant concentration was done by calibration. Since the model is very sensitive to most input data, the storm starting time was lagged to account for storm travelling time, and pollutant load rates and meteorological data were adjusted to match the predicted results with the observed data. The average pollutant fraction for different sources of DD used in the calibrating storms is given in Table 8.6. The typical observed and calibrated pollutographs (BOD, SS, TKN, TP) and hydrographs for CHGQUAL and SWMM3 are plotted in Figures 8.6, 8.7, 8.8, 8.9 and 8.10. The pollutographs produced by CHGQUAL agree well with observed data when compared to SWMM3 results. Finally, the results predicted by both CHGQUAL and SWMM3 models are compared statistically as shown in Figure 8.11 and Table 8.7. The statistical criteria discussed in section 2.3.5 are used for model comparison. The statistics of both best fit lines of CHGQUAL and SWMM3 were compared with ideal line. The statistics results indicated that CHGQUAL predicts better than SWMM3.

8.6. VALIDATION

8.6.1. Introduction:

Validation is defined as testing the model against a new set of data not previously used in calibration (James

and Robinson, 1981). A favourable comparison of output from the calibrated model against sufficient observed independent field data sets would validate the model. If the model is correct then the validated results must be same as observed data. Whatever the model sophistication, it is hard to match the observed data exactly because of the complexity of the real process. After satisfactory results are obtained in validation a model could be applied with more confidence to real situations.

8.6.2. Validation of CHGQUAL model:

After calibration, CHGQUAL was subjected to validation. The data used for validation were collected in the summers of 1981 to 1983. Pollutant parameters used for validation were BOD, SS, total nitrogen, and total phosphorous. Most of the observed pollutant concentration results for 1981-1983 were almost equal to the baseflow concentration because of the frequency of late night or weekend storms. Therefore, only a few data sets were available. These observed and validated hydrographs and pollutographs are plotted in Figures 8.12, 8.13 and 8.14. The validated results are good with respect to time to peak and peak concentration. The observed and predicted results were compared statistically using the criteria discussed in section 2.3.5. The statistical results are tabulated in Table 8.8 and plotted in Figure 8.15. The CHGQUAL predicted

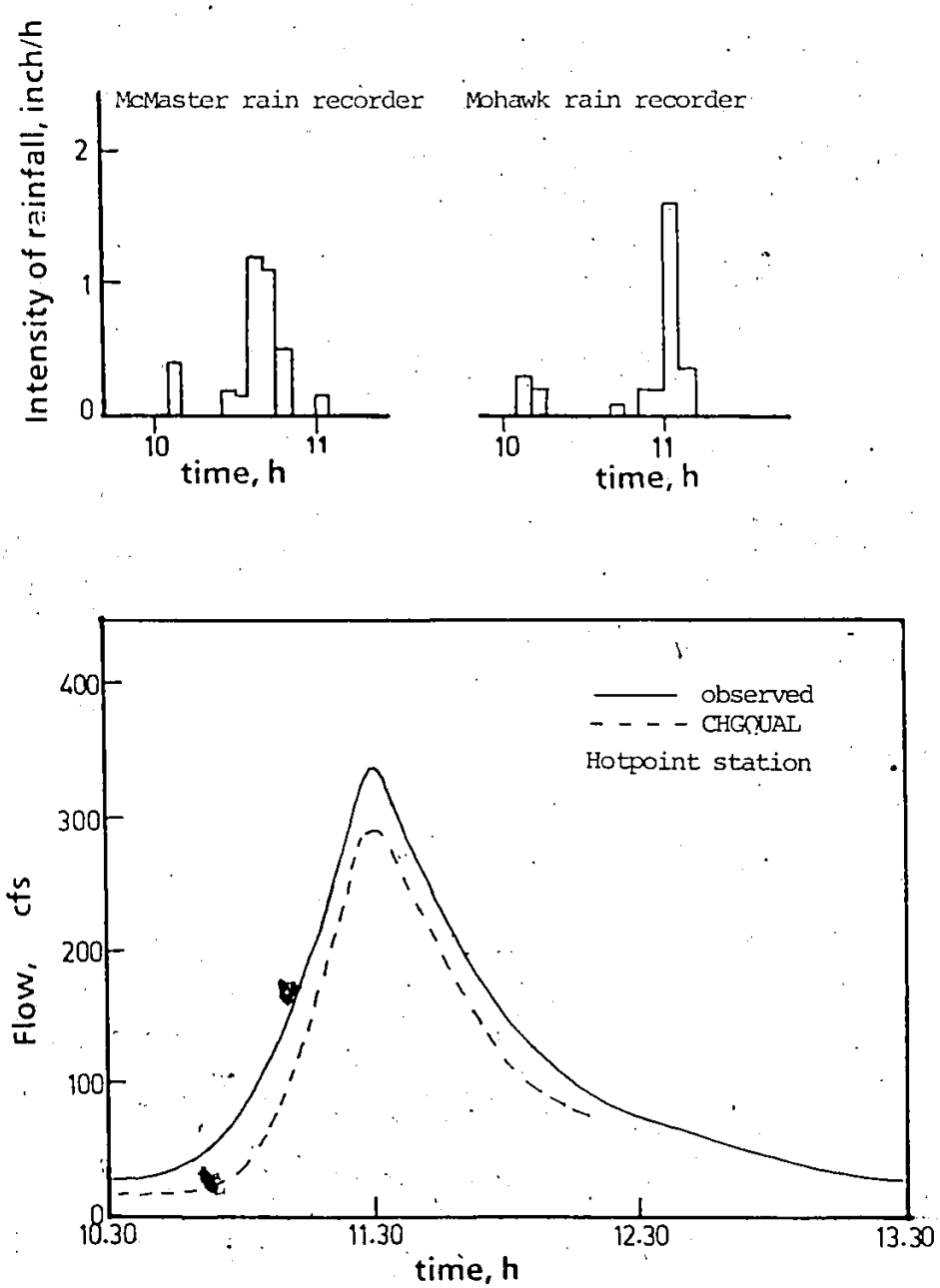

Figure 8.12 CHGQUAL validated and observed hydrograph and pollutograph (June 22, 1981).

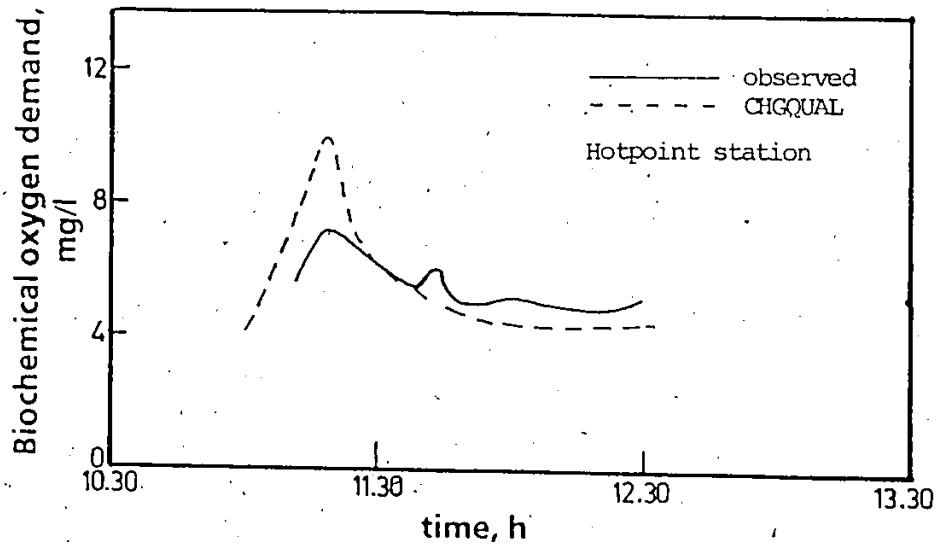

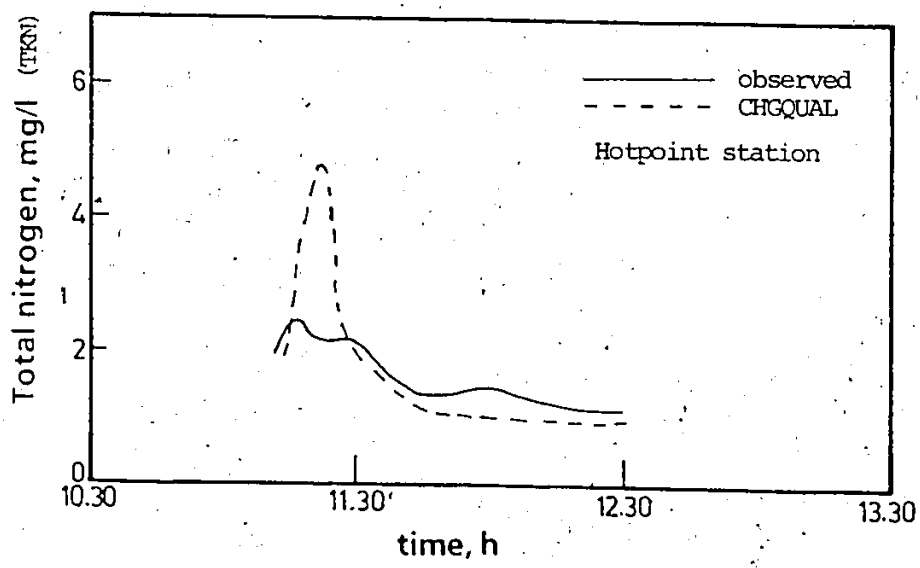

Figure 8.12 continued. (June 22, 1981)

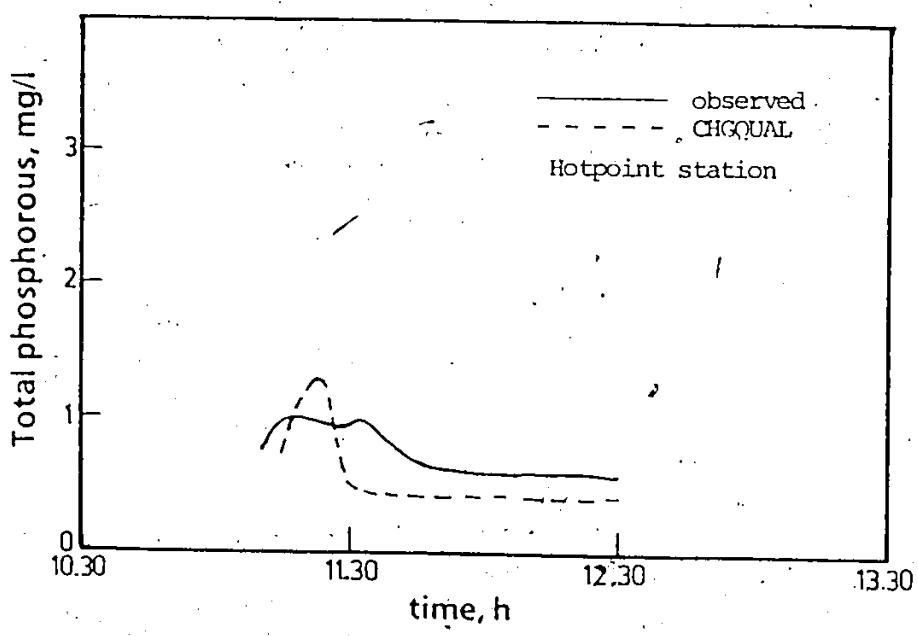

Figure 8.12 continued. (June 22, 1981)

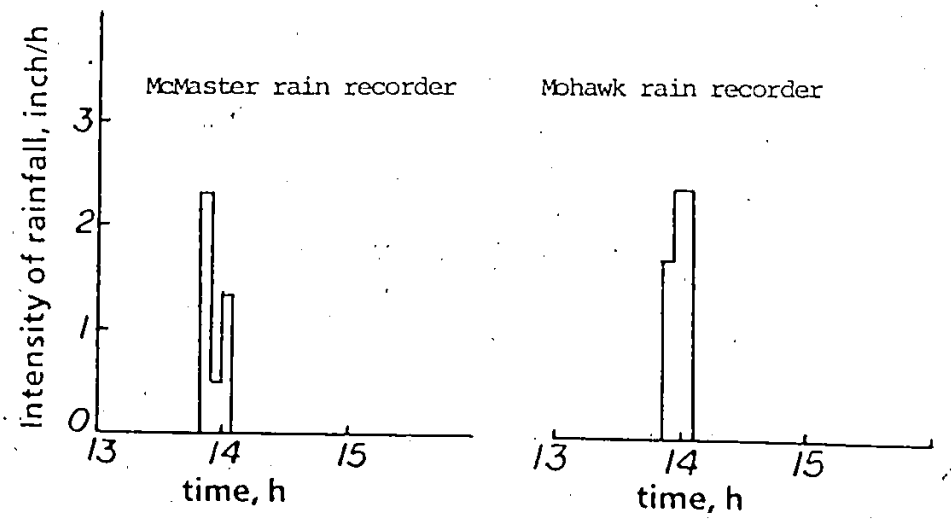

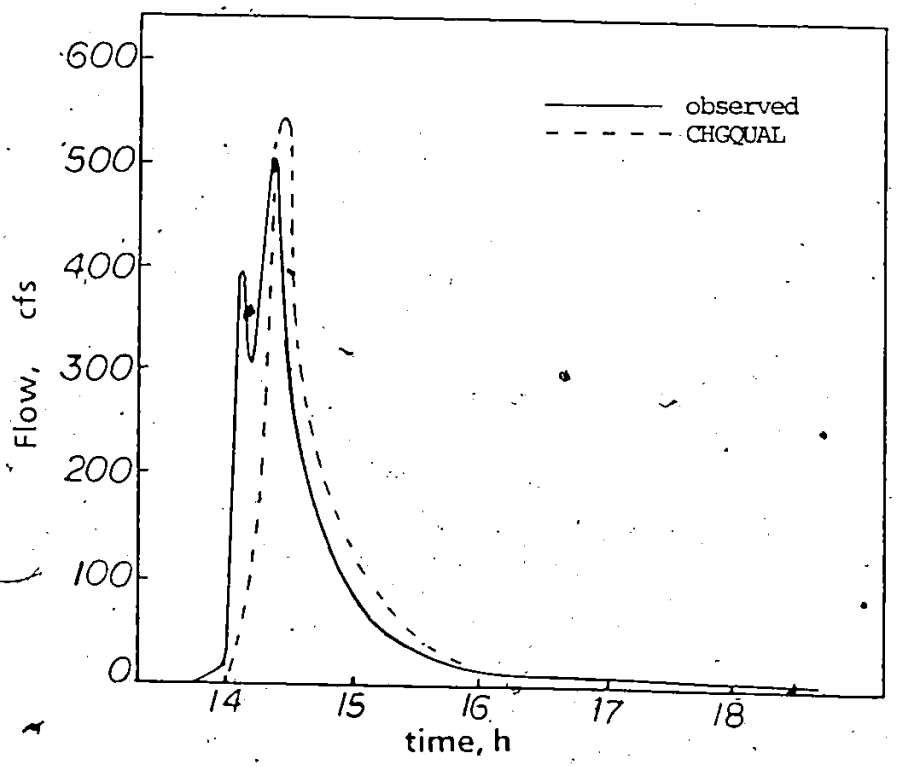

Figure 8.13 CHGQUAL validated and observed hydrograph and pollutographs (July 9, 1981, Hotpoint station).

Figure 8.13 continued. (July 9, 1981, Hotpoint station)

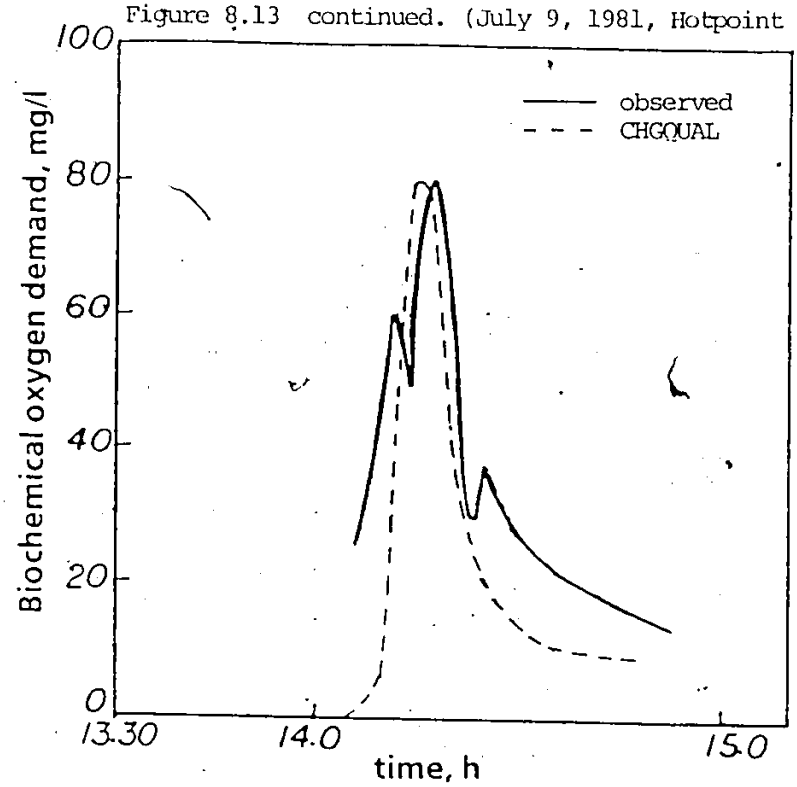

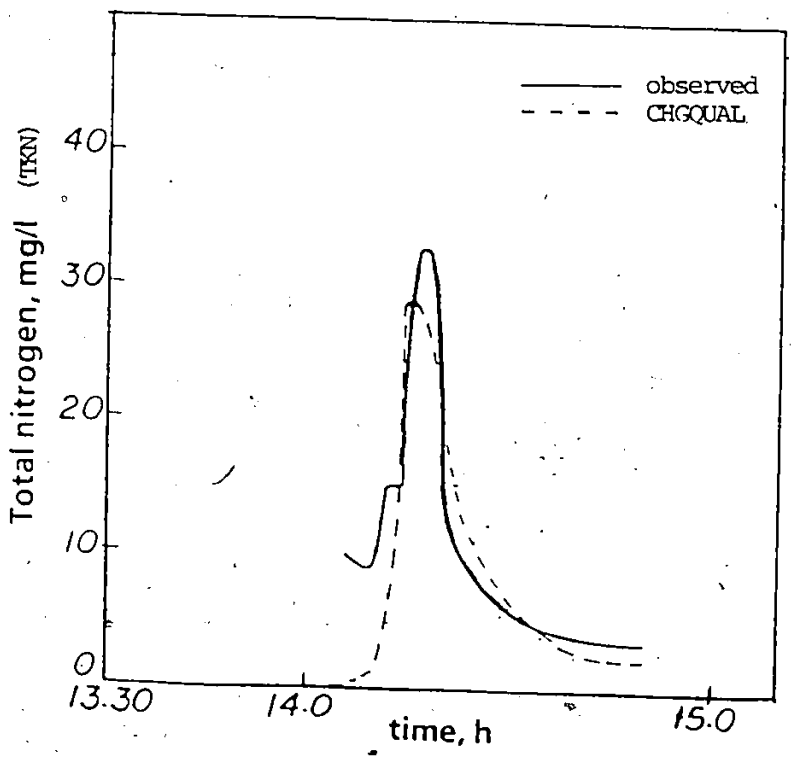

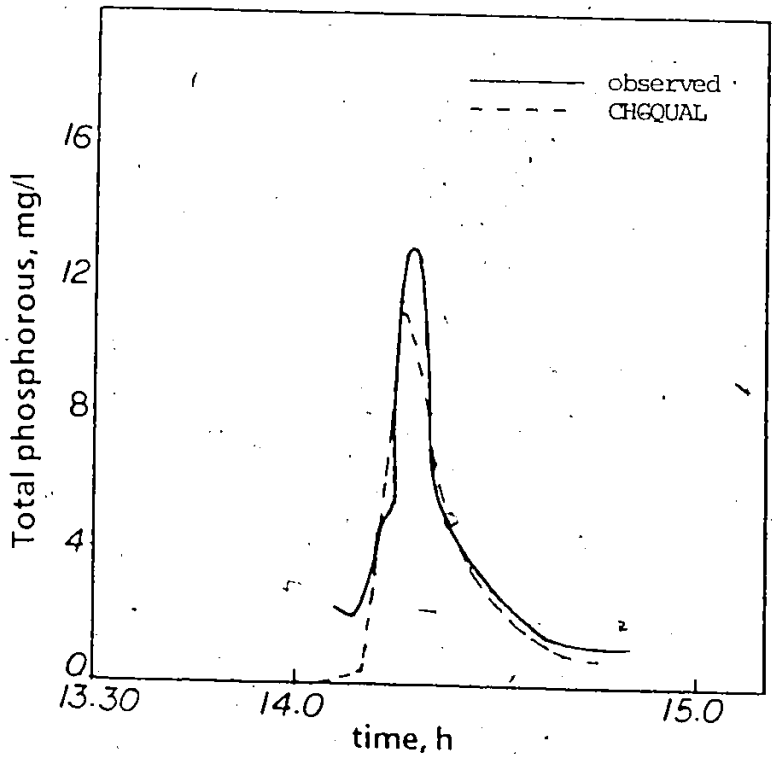

Figure 8.13 continued. (July 9, 1981, Hotpoint station)

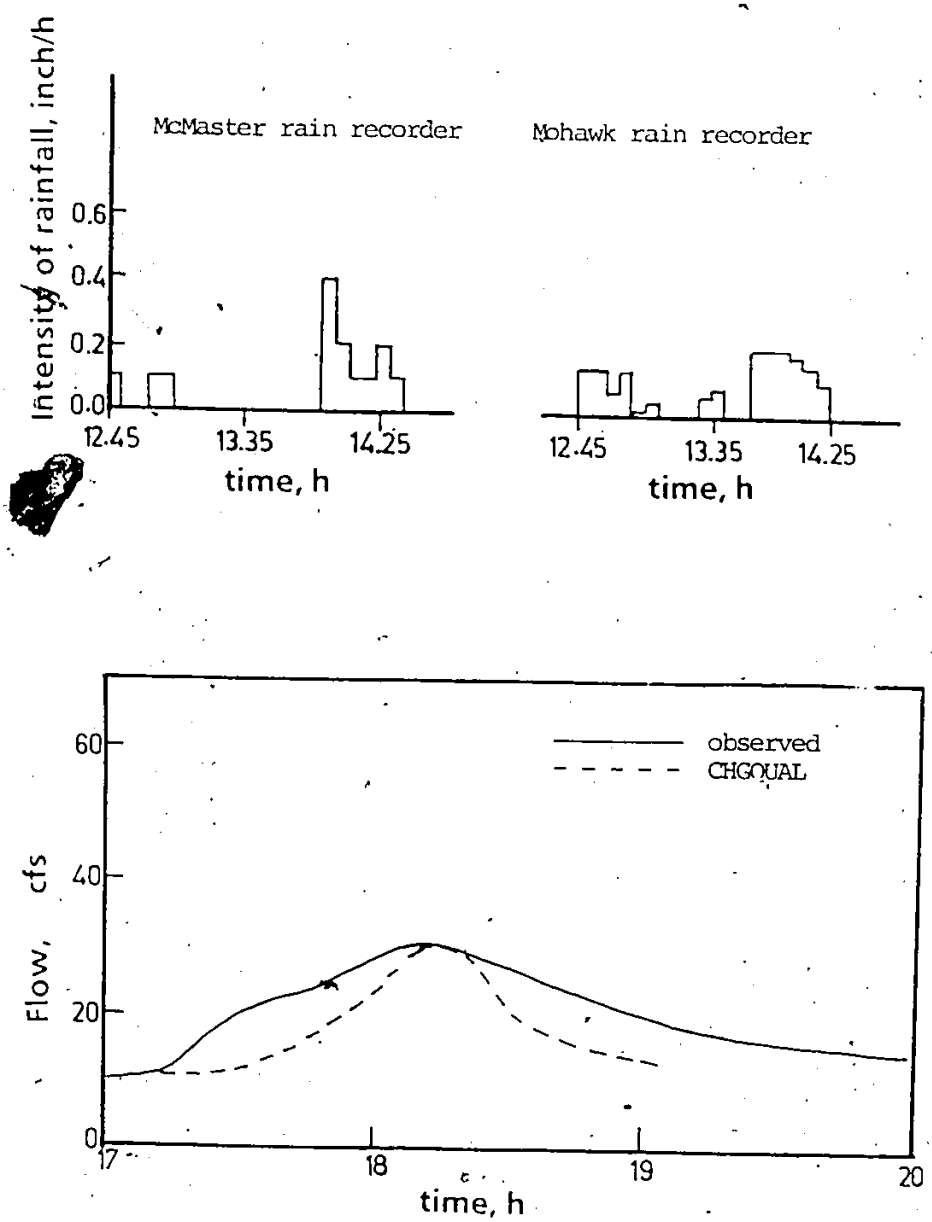

Figure 8.14 CHGQUAL validated and observed hydrograph and pollutographs(July 27, 1982, Hydro station).

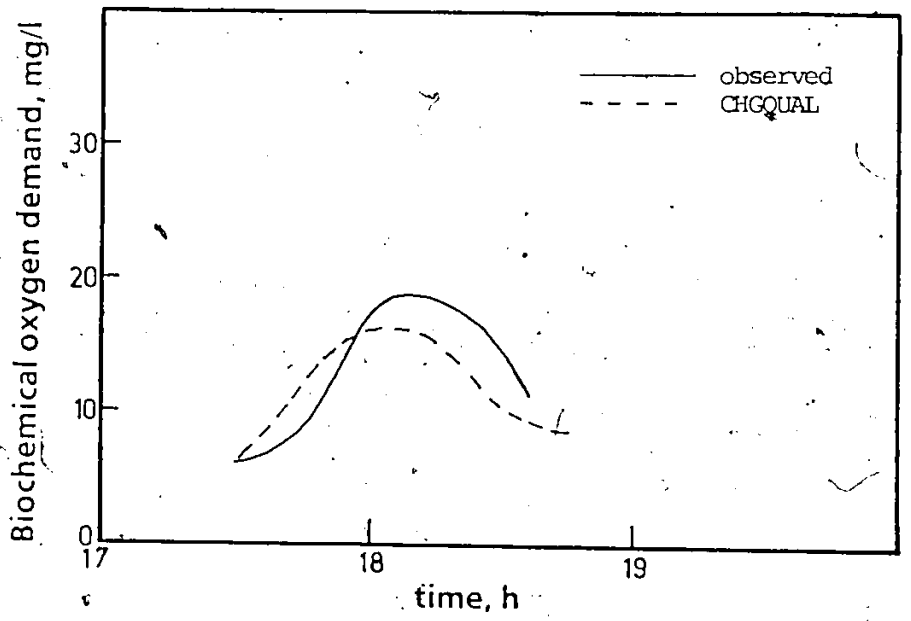

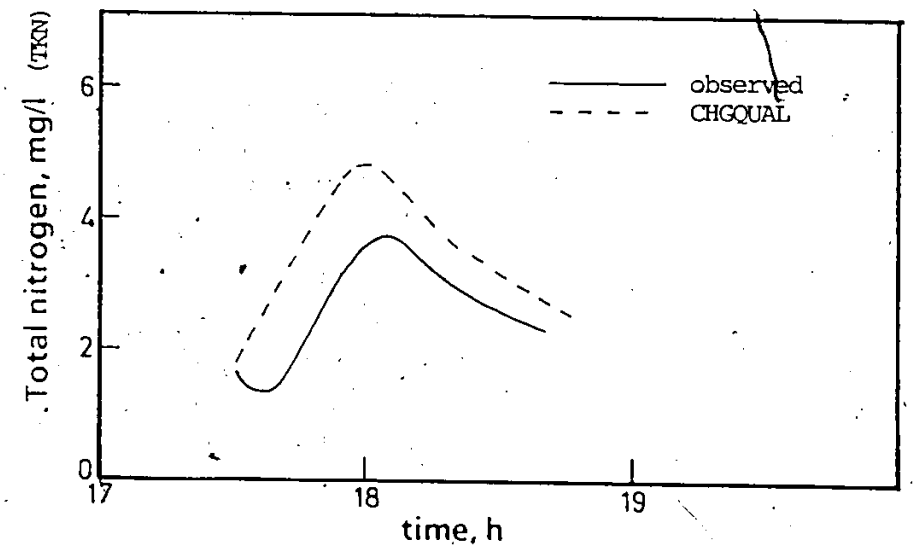

Figure 8.14 continued. (July 27, 1982, Hydro station)

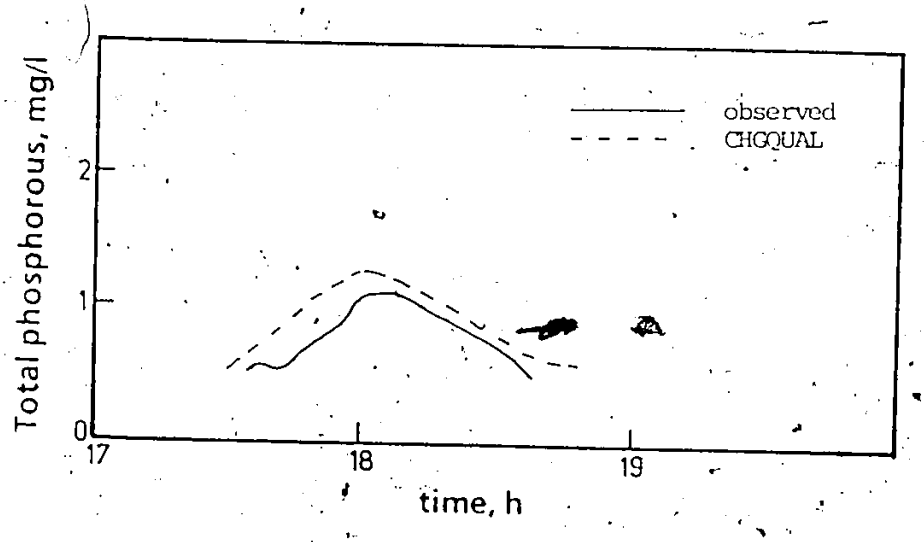

Figure 8.14 continued. (July 27, 1982, Hydro station)

Table 8.8 Statistical analysis on CHGQUAL validation results.

statistical parameter	values for best fit lines			
	flow	BOD	TKN	TP
a	-4.30	-0.30	0.19	0.14
b	0.88	0.85	0.92	0.89
std. dev.	34.59	7.54	1.80	0.51
covariance	40.04	47.91	36.92	27.20
cor. coef.	0.96	0.91	0.96	0.98
RMSE	33.18	7.29	1.74	0.49
rel. error	0.20	0.15	0.19	0.21

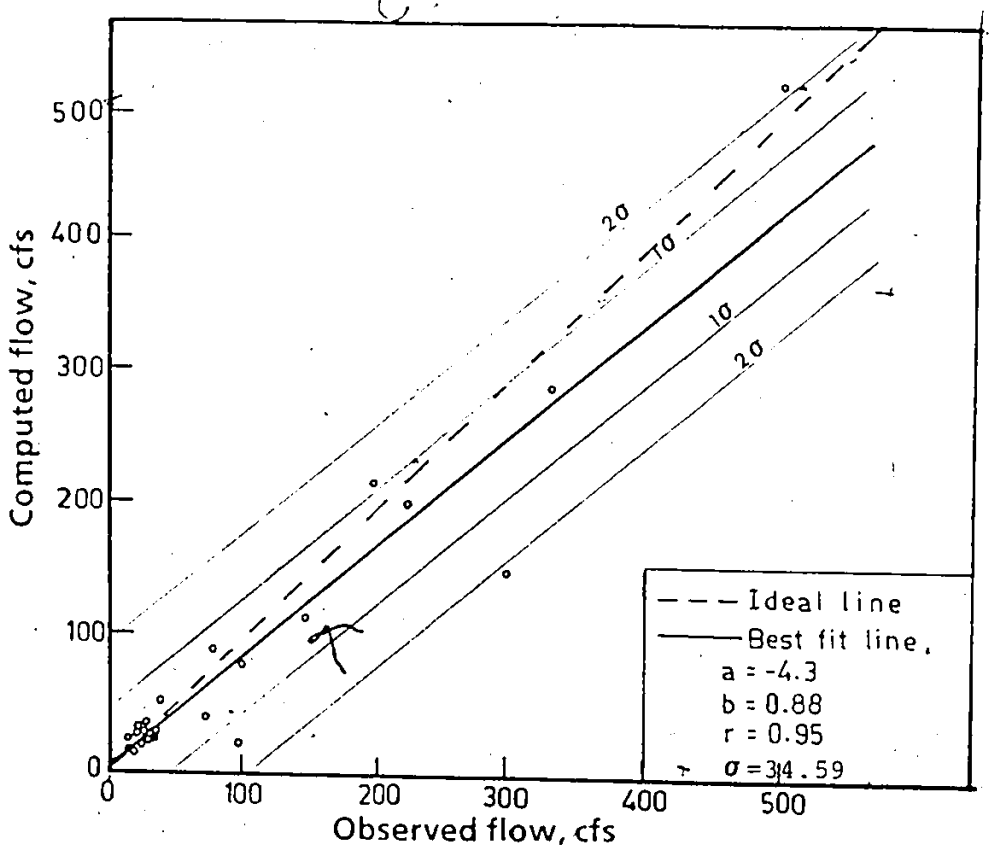

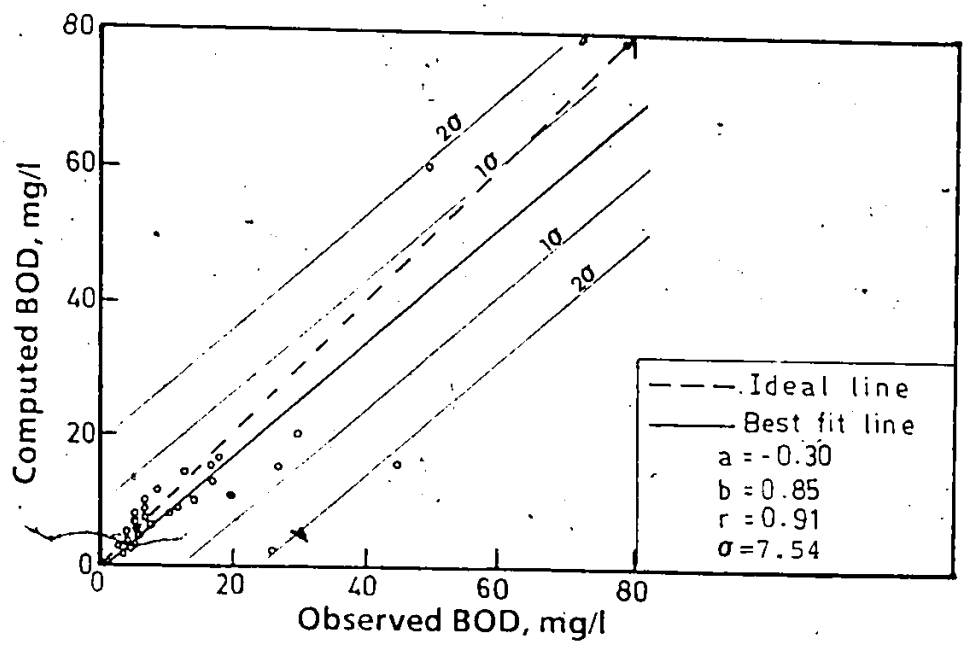

Figure 8.15 Statistical comparison between observed and validated hydrograph and pollutographs.

Figure 8.15 continued.

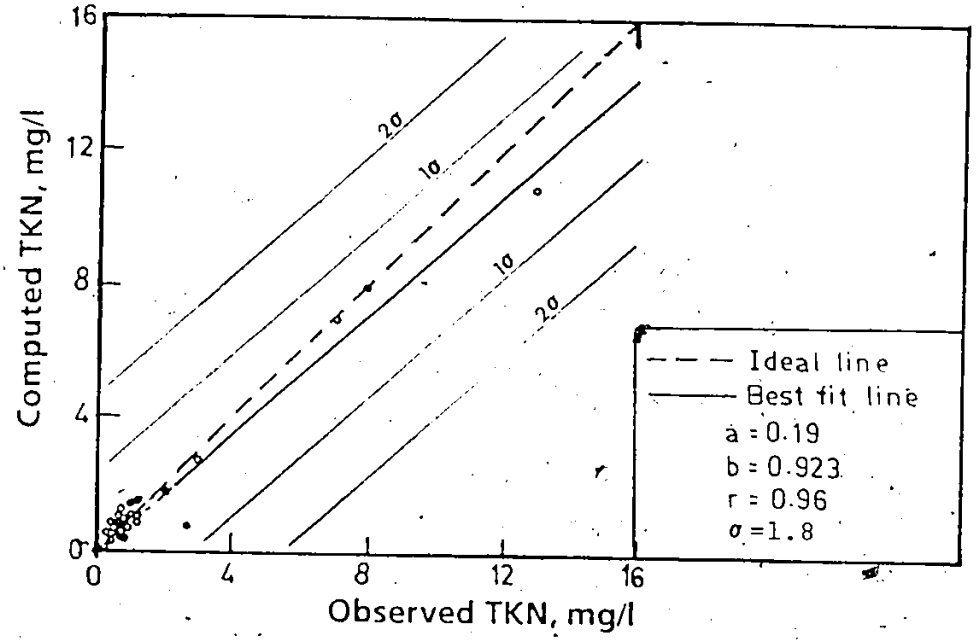

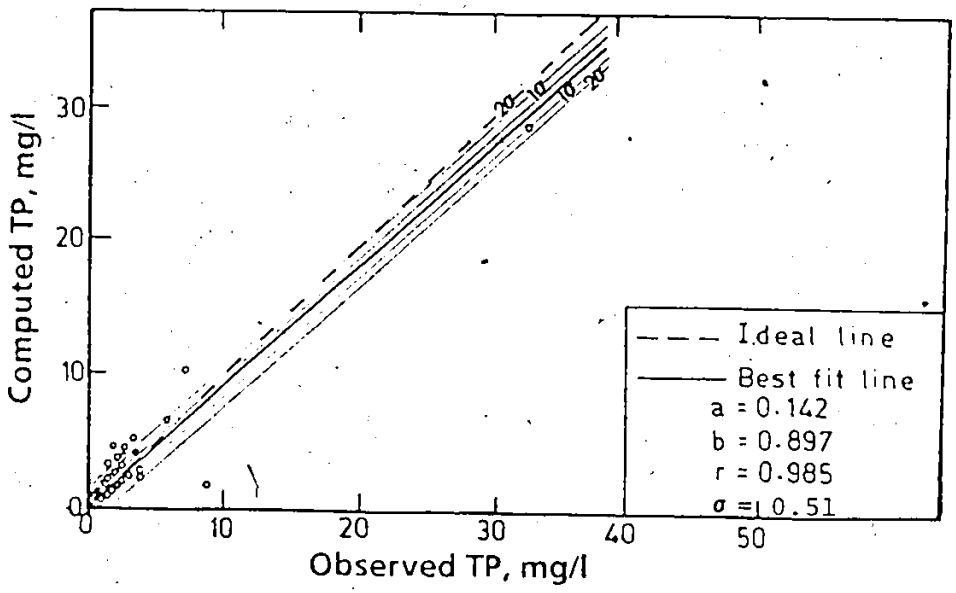

results under validation for Chedoke Creek test catchment were quite satisfactory.

CHAPTER IX

DISCUSSIONS AND CONCLUSIONS

9.1. Discussions:

Deterministic models may be constructed to compute storm water runoff quality in sequential steps. Estimation of DD accumulation during inter-event drydays is the first stage and estimation of washoff of the DD during runoff events is the second stage. Routing is a third stage, if pollutant concentration is to be computed at the downstream end of the storm sewer network. Pollutant sedimentation, dispersion and transport in the receiving water is the final stage. Since the processes of accumulation, washoff, transport and dispersal are complex in nature, a general model for the complete process suitable for application to all catchments has yet to be developed. This study should be seen as a small step in that direction.

The data collected by researchers on DD and pollutant buildup show linear and non-linear accumulations, with a high degree of scatter. The scatter represents variations due to unexplained processes. Because of this, using a fitted equation to estimate DD for a specific storm day may not reflect the actual data. For example, high winds transport DD from effective to ineffective areas; unreported street sweeping prior to a storm considerably

reduces DD; thermal inversions in Hamilton may significantly increase fallout. Clearly a simple linear or exponential equation using the number of drydays as the only independent variable is not sufficient to depict the complex buildup processes. For these reasons this study focussed on overcoming the shortcomings of the current methods of computing DD buildup by developing process oriented buildup algorithms, based on daily mass balances of DD or a pollutant. This approach computes DD or pollutant loadings available at the onset of the storm. Several FORTRAN codes were written by the author to interface with the SWMM3 package. The NEWBULD routine in CHGQUAL calculates buildup on all the subcatchments on an individual basis; it is not based on the five land use classifications. This gives the user a capability of modelling management strategies for reducing buildup.

After Sartor and Boyd's experiments on washoff in 1972 most urban runoff quality models defined washoff as an exponential function of runoff rate dependent on DD quantity available for washoff. But washoff is really the joint effect of raindrop impact, overland flow and traffic during a storm. The impact of raindrops dislodges particles. Overland flow erodes the surface and transports DD while moving vehicles induce turbulence which accelerates washoff.

These processes are modelled in CHGQUAL for DD or pollutant washoff. Three constants W_1, W_2 and W_3 are obtained by calibrating CHGQUAL against Sartor and Boyd's experimental data. Hence CHGQUAL washoff is sensitive to rain intensity overland flow and the number of vehicles moving during the storm. SWMM3 washoff is sensitive only to runoff rate.

Pollutant washoff is sensitive to time step because of its dependency on the quantity remaining for washoff. Most models use a constant timestep of 1 min to 5 min for single event and 1 hr for continuous modelling. The smaller the timestep, the more accurate the results, but the computational cost becomes very high. Longer timesteps reduce computational cost but the results may deviate substantially from reality. Therefore a variable timestep has been provided in CHGQUAL to increase the accuracy and reduce computational cost.

In addition to impervious area washoff, (a) aerosol and gas scavenging, (b) canopy washoff and (c) pervious area erosion add to runoff water quality during the storm. SWMM3 treats both aerosol and gas scavenging together as a constant concentration throughout the simulation. Randall et al. (1978) and other researchers have found that aerosol scavenging varies exponentially with the intensity of rainfall. It also varies with particle radius and collection efficiency. Gas scavenging remains almost constant throughout the simulation because it is not rate

limited and attains equilibrium concentration within a small distance of travel. These two processes are modelled separately in CHGQUAL.

The vegetation canopy accumulates more dustfall than the land surface because of the large surface area of leaves and air filtration through the canopy. Pollutants washed off the canopy during a storm joins the runoff only after satisfying depression storage and exceeding infiltration. Among the total quantity of pollutant washed off from the canopy only a portion joins the runoff. The remainder either infiltrates or is arrested in the grass filtration blanket. Consequently the net canopy effect on pollutant runoff may not be significant under normal conditions when the grass filtration blanket is absent or thin and/or when the location of the catchment is very close to dust prone areas, the canopy effect may be significant. In Ontario, the forest canopy is widespread, and so this phenomena was also modelled in CHGQUAL.

Runoff pollutants are routed through a sewer network. Gutter flow is usually treated as completely mixed with continuous or purged pollutant input. This applies in SWMM3 until the ratio of time step (Δt) to detention period (t_d) is greater than 16.0. Actually if t_d is greater than Δt, flow from the previous time step is still present in the gutter and this allows pollutants to mix with the incoming

pollutants. Therefore both continuous and purged sources are necessary to compute runoff quality. On the other hand, if t_d is smaller than Δt, the flow has already left the gutter and no mixing of pollutant from the previous time step occurs. A continuous source with complete mixing condition is sufficient to model the situation. But in SWMM3 until the ratio $\Delta t/td$ is 16.0 both continuous and purged sources are used. This results in about 100% total pollutant summation error. The effect of the purged source is restricted to $\Delta t/td$ less than 1 in CHGQUAL, which reduces the total pollutant summation error to about 1%.

Field data are necessary to validate the model developed. In Hamilton this required construction of a weir to measure streamflow. The ponding of water behind the weir might cause solids settling during low flow. During high flow, these solids scoured. A critical condition occurs between these two stages when neither sedimentation nor scouring takes place. Thus the construction of a weir alters the time distribution of concentration of suspended solids, depending upon the volume of the pond upstream of the weir and the grain size distribution of the particles. The removal of SS impacts on the concentration of associated pollutants. There is no provision to simulate this weir effect on the pollutant concentration in any of the known storm water models. The algorithm included in CHGQUAL

facilitates weir modelling at any point in the sewer network.

Generally, a storm sewer network carries base flow which is almost constant both in quantity and quality. This impacts on pollutant concentration during the initial simulation period when storm flow is low and pollutant concentration is high. If computed pollutant concentration is not initially reduced because of dilution with baseflow, unrealistic concentrations will be predicted by the model, especially if exponential washoff relations are used and the amount of solids available is high. The remaining surface DD becomes very small soon after the storm starts and computed concentration tends to zero. The constant observed concentrations at the end of the storm are mainly due to background baseflow concentration rather than pollutant washoff from the buildup. Algorithms for the inclusion of baseflow and its concentration at any point were inserted in CHGQUAL. The addition of this background concentration to CHGQUAL produced a recession limb of the pollutograph that yielded a better fit to the observed data. CHGQUAL was finally subjected to verification, calibration and validation tests using data from the Chedoke Creek catchment in Hamilton. CHGQUAL was calibrated against observed data for summer 1980 . During the calibration, it was found that the peak of the observed and predicted data did not coincide. Shifting the storm onset time by 5 to 10 minutes

made it possible to fit the computed to observed time for peak flow and concentration. Since storms are dynamic rather than stationary the initial starting time for an individual subcatchment is dependant upon the storm speed and direction. The error in predicting time to peak flow and concentration could be attributed to the assumption of stationary storms. Therefore a dense data collection network is recommended to provide better rain data.

Most of the computed pollutographs calibrated well against observed pollutographs by adjusting model input parameters rather than model constants. This confirms the necessity for careful sensitivity analysis. CHGQUAL was validated against 1981-83 summer data using average calibrated model parameters. Unfortunately most of the data collected during 1981-1983 were almost background concentrations, because the few storms that did occur typically started at inconvenient times and were not adequately sampled. Nevertheless the validated results are good with respect to time to peak and peak concentrations.

9.2. CONCLUSION:

The present art of modelling urban storm water quality is still in the preliminary stages. A larger data base and better knowledge of pollutant buildup, washoff and transport is essential. The attempt made in this study to better approximate the basic physics of processes involved

in the storm water quality is a start towards a process oriented model. The statistical comparison between SWMM3 and CHGQUAL for both calibration and validation showed that CHGQUAL probably represents an improvement. However the tests were carried out on a very small data set, so it is too soon to make generalised statement on the predictibility of CHGQUAL. Since CHGQUAL is process oriented, more capabilities for investigating sophisticated management techniques based on the physical processes are now possible.

The algorithms used in CHGQUAL are by no means the final solution to the problem of storm water quality modelling. But an attempt has been made to identify the processes, to model them separately and to use them in an overall model for management of runoff water quality. Until a sufficiently large data base is available which will allow further description of the processes involved in urban runoff water quality, CHGQUAL should be used with caution.

REFERENCES

Acres Consulting Services, "Atmospheric Loading of the Lower Great Lakes and the Great Lakes Drainage basin", Department of Fisheries and Environment, Canada Centre for Inland Waters, 1977.

Air Quality Report on Hamilton city, Ministry of Environment, Ontario, 1980.

Alaa Eldin Elzawahry, "Algorithm for Transient Sediment Deposition and Resuspension in a One-Dimensional Zone between an Outfall and Receiving water", M.Eng. Thesis, McMaster University, 1981.

Alley M. W., "Estimation of Impervious-Area Washoff Parameters", Water Resources Research, Vol. 17, No. 4, pp. 1161-1166, 1981.

American Public Works Association, "Water Pollution Aspects of Urban Runnoff", Federal Water Pollution Control Administration, Report WP-20-15, U.S. Department of the Interior, Washington, D.C. 1969.

Ammon C. D., "Urban Stormwater Pollutant Buildup and Washoff Relationships", M.Engineering Thesis, University of Florida, 1979.

Asplund, F., Max W. B., and Ferguson F. J., "Total Suspended Solids in Highway Runoff in Washington State", J.ASCE, Environmental Engineering Division, Vol.108, pp 391-404, 1982.

Barkdoll, M.P., "An Analysis of Urban Storm Water Quality and the Effect of Dustfall on Urban Storm Water Quality", M.S. Thesis, University of Tennessee, Knoxville, 1975.

Barton, S. C., Hunt, J. E., Kane, D. M. and Weisman, "An Assessment of Street Dust and Other Sources of Airborne Particulate Matter in Hamilton, Ontario", Technology Transfer Seminar, Toronto, Sponsored by MOE, November 24, pp. 1-11, 1981.

Blanchard, D.C., "Behaviour of Water Drops at Terminal Velocity", Transactions of the American Geophysical Union, 31, pp. 836, 1950.

Chamberlain, A. C., and Chadwick, R. C., " Transport of

Iodine from atmosphere to ground", Tellus, XVIII (2), pp. 226-237, 1966.

Chamberlain, A. C., Proceedings of Royal Society, A 296, pp.45, 1967.

Chan, C.H., and Kuntz, K.W., "Lake Ontario Atmospheric Deposition 1969 - 1978", Canada Centre for Inland Waters, Water Quality Branch Report, Ontario Region pp. 1-28, 1981.

Chen W. C., Hudson J. M. R., Cherini A. S., Dean J. D., and Goldstein A. R., "Acid Rain Model: Canopy Module", J.ASCE, Vol. 109, No. 3, pp 585-603, 1983.

Dick, T.M., Marsalek, J., "Exchange Flow Between Lake Ontario and Hamilton Harbour", Scientific series No.36, Environment Canada, pp 1-22, 1973.

Donigian, A. S., Jr. and Crawford, N.H., "Modelling Non-Point Pollution from the Land Surface", EPA-600/3-76-083, Environmental Protection Agency, 1976.

Eid, M. F. B., " Investigation into Interfacial Transports and Exchange Flows for Lake Models", Ph. D. Thesis, McMaster University, 1981.

Eisenreich J. S., "Atmospheric Pollutnats in Natural Waters", Ann Arbor Science Publishers Inc., pp 23-55, 1981.

Ellis, F. W., and Sutherland, R. C., "An approach to Urban Pollutant Washoff Modelling", International Symposium on Urban Storm Runoff, Proceedings, University of Kenteky, Lexington, pp. 325-340, 1979.

Farhang, A.C., "Meteorology and Climatology of Hamilton (Ontario) and its Surroundings", Urban Air Environment Group Report, McMaster University, pp 1-123, 1982.

Frizzola, J. A., and Joseph, H. B., "Contaminants in Rainwater and their Relation to Water Quality", Part I, Water and Sewage Works, August, pp. 72-75, 1975.

Geiger, W.F. and Dorsch, H.R., "Quantity-Quality Simulation (QQS): A Detailed Continuous Planning Model Description, Testing and Applications", EPA-600/2- 80-011, Environmental Protection Agency, Cincinnate, OH, 1980.

Goettle, A., "Atmospheric Contaminants, Fallout and

Their Effects on Storm Water Quality", Progress in Water Technology, Vol. 10, Nos. 5/6, pp.455-467, 1978.

Gupta, M. K., Agnew, R. W., and Kobriger, N. P., "State-of-the art report on Highway Runoff Constituents, Envirex Inc. for FHWA Contract DOT-FH-8600, 1978.

Hales, J.M., "Fundamentals of the Theory of Gas Scavenging by Rain", Journal of Atmospheric Environment, Vol.6, No. 635, 1972.

Haro, H., Kitai, R., and James, W., "Precipitation Instrumentation Package for Sampling of Rainfall", Institute of Electrical and Electronics Engineers (Transactions on Instrumentation and Measurement), Vol. IM32, No.3, pp. 423-429, September 1983.

Haro, H., "Instrumentation for Rainfall Sampling", Ph.D. Thesis, McMaster University, January 1984.

Heaney, J.P., and Huber, W.C., "Storm Water Management Model, Refinements, Testing and Decision Making", Department of Environmental Engineering and Sciences, University of Florida, 1973.

HEC (Hydrologic Engineering Center), US Army, Crops of Engineers, "Storage, Treatment, Overflow, Runoff Model (STORM)", Computer Program 723-58-17520, Davis, California, 1976.

Heidorn, K.C., "Air Pollution Incidents and Wind Variability in Southern Ontario", J. Atmospheric Environment Vol. 12, pp. 2251-2257, 1978.

Heinemann, K., Vogt, K.G., and Angeletti, L., "Atmosphere Surface Exchange of Particles and Gases", ERDA Conference Series, 1975.

Hill, A.C. and Chamberlain, E.M. "Removal of Water Soluble Gases from the Atmosphere by Vegetation", Atmosphere-Surface Exchange of particles and Gases, ERDA Symposium Series, 38, pp.153-170, 1974.

Huber, W. C., Heaney, T. P., Nix, S. J., Dickenson, R. E. and Polmann, D. J., "Storm Water Mangement Model User's Manual, Version III", U. S. Environmental Protection Agency, Cincinnati, OH, 1981.

Hudson, N., "A Review of Methods of Measuring Rainfall Characteristics Related to Soil Erosion", Research Bulletin 1, Department of Conservation, Salisbury

Rhodesia, 1964.

James, W., and Robinson, M.A., "Standard Terms of Reference to Ensure Satisfactory Computer-based Urban Drainage Design Studies", Candian Journal of Civil Engineering, Vol. 8, No. 3, pp. 294-303, March 1981.

James, W., and Mitri, H., "Modelling Sideweir Diversion Structures for Stormwater Management", Canadian Journal of Civil Engineering, Vol. 9, No. 2, pp. 197-205, June 1982

James, W., Haro, H., Robinson, M. A., and Kitai, R., "Hydrologic Data Acquisition: Innovative, High resolution, Programmable Instruementation for Storm Water Mangement", Proceedings of the Conference on Storm Water and Water Quality Management Modelling, U. S. EPA. Washington, D. C., EPA 600/9-82-015, pp. 128-151, 1982.

James, W., and Henry, D., "Stormwater Management Model for Hamilton Harbour, Summer Field Program 1981 (Development of a Stormwater Overflow Model for Pollutional Loadings to Hamilton's Receiving Water, Summer Field Program and Data for Period May to October 1981)". Report to the Ontario Ministry of the Environment. CHI Publications, (about 300 pp.) March 1982.

James, W., and Shivalingaiah, B., "Stormwater Quality and Atmospheric Pollution Modelling in an Industrial City", 6th Canadian Hydrotechnical Conference, Ottawa, pp. 707-722, June 1983.

James, W., and Henry, D., "stormwater Management Model for Hamilton Harbour, Summer Field Program 1982 (Development of a Stormwater Overflow Model for Pollutional Loadings to Hamilton's Receiving Water, Summer Field Program and Data for Period March - October, 1982)". Report to the Ontario Ministry of the Environment. CHI Publications, Hamilton, (about 300 pp.) January 1983.

Jeffries, D. S., "Ontario Precipitation Chemistry and Heavy Metal speciation", Ph.D. Thesis, McMaster University, pp. 1-125, 1975.

Junge, C.E., "Air Chemistry and Radioactivity",Academic Press Inc., New York, 1963.

Kohli, B., "Mass Exchange between Hamilton Harbour and Lake Ontario", Ministry of the Environment Report, pp

1-74, 1977.

Kramer, J., Private communication from Dr. Kramer, J., Department of Geology, McMaster University, 1982.

Laws, J.O., "Measurements of Fall Velocity of Water-Drops and Raindrops", Transaction of the American Geophysical Union 22,pp. 709, 1941.

Malmquist, P.A., "Atmospheric Fallout and Street Cleaning Effects on Urban Storm Water and Snow", Prog. Wat. Tech., Vol. 10, Nos. 5/6, pp 495-505, 1978.

Mance, G., and Harman, M., "The Quality of Urban Stormwater Runoff", Urban Storm Drainage, Proceedings of International Conference on Urban Storm Drainage, Southampton, England, 1978.

Manning, M.J.; Sullivan, R.H. and Kipp,T.M. "Nationwide Evaluation of Combined Sewer Overflows and Urban Storm Water Discharges, VolumeIII: Characterization of Discharges, Environmental Protection Technology Series, EPA-600/2-77-064, U.S. Environmental Protection Agency, Cincinnati, 1977.

Marsalek, J., "Stormwater Quality in the Malvern Catchment", Presented at the Stormwater Management Model Users Group Meeting, Toronto, Ontacio, 1976.

McCuen, R.H. and Sutherland, R., "Flood Runoff From Urban Areas", Technical Report No. 33, Water Resources Research Center, University of Maryland, College Park, Maryland, 1975.

Medina, M.A., Jr. "Interaction of Urban Storm Water Runoff, Control Measures and Receiving Water Response", Ph.D. Dissertation, University of Florida, Gainesville, Florida, 1976.

Metcalf and Eddy, Inc., University of Florida Water Resources Engineers, Inc.; "Storm Water Management Model Volume I, Final Report", Water Pollution ontrol Research Series, 11024 DOC 07/71, U.S. Environmental Protection Agency, Washington, D.C., 1971.

Metcalf and Eddy, Inc., "Waste Water Engineering", McGrew-Hill Series in Water Resources and Environmental Engineering, 1972.

Miller, R.A., Mattraw, H.C. and Jennings, M.E., "Statistical modelling of Urban Storm Water Processes,

Broward County, Florida", Proceedings, International Symposium on Urban Storm Water Management, University of Kentucky, Lexington, pp 269-273, 1978.

Novotny, V., Goodrich-Mahoney,J., "Comparitive Assessment of Pollution Loadings from Non-point Sources in Urban Land Use", Progress in Water Technology, Vol.10 Nos. 5/6, pp. 775-785, 1978.

Novotny, V., "Acidity of Urban Precipitation and its Buffering During Overland Flow", Second International Conference on Urban Storm Drainage, Urbana, Illinois, U.S.A. June 1981.

Nunno,T.J., "Application and Testing of Stormwater Modeling Technology", M.S. Project, Department of Civil Engineering, University of Massachusets, Amherst, 1978.

Pitt, R., The Potential of Street Cleaning in Reducing Non-point Pollution", Urban Stormwater Management Workshop Proceedings, EPA-600/9-78-017, U.S. Environmental Agency, Cincinnati, pp. 91-119, 1978.

Postma, A. K., "Precipitation Scavenging", AEC Symposium Series, 1970.

Prasad, D., Henry, J.G., and Kovacko, R., "Pollution Potential of Autumn Leaves in Urban Runoff", International Symposium on Urban Storm Runoff, Lexington, Kentuck, pp. 197-201, 1980.

Rafael G. Q. and Ali-Bux B., "Rainfall Energy from Drop Size Data", IAWPRC and IAHR Specialised Seminar, Copenhagen, Denmark, pp 239-252, 1983.

Randall, C.W., Helsel, D., Grizzard, T., and Hoehn, R., "The Impact of Atmospheric Contaminants on Storm Water Quality in an Urban Area", Prog. Wat. Tech., Vol.10, Nos. 5/6, pp. 417-431, 1978.

Randall, C.W., Grizzard, T.J., Helsel, D.R. and Griffin, D.M., "Comparison of Pollutant Mass Loads in Precipitation and Runoff in Urban Areas", Second International Conference on Urban Storm Drainage, Urbana, Illinois, pp. 29-38, 1981.

Robinson, M. A., and W.James, "Continuous SWMM Modelling of Summer Storm Water Runoff Quality in Hamilton: Analysis of preliminary output time series based on discrete-event calibrations from non-industrial areas", CHG Publications, Hamilton, 1981.

Rouse, W.R., and McCutcheon G.J., "The Effect of the Regional Wind on Air Pollution in Hamilton, Ontario", Canadian Geographer, xiv, 4, pp 271-285, 1970.

Rouse, W.R., Noad, D. W., McCutcheon, G. J., and Donald, N., "Atmospheric Emissivities in a Polluted Urban Atmosphere at Hamilton, Ontario", J.Applied Meteorology, Vol. 12, pp. 798-807, 1972.

Rutherford, G. K., "A Preliminary Study of the Composition of Precipitation in SE. Ontario", Canadian Journal of Earth Sciences, Vol. 4, pp. 1151-1160, 967.

Sartor, J. D., and Boyd, G. B., Water Pollution Aspects of Street Surface Contaminants, Environmental Protection Technology Series, EPA-R2-72-081, U.S. Environmental Protection Agency, Cincinnati, 1972.

Scheckenberger, R." Dynamic Spatially Variable Rain Models for Storm Water Management", M.Eng. Thesis, McMaster University, 1983.

Sehmel, G. A., "Particle Resuspension from an Asphalt Road caused by car and Truck Traffic", Atmospheric Environment Pergamon Press, Vol. 7, pp 291-309, 1973.

Sehmel, G.A., "Atmosphere Surface Exchange of Particles and Gases", ERDA Conference Series, 1975.

Sehmel, G. A., "Particle and Gas Dry Deposition: A Review", Atmospheric Environment, Vol. 14, pp 983-1011, 1980.

Semkin, R.G., Mclarty, A.W., and Craig, D., "A Water Quality Study of Cootes Paradise", Ministry of the Environment Report, 1977.

Shaheen, D. G., "Contributions of Urban Roadway Usage to Water Pollution", Environmental Protection Technology Series, EPA-600/2-75-004, U. S. Environmental Protection Agency, Cincinnati, 1975.

Shivalingaiah, B., and James, W., "Atmospheric Pollution in relation to storm water quality modelling; Literature Review for an Industrial City", Storm Water Quality Model User's Group Meeting, Washington, D. C. EPA-600 9-82-015, pp 274-295, 1982.

Shivalingaiah, B., Robinson, M.A. and James, W., "Enhancements to SWMM3 Runoff Quality Algorithms", Proceedings of the Conference on Stormwater and Water

Quality Management Modelling, Montreal, Quebec. Report Gremu 83/03, Ecole Polytechnique, pp. 64-74, September 8-9, 1983a.

Shivalingaiah, B., and James, W., "Atmospheric and Land-Based Loadings for Storm Water Runoff Quality Models", International Symposium on Urban Hydrology, Hydraulics and Sediment Control, Lexington, Kentucky, pp. 115-121, July 25-28, 1983b.

Shivalingaiah, B., and James, W., "Atmospheric Dustfall Model for Runoff Water Quality in Hamilton, Ontario", Report to Inland Waters Directorate, Environment Canada (75pp.) February 1983c.

Shivalingaiah, B., and James, W., "CHGQUAL User's Manual", CHG Publication, Hamilton, 1984 (under publication).

Shtifter, Z., "A Kinematic Storm Model for Urban drainage studies", M.Eng. Thesis, McMaster University, May 1980.

Slinn, W. G. N., "Precipitation Scavenging: Some Problems, Approximate Solutions and Suggestions for Future Research", Precipitation Scavenging ERDA 41 Symposium Series, CONF-741003, pp. 1-60, 1974.

Slinn, W. G. N., "Formulation and a Solutionn of the Diffusion, Deposition, Resuspension Problem", Atmospheric Environment, Vol. 10, Nos. 9, pp. 763-768, 1976.

Slinn, W.G.N. "Some Approximation for the Wet and Dry Removal of particles and Gases from the Atmosphere", Water, Air, Soil Pollution, 7, pp 515-543, 1977.

Smith, P. E., and Jennings, M. E., "Accumulation and Washoff of Pollutants on Urban Watersheds", EOS, Transactions of American Geophsical Union, Vol. 60, nos. 18, pp. 259, 1979.

Snodgrass, W., "Material Budget For Hamilton Harbour", Ministry of the Environment Report, 1981.

Stewart, I.M., and Matheson, D. H., "Methods of Relating High Volume Sampler Particulate Loadings to Wind Direction", Atmospheric Environment, Pergamon Press, Vol. 2, pp. 181-185, 1967.

Terstriep, M. L., Bender, G. M., and Benoit D. J.,

"Buildup, Strength, and Washoff of Urban Pollutants," Preprint 3439, Presented at American Society of Civil Engineers Convention, Chicago, 1978.

Thomann, V. R., "Verification of Water Quality Models", J.ASCE, Environmental Engineering Division, Vol.108, pp 923-940, 1982

Waller, D. H., "Factors that Influnce Variations in the Composition of Urban Surface Runoff, "Water Pollution Research in Canada, No.7, pp. 68-95, 1972.

Wanielista P. M., "Stormwater Mangement Quantity and Quality", Ann Arbor Science Publications Inc., 1979.

Weisman, B., Matheson, D. H., and Hirt. M., "Air Pollution Survey for Hamilton, Ontario", Atmosphere Environment, Pergamon Press 1969. Vol. III, pp. 11-23. Printed in Great Britain.

Wischmeier, W.H. and Smith, D.D., "Rainfall Energy and its Relationship to Soil Erosion", Transactions American Geophysical Union, Vol. 39, No.2, pp. 285-291, 1958.

Wischmeier, W.H. and Smith, D.D., "Predicting Rainfall-Erosion Losses from Cropland East of the Rocky Mountains", Agricultural Handbook 282, U.S. Department of Agriculture, Washington, D.C., 1965.

LIST OF ABBREVIATIONS

a	= aerosol particle radius, cm [6.10]
	= exchange coefficient [7.26]
a, b, c	= empirical coefficients [3.9]
a_i, b_i	= regression constants for dustfall station i [2.26]
a_i, b_i, c_i	= multiregression constants [2.27]
A	= area, ha [2.30]
	= special activity area, ha [2.31]
	= subcatchment area in ha. [5.6]
	= area, cm^2 [5.13]
	= area of canopy, m^2 [6.23]
	= area of subcatchment, m^2 [6.15]
	= total canopy area, m^2 [6.19]
A_c	= area leading to collision, cm^2 [2.10]
A_f	= atmospheric fallout (g/m^2-d) [2.4]
A_i	= availability factor, dimensionless. [5.1]
A_v	= availability factor [2.36]
A_x	= projected area of obstacle, cm^2 [2.10]
b	= washoff coefficient, 1/mm [5.1,5.6]
B	= biomass per unit volume, mass/m^3 [2.24]
C	= canopy removal rate, s [2.23]
	= mean atmospheric aerosol concentration, mg/m^3 [6.15]
	= influent pollutant concentration, mg/l

= cropping mangement factor or cover index factor [6.24]

= gutter outlet concentration at time t, mg/l [7.19]

= weir influent solids concentration, mg/l [7.21]

C_a = influent concentration, mg/l [7.17]

= additional concentration due to scouring, mg/l [7.24]

C_c = pollutant concentration in canopy, mg/l [6.23]

= pollutant concentration at the previous timestep, mg/l [7.18]

= gutter purged source concentration (previous timestep concentration), mg/l [7.19]

C_D = drag coefficient [2.17]

C_e = equilibrium concentration of gaseous pollutant in the drop [6.13]

C_f = washoff coefficient, $(mm/h)^{-W} s^{-1}$ [5.7]

= washoff coefficient in empirical units [5.21]

= collection efficiency, (10^{-2} to 10^{-1} for particle size 1-5 μm and drop radius 0.1-1.00 mm [6.16]

C_f = coefficient, kg/d [3.3]

C_h = average concentration in the harbour, mg/l [7.26]

C_i = incoming concentration, mg/l [7.25]

= average input concentration to harbour, mg/l [7.26]

C_{it} = influent concentration of tracer, mg/l [7.4]

C_i = concentration of pollutant at the inflow, mg/l [7.14]

C_j = outlet pollutant concentration for gutter number j, mg/l [7.18]

C_l = average lake concentration, mg/l [7.26]

C_o = gutter continuous source influent concentration mg/l [7.19]

= concentration of pollutant at the outflow, mg/l [7.14]

C_q = equilibrium concentration, mg/l [6.18]

C_T = total concentration, mg/l [7.25]

C_t = outlet concentration at time t, mg/l [7.3]

= effluent and reservoir pollutant concentration, mg/l [7.4]

C_t = effluent concentration, mg/l [7.9]

C_1 = canopy washoff coefficient, 1/mm [6.20]

C_1 , C_2 = pollutant concentration from pipe 1 and 2, mg/l [7.17]

d = average depth between first and the second fluid parcel, m [7.15]

= average depth of fluid, m [7.16]

= depth of flow, m [7.14]

d_1 = depth of incoming fluid parcel, m [7.15]

D = molecular diffusion coefficient, cm^2/s [6.10]

= atmospheric dust, mg/eff.h-m^2 [6.19]

= Brownian or molecular diffusivity, m^2/s [2.14]

= pollutant deposition during time interval, (t/ha) [3.7]

DD = dust and dirt accumulated near the curb, g/m [2.14]

D_d = limiting buildup quantity, kg [3.6]

= dust and dirt loading rate (g/d-100m) [3.6]

D_f = coefficient, half time constant, kg/100m,

curb-d [3.1]

D_g = surface deposition, mg/m^2 -s [6.13]

D_i = diurnal variation factor at time of the day d, dimensionless, [5.8]

D_m = gutter length, m, or subcatchment area, ha

E = average annual Lake exchange rate, m^3/s [7.27]

= collection efficiency, (collision efficiency multiplied by retention efficiency which is taken to be unity) [6.9]

= collision efficiency [2.11]

= total energy, t-m/ha-mm [4.1]

= efficiency of street cleaning on the impervious area [3.8]

= sediment loss to stream from impervious areas in time t, t/ha [4.6]

E_f = number of effective hours, h(24 X wind frequency) [6.19]

E = sediment loss to stream from impervious area, t/ha [5.11]

E_i = jet collection efficiency [2.23]

E_l = pollutant buildup, (mg or MPN) [3.3]

E = total rainfall energy, 100ft-t/ac [6.26]

E_s = energy, $ergs/cm^2$-mm [4.2]

f = frequency of street cleaning

F = pollutant fraction in aerosol, mg/mg [6.15]

= flux of pollutant per unit area, $mg/s\text{-}m^2$ [2.12]

= collection efficiency [2.11]

= fraction of impervious area [3.8]

F_o = average pollutant flux over the timestep, mg/s [7.18]

F_c = pollutant flux in canopy, mg/s [6.23]

F_o = fraction of impervious overland flow reaching the stream [5.11]

= fraction of impervious overland flow reaching the stream in time t [4.6]

g = acceleration due to gravity, cm/s^2

G = total gutter or curb length in subcatchment, 100m [3.6]

G, L = gain and loss of contaminant associated with particles because of condensation, evaporation, coagulation etc., mg [6.1]

H = canopy depth, m [2.23]

= curb height, cm [2.4]

= Henry's law constant [6.13]

= atmospheric mixing height, m [6.15]

i = excess intensity of rainfall, cm/s [5.13]

= excess intensity of rainfall, cm/h [5.19]

I = effective precipitation, mm/5 min [5.8]

= rain intensity, mm/h [5.20]

= intensity of rainfall, mm/h [6.16]

= inflow rate, l/s [7.4]

j = impervious area exponent of transport [4.4]

k = 0.4 = Von Karman's constant [2.21]

= bR = proportionality constant, 1/h [4.3]

K = decay coefficient, 1/d [2.32]

= impervious area coefficient of transport [4.4]

= turbulent diffusivity, cm^2/s [6.1]

= soil erodibility factor [6.24]

= decay coefficient (decomposition) or solid removal rate, w/d (sedimentation), 1/s [7.14]

= decay coefficient, 1/s [7.4]

K_b = fraction of pollutant decay by biochemical processes [3.8]

K_d = deposition rate per axle, kg/axle-km [2.1]

K_e = impervious area coefficient at transport [5.9]

K_Z = the Z component of turbulent diffusivity, m /s [2.15]

K_1 = loss rate per axle [2.1]

K_i = constant, 1.0 [5.20]

K_2 = rain impact exponent =2.0 [5.20]

L = mass of DD produced per vehicle per km travelled (800mg/axle-km in Hamilton) [2.28]

= per capita mass of pollutants/day, (200mg/cap-d in Hamilton) [2.29]

= the pollutant loading, kg/km [2.3]

= accumulated loading, mg [2.5]

= pollutant accumulation during dry period, kg/ha [3.9]

= cumulative weight of material of a given particle washed off, kg/1000m^2 [4.3]

= amount of material on the impervious area, t/ha

$\overline{L}$ = average vertical component of dry flux [2.14]

L_a = DD present before sweeping, mg [2.36]

= daily mass flux of atmospheric dustfall, mg/d [2.9]

L_e = daily mass flux of pollutants from vegetation mg/d [2.9]

= vegetation input DD, mg/d [2.30]

L_m = K_d/K_1 = maximum pollutant loading, kg/km [2.2]

= maximum pollutant loading (kg/ha) [3.9]

= maximum accumulation DD, kg/ha [T 2.2]

L_o = initial load of material of a given particle kg/1000m [4.3]

L_p = total mass of DD due to population, mg/d [2.29]

= daily mass flux of pollutants from population related activities such as lawn cutting, insecticides and pesticides, spray and fertilizer on lawns, mg/d [2.9]

$L_{nj(t-1)}$ = quantity of pollutant j on subcatchment n at time t, mg [5.2]

L_{njt} = quantity of pollutant 'j' on subcatchment 'n' at time step t, mg [5.2]

$L_{nj(t-1)}$ = quantity of pollutant 'j' washed off subcatchment 'n', at timestep (t-1), mg [5.2]

L_S = total mass of DD produced by special activities in mg/d [2.31]

= daily mass flux of pollutants from special activities such as construction, demolition of structures, mg/d [2.9]

L_t = pollutant loading on subcatchment at time 't' (mg) [3.6]

L_S = slope length gradient ratio [6.24]

L_t = pollutant loading on subcatchment at time 't' (mg) [3.6]

L_{t-1} = pollutant accumulation at time(t-1), (t/ha) [3.7]

L_t = amount of material on the impervious surface, t/ha [4.5]

L_{t-1} = pollutant loading on subcatchment at t-1, (mg) [3.6]

L_v = mass of DD produced by vehicles mg/d [2.28]

= daily mass flux of pollutants from vehicles, mg/d [2.9]

M = total length of road in subcatchment, km [2.28]

n = number of records for the month m and station i [2.25]

= washoff exponent = 0.8, [5.24]

N = number of vehicle axles active each day in a subcatchment, assuming two axles per vehicle (product of total population and P) [2.28]

= 40,000 axle/d [2.3]

= number of vehicles in a subcatchment [2.33]

= average daily traffic (vehicles/d) [2.6]

= number of vehicles in thousands [5.22]

O_i = overland flow washoff component, l/h [5.23, 5.21]

O_t = outflow rate, l/s [7.4]

O_v = impervious area overland flow occuring in time interval t, min [5.9]

P = population to vehicle ratio = 0.4 to 0.5 [2.28]

= total population in a subcatchment [2.29]

= average mass of DD available on the surface mg/d [2.32]

= DD available for eddy-transport, mg/d [2.33]

= erosion control practice factor [6.24]

P_a = percent open area near the site [2.4]

= daily mass flux of pollutant accumlated, mg/d [2.9]

P_c = total pollutant quantity on the canopy before the rain, mg [6.19]

P_d = population density, persons/ha [2.37]

= total mass flux of previously deposited pollutants scoured from storm sewers and catch basins, mg/s [2.7]

P_e = pectlet number [6.10]

P_g = rate of pollutant added to the runoff water, mg/s [6.18]

P_i = total mass flux of accumulated pollutants washed off impervious areas, mg/s [2.7]

P_l = solids remaining after washoff at time t, mg [5.24]

P_o = solids accumulated on the impervious area, mg [5.24]

P_m = total water precipitation during month, mm (water equivalent) [2.27]

P_{nj} = quantity of pollutant 'j' washed off subcatchment 'n', mg [5.1]

= quantity of pollutant j available for washoff from subcatchment n, mg [5.6]

P_p = total mass flux of pollutants washed off pervious areas, mg/s [2.7]

P_r = total mass flux of pollutants in the subcatchment pollutograph mg/s [2.7]

P_s = total mass flux of pollutants scavenged by rain during its motion through the atmosphere, mg/s [2.7]

= pollutant scavenging rate, mg/s [6.17]

P_t = pollutant washed off at time t, kg/ha [5.8]

P_w = total washoff coefficient, 1/h [5.24]

= quantity of pollutant remaining in the canopy after washoff at time t, mg [6.20]

$P_{z,t}$ = precipitation rate at elevation z and time t, mm/s [6.9]

q = quantity of flow joining runoff water, 1/s [6.23]

Q = fraction of dust and dirt consisting of pollutant, in mg/g [3.6]

= flow rate, m^3/h [5.6,7.22,6.18]

= flow, 1/s [7.1,7.9]

= runoff rate, 1/s [7.25]

= average annual inflow rate to harbour, m^3/s [7.27]

Q_a = average flow rate over the timestep, l/s [7.18]

Q_i = impervious area overland flow occuring in time interval t, mm

Q_1, Q_2 = flow from pipe 1 and 2, l/s [7.17]

r_i = rain impact component, l/h [5.24]

R_v = daily mass flux of pollutants removed by vehicle generated eddies, mg/d [2.9]

R = retention efficiency (approximately equal to unity) [2.11]

= runoff rate, mm/h [5.1,5.6,5.7,5.20,5.21,5.22]

R_a = rain scavenging rate, l/s [6.14,6.17]

R_b = total mass of DD removed by biological decomposition, mg/d. [2.32]

= daily mass flux of pollutants removed by biological decomposition, mg/d [2.9]

R_c = $\Delta t/t_d$ = constant [7.18,7.19]

R_d = residential density (dwellings/ha) [2.4]

R_e = Reynold's number [6.10]

R_f = removal efficiency [2.37]

= rainfall factor [6.24]

R_g = general removal fraction [3.7]

R_i = DD removed by sweeping = $A_v R_f$ [2.36]

= daily intentional removal of pollutants, e.g. street cleaning, mg/d [2.9]

R_m = mean rain drop radius, cm [6.10]

R_{ma} = DD remaining on subcatchment surface, mg [2.36]

R_n = rainfall duration factor, dimensionless [5.8]

R_I = maximum average 30 minute rainfall intensity, mm/h [6.25]

R_v = mass of DD removed due to vehicle generated eddies, mg/d [2.33]

= daily mass flux of pollutants removed by vehicle generated eddies, mg/d [2.9]

R_w = daily removal of pollutants by natural wind, mg/d [2.9]

= fraction of DD lost due to wind [2.35,3.8]

S = vehicle speed, km/h [2.34]

= Stoke's number [6.10]

= average slope over the given runoff length, ft/ft [6.24]

S_a = total quantity of deposited solids at the weir, mg [7.23]

S_c = the Schmidt number [2.21,6.10]

= quantity of aerosol remaining in the atmosphere at time t, mg [6.14]

= pollutant quantity remaining in the atmosphere mg [6.17]

S_d = concentration of removed solids, mg/l [7.21]

S_L = DD loading, mg/ha-d [2.31]

S_o = quantity of aerosol present before the scavenging, mg [6.14]

S_* = critical Stoke's number [6.10]

t = time elapsed since rainfall or street sweeping, days [2.2, 2.3]

= number of days [2.32]

= time in days [3.4]

= time since beginning of runoff, h [4.3]

= time, h [5.23]

= time, s [5.19,6.20,7.4,7.9]

= time since start of effective precipitation, min [5.8]

= dry days, d [6.19]

t_d = time, d [2.4]

= detention period, s [7.19,7.23]

t_d, t_c = detention and critical detention periods, s [7.21]

t_d = detention period, s ($t = V/Q$) [7.3]

T = total traffic, axles [2.1]

= sediment transport for time interva t, t/ha [5.9]

T_c = average flux of solids scoured during the timestep, mg/s [7.23]

T = scoured pollutant flux, mg/s [7.24]

T_c = traffic speed (km/h) [2.4]

T_d = traffic density [2.4]

T_R = quantity of solids removed during timestep, mg [7.22]

T_s = total solids (kg/km-d) [2.6]

T = sediment transport for time interval t, t/ha [4.4,4.5]

$\overline{U}_c$ = mean wind speed in canopy, m/s [2.24]

$\overline{U}_g$ = mean wind above canopy, m/s [2.23]

U_L = upper limit for load, kg [3.4,3.5]

U_{n-1} = transformation function, kg/ha-mm [5.8]

U_* = friction velocity, m/s [2.23]

V = vegetation load rate to DD which varies with the landuse, and density of trees , mg/ha-d [2.30]

V = wind speed, cm/s [6.1]

= ratio of dynamic viscosities, water to air [6.10]

= volume of the tank, l [7.1,7.9]

= deposition velocity, m/s

= horizontal velocity, m/s [7.14]

= average volume of water in the gutter over the timestep, l [7.18]

= reservoir volume, l [7.4]

V_a = average fluid velocity with which pollutant concentration is moving, m/s [7.15]

= average fluid velocity, m/s [7.16]

V_c = celerity, m/s [7.16]

V_d = particle deposition velocity, m/s [2.23]

V_s = particle settling velocity, m/s [2.23]

$\overline{V}_d$ = the time average, deposition velocity, m/s [2.14]

V_{dx} = drop velocity component in x-direction, cm/s [5.13]

V_g = gravitational settling speed m/s [2.14]

V_i = vehicle induced washoff component, l/h [5.22]

V_{md} = average wind velocity for the month m and direction d, (km/h) [2.26]

V_t = terminal drop velocity, cm/s [6.10]

V_w = mean horizontal velocity of the overland flow, cm/s [5.19]

V_1 = velocity of oncoming fluid, m/s [7.15]

W = wind speed (km/h) [2.35]

= street width (m) [2.4]

W = exponent [5.7]

W_a, W_s = the vertical components (positive, up) of the air and slip velocities, m/s [2.14]

W'_a, W'_s = the fluctuation in air and slip velocities, m/s [2.14]

W_r = deposition rate exponent, 1/s [7.21]

W_s = wind speed, km/h [2.4]

W_s = scour exponent, s [7.23]

W_1 = drop energy damping exponent, h/mm [5.20]

W_2 = washoff exponent [5.21]

W_3 = vehicle washoff constant, 1/in-1000 vehicle [5.22]

x = horizontal distance in the x-direction, cm [5.19]

= longitudinal distance, m [7.14]

x_{im} = predicted average dustfall for month m and station i, g/m -30d [2.25]

Y = depth of water, cm [5.13]

= depth of overland flow, cm [5.19]

Y_{im} = observed dustfall for month m and station i, g/m -30d [2.25]

z = dry period (number of 5 minute intervals) [3.9]

Z = vertical height, m [2.14]

$\alpha, \beta, \gamma, \delta$ = empirical constants

δ = fraction of particles resuspended from the canopy

λ = typical length scale of individual fibres, m

Ξ = particle/canopy collection efficiency

Ψ = precipitation scavenging rate coefficient, 1/s

X = amount of contaminant per unit volume, mg/cm^3

X_g = pollutant concentration in the gas, mg/m^3

X' = pollutant concentration fluctuation in air, mg/m^3

X_c = pollutant concentration in the canopy layer per m^3

X_B = pollutant concentration in the boundary layer per m^3

τ_w = wind shear stress on the water, g/cm^2

τ_i = shear stress due to rain drop, g/cm^2

τ_b = bed shear stress, g/cm^2

Φ = surface slope

ρ = density of water, g/cm^3

$\bar{\rho}$ = average mass density of the foliage, $mass/m^3$

ν = kinematic viscosity of air, cm^2/s

ϵ_p = particle eddy diffusivity, m^2/s

ρ_a = density of air, g/cm^3

θ_1 = maximum fraction of DD removed

θ_2 = decay coefficient, h/km

Δt = timestep,